From Copper Dyshomeostasis to Neurotoxicity: Investigating the Interplay of Copper Regulation, Oxidative Stress and Neuronal Integrity in *Caenorhabditis elegans*

Dissertation

Zur Erlangung des Doktorgrades

der Naturwissenschaft (Dr. rer. nat.) in der Fachgruppe Chemie und Biologie

der Mathematisch Naturwissenschaftlichen Fakultät

der Bergischen Universität Wuppertal

vorgelegt von

Ann-Kathrin Weishaupt

aus Fulda

– 2024 –

Dekan: Prof. Dr. Francesco Knechtli

Erste Gutachterin: Prof. Dr. Julia Bornhorst

Zweiter Gutachter: Prof. Dr. Heiko Hayen

Tag der mündlichen Prüfung: __.__.____

Introductory remarks

This dissertation follows a semi-cumulative style and consists of 7 chapters, whereof chapters 3 – 6 are based on first-author publications, which have either been published or submitted to peer-reviewed journals. These 4 chapters incorporate remarks and suggestions of all co-authors as well as of reviewers and editors due to peer-reviewing. Every publication starts with a specific and detailed introduction, therefore, chapter 1 and 2 will give more general background information about the entirety of the project. Chapter 7 concludes with an overview of all data, discussion and future perspectives.

The publications were published in different journals with varying styles, therefore, it was chosen to summarize all references, figures and tables using consecutive numbers for clarity and comprehensibility. Differences and Inconsistency in abbreviations, nomenclature and spelling (British and American English) might be noticeable due to journal standards. The source of each publication is clearly stated in the beginning of every publication-based chapter.

The following nomenclature was applied for the use of mutants of *C. elegans* (*Caenorhabditis elegans*): Deletion mutants (loss-of-function) are accompanied by a delta (Δ), while knock-out mutants bear the designation 'KO' behind the name of the gene. Mammalian *GENES* are written in italic and upper-case letters, while *genes* of *C. elegans* is written in italic and lower-case letters. Mammalian PROTEIN names are written in upper-case letters, those of *C. elegans* are not.

Table of Content

Figures

Tables

Abbreviations

6-OHDA	6-hydroxydopamine
8oxodG	8-oxoguanine
ACh	acetylcholine
AChE	acetylcholinesterase
ACN	acetonitrile
AD	Alzheimer's Disease
ADE	anterior deirid dopaminergic neurons
ADP	adenosine diphosphate
AMP	adenosine monophosphate
APP	amyloid precursor protein
ARE	antioxidative response element
ATOX1	antioxidant protein 1
ATP	adenosine triphosphate
Aβ	amyloid β
BHA	2- or 3-*tert*-butyl-4-hydroxyanisol
BSR	basal slowing response
C. elegans	*Caenorhabditis elegans*
CAD	collision gas
CE	collision energy
CEP	cephalic dopaminergic neurons
CF4	Copper Fluor-4
ChAT	choline acetyl transferase
ChT	choline transporter
CL	cardiolipins
Cu	copper
COX-17	cytochrome c oxidase copper chaperone
CTR-1	high affinity copper uptake protein
CXP	collision cell exit potential

DA	dopamine
DAD	diode array detector
dat-1	dopamine transporter 1
DMT-1	divalent metal transporter
DNA	deoxyribonucleic acid
DOPAC	3,4-dihydroxyphenylacetic acid
DOPAL	3,4-dihydroxyphenylacetaldehyde
DP	declustering potential
E. coli	Escherichia coli
EFSA	European food safety authority
ERK	extracellular signal-regulated kinases
ESI	electrospray ionization
FA	formic acid
Fe	iron
FLD	fluorescence detector
FOXO	Forkhead box O
GABA	γ-amino butyric acid
GCLC	glutamate-cysteine ligase catalytic subunit
GFP	green fluorescent protein
Glu	glutamate
GPx	glutathione peroxidase
GR	glutathione reductase
GSH	glutathione
GSSG	glutathione disulfide
ICP-OES	inductively coupled plasma-optical emission spectrometry
ITO	indium tin oxide
JNK	c-Jun N-terminal kinases
LC-MS/MS	liquid chromatography-tandem mass spectrometry
L-DOPA	L-dihydroxyphenylalanine
LOD	limit of detection

LOQ	limit of quantification
LRRK2	leucine-rich repeat kinase 2
m/z	mass to charge ratio
MAPK	mitogen activated kinases
MDA	malondialdehyde
MeOH	methanol
Mn	manganese
MtBE	methyl-*tert*-butyl ether
mtDNA	mitochondrial DNA
mtl	metallothionein
NADH/NAD$^+$	nicotinamide adenine dinucleotide
NADPH/NADP$^+$	nicotinamide adenine dinucleotide phosphate
NanoSIMS	Nano Secondary Ion Mass Spectrometry
NGM	nematode growth medium
NLS	nuclear localization signal
Nrf2	nuclear factor erythroid 2-related factor
PARG	poly-(ADP-ribose) glycohydrolase
PARP	poly-(ADP-ribose) polymerase
PARylation	poly-(ADP-ribosyl)ation
PC	phosphatidylcholine
PD	Parkinson's Disease
PE	phosphaditylethanolamine
PFP	pentafluorophenyl
PQ	paraquat
p-tau	protein tau
RONS	reactive oxygen and nitrogen species
RT-qPCR	reverse transcription-quantitative polymerase chain reaction
S/N	signal to noise ratio
SD	standard deviation
Se	selenium

SEM	standard error of the mean
sMRM	scheduled multiple reaction monitoring
SOD	super oxide dismutase
SRT	serotonin
STEAP	six transmembrane epithelial antigen of the prostate
TBA	2-Thiobarbituric acid
t-BOOH	*tert*-butylhydrogenperoxide
TCA	trichloric acid
TMP	1,1,3,3-Tetramethodypropane
ToF-SIMS	Time-of-Flight Secondary Ion Mass Spectrometry
WD	Wilson's Disease
Y	yttrium
Zn	zinc

Summary

Copper (Cu) is vital for biological processes as an enzyme cofactor, primarily obtained from drinking water, grains and vegetables in the general population. Industrial and agricultural activities introduce excess Cu into the environment via emissions, runoff and waste disposal, posing risks to ecosystems and human health. Excess Cu is supposed to induce oxidative stress on a cellular level, which is defined as an imbalance between the production of reactive oxygen and nitrogen species (RONS) and antioxidants. The overproduction of RONS leads to damage of cellular structures and macromolecules like proteins, lipids and DNA. Its ability to catalyze Fenton-like reactions associates Cu with oxidative stress and mitochondrial impairment, as well as neurodegeneration. The molecular mechanisms underlying Cu toxicity remain poorly understood. In order to investigate Cu-mediated toxicity, it is essential to assess the Cu status of individuals first. Disrupted Cu levels have been observed in patients diagnosed with neurodegenerative diseases. Additionally, protein-bound Cu shifts to labile Cu pools, potentially causing greater damage. Therefore, this thesis focused on identifying reliable Cu markers and elucidating the molecular mechanisms underlying Cu toxicity. For this purpose, the *in vivo* model organism *Caenorhabditis elegans* (*C. elegans*) was used. Loss-of-function mutants deficient in Cu chaperone atox-1 and Cu storage protein ceruloplasmin were used to model Cu dyshomeostasis. Furthermore, the consequences of excess Cu on individuals genetically susceptible to neurodegenerative disorders such as Alzheimer's disease (AD) and Parkinson's disease (PD) were examined.

Behavioral assays and neuron morphology studies by fluorescence microscopy are established methods to assess neurotoxicity in *C. elegans*. However, these methods lack quantitative evaluation of neurotransmitter levels. To better understand neurodegenerative processes, the initial step of this thesis was to develop a highly sensitive and specific technique to quantify neurotransmitters. A liquid chromatography-tandem mass spectrometry (LC-MS/MS)-based

method was developed and addressed high sensitivity and specificity for dopamine, serotonin, γ-amino butyric acid and acetylcholine in *C. elegans*, but was further adopted to mouse brain tissue. Neurotransmitter quantification is crucial for understanding neurotoxic mechanisms and identifying therapies, although it requires a combination of approaches for comprehensive evaluation. *C. elegans*, combined with sensitive analytical techniques, offers a reliable platform for neurotoxicity studies, enabling molecular level neurotransmitter analysis alongside behavioral and morphological assessments.

Excess Cu and genetic deficiencies in atox-1 and ceruloplasmin were investigated to understand Cu homeostasis in *C. elegans*. Wildtype and mutant worms were exposed to $CuSO_4$-enriched *Escherichia coli* for 24 hours. While wildtype worms tolerated doses up to 2 mM Cu, atox-1 and ceruloplasmin mutants showed reduced survival rates, indicating Cu hypersensitivity. Total Cu analysis via inductively coupled plasma-optical emission spectrometry (ICP-OES) showed no basal differences but decreased Cu uptake in mutants after Cu treatment. Time-of-Flight Secondary Ion Mass Spectrometry (ToF-SIMS) analysis demonstrated uniform Cu distribution, with depth profiling confirming reduced total Cu content in both deletion mutants. Fluorescence probe Copper Fluor-4 (CF4) indicated elevated labile Cu levels in mutants, exacerbated by Cu treatment. Furthermore, gene expression changes in Cu homeostasis regulators were observed in both mutants. These findings emphasize the importance of maintaining regulated Cu homeostasis and monitoring labile Cu levels for assessing Cu imbalance.

After characterizing Cu homeostasis in *C. elegans*, toxic mechanisms due to disrupted Cu balance and excess Cu were examined, focusing on oxidative stress and its impact on genomic and neuronal stability. Data revealed reduced glutathione (GSH) levels in all worm strains after Cu exposure, with atox-1 and ceruloplasmin mutants exhibiting increased mRNA levels of *gcs-1/GCLC*, suggesting enhanced GSH synthesis. Ceruloplasmin mutants showed lower

ATP levels, further reduced by Cu, indicating higher energy demand and mitochondrial impairment due to reduced cardiolipin (CL) content. Elevated 8-oxoguanine levels, a marker for oxidative DNA damage, were observed in ceruloplasmin mutants exposed to Cu. Moreover, decreased γ-amino butyric acid content in these mutants underscores ceruloplasmin's role in Cu homeostasis and mitochondrial integrity for genomic and neuronal stability. Atox-1 mutants displayed elevated markers of oxidative stress, such as malondialdehyde (MDA) and reduced neurotransmitter levels after Cu exposure, highlighting its importance in Cu homeostasis and neuronal survival in Cu-mediated neurotoxicity.

Understanding the mechanisms underlying neurodegenerative diseases like AD and PD remains incomplete, influenced by both genetic and environmental factors. An amyloid β-expressing transgenic strain (CL2006) was used to model AD, while deletions of pdr-1/PARKIN and the g2019s mutation of LRRK2 were employed as models for PD. Cu exposure did not affect neuronal stability in wildtype worms, but both PD models showed reduced dopamine levels, exacerbated by Cu. This was confirmed by alterations in the basal slowing response assay, a behavioral assay dependent on dopamine. Crossbreeding PD mutants with BY200 (dat-1::GFP) strain revealed severe impairments in dopaminergic neuron morphology induced by Cu, confirming reduced DA levels. These findings highlight the hypersensitivity of *C. elegans* PD models to Cu.

Taken together, this thesis emphasizes the complexity of Cu toxicity, highlighting the risks associated with excess Cu and a disrupted Cu homeostasis. The condition of elevated Cu levels, Cu dyshomeostasis or a genetic predisposition to PD lead to oxidative stress as well as genomic and neuronal instability. This underlines the importance of a proper regulated and well-functioning Cu homeostasis to maintain RONS balance, mitochondrial and neuronal integrity.

Chapter 1 – Motivation and Scope of the Thesis

Chapter 1 – Motivation and Scope of the Thesis

Motivation of the Thesis

Copper (Cu) is an essential trace element which primarily enters the body through drinking water and dietary sources, such as fish, nuts and legumes [1,2]. The recommended daily intake for adults ranges from 1.3 to 1.6 mg, which is typically met by a normal diet and renders a Cu deficiency as uncommon [3]. However, excessive Cu is introduced into the environment through various human activities including industrial processes, agriculture, urban runoff and improper waste disposal, which possesses a significant risk to ecosystems and human health if not appropriately managed [4,5]. Cu plays a vital role in the redox biology of organisms, serving as an essential electron donor crucial for the catalytic function of an array of enzymes in biological processes [6]. The involvement of Cu spans from energy metabolism and antioxidant defense mechanisms to cellular respiration [7]. Conversely, excess Cu leads to the formation of reactive oxygen and nitrogen species (RONS) [8–10], which have the capacity to damage biological macromolecules, such as lipids, proteins and DNA [11,12]. Fenton-like reactions generate highly reactive hydroxyl radicals, which can induce oxidative stress, an imbalance of RONS and antioxidants, which in turn can promote neurodegenerative processes [13,14]. Little is known on how Cu toxicity is mediated on a molecular level. To evaluate Cu toxicity, it is of paramount importance to dispose selective and sensitive techniques, which provide insights into the Cu status of an individual [15]. Studies revealed disturbed Cu levels in the brain of patients diagnosed with Alzheimer's disease (AD) and Parkinson's disease (PD) [16,17]. Moreover, studies exposed a shift of protein bound Cu into labile Cu pools, which seems to be the readily available and therefore more damaging Cu species [18,19].

Therefore, the motivation of this thesis was to investigate molecular mechanisms, which underlie Cu toxicity. Transgenic strains of *Caenorhabditis*

elegans (*C. elegans*), which were deficient in Cu chaperone atox-1 or Cu storage protein ceruloplasmin were used to model Cu dyshomeostasis. Total Cu, labile Cu and gene expression of Cu-homeostasis related proteins were analyzed to characterize Cu dyshomeostasis in *C. elegans*. To reveal consequences of excess Cu and Cu dyshomeostasis, a variety of markers related to oxidative stress as well as genomic and neuronal instability were assessed using highly selective and sensitive techniques. Additionally, *C. elegans* models of AD and PD were treated with excess Cu, in order to gain insights into the interplay of Cu and the genetic predisposition to neurodegenerative diseases.

Scope of the Thesis

This work focused on the following key points:

- Development of an LC-MS/MS-based method for neurotransmitter quantification as highly selective marker for neurotoxicity in *C. elegans*
- Assessment of total and labile Cu levels and characterization of Cu homeostasis with special focus on Cu chaperone atox-1 and Cu storage protein ceruloplasmin in *C. elegans*
- Analysis of the consequences of a disturbed Cu homeostasis regarding oxidative stress as well as genomic and neuronal stability in *C. elegans*
- Investigation of the impact of a genetic predisposition to neurodegenerative diseases in Cu-induced neurotoxicity in *C. elegans*

Chapter 2 – General background Information

Chapter 2 – General background Information

2.1. The model organism *Caenorhabditis elegans*

Toxicology – examining how chemicals interact with biological systems – is relevant for human health and disease [20]. This requires test systems, which can range from microorganisms to *in vitro* cell culture and *in vivo* model organisms to animal experiments. Each of these models possesses unique strengths and weaknesses, rendering them (un)suitable for different applications [21]. In this thesis, the *in vivo* model organism *Caenorhabditis elegans* (*C. elegans*) was employed. As the following parts of this chapter will mention orthologs and suchlike information of *C. elegans*, the worm will be introduced initially for a better comprehension. The nematode constitutes an alternative to animal experiments, aligning with the principles of the 3Rs: Reduce, Replace, and Refine [22]. Sydney Brenner pioneered the use of *C. elegans* in the 1960s as a model for genetic and biomolecular research. He envisioned an in vivo model system which is both simple but yet sufficient on a cellular and molecular level compared to mammals [23]. Over time, research on *C. elegans* has expanded to explore a wealth of diverse areas in modern biology, including studies of basic cellular functions as well as more complex inquiries such as processes implicated in human diseases [23]. The nematode features several advantages, including its transparency, a fully sequenced genome, cell consistency as well as a short lifespan and short generation time. Furthermore, cultivation on agar plates coated with *Escherichia coli* (*E. coli*), which is the food source of worms, is easy to handle [24]. Measuring about 1 millimeter in length, it comprises three main regions: head, midbody, and tail. The head contains sensory organs and a nerve ganglion, while the midbody houses the digestive tract, gonads, and longitudinal muscle cells. The tail, with the anus and locomotion-specialized cells, completes the structure. *C. elegans* is surrounded by a cuticle, which serves as a protective barrier, maintains the

worm's shape, and facilitates sensory function. It controls permeability and primarily consists collagen-like proteins [25]. Internally, it possesses a complete digestive and reproductive system, alongside a relatively simple but organized nervous system of 302 neurons. *C. elegans* exhibit cellular consistency, maintaining a constant number of 959 somatic cells [25,26]. The worm exists in two sexes: hermaphrodites, which possesses both male and female reproductive organs and males, which only have male reproductive organs. Males occur naturally, comprising only < 0.2 % of the population. As hermaphrodites cannot cross with each other, males are introduced into populations of hermaphrodites for research use to facilitate crossbreeding between different strains. This allows to create progeny with combinations of desired genetic traits [27]. Hermaphrodites are capable of self-fertilization and produce up to 300 genetically identical offspring [27]. The transformation from an egg to an egg-laying adult worm is intricately linked to temperature and lasts around 3 days at 20 °C. When hatched, larvae find themselves in the L1 stage, where they remain unless food in the form of *E. coli* is provided (Figure 1). Under optimal feeding conditions, these L1 larvae seamlessly transition through the developmental stages of L2 to L4, ultimately reaching adulthood as egg-laying worms [28]. Due to adverse environmental conditions and the scarcity of food, an alternative larval stage in *C. elegans* is triggered, which is named dauer stage. During dauer, worms undergo a developmental arrest enabling them to endure harsh conditions. This stage can significantly extend lifespan. Once environmental conditions improve, *C. elegans* exit dauer and resume normal development to L4 stage worms [29].
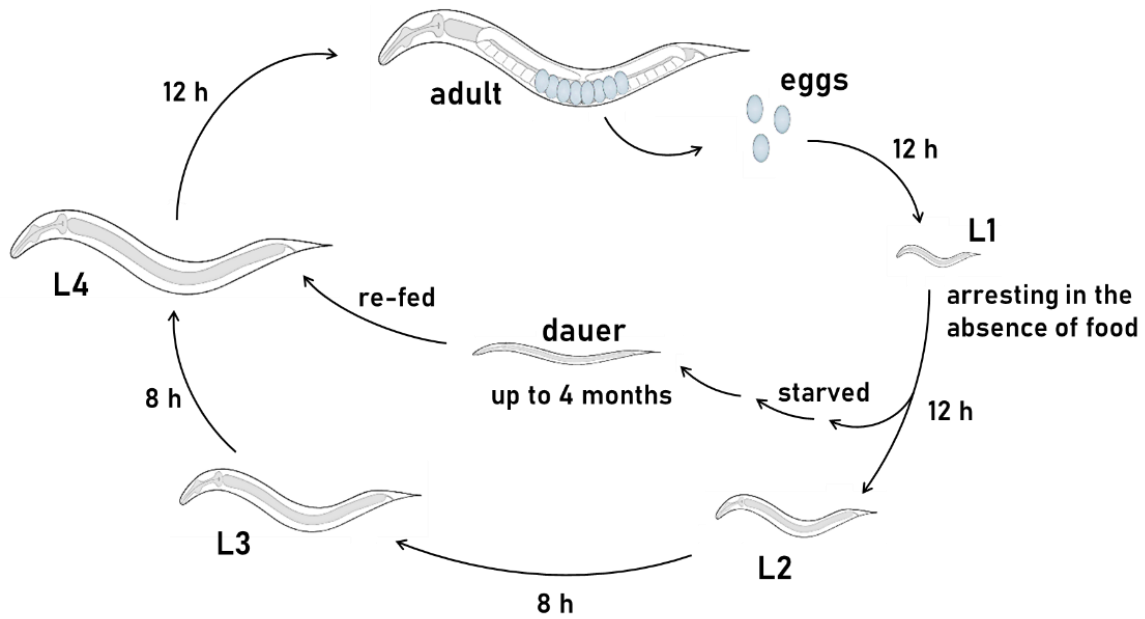
Figure 1:   *C. elegans* life cycle at 20 °C. When well-fed, the life cycle of worms spans approximately 3 days. However, in times of starvation, worms transition into the alternative dauer larval stage, which entails a considerably extended life cycle (adapted and modified from Kimble et al. [30]).

The fully sequenced genome of *C. elegans* provides a comprehensive understanding of its genetic makeup. This knowledge enables the creation of deletion mutants, in which a specific segment of a gene has been intentionally removed or deleted. This manipulation results in the loss of function of the affected gene, allowing to study the resulting phenotype and to deduce the function of the gene and its encoded protein [31]. RNA interference (RNAi) feeding in *C. elegans* utilizes ingested double-stranded RNA to induce gene silencing, offering another powerful approach for studying gene function in the nematode [32]. Furthermore, worms displaying fluorescence-tagged proteins are commonly used to study protein expression, localization and dynamics within the nematode. This involves genetically fusing a fluorescent protein, such as green fluorescent protein (GFP), to the protein of interest. When expressed in the transparent worm, the fluorescently tagged protein can be visualized by a fluorescence microscope, allowing to track its localization and expression in a living organism [33]. The genome of *C. elegans* reveals that worms share a significant portion of its genes with humans, meaning they are evolutionary

related and likely perform similar functions across species. In detail, 60 – 80 % of genes share orthologs with humans [34], while about 40 % of human disease-related genes are encoded in *C. elegans* [35].

Despite its simplicity compared to the mammalian nervous systems, *C. elegans* possesses a well-defined nervous system consisting of precisely mapped neurons, which allows for detailed studies of neurotoxic effects on neuronal structure and function. The neuronal system spans the entire body of the nematode, with the majority of neurons in the head region [24,36]. These neurons possess dendrites, which form a nerve ring – a dense bundle of axons wrapped around the pharynx. [37]. The dendrites transmit information via neurotransmitters. *C. elegans* shares neurotransmitters like dopamine, serotonin, acetylcholine, γ-amino butyric acid, and glutamate with humans, facilitating research on signal transduction pathways [38]. Many fundamental aspects of neurobiology, including synaptic transmission, neuronal development and behavior are conserved in the nematode. *C. elegans* exhibits a wide range of behavior that can be quantified and manipulated, including locomotion, basal slowing, and chemotaxis [39]. Changes in behavior induced by neurotoxic compounds provide valuable insights into their effects on neuronal function and integrity. As *C. elegans* is transparent, it allows for the visualization of neuronal morphology and activity in living worms. An example is the fluorescence microscopy of dopaminergic neurons using mutant strain BY200 (dat-1::GFP) [40]. Strain BY200 expresses GFP in the dopamine transporter 1 (dat-1), which exclusively occurs within dopaminergic neurons, shown in Figure 2.
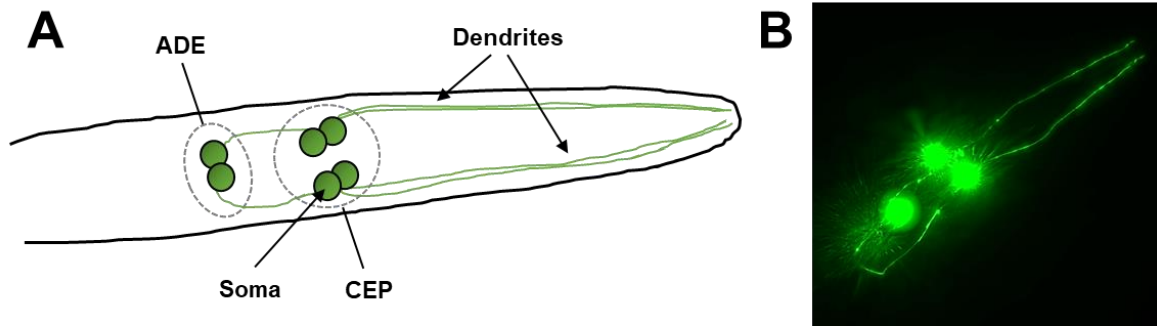
Figure 2: (A) The dopaminergic neurons (ADE (anterior deirid) and CEP (cephalic)) as well as dendrites in the worms head region are depicted schematically. (B) These neurons can be observed by fluorescence microscopy using mutant strain BY200 (dat-1::GFP). Parameters for capturing the fluorescence image are stated in section 6.2.8.

Like any other model organism, using *C. elegans* has its limitations. Although its small size is beneficial, worms present a relatively simple body plan with only a few hundred cells, limiting its suitability for studying complex tissue interactions and organ systems found in higher organisms. Additionally, most studies are carried out in whole worm homogenates. Therefore, information can only be obtained for the total worm body instead of a specific location or tissue. While many genes and biological pathways are conserved between *C. elegans* and mammals, there are also notable differences. This can limit the direct translation of findings from *C. elegans* to higher organisms [41,42]. No model can be used to answer every research question. Thus, it is of paramount importance to decide whether a model organism is suitable depending on the issue being addressed. For instance, *C. elegans* offers utility in the realm of neurodegeneration research, thanks to its extensively studied and analogous nervous system. However, its utility in immunology research is limited due to the lack of an immune system [43]. Despite the limitations, the conservation of genes and biological processes between *C. elegans* and humans, along with the experimental advantages offered by this model organism, make it a valuable tool for studying human biology and disease mechanisms, as well as investigating the mechanisms underlying neurotoxicity and potential therapeutic

interventions for neurodegenerative diseases, given its simple yet conserved neurobiology, genetic tractability, transparent body and short lifespan.

2.2. Copper

Copper (Cu), is an essential micronutrient and trace element for all living species like mammals, plants or microorganisms, which occurs predominantly in oxidation states 0, +1 and +2 in the environment. It serves as both a cofactor and electron transporter crucial for the proper function of diverse enzymes and biological processes [6]. As a part of cytochrome c oxidase, Cu is involved in energy production and cellular respiration, as it is crucial for the final step of the electron transport chain in mitochondria. This process generates adenosine triphosphate (ATP), the primary energy molecule utilized by cells for various metabolic activities [7]. Cu-containing superoxide dismutases detoxify superoxide radicals, providing antioxidant defense [44]. Cu is required for the activity of lysyl oxidase, an enzyme involved in the cross-linking of collagen and elastin fibers. This cross-linking process is essential for the structural integrity and strength of connective tissues, including skin, bones, cartilage, and blood vessels [45]. Furthermore, Cu-dependent enzymes participate in the biosynthesis of neurotransmitters. It acts as cofactor for enzymes such as the tyrosinase, which catalyzes the hydroxylation of L-tyrosine to L-DOPA, which is a precursor of dopamine [46]. These functions underscore the essential role of Cu in various physiological processes, including energy metabolism, tissue formation, neurotransmitter regulation, and antioxidant defense. Therefore, maintaining adequate Cu levels is crucial for overall health and well-being.

Typically, an adult human body stores an average of 80 to 100 mg of Cu. As advised in 2015 by the European Food Safety Authority (EFSA), an appropriate daily intake for humans of Cu ranges from 1.3 to 1.6 mg for adults, varying with gender [3]. Cu intake has seen a noticeable rise across Germany in recent years, with vegetarians exhibiting notably higher levels, averaging between 2.1 and 3.9 mg per day [47]. The primary sources of Cu exposure for the general

population are food and drinking water. Foods such as fish, seafood, nuts, and legumes are notably rich in Cu. Approximately 6-13 % of Cu intake emanates from drinking water, a percentage that can be further elevated by Cu-containing water pipes, depending on the water's pH level [48]. Excess Cu can infiltrate the environment through various channels. Firstly, industrial operations such as mining, smelting, and manufacturing emit Cu into the air, water and soil via both emissions and waste discharge. Secondly, agricultural activities contribute to Cu accumulation in soil and water systems through the application of Cu-based pesticides and fertilizers [49]. Urban areas further exacerbate the issue as Cu from roofing materials, plumbing systems, and vehicle emissions is washed into water bodies by urban runoff, especially during rainfall events [50]. Improper waste disposal worsens the problem, as electronic waste, batteries and other Cu-containing products leach Cu into soil and groundwater in landfills. Overall, human activities are significant contributors to the introduction of excess Cu into the environment, posing risks to ecosystems and human health when not managed properly [49,50].

2.3. Cu homeostasis: import, distribution, storage and excretion

In humans, Cu absorption primarily occurs in the small intestine, typically ranging from 30 % to 50 %, with absorption rates impacted by various food components. Cu bound to amino acids or complexed with organic acids tends to be more readily absorbed, while other metal ions like zinc, iron, or calcium can hinder Cu absorption. The liver contains the highest Cu concentration, where it is stored in hepatocytes, released into the plasma, or excreted through bile. Bile excretion stands as one of the crucial homeostatic mechanisms for Cu regulation [51]. Cu exists in two physiological relevant oxidation states: +1 and +2, which both can be transported into a cell. The majority of Cu enters the cell as Cu^+ via a Cu^+-specific high affinity copper uptake protein (CTR-1). In mammals, divalent Cu can be reduced by the six transmembrane epithelial antigen of the prostate (STEAP) metalloreductase [52]. While this reductase is

absent in *C. elegans*, Cu in the worm undergoes reduction to Cu^+ by a yet unidentified reductase and is then transported into the cell through CTR-1. Cu^{2+} ions, which remain in the oxidized state (+II), can enter the cell through the divalent metal transporter 1 (DMT-1). This transporter, while not exclusively dedicated to Cu, serves as a conduit for various divalent metals such as iron, zinc or manganese [53]. Mouse experiments revealed that the absence of DMT-1 did not alter Cu uptake. In contrast, the absence of CTR-1 led to severe Cu deficiency and early lethality. This underlines that Cu is mainly imported via the high affinity CTR-1 transporter [54]. Figure 3 displays how Cu is distributed, stored and excreted within the cell.
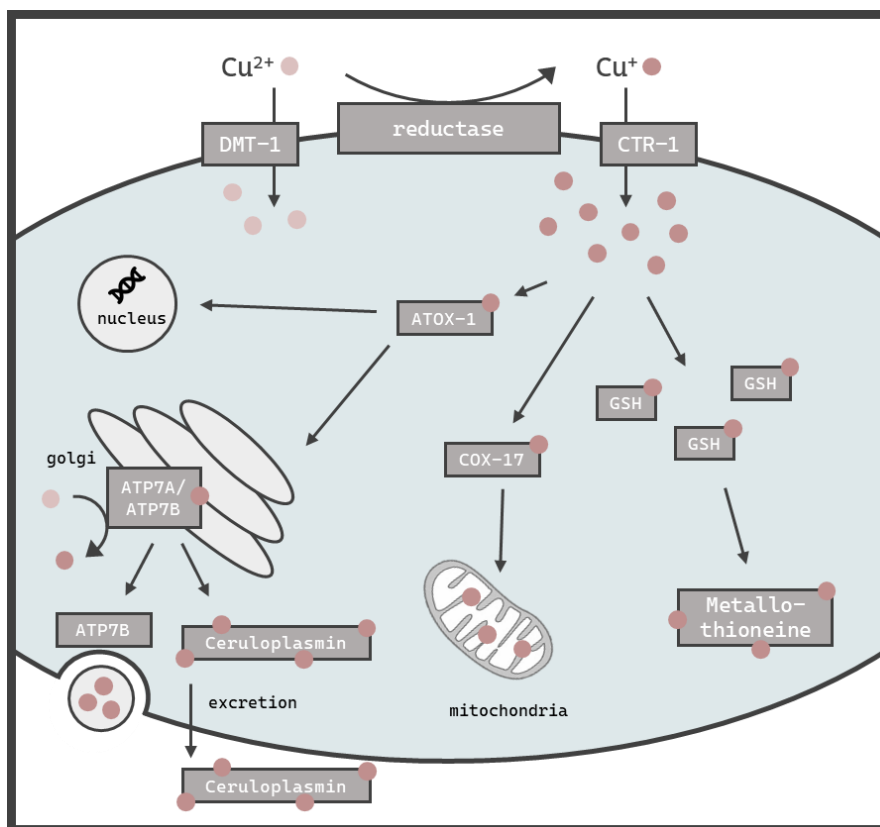
Figure 3: Schematic representation illustrating the presumed intracellular pathways of Cu import, distribution, storage and excretion. Cu uptake primarily occurs as Cu^+ via CTR-1 or alternatively as Cu^{2+} via DMT-1. Cu^{2+} can be reduced in the golgi. ATOX-1 facilitates Cu distribution to various cellular compartments such as the golgi, nucleus or to COX-17, which delivers Cu into the mitochondria. Excess Cu is believed to be chelated by GSH and metallothionein, with the majority stored in ceruloplasmin. ATP7B facilitates the efflux of surplus Cu via vesicular sequestration (adapted from previously published work [55]).

Antioxidant protein 1 (ATOX-1), acting as a Cu metallochaperone, acquires Cu from CTR-1 and facilitates its intracellular transport to specific organelles such as the nucleus or golgi apparatus [56]. Given Cu's role as a cofactor for numerous mitochondrial enzymes, the cytochrome c oxidase copper chaperone (COX-17) governs the import of Cu into the mitochondria [57]. The primary carrier of Cu in the blood is the multifunctional protein ceruloplasmin, which stores approximately 90 % of the total Cu [58]. Another type of metal storage protein is metallothionein (MT), which serves as binding agent for metal ions such as cadmium, zinc and Cu, providing detoxification and shielding against oxidative stress [59]. ATP7A, a P-type ATPase provides certain enzymes with Cu, such as the lysyl oxidase. Furthermore, it takes part in human Cu resorption as it transports Cu from the small intestine into the blood [60]. Genetic disorder of *ATP7A* causes Cu deficiency which results in Menke's disease [61]. Another P-type ATPase is ATP7B, which like ATP7A is located in the golgi network, especially in the liver and brain. ATP7B serves two primary functions: facilitating Cu loading onto Cu storage protein ceruloplasmin and orchestrating the vesicular sequestration and excretion of excess Cu into the bile [62]. Genetic disorder in *ATP7B* results in Wilson's disease. This condition leads to the accumulation of Cu in tissues, mainly the liver and the brain, which can manifest in neurological symptoms and liver diseases [63]. Mammals encode genes for both P-type ATPases *ATP7A* and *ATP7B*, while *C. elegans* carries only a single gene of *atp7a/b*, nevertheless expressing both atp7a and atp7b with high sequence similarity to human orthologs [64]. The following table lists the orthologs of *C. elegans* taking part in Cu homeostasis.

Table 1: Human proteins and genes taking part in Cu homeostasis as well as their orthologs in *C. elegans.*

Humans		*C. elegans*		Reference
protein	gene	protein	gene	
CTR-1	*SLC31A1*	ctr-1	*chca-1*	[65]
		smf-1	*smf-1*	
DMT-1	*SLC11A2*	smf-2	*smf-2*	[66,67]
		smf-3	*smf-3*	
ATOX-1	*ATOX-1*	atox-1	*cuc-1*	[68,69]
CCS	*CCS*	no ortholog		[70,71]
COX-17	*COX-17*	cox-17	*cox-17*	[66]
MT1A	*MT1A*	mtl-1	*mtl-1*	[59,72]
MT2A	*MT2A*	mtl-2	*mtl-2*	
ATP7A	*ATP7A*	atp7a	*cua-1*	[64]
ATP7B	*ATP7B*	atp7b		
Ceruloplasmin	*CP*	ceruloplasmin	F21D5.3	[66,73]

2.3.1. Cu chaperone ATOX-1

ATOX-1 mediates the transfer of Cu to the Cu-transporting ATPases ATP7A and ATP7B, found in the trans-Golgi network and endocytic vesicles. ATOX-1 engages in a direct interaction with the N-terminal Cu binding domain of ATP7A and ATP7B, facilitating the transfer of Cu ions. This intricate molecular interplay serves as a crucial mechanism for coordinating Cu homeostasis within the cell and regulating the activity of Cu-dependent enzymes [74]. In line with its role, ATOX-1 knockout mouse embryonic fibroblasts exhibit aberrantly elevated levels of intracellular Cu, underscoring the importance of ATOX-1 in Cu homeostasis [75]. The primary function of ATOX-1 is serving as a Cu chaperone, effectively binding and controlling Cu reactivity while transporting it to specific destinations within a cell. Secondly, ATOX-1 takes part in maintaining cellular redox balance and responding to oxidative stress. Elevated activity of

ATOX-1 possesses antioxidative properties, as increased endogenous ATOX-1 levels protects against oxidative stress and promote neuronal survival [76,77]. The role of atox-1 in *C. elegans* will be discussed in Chapter 4.

2.3.2. Cu storage protein ceruloplasmin

Ceruloplasmin is a multifunctional Cu-binding protein which is, in humans, primarily synthesized in liver and found in the blood plasma. Furthermore, ceruloplasmin, which contains six cupredoxin domains, is the major Cu storage protein [78]. It plays a crucial role in Cu metabolism and homeostasis as it is the major Cu transport protein, carrying approximately 70 % of plasma Cu. Ceruloplasmin indirectly contributes to Cu excretion by facilitating its transport to the liver for further processing by ATP7B and elimination. In the liver, Cu is incorporated into the bile and excreted into the intestinal lumen via the bile ducts. From there, Cu is eliminated from the body through fecal excretion [62]. In addition, ceruloplasmin functions as a ferroxidase, catalyzing the conversion of ferrous iron (Fe^{2+}) to ferric iron (Fe^{3+}). This activity facilitates iron binding to transferrin for distribution and prevents iron toxicity by reducing free ferrous iron levels. Dysregulation can lead to iron metabolism disorders, including iron overload and may contribute to neurodegenerative diseases [79]. Inherited deficiency of the protein leads to aceruloplasminemia, an autosomal recessive disorder marked by gradual neurodegeneration of the retina and basal ganglia due to specific mutations in the ceruloplasmin gene. The disease is characterized not only by elevated Cu levels but also by elevated iron levels, as excess iron gets accumulated in various organs [80]. The role of ceruloplasmin in *C. elegans* will be discussed in Chapter 4.

2.4. Biomarkers for Cu status

Symptoms of Cu deficiency include anemia, fatigue, impaired immune function, as well as bone abnormalities. Conversely, Cu overload is accompanied by symptoms like vomiting, gastrointestinal distress and liver damage [81]. Given the widespread exposure to Cu and the absence of reported deficiencies among

the general population, the German Institute for Risk Assessment advised against Cu supplementation in 2021 [82]. As alterations in Cu levels have severe consequences for human health, the diagnosis of Cu dyshomeostasis is crucial to prevent the onset and progression of Cu-related diseases [83]. Other trace elements such as Cu, zinc, iron and selenium also play pivotal roles in maintaining physiological balance. Both deficiency and excess of these elements are recognized as significant risk factors for various diseases. Hence, accurate assessment of the trace element status is paramount. Rather than solely focusing on total amounts, incorporating functional trace element markers is essential for a more nuanced understanding of individual trace element levels and overall health status [84]. To assess selenium status, measurements of selenoprotein P and glutathione peroxidase are conducted in serum and plasma, alongside the evaluation of total selenium levels [85]. Serum ferritin and transferrin saturation serve as vital functional markers in evaluating the iron status [86]. Free zinc is regarded as the exchangeable and biologically active form of zinc in serum, making it a promising biomarker for changes in zinc homeostasis and associated diseases [87].

Tools for an early detection of Cu imbalance are essential to effectively treat and prevent Cu-related disorders. Consequently, it exists a pressing need for robust and readily applicable biomarkers to gauge individual Cu status in humans. Regular monitoring of Cu status and prompt detection of deviations are pivotal steps towards an early diagnosis and the implementation of appropriate therapeutic interventions [88,89].

2.4.1. Current markers

Standard diagnostic parameters commonly employed to assess the Cu status include the measurement of total Cu levels and the concentration of ceruloplasmin in serum [83]. Nevertheless, relying solely on these markers is a subject of contentious debate, given their limited predictive accuracy and clinical significance, which complicates their interpretation as standalone indicators

[90,91]. Numerous factors, such as medication, hormonal fluctuations and inflammatory conditions impact these parameters, which reduces their specificity to assess Cu dysregulation [92]. The ceruloplasmin levels in serum are affected by age and gender, which must be taken into account [93]. Furthermore, these markers are unable to detect marginal changes in the individual Cu status but rather unsatisfactory heavy alterations [83,94]. Other markers which are mainly focused on the diagnosis of WD are the ceruloplasmin activity in serum and the urinary Cu excretion, which can give, under certain circumstances, false negative results (Table 2).

Table 2: Overview of current Cu markers as well as their limitations and quantification methods in mammals

Marker	Limitations	Methods
Total Cu levels in serum	Cu levels may be normalized to due reduced ceruloplasmin levels in WD patients	Atomic absorption spectroscopy [95]
Ceruloplasmin level in serum	Level can be in normal range in certain circumstances (inflammation or hormonal fluctuations)	Immunoturbidimetry [96] or Immunonephelometry [93,97]
Ceruloplasmin activity in serum	False negative results during inflammation or in pregnancy	Colometric method [98] using commercial kits
Urinary Cu excretion	False negative results in children and asymptomatic WD patients	Total Cu quantification in a 24 h urine collection [99]

Others recommend the assessment of Cu-containing enzymes such as erythrocyte superoxide dismutase and cytochrome-*c* oxidase, as the enzyme activity is said to be proportional to changes in the Cu stores [100]. However, alternative studies indicate that these markers lack reliability and sensitivity [91]. For instance, it has been demonstrated that the enzyme activity of erythrocyte superoxide dismutase 1 can be influenced by dietary carbohydrate intake [101]. In order to diagnose the genetic Cu-metabolism disorder Wilson's disease (WD), a liver biopsy, and therefore surgery, is needed [102]. Therefore, it becomes imperative to identify marker that can be rapidly assessed in blood serum or

plasma, thus avoiding the need for invasive medical procedures and facilitating a quicker diagnosis.

2.4.2. Labile Cu

Around 70 – 90 % of Cu residues within ceruloplasmin, with the remaining Cu, often termed as loosely bound Cu, associated with small molecules like albumin (10 – 15 %), α-macroglobulin (5 – 15 %), clotting factors, enzymes like superoxide dismutases or metallothionein [103,104]. Loosely bound Cu encompasses all Cu not bound to ceruloplasmin, while labile Cu refers to a subset of this pool that is defined only to be in equilibrium with low molecular weight (LMW) ligands like amino acids (Figure 4) [105], while free ionic Cu does almost not exist [106].
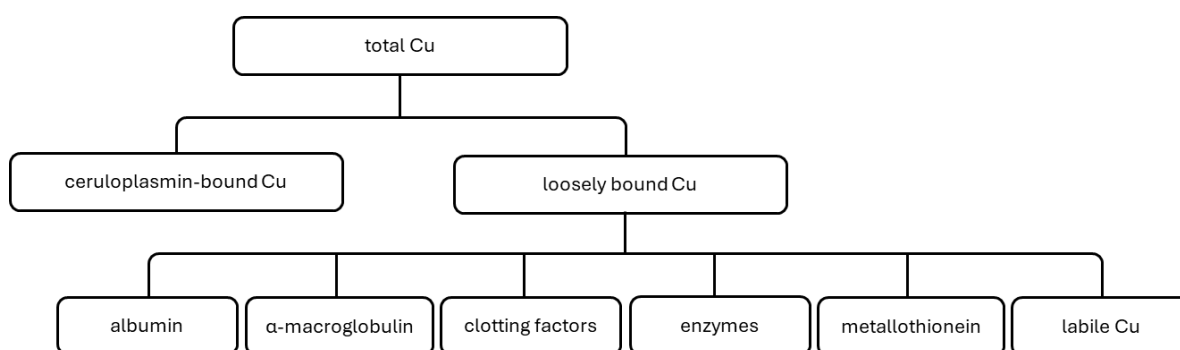
Figure 4:   Overview of how Cu ions can be bound or complexed: Most of the total Cu is stored in ceruloplasmin, while the remaining Cu (non-ceruloplasmin bound) is termed as loosely bound Cu, which is complexed with a variety of proteins. Labile Cu, which is merely in an equilibrium with low molecular weight ligands represents a special sub-group of loosely bound Cu.

Labile Cu levels can be estimated by calculation using total Cu levels and ceruloplasmin content, however, this is imprecise [107]. In recent years, increasing effort has been made to develop methods for the quantification of labile Cu in serum or tissue. These methods range from the use of fluorescent probes [104,108] to analytical approaches [83]. A fluorescent sensor for labile

Cu detection requires Cu-dependent fluorescence changes, high selectivity, sensitivity, suitable Cu affinity and reversible metal binding. Most of total Cu is associated with high affinity binding proteins, therefore, sensors must present high enough affinities to compete for Cu within its biological window (Figure 5) [104,109]. Available fluorescent probes for labile Cu detection present affinities of about $K_D = 10^{-13}$ M [104,108,109].
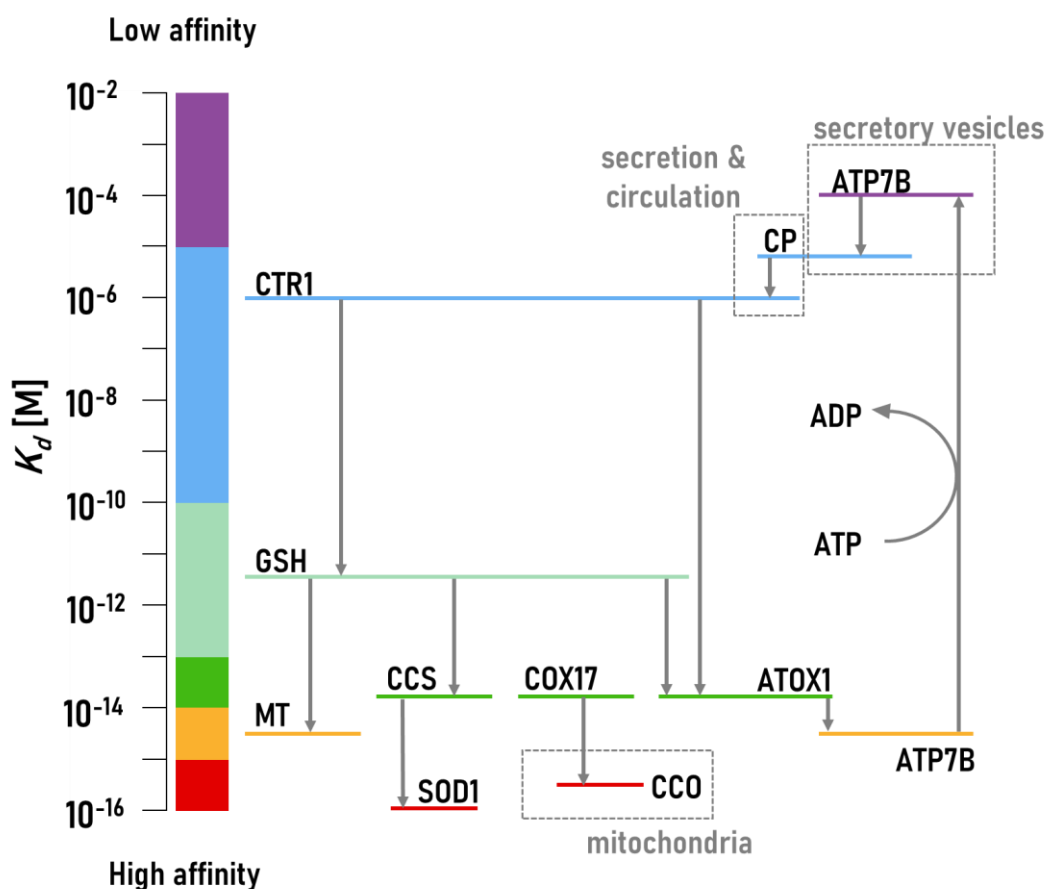
Figure 5: Affinities to Cu of mammal proteins involved in Cu metabolism. Cu gets transported, which is represented by arrows, from a protein with lower to a protein with higher affinity. Cu affinity of ATP7B changes upon an ATP-dependent conformational transition (adapted and modified according Hatori et al. [74]).

The labile Cu pool is considered to be readily bioavailable for cellular uptake and has been discussed as potentially crossing the blood-brain-barrier as an LMW-Cu complex. Due to Cu's redox activity, tight control is essential to prevent

an increase in labile Cu leading to the formation of reactive oxygen species and consequently oxidative stress [104]. Dependence solely on labile Cu levels is presently deemed inadequate due to the complexity of analysis and limited available methodologies. Nonetheless, when integrated with total Cu and ceruloplasmin measurements, the assessment of labile Cu holds promise as a valuable and robust tool for evaluating Cu status, thereby aiding in the risk assessment or diagnosis of Cu dysregulation-related disorders [14].

2.5. Oxidative stress

Reactive oxygen and nitrogen species (RONS) represent metabolic byproducts within biological systems. Primarily mitochondria generate RONS under both physiological and pathological conditions. RONS play pivotal roles in fundamental processes like protein phosphorylation and apoptosis [110,111]. However, an escalation in RONS production poses detrimental risks to cellular structures including proteins, lipids and deoxyribonucleic acid (DNA). Hence, it is crucial to uphold an equilibrium by ensuring that RONS formation remains balanced with antioxidants, thereby safeguarding proper cellular function [112]. If the equilibrium is shifted towards an excessive RONS formation, it is commonly referred to as oxidative stress (Figure 6) [111,113].
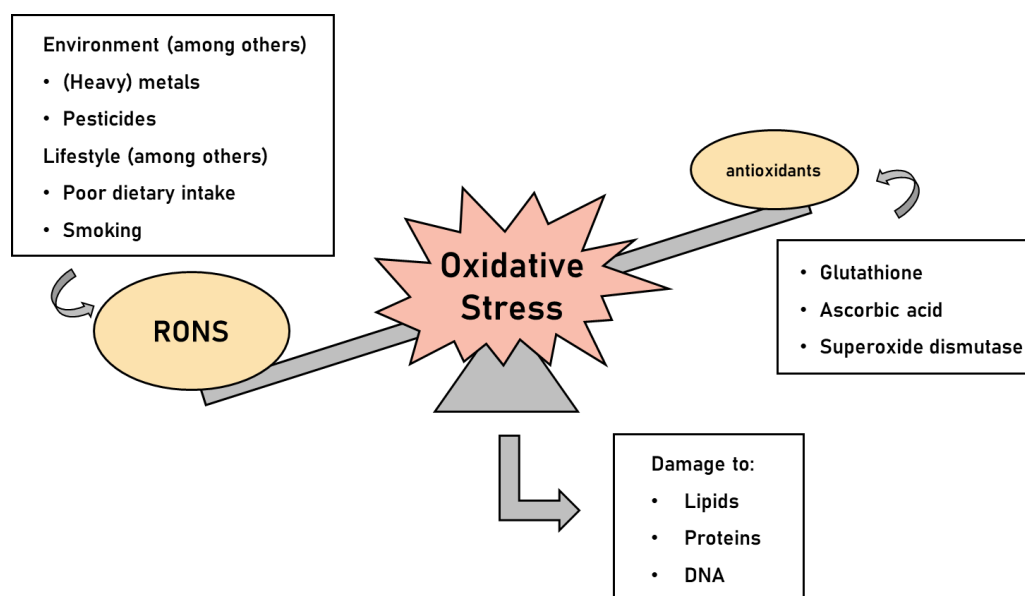
Figure 6: Examples for typical factors which can, among others, cause oxidative stress, which is the consequence of a disturbed balance of excessive RONS formation and/or weakened antioxidative capacity (adapted and modified from Takeshima et al. [113]).

Cells are equipped with a variety of intrinsic RONS scavengers with antioxidative properties. These include, among others, essential vitamins like ascorbic acid or tocopherol and phytochemicals like carotenoids. The most prominent antioxidant is reduced glutathione (GSH), which protects cells against free radicals. GSH acts as electron donor and cofactor for the detoxification of peroxides by the enzyme glutathione peroxidase (GPx) [114]. Furthermore, superoxide dismutases (SODs) are a group of enzymes, which catalyze the formation of superoxide anions into oxygen and hydrogen peroxide. SODs control the levels of RONS and therefore limit their potential toxicity and protect cellular structures and functions [115]. RONS are molecules with an enormous range of reactivity and chemical nature. Common reactive oxygen species are, among others, hydrogen peroxide (H_2O_2), hydroxyl radicals ($^{\bullet}OH$) or superoxide radicals ($O_2^{\bullet-}$). Some of the reduction byproducts of oxygen exist as free radicals, characterized by having unpaired electrons. In contrast, e.g. hydrogen peroxide lacks radical properties and thus remains a chemically stable molecule. Common reactive nitrogen species are nitrogen dioxide radicals ($NO_2^{\bullet}$) or nitrite

(NO_2^-) and nitroxyl anions (NO^-) [116]. Endogenously, RONS are mainly formed as byproduct of mitochondria in processes like cellular respiration [110]. Exogenously, RONS formation can be triggered by environmental pollutants like pesticides [117] or (heavy) metals, such as cadmium, arsenic, iron and Cu, which catalyze Fenton(-like) reactions [118,119]. In addition, drugs, chemical solvents and lifestyle vices (alcohol or smoking) can stimulate the formation of RONS [120,121]. Excessive RONS are capable to interact with various cellular components and to induce alterations in cellular structures and function. The reactive species damage the cell integrity by attacking, among others, the structure of proteins, as well as the cell membrane, which initiates lipid peroxidation of membrane lipids. Furthermore, RONS can induce oxidative DNA damage [116,122]. Therefore, oxidative stress is an often-discussed mechanism to cause the onset of various diseases, especially neurodegenerative disorders [123].

2.5.1. Biomarkers

The association between oxidative stress and numerous neurological diseases underscores its significance as either a primary or secondary contributor to various multifactorial syndromes. This emphasizes the necessity of a quantitative evaluation of oxidative stress across diverse research fields. One marker for oxidative stress are obviously RONS itself. Several techniques have been devised for the quantification of RONS, including chemiluminescent or fluorescent probes [124]. These have also been applied in model organisms like *C. elegans* [117], but do lack specificity and do not allow subcellular localization [124]. Excessive levels of RONS initiate signaling cascades that lead to the activation of several transcription factors responsible for orchestrating the antioxidant response, for example GSH synthesis. RONS activate mitogen-activated protein kinases (MAPKs), which phosphorylate, among others, transcription factors that regulate the antioxidative response and cell functions like gene expression, cell survival and apoptosis [125,126]. There exist three distinct subgroups of MAPKs: the extracellular signal-regulated kinases

(ERKs), the c-Jun N-terminal kinases (JNKs) and the p38 MAPKs [126]. Under stressed conditions, Nuclear Factor Erythroid 2-related factor (Nrf2) dissociates from Keap1 following phosphorylation by ERK family kinases. Subsequently, Nrf2 translocates into the nucleus where it binds to antioxidant response elements (AREs). The expression of a majority of antioxidants is governed by ARE-driven genes, which are under the transcriptional regulation of Nrf2 [127]. Furthermore, RONS trigger the phosphorylation of Forkhead box O (FOXO) by p38 and JNK kinases, resulting in nuclear translocalization and attachment to DNA [128]. Like Nrf2, FOXO coordinate the antioxidative response, but also other essential cellular processes like apoptosis [129]. Activation of MAPK signaling cascades can be assessed by protein and mRNA expression levels by western blotting and reverse transcription-quantitative polymerase chain reaction (RT-qPCR) [130]. The translocalization of Nrf2 or FOXO can be assessed through Western blot analysis of cytosolic and nuclear fractions or by utilizing cells expressing a green fluorescent protein (GFP)-tagged version of the target protein [131,132]. In *C. elegans*, orthologs are skn-1 (human Nrf2) and daf-16 (FOXO), which can be visualized using GFP-tagged mutant strains. Due to the transparency of the worm, translocalization of skn-1 or daf-16 can be assessed by fluorescence microscopy (Figure 7) [133].
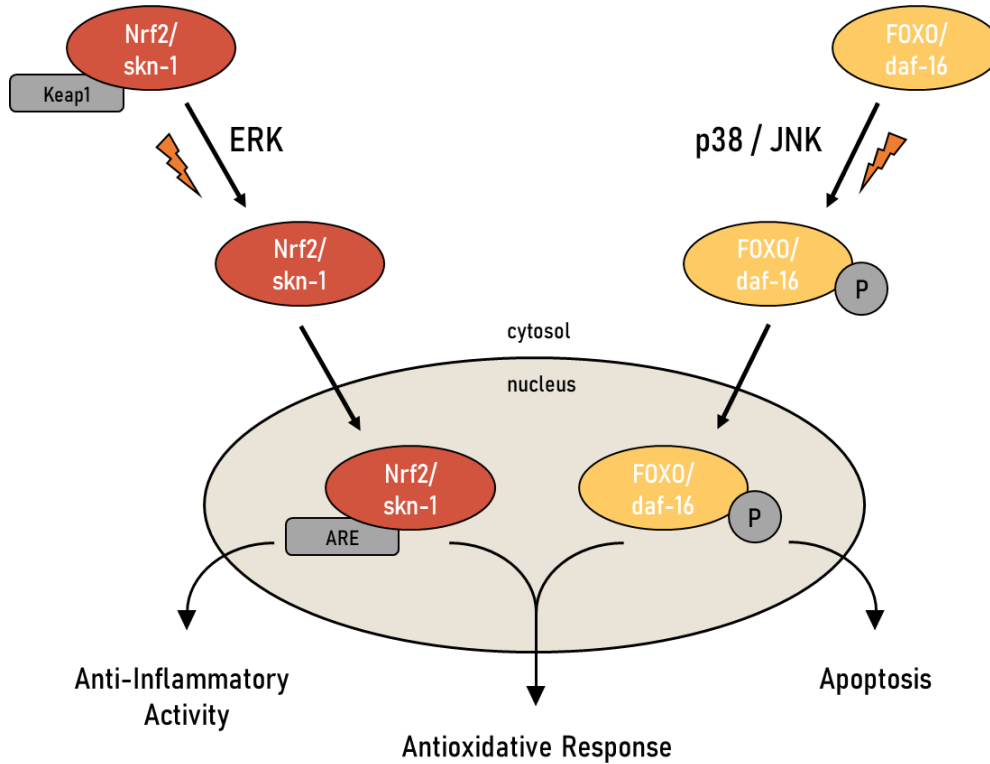
Figure 7:   Scheme on Nrf2 (skn-1 is the ortholog in *C. elegans*) and FOXO (daf-16 is the ortholog in *C. elegans*) activation due to oxidative stress. Nrf2 gets released from Keap1 and phosphorylated by ERK kinases, following nuclear translocalization and binding to antioxidant response elements (AREs). P38 and JNK kinases phosphorylate FOXO to translocalize into the nucleus. Both transcription factors induce signaling pathways of the antioxidative apparatus. This activation leads to the expression of genes involved in antioxidative defense, detoxification and cellular repair processes, ultimately mitigating the effects of oxidative stress (adapted and modified from Hammad et al. [134] and Nguyen et al. [135]).

The prominent antioxidant GSH, which is a tripeptide consistent of γ-glutamyl-cysteinylglycine, is an important marker for the antioxidative capacity of an organism [136]. In its reduced form, GSH is used as electron donor by GPx to detoxify H_2O_2, while 2 molecules of GSH react to its oxidized form GSSG (Figure 8).
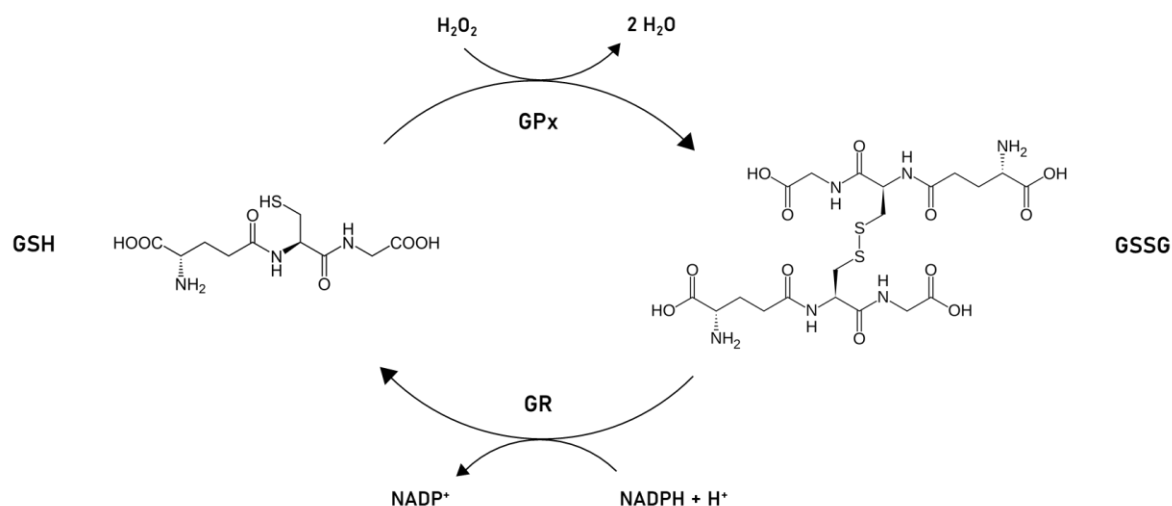
Figure 8: Mechanism behind the antioxidative property of GSH. H_2O_2 gets detoxified by glutathione peroxidase (GPx). Thereby, 2 molecules of GSH act as electron donor and oxidize to GSSG. Under NADPH consumption, glutathione reductase (GR) reduces GSSG back to GSH (adapted and modified from Jozefczak [136]).

Thus, a reduction in GSH, an increase in GSSG as well as alterations of the GSH/GSSG ratio serve as pivotal indicators of oxidative stress [137,138]. Quantification of GSH and GSSG can be carried out in different matrices, among others in *C. elegans*, by different techniques like the use of a fluorescence-based redox-cycling assay [139] or analytical approaches like liquid-chromatography tandem-mass spectrometry (LC-MS/MS) [140]. However, due to the lack of specificity and sensitivity of the redox-cycling assay, analytical methods for quantification should be prioritized [140]. Other major antioxidants besides GSH are, among others, the family of superoxide dismutases, catalase and GPx. Examining the expression and activity of antioxidant enzymes serves as an indirect marker to gauge oxidative stress and the redox status of an organism. Enzyme activity can be determined using (fluorescent) dye-based assays. Typically, a substrate is introduced, which gets converted by the enzyme into an absorbent or fluorescent product that can be quantified [141]. Additionally, mRNA levels of antioxidants can be assessed by real-time quantitative polymerase chain reaction (RT-qPCR), which can as well be conducted in *C. elegans* using TaqMan Gene Expression Assay probes. This

signifies the activation of specific signal cascades, due to a relative-fold change of transcription levels [142]. As previously stated, RONS possess the capacity to harm macromolecules, including lipids. Hence, another marker of oxidative stress is malondialdehyde (MDA), which is a byproduct of lipid peroxidation of polyunsaturated fatty acids [143]. MDA quantification can be carried out using fluorescent dyes [144] or by HPLC-based fluorescent detection [143]. The advantages of (fluorescent) dyes are that these assays are rapidly performed, but often lack specificity as well as sensitivity. An example of this is the redox-cycling assay for GSH assessment, which unspecifically binds to every thiol group [140]. In contrast, analytical techniques offer greater specificity and, if using mass spectrometry, way better sensitivity. Nevertheless, the stability of relevant molecules may be a concern due to partially extensive sample preparation for analytical approaches [140]. Since RONS can induce various signal cascades and alter different metabolic pathways, possessing a combination of different markers is of paramount importance to identify the underlying mechanisms of oxidative stress.

2.5.2. Mitochondria as target of oxidative stress

The primary function of mitochondria is to synthesize adenosine triphosphate (ATP), the energy currency of cells. Additionally, mitochondria play a crucial role in the biosynthesis of amino acids, nucleic acids, purines and various other essential metabolites. They also regulate intracellular calcium ion (Ca^{2+}) homeostasis and oversee processes such as cell division and apoptosis [145]. In periods of intense oxidative metabolism, mitochondria produce and sequester RONS. The majority of RONS, particularly the superoxide anion, originate from mitochondrial respiration and are generated in the different complexes of the electron transfer chain [146]. In instances of RONS overproduction or compromised mitochondrial antioxidants, it can lead to damage of biomolecules like mitochondrial proteins and potentially impairing mitochondrial function [147].

The synthesis of ATP is intricately linked to the levels of adenosine diphosphate (ADP) and adenosine monophosphate (AMP), which are produced during metabolic activities by removing one or two phosphate groups from ATP. ADP and AMP are subsequently utilized within the mitochondria during oxidative phosphorylation to regenerate ATP, creating a direct correlation among the concentrations of these three adenine nucleotides [148]. Additionally, another crucial group of energy-related nucleotides within the mitochondria includes the oxidized and reduced forms of pyridine nucleotides: nicotinamide adenine dinucleotide (NAD+/NADH) and its phosphorylated variant (NADP+/NADPH). These molecules serve as co-substrates in various biochemical reactions. For instance, phosphorylated NADPH plays a vital role in replenishing glutathione within the antioxidant system (Figure 9), thus directly mitigating damage caused by oxidative stress. Furthermore, energy-related nucleotides are indispensable in a plethora of cellular processes beyond the mentioned examples [149].
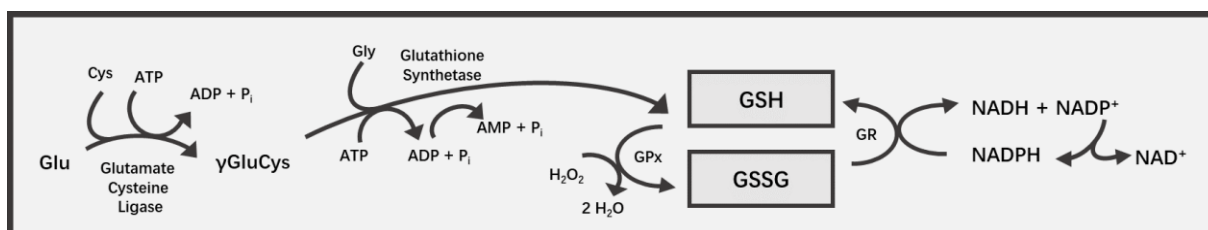
Figure 9:   Interplay of energy-related nucleotides and glutathione synthesis and redox cycling.

Mitochondria feature both an outer and inner membrane. The inner membrane envelops the mitochondrial matrix, housing intricate multi-subunit enzyme complexes integral to the respiratory chain, along with all the enzymes crucial for ATP production. Therefore, the preservation of mitochondrial membrane integrity and the membrane potential are of paramount importance [150]. Mitochondrial membranes are enriched with phospholipids, notably phosphatidylcholine (PC), phosphatidylethanolamine (PE), and cardiolipin (CL). CLs are exclusively to mitochondria, constituting approximately 10 – 15 % of total mitochondrial phospholipid content. Located mainly in the inner mitochondrial membrane, CLs play a critical role in preserving membrane

integrity and shaping cristae morphology. Beyond its contribution to membrane architecture, CLs actively engage in the stabilization of the respiratory chain complexes [151]. During periods of stress, CLs are translocated to the outer mitochondrial membrane, where they serve as a signaling molecule, facilitating the activation of mitophagy and apoptotic signaling pathways [152]. CLs have garnered significant attention in neurodegenerative disease research, as irregularities in CL content, structure and distribution have been associated with compromised neurogenesis and neuronal dysfunction, thereby contributing to aging and the onset of neurodegenerative diseases. Moreover, the unique acyl chain composition of CL constitutes a promising biomarker for diagnosing and monitoring the progression of various neurological disorders [151,153–155].

2.5.3. Oxidative DNA damage and DNA damage response

The excess formation of RONS presents significant danger to cellular components like the DNA. For instance, highly reactive hydroxyl radicals have the capability to interact with individual DNA bases and to form adducts, leading to an array of DNA base damage [156]. Among the most prevalent types of DNA damage is the oxidation of the DNA base guanine to 8-oxoguanine (8oxodG), making it a useful marker to assess the impact of oxidative stress on DNA [157]. Furthermore, oxidative DNA damage can manifest in various forms, such as single or double strand breaks, damages to the DNA sugar backbone and the deletion or translocalization of individual bases. The spectrum of oxidative DNA damage is intricately linked to processes like aging, the onset of diseases and carcinogenesis [122].

To cope with constant DNA damage, cells employ diverse repair mechanisms tailored to address different types of damage. DNA damage response, first action following DNA damage, encompasses a myriad of mechanism which impact DNA damage detection, DNA damage repair and apoptosis. The major DNA damage response mechanism is the posttranslational modification of proteins via poly-(ADP-ribosyl)ation (PARylation) [158]. PARylation is an

NAD$^+$-consuming mechanism, beginning with poly-(ADP-ribose) polymerases (PARPs), which catalyze the formation of ADP-ribose chains on target proteins and DNA ends. This leads to a recruitment of downstream repair enzymes and consequently DNA repair [159]. For instance, base excision repair involves the removal of the damaged base followed by its replacement with an intact base of the same type, effectively repairing individual base damage. Alternatively, nucleotide excision repair can be employed for extensive DNA lesions, wherein a segment comprising several adjacent bases is substituted with an undamaged sequence, facilitating the repair of broader damage [160]. Following successful DNA repair, a rapid hydrolytic degradation of the ADP-ribose chains occurs, which is catalyzed by poly-(ADP-ribose) glycohydrolases (PARGs) [161]. Next to DNA damage response, PARylation takes part in, among others, chromatin regulation, telomer maintenance and genomic stability [162].

2.5.4. Overexposure of (labile) Cu

Cu, an essential micronutrient, serves as a critical catalytic cofactor in numerous biological processes, encompassing mitochondrial respiration, antioxidant defense and biocompound synthesis. Maintaining an optimal intracellular Cu concentration is crucial, as deviations from the optimal range, even moderate increases, can induce oxidative stress, cytotoxicity and cell death. Therefore, the uptake, distribution and elimination of Cu has to be rigorously regulated to ensure cellular homeostasis [163].

Exceeding the physiological range, Cu exhibits toxic properties. He et al. demonstrated that Cu nanoparticles decrease the ratio of GSH and GSSG, thereby compromising antioxidative capacity [9]. Similarly, Baldissera et al. found elevated levels of RONS in *Cichlasoma amazonarum*, resulting in reduced ATP levels [8]. Similar findings were replicated in *C. elegans*. Exposure to CuSO$_4$ resulted in heightened levels of RONS, H$_2$O$_2$ and MDA [144]. Additionally, the expression of genes associated with oxidative stress, such as *gcs-1/GCLC* (glutamate-cysteine ligase catalytic subunit) were

upregulated in *C. elegans* [164]. As discussed in 2.4.2., the question arises whether Cu toxicity is induced by the total Cu fraction or by a specific Cu species. The current research spotlight is on labile Cu, known for its high bioavailability and redox activity. This reactivity renders labile Cu more likely to interact with various cellular components, including proteins, nucleic acids and lipids, potentially leading to cellular damage and dysfunction [165]. It is suggested that in the aging human brain, there is a transition from bound metal ion pools to labile ones. This shift leads to the loss of energy production and antioxidant function, while facilitating gain-of-function oxidative stress [18]. Chelators, with lower binding affinity compared to cuproenzymes, selectively bind available labile Cu. Lichtmannegger et al. observed in ATP7B knockout rats, a model for WD, that Cu accumulates in the liver and causes mitochondrial dysfunction. Using a specific Cu chelator, these effects could be suppressed [166]. Another study demonstrated that chelator therapy protects against Cu-induced oxidative stress in both *in vitro* and *in vivo* models [167]. This underscores the hypothesis that toxic mechanisms of Cu are primarily mediated by labile Cu [165]. Boll et al. reveal elevated labile Cu levels in cerebrospinal fluid in the brain of patients diagnosed with Parkinson's disease. Furthermore, elevated nitric oxide activity and lipid peroxidation products were observed [13]. This suggests that labile Cu isn't just a catalyst for oxidative stress; it seems like it actively contributes to neurotoxicity and the development of neurodegenerative diseases [13,14,163].

2.6. Neurotoxicity

Neurotoxicity refers to any reversible or permanent harmful impact on the structure or operation of both the central and peripheral nervous systems caused by a variety of biological, chemical, or physical agents [168]. As consequence, neurotoxicity can lead to neurodegeneration, which is characterized by protein accumulation, synaptic reduction, neuronal dysfunction and lastly death [169]. Pesticides, metals, genetic risk factors and aging possess

risk factors, which contribute to neurotoxicity [169]. Nerve cells, in particular, are highly vulnerable to neurotoxins. The excitable membrane of neurons is a prime target for an extensive variety of neurotoxins, which disrupt the essential ion channels necessary for the proper functioning of neurons, axons and muscles [170]. Another target of neurotoxins are diverse structures in the synaptic cleft, which suppresses sufficient transmission of neurotransmitters [171]. Moreover, a defining characteristic of neurotoxicity is the accumulation of misfolded protein aggregates, contributing to the breakdown of cellular protein homeostasis. This may result in a toxic gain- or loss-of-function leading to cellular toxicity and ultimately neuronal death [172]. With its transparency, the nematode *C. elegans* allows for convenient examination of its neurons. Detailed descriptions of the morphology of every neuron type have been established, alongside the presence of neuronal fate markers for nearly all neurons, often in the form of fluorescent reporter genes. Leveraging fluorescence microscopy to "phenotype" neurons renders the nervous system of *C. elegans* an ideal model system for investigating the impacts of exogenous toxins and genetic mutations on neuronal morphology [173,174]. Due to advancements in characterizing *C. elegans* behaviors and their correlation with specific neural circuits, additional insights into underlying mechanisms have been gained. Therefore, neurotoxicity can be assessed through behaviors, such as thrashing, chemotaxis or pharyngeal pumping. Another common behavior assay used in *C. elegans* is the basal slowing response (BSR) assay, which evaluates the functionality of the dopaminergic system. When bacteria are present, wildtype worms exhibit decreased movement speed compared to their activity in the absence of bacteria. This bacterial sensing is facilitated by dopamine-containing neural circuits. Consequently, a diminished movement slowdown occurs on food when there is a loss of functionality in dopaminergic neurons [175]. Neuronal cells in *C. elegans* function as sophisticated information processing units. They exhibit intricate wiring patterns to other neurons and express a remarkable array of signaling molecules, including neurotransmitters and their receptors.

Transcriptome analysis have revealed that *C. elegans* possesses up to 14 different neurotransmitter receptors per sensory neuron [176].

2.6.1 Neurotransmitter as Target

Neurotransmitters are messenger molecules, which transmit excitation between neurons across a chemical synapse. This enables the brain to sense perceptions and to coordinate complex behavior [177]. The most important neurotransmitters, which are present both in mammals and *C. elegans*, are dopamine (DA), γ-amino butyric acid (GABA), glutamate (Glu), serotonin (SRT) and acetylcholine (ACh) [178–181]. Misregulation of the mentioned neurotransmitters is associated with the onset of various neurodegenerative diseases [179]. Neurotoxins interfere with neurotransmitters and disrupt their metabolism in various ways. These include enzymes for neurotransmitter synthesis as well as enzymes for metabolization, disturbed uptake and release processes, blocking of receptors or ion channels and post synaptic events associated with receptor activation. Therefore, the assessment of neurotransmitter levels is an essential marker to assess neurotoxicity [171,182,183]. Studies further advocate to use neurotransmitter ratios as indicator for neurodegenerative diseases [184,185].

DA, synthesized in the substantia nigra [186], is essential for cognitive and motor functions [187]. Dopaminergic neurons are under constant oxidative stress due to DA metabolism. Due to excitation of dopaminergic neurons (DAergic neurons), DA is released into the synaptic cleft (Figure 10). However, excess DA has to be removed for signal interruption [188] by either reuptake or degradation. Oxidative deamination of DA catalyzed by monoamine oxidases results in the formation of toxic metabolites like 3,4-dihydroxy-phenylacetaldehyde (DOPAL), 3,4-dihydroxyphenylacetic acid (DOPAC) and H_2O_2 [189]. Since the brain consumes about 20 % of total oxygen, neurons are particularly susceptible to RONS [190]. However, metabolic balance in DAergic

neurons is essential, as reduced DA levels are associated with neurodegenerative diseases, such as Parkinson's disease [191,192].
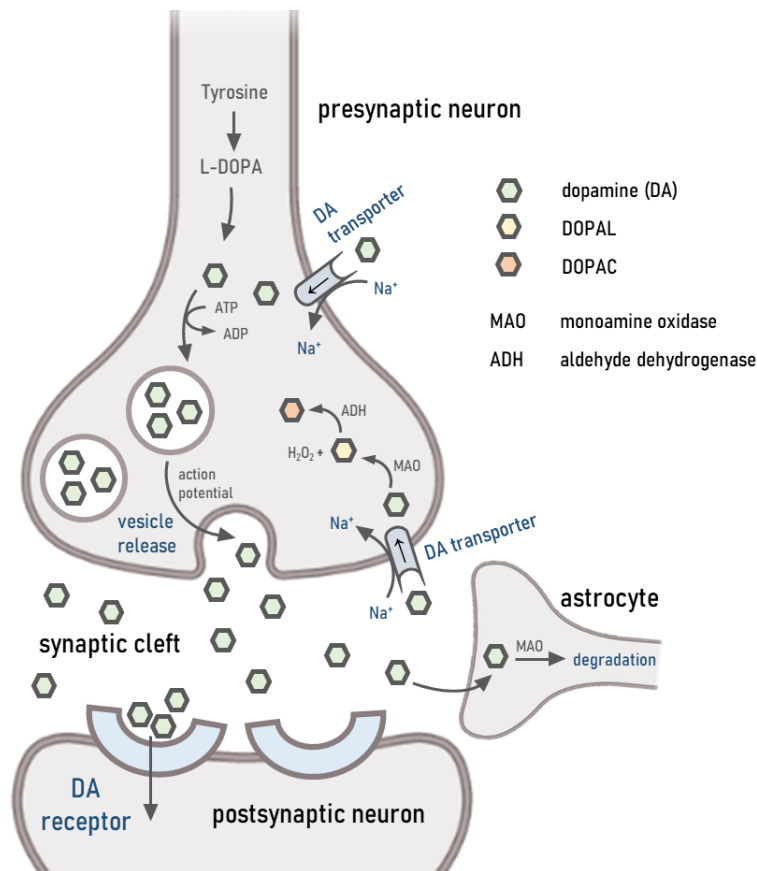
Figure 10: DA metabolism in dopaminergic neurons (adapted and modified from Xu et al. [193]). DA gets either taken up by the DA transporter or synthesized from tyrosine via L-dihydroxyphenylalanine (L-DOPA). Newly synthesized DA is stored in vesicles, which can be secreted into the synaptic cleft following an action potential. Cytosolic DA can be degraded in dopaminergic neurons or astrocytes to homovanillic acid or can be oxidized to form metabolites (DOPAL and DOPAC) as well as hydrogen peroxide (H_2O_2).

SRT, which is synthesized in the brainstem raphne nuclei [194], regulates a broad variety of functions in the central nervous system, like the sleeping cycle or appetite. The most clinical relevance of SRT is its role in psychological disorders, as its reduction is associated with depression [195,196]. Changes in the ratio of GABA and Glu leads to alterations in the control of cortical excitability, as GABA is the main inhibitory and Glu the main excitatory neurotransmitter in the cortex. Therefore, synthesis of GABA out of Glu via the tricarboxylic acid cycle is tightly regulated [197], to ensure adequate rhythmic

activity [198]. ACh coordinates cognitive and affective functions through proper signaling of the muscarinic ACh receptor and nicotinic ACh receptor [199]. Synthesized out of mitochondrial acetyl-CoA and choline and stored in vesicles, ACh is Ca^{2+}-dependent released into the synaptic cleft (Figure 11) [200]. Excess ACh has to be degraded by the enzyme acetylcholinesterase (AChE) [201]. The modulation of AChE activity has gained attention for the treatment of neurodegenerative diseases with lowered ACh synthesis, as inhibition of AChE elevates ACh levels [202]. On the other hand, AChE inhibitors are applied as insecticides or nerve agents to induce ACh accumulation and hyperstimulation of muscarinic and nicotinic receptors [203], which can cause rapid death [204].
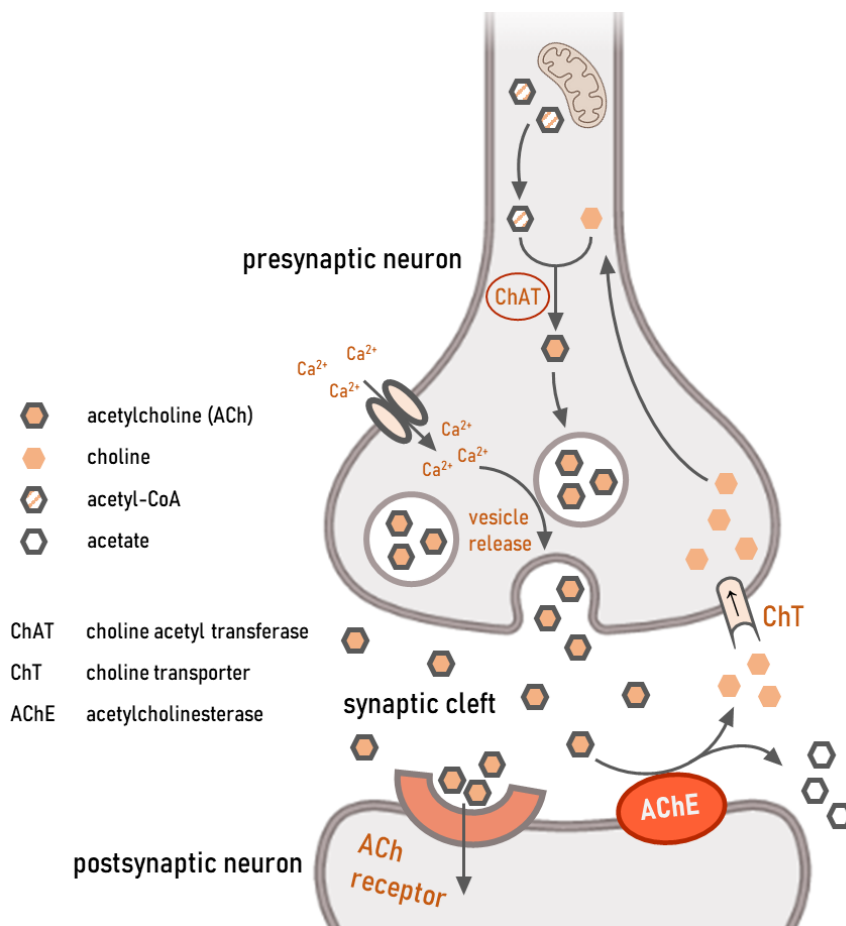
Figure 11: ACh metabolism in cholinergic neurons (adapted and modified from Stanciu et al. [200]). The choline acetyl transferase (ChAT) catalyzes the synthesis of ACh out of choline and mitochondrial acetyl-CoA. ACh is stored in vesicles which can, dependent on Ca^{2+}, be sequestrated into the synaptic cleft. Excess ACh gets degraded by the acetylcholinesterase to acetate and choline, which can be resumed via the choline transporter (ChT).

2.6.2. Neurodegenerative diseases

Neurodegenerative diseases manifest when nerve cells in the brain or peripheral nervous system gradually loose function and eventually perish. While certain treatments may alleviate some physical or mental symptoms linked to these diseases, slowing their progression remains elusive, and no cures are currently available [205]. Neurological disorders represent the foremost cause of both physical and cognitive disabilities globally, affecting approximately 15 % of the world's population. Over the past three decades, there has been a significant rise in the absolute number of individuals affected by these conditions [206]. The most common neurodegenerative diseases worldwide are Alzheimer's disease (AD) and Parkinson's disease (PD) [207].

With aging being the main risk factor, AD is defined by a progressive decline in cognitive function accompanied by escalating behavioral challenges and neuropsychiatric symptoms [208]. The primary hallmarks of Alzheimer's pathology consist of amyloid plaques and neurofibrillary tangles [209]. The peptide amyloid β (Aβ) is generated through the sequential cleavage of amyloid β precursor protein (APP). APP, a transmembrane protein, holds considerable importance in neuronal development and growth [210]. Following cleavage, the released Aβ peptides can undergo oligomerization and subsequent fibrillization, ultimately forming the distinctive Aβ plaques observed in the atrophied brain tissue of deceased AD patients [211]. Aβ plaques are rich in redox active trace elements, as single peptides are linked via divalent metals [212]. Furthermore, the accumulation of Aβ in the brain seems to precede other pathomechanistic alterations in the biological continuum of AD, including the propagation of neurofibrillary tangles and the onset of neuronal and synaptic loss [213]. In addition to Aβ, tau protein (p-tau) stands as the primary component of neurofibrillary tangles in AD. Under normal circumstances, p-tau plays a crucial role in maintaining microtubule stability and contributes to the regulation of intracellular trafficking. However, in AD, the normal function of p-tau becomes disrupted, leading to the formation of neurofibrillary tangle pathology. The

progression of p-tau pathology is a multifaceted process involving post-translational modifications, disturbances in cytoskeletal integrity, and deficiencies in protein degradation mechanisms [214]. Consequently, this results in impaired neuronal function, particularly affecting cholinergic neurons AD. In addition to decreased DA levels, AD is characterized by reductions in choline acetyltransferase activity and ACh synthesis, along with alterations in choline uptake and release in the brain tissue of affected patients [215].

Symptoms of PD are diverse and encompass bradykinesia, tremor, rigidity, alongside numerous non-motor symptoms [216]. In industrialized countries, the prevalence of PD is 0.3 % in the general population, rising to 1 % among individuals over the age of 60 and further increasing to 3 % among those over 80 years old. Consequently, age stands as one of the most significant risk factors for PD. The hallmark of the pathophysiology of PD is the loss of dopaminergic neurons and therefore DA deficiency, which is commonly associated with the motor deficits in PD. Decades of research suggest that dysfunction or dysregulation of axonal dopamine release occurs before neuronal loss, indicating a complex interplay of factors in the pathogenesis of the disease [191,192]. While the majority of PD cases are idiopathic, mutations in several genes have been linked to the development of the disease [217]. These genes listed in Table 3 and their associated proteins play critical roles in various cellular processes, including protein aggregation, mitochondrial function, oxidative stress response, and lysosomal degradation. Mutations in these genes can disrupt these cellular processes, increasing the risk for the development of PD.

Table 3: Overview of genes whose mutation is associated with the onset of PD as well as the associated proteins and their function in a healthy individual.

Protein	Gene	Function
PARK1/4	*SNCA*	α-synuclein, a transport protein which forms membrane channels and regulates dopamine release [218]
PARK2	*PARKIN*	marks defect proteins in dopaminergic neurons by ubiquitination, defect proteins are then removed and degraded [219]
PARK5	*UCHL1*	antagonist of PARK2 → catalyzes the hydrolyzation following ubiquitination to regain ubiquitin monomers [218]
PARK6	*PINK1*	enables PARK2 to bind to depolarized mitochondria to induce autophagy, furthermore triggers neuronal differentiation [219]
PARK7	*DJ1*	a protein deglycase that inhibits the aggregation of α-synuclein and protects neurons against oxidative stress and cell death
PARK8	*LRRK2*	A kinase taking part in cellular signaling processes including the regulation of protein translation, vesicle trafficking and neurite outgrowth [217]
PARK9	*ATP13A2*	Involved in the transport of divalent transition metal cations and appears to protect cells from metal toxicity [220]

In addition to cases of PD in patients with a genetic predisposition, the majority of individuals with PD (about 90 %) are of unknown cause. It is plausible to consider, next to aging, that environmental factors play a role in the onset of PD. Among these factors, pesticides and metals are of particular interest due to their documented ability to induce oxidative stress [221]. Chronic exposure to (heavy) metals disrupts redox homeostasis by inducing free radical generation and decreasing antioxidant levels [222]. Moreover, the substantial increase in oxidative stress linked to metal exposure compromises the activity of the ubiquitin-proteasome system, leading to protein aggregation. These aggregated proteins disrupt cellular processes, ultimately culminating in cell death [223]. Studies have revealed significant alterations in metal concentrations in the brains of deceased PD patients compared to age-matched non-PD controls, implying a strong association between metal exposure and the incidence of PD [224]. Chapter 6 will discuss the interaction of neurodegenerative diseases and excess Cu in *C. elegans* in more detail.

2.6.3. Cu (dyshomeostasis)-mediated Neurotoxicity

In conjunction with the toxic effects of Aβ and p-tau, it is evident that oxidative stress significantly contributes to the advancement of AD symptoms and ultimately leads to the demise of afflicted patients [225]. The primary event in AD is the development of fibrils and plaques in the brains of affected patients. Aβ plaques exhibit elevated concentrations of trace elements, including Cu, Fe and Zn. Cu^{2+} ions demonstrate a strong affinity for Aβ peptides and can promote the formation of β-sheet and α-helix structures within these peptides, potentially contributing to Aβ aggregation. Various concentrations of Cu ions have been found to enhance fibril formation and the binding of Cu ions to Aβ notably increases its toxicity to cells [212]. The neurotoxic effects of Aβ peptides are believed to stem from oxidative stress, which arises from the redox cycling of Cu ions bound to Aβ peptides and the subsequent generation of hydrogen peroxide (Figure 12) [226].
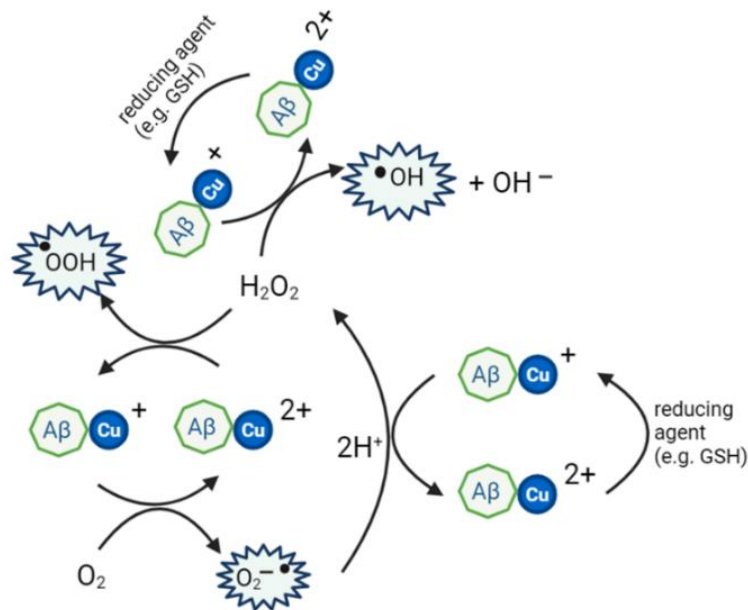
Figure 12: Scheme of the proposed mechanism of RONS production by Aβ-bound Cu. Cu within Aβ plaques remains redox active and is able to cycle between its two oxidation states +I and +II, which results in the formation of reactive radicals (adapted and modified from Arrigoni et al. [227]).

Despite overall lowered total Cu levels in the brains of AD patients compared to healthy individuals, numerous studies have consistently demonstrated elevated levels of labile Cu in the AD brain. Alterations in the distribution of serum Cu, marked by an increase in a Cu fraction not accounted for by ceruloplasmin, appear to be a distinctive feature of AD and could potentially play a role in its pathogenesis [228–231]. Similar to AD, total Cu levels in the brain of PD patients are lowered, while labile Cu is increased [232]. Additionally, Boll et al. demonstrate heightened levels of labile Cu in the cerebrospinal fluid within the brains of individuals diagnosed with PD in correlation with elevated oxidative stress markers [13]. Moreover, increased levels of ceruloplasmin were identified in the brains of patients with PD, suggesting either an acute phase response or a compensatory mechanism in response to escalating oxidative stress [233]. In summary, the intricate interplay between Cu dyshomeostasis, oxidative stress, protein aggregation and plaque formation significantly contribute to the progression of neurodegenerative diseases like AD and PD. Elevated levels of labile Cu in the brain of patients with neurodegenerative diseases coupled with increased oxidative stress markers, underscore its role in the pathogenesis of these neurodegenerative disorders. Understanding these mechanisms holds promise for targeted therapeutic interventions aimed at mitigating disease progression and improving patient outcomes.

Abstract

Neurotransmitters like dopamine (DA), serotonin (SRT), γ-aminobutyric acid (GABA) and acetylcholine (ACh) are messenger molecules playing a pivotal role in transmitting excitation between neurons across chemical synapses, thus enabling complex processes in the central nervous system. Balance of the neurotransmitter homeostasis is essential, and altered neurotransmitter levels are associated with various neurological disorders, e.g. loss of dopaminergic neurons (Parkinson's disease) or altered ACh synthesis (Alzheimer's disease). Therefore, it is crucial to possess adequate tools to assess precise neurotransmitter levels, and to apply targeted therapies. An established *in vivo* model to study neurotoxicity is the model organism *Caenorhabditis elegans* (*C. elegans*), as its neurons have been well characterized and functionally are analogous to mammals. We have developed a liquid chromatography-tandem mass spectrometry (LC-MS/MS) method including a sample preparation assuring neurotransmitter stability, which allows a simultaneous neurotransmitter quantification of DA, SRT, GABA and ACh in *C. elegans*, but can easily be applied to other matrices. LC-MS/MS combined with isotope-labeled standards is the tool of choice, due to its otherwise unattainable sensitivity and specificity. Using *C. elegans* together with our analytically validated and verified method provides a powerful tool to evaluate mechanisms of neurotoxicity, and furthermore to identify possible therapeutic approaches.

Chapter 3 – A Reliable Method Based on Liquid Chromatography-Tandem Mass Spectrometry for the Simultaneous Quantification of Neurotransmitters in *Caenorhabditis elegans*

Chapter 3 – A Reliable Method Based on Liquid Chromatography-Tandem Mass Spectrometry for the Simultaneous Quantification of Neurotransmitters in *Caenorhabditis elegans*

3.1. Introduction

Neurotransmitters are messenger molecules transmitting excitation between neurons across chemical synapses, which enable the brain to sense perceptions and coordinate complex behavior [177]. Here, the most important neurotransmitters, dopamine (DA), serotonin (SRT), γ-aminobutyric acid (GABA) and acetylcholine (ACh) will be discussed, as their dysregulation, among others, is associated with several neurological diseases. DA regulates body movement control, as well as memory function and cognition [234,235]. The most common DA-associated neurodegenerative disorder is Parkinson's disease (PD), which is associated with the progressive loss of dopaminergic neurons in the substantia nigra [236] and is characterized, among other things, by the presence of alpha-synuclein inclusions (Lewy Bodies) [237]. SRT acts as a neurohormone controlling the function of several peripheral organs and modulates mood, cognition, sleep, learning and anxiety [238,239]. Hypofunction of serotonergic neurons is associated with depression, and disturbances in SRT levels lead to anxiety disorders [239]. GABA, among other functions, regulates blood pressure and heart rate. In addition, it binds to receptors at inhibitory synapses, thus decreasing neuronal excitability [240]. The balance between excitation and inhibition is a requisite for proper neural function; as a consequence, a disequilibrium contributes to neurodegeneration [241]. The cholinergic system, including in particular the neurotransmitter ACh, is known to be required for a variety of critical physiological activities, such as attention, learning and memory [242]. A decreased activity of choline acetyltransferase

44

(ChAT) and the subsequent altered ACh synthesis are correlated with an increased formation of ß-amyloid (Aβ) plaques in the brains of patients with Alzheimer's disease (AD) [243]. Furthermore, a deficiency of ChAT, choline uptake and ACh secretion are concomitant symptoms of neuronal loss associated with learning deficits and memory loss [244]. Therefore, the analysis of basal levels of neurotransmitters is an essential tool for neurotoxicity assessment, especially in terms of neurodegenerative diseases such as PD and AD. In addition, neurotransmitter ratios are of great interest, as they interact and depend on each other, and in most neurodegenerative diseases the entire neurotransmitter system is disturbed [245,246]. In brief, it is crucial to have the ability to determine which neurotransmitter(s) are impaired, in order to apply targeted therapies.

Neurotransmitter quantification in mouse tissue, such as the brain [247] or cerebrospinal fluid [248], can be employed to assess the neurodegenerative potential of chemical or physical agents that may be harmful, as well as to identify therapeutic strategies. However, animal experiments provoke great ethical debate, requiring novel model organisms to substitute and complement animal experiments for testing neurodegenerative potentials. For this purpose, zebrafish (*Danio rerio*), flies (*Drosophila melanogaster*) and worms are commonly used [249,250]. The nematode *Caenorhabditis elegans* (*C. elegans*) constitutes a distinguished *in vivo* model featuring a well-elucidated nervous system. All neurons are well characterized and mapped over the worm body, and they are structurally and functionally similar to mammals [39]. Furthermore, in *C. elegans,* orthologs are present for 60–80% of human genes related to various diseases, including neurodegenerative disorders [23]. Therefore, *C. elegans* is a well-established model organism in the field of neurotoxicity and neurodegeneration. In addition, worms are easily genetically manipulated, providing a variety of mutants, especially for PD [251,252] and AD [253,254].

Neurotoxicity in *C. elegans* is predominantly assessed by behavioral assays. Commonly performed assays include that of the basal slowing response, which examines dopamine-dependent behavior in the presence of food [175], the determination of serotonin-dependent pharyngeal pumping [255], the synaptic transmission at neuromuscular junctions using the aldicarb-induced paralysis assay [256] and the assessment of functional changes in locomotion [175]. Additionally, genetically modified worms with fluorescence tags in neurons have been used to study neurodegeneration via fluorescence microscopy [257,258]. However, these techniques have the limitation, among others, of not being able to quantify absolute neurotransmitter levels. Furthermore, the majority of assays, such as that of basal slowing, are focused on a solitary neurotransmitter, in this case, DA. Other assays, namely those of locomotion, are mediated by several neurotransmitters, such as acetylcholine and dopamine; these provide broader outcomes, but can be problematic in interpretation. So far, only Schumacher et al. have assessed DA and SRT [38], but, to date, GABA and ACh have not been quantified in *C. elegans*. Therefore, a method is required for the simultaneous quantification of multiple neurotransmitters in *C. elegans.*

The demands of such a technique are challenging, as the analysis must be specific for the individual neurotransmitters and, on the other hand, requires good sensitivity, as the basal levels of neurotransmitters are low. In addition, neurotransmitters display poor stability. Methods do already exist to quantify neurotransmitters in a variety of matrices by electrochemical detection [259,260], fluorescence detection [261,262] or fluorescent dyes [263–265]. However, here, we opted for liquid chromatography–tandem mass spectrometry (LC-MS/MS) as the preferred choice due to its high sensitivity and unmatched specificity, and given its propensity to detect distinctive mass transitions of each analyte, and therefore, its capacity for unequivocal identification. In addition, mass spectrometry allows the use of isotope-labeled standards, which

correspond analogously to their respective analyte throughout the entire analytical procedure, from sample preparation to detection. The combination of mass spectrometry and isotope-labeled standards of target analytes is a top-notch technique for the analysis of several biological samples [266]. In recent years, a handful of LC-MS/MS-based methods have been published to quantify neurotransmitters. These refer almost exclusively to mouse [247,248] and rat [267,268] brain tissue and mostly do not provide sufficient LOQs for neurotransmitter quantification in model organisms like *C. elegans*. Only Tufi et al. present an LC-MS/MS analysis in zebrafish *Danio rerio* [269], while Barata et al. published a method for neurotransmitter and related metabolites quantification in *Daphnia magna* [270]. A tool for the simultaneous quantification of neurotransmitters, especially GABA and ACh, in *C. elegans* with sufficient sensitivity has yet to be reported.

Here, we aim to present an established and validated LC-MS/MS-based method, which allows the simultaneous quantification of neurotransmitters, specifically DA, SRT, GABA and ACh, in *C. elegans*. A new extraction protocol assured stability and high recovery for all four analytes. The use of isotope-labeled standards and LC-MS/MS analysis in multiple-reaction-monitoring mode provided an unequivocal identification, as well as specificity of all analytes and greater sensitivity compared to other techniques. As method validation parameters, the linear range, limit of detection (LOD), limit of quantification (LOQ), accuracy, recovery and precision were assessed. Further, we analyzed neurotransmitter profiles of transgenic *C. elegans* strains with altered neurotransmitter homeostasis and characterized their synaptic transmission by the aldicarb-induced paralysis assay in order to corroborate the analytical LC-MS/MS data.

3.2. Results

3.2.1. Method Development for Neurotransmitter Quantification via LC-MS/MS

The aim of the chromatography was to establish a baseline-separated elution for all analytes, as well as maximum sensitivity with subsequent mass spectrometric detection. Different solvents (MeOH and ACN) were tested, with ACN demonstrating sharper peaks, lower noise and quicker elution of all analytes when we used the YMC-Triart PFP column. ACN modified with 10 mM FA resulted in a higher response compared to 5 mM FA. For further optimization, the column temperature was varied (20–40 °C), with 30 °C leading to the best result. A gradient of a total of 12 min (including equilibration) was generated with the following retention times for all analytes and their respective deuterated internal standards (used for internal calibration and unambiguous identification): GABA—2.50 min, DA—5.92 min, ACh—7.22 min and SRT—8.38 min. The respective chromatograms of the quantifiers of all analytes and all internal standards in a *C. elegans* matrix (wildtype) are shown in Figure 13.

Ion source parameters were optimized with standard solutions using the Compound Optimization software wizard of the Sciex Analyst Software (Version 1.7.2); they are listed in the materials and methods Section 2.4. To determine mass-to-charge (m/z) ratios for the precursor ions, standard solutions of the analytes and deuterated analytes were injected and Q1 scans were performed. Fragment ion scans with varying intensity in collision energy were conducted to determine the m/z ratios of the respective fragments. The aim was to identify at least two MRM transitions for each analyte with optimal intensity. The following mass transitions revealed the highest responses (Figure 13C–F) and were therefore used as quantifiers: DA m/z 154 > 91, DA$_{d4}$ m/z 158 > 95, SRT m/z 177 > 160, SRT$_{d4}$ m/z 181 > 164, GABA m/z 104 > 69, GABA$_{d6}$ m/z 110 > 73, ACh m/z 146 > 87 and ACh$_{d4}$ m/z 150 > 91. Quantifier precursor and fragment

ion structures are stated in Figure 14. Further mass transitions (qualifiers) are listed in Table 4.
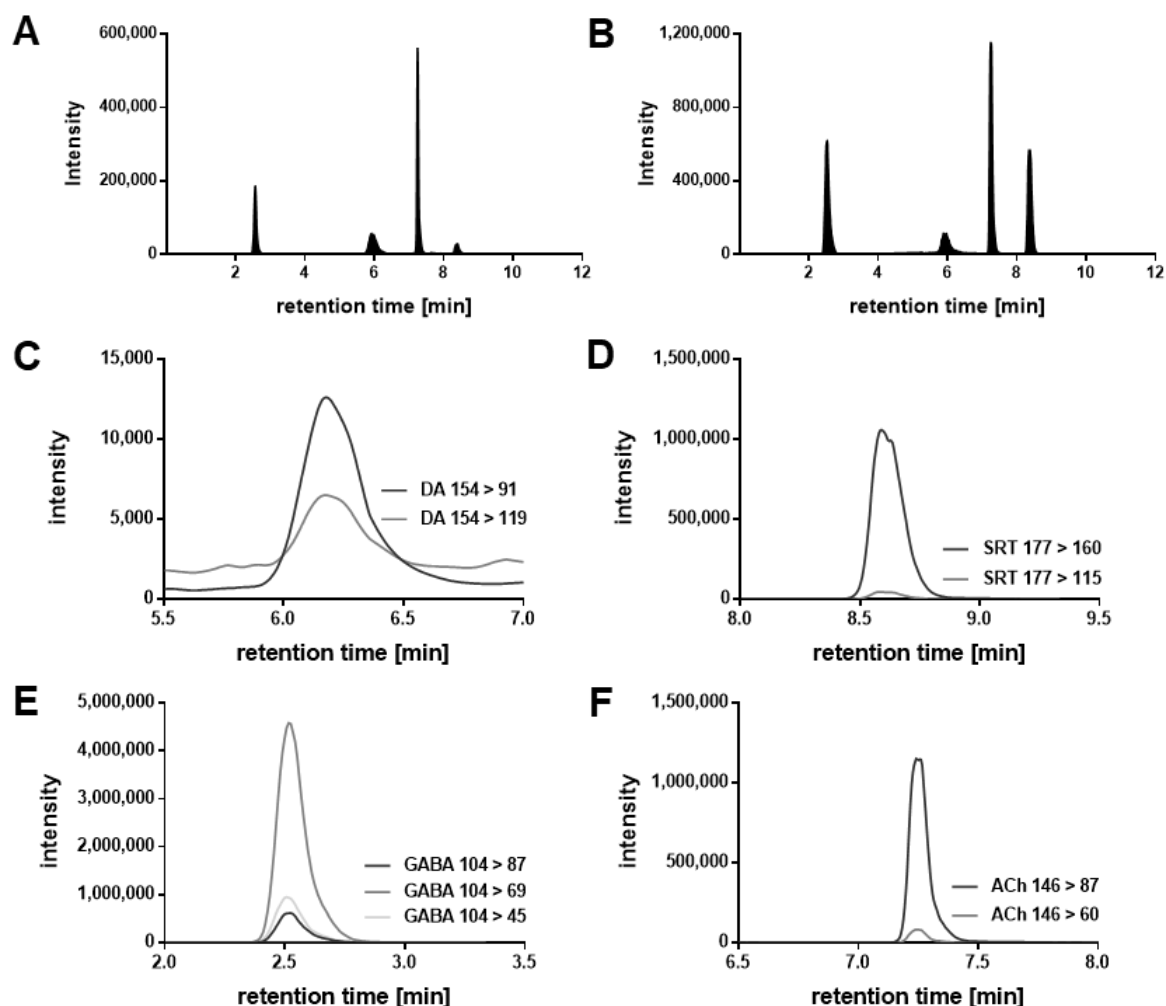
Figure 13: sMRM chromatograms of all analytes (A) and their respective deuterated internal srandards (B) (25 nM of DA$_{d4}$, 25 mMSRT$_{d4}$, 500 nM of GABA$_{d6}$ and 25 nM ACh$_{d4}$) in *C. elegans* worm homogenate (wildtype). (**A**,**B**) only the quantifier mass transitions (Table 4) of DA, SRT, GABA, ACh and the accordant internal standards are presented. The most intensive mass transitions (listed in Table 4) of DA (m/z 154 > 137 not found in matrix) (**C**), SRT (**D**), GABA (**E**) and ACh (**F**) are displayed in matrix.

Table 4: sMRM parameters for DA, SRT, GABA, ACh and their respective internal standards. The quantifiers are highlighted in bold. All transitions are single-protonated ions ([M + H]$^+$).

Compound	Q1	Q3	CE	DP	CXP	Retention Time (min)
DA	154	137	15	30	15	
		119	25	30	15	
		91	32	30	15	5.92
DA$_{d4}$	158	141	15	30	15	
		123	25	30	15	
		95	32	30	15	
SRT	177	**160**	15	15	17	
		115	51	30	41	8.38
SRT$_{d4}$	181	**164**	15	15	17	
		118	51	30	41	
GABA	104	87	15	17	10	
		69	21	18	10	
		45	28	25	11	2.50
GABA$_{d6}$	110	93	15	17	10	
		73	21	18	10	
		49	28	25	11	
ACh	146	**87**	19	27	13	
		60	16	32	9	7.22
ACh$_{d4}$	150	**91**	19	27	13	
		60	16	32	9	
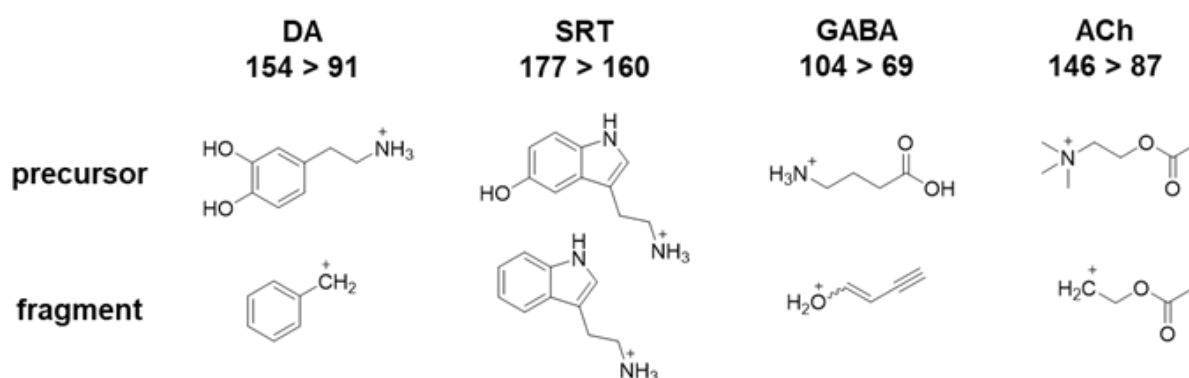
Figure 14: Chemical structures of precursors and their underlying fragment ions [M + H]$^+$ (quantifiers) for DA, SRT, GABA and ACh.

3.2.2. Sample Preparation and Neurotransmitter Extraction

Following optimization of the LC-MS/MS conditions, the method was applied to
C. elegans homogenates. The extraction of neurotransmitters was improved by
optimizing the composition of the applied extraction buffer. We tested the pH
effect (acidic and neutral) on the stability and recovery of all four analytes.
Whereas DA seems to be stable only in acidic pH, GABA shows the highest
recovery in neutral pH. In contrast, both SRT and ACh demonstrate no
differences in recovery in acidic or neutral pH. In order to identify a suitable
compromise, various acids (perchloric acid and formic acid) and pH values (pH
= 1–7) were tested. A sufficient response of all four analytes was obtained by
adding 2.5 mM perchloric acid (pH = 4). In addition, we analyzed the impact of
different amounts (10, 20 and 30%) of organic modifiers (MeOH and ACN) in
the extraction buffer. A higher response, especially for GABA, was observed
when we modified the buffer with 10% MeOH. The sample extracts were purified
by a Spin-X® Centrifuge Tube Filter 0.22 µm (Corning). The recovery of the
neurotransmitters as well as the protein content with and without purification
steps were determined, and showed statistically indistinguishable results.

3.2.3. Method Validation

Samples were spiked with DA, SRT and ACh from 0 to 500 nM and with GABA
from 0 to 10 µM. Linearity was observed for all analytes in the indicated range
(Figure 15); correlation coefficients are listed in Table 5.

Table 5: Method validation parameters assessed in *C. elegans* matrix (wildtype). How parameters were assessed is listed in section 4.4.5.

	DA	SRT	GABA	ACh
Concentration in samples [#]	11.9 nM	2.2 nM	2.6 µM	38.8 nM
Correlation coefficient (R^2)	0.9966	0.9939	0.9873	0.9993
Limit of detection (nM)	0.204	0.097	15.628	0.0009
Limit of quantification (nM)	0.679	0.324	52.094	0.0029
Recovery (%)	103 ± 2.7	64 ± 2.3	80 ± 4.1	56 ± 11.9

[#] analyte concentration of worm homogenates (3000 L4 stage worms in 150 µL extraction buffer) before protein normalization.
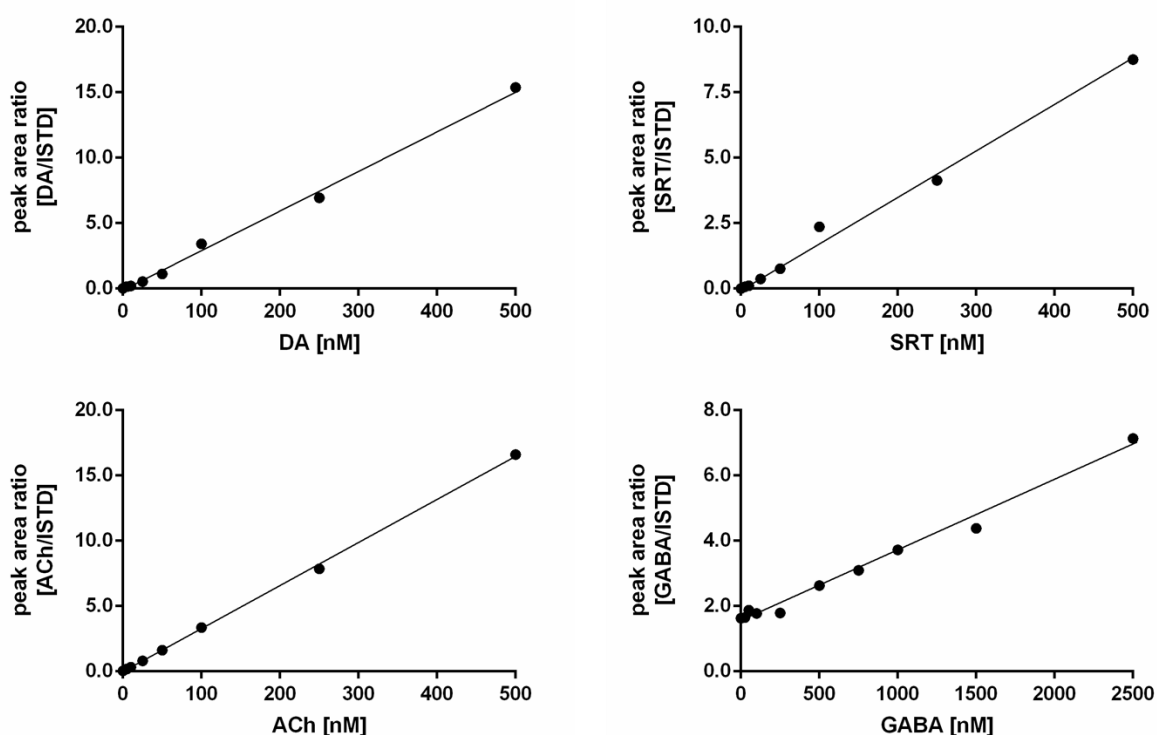
Figure 15: Calibration curves for all four neurotransmitters in the concentration range of up to 500 nM for DA, SRT and ACh and up to 2500 nM for GABA. Correlation coefficients are stated in Table 5.

The LOD was defined as LOD = $3\times SD_y/b$ (SD_y = standard deviation of analyte concentration in ≥12 blank measurements, b = slope of calibration curve), with 0.204 nM for DA, 0.097 nM for SRT, 15.628 nM for GABA and 0.0009 nM for

ACh. The LOQ was defined as LOQ = 10 × SD_y/b, with 0.679 nM for DA, 0.324 nM for SRT, 52.094 nM for GABA and 0.0029 nM for ACh. Thus, the LOQs were far below the analyte concentrations in *C. elegans* homogenates (3000 L4 stage worms in 150 µL extraction buffer), which were 11.9 nM of DA, 2.2 nM SRT, 2.6 µM GABA and 38.8 nM ACh (n ≥ 20). The LOQs underline the sensitivity of the method and show that considerably less than 3000 worms can be used for the analysis. The recovery of deuterated standards in matrix amounted to 103 ± 3% for DA, 64 ± 2% SRT, 80 ± 4% for GABA and 56 ± 12% for ACh, compared to deuterated standards in extraction buffer only. This indicates sufficient recovery, as the loss of neurotransmitters during sample preparation and analysis was always balanced by the respective deuterated standards.

Accuracy was determined in samples with low (25 nM), middle (250 nM) and high (2500 nM) concentrations of all analytes and was within ± 20% of the nominal concentration (Table 6). The variation in neurotransmitter quantification from eight samples on the same day was defined as intraday precision and was 3.1% for DA, 6.1% for SRT, 3.4% for GABA and 7.6% for ACh. The variation from eight samples analyzed on different days was defined as interday precision and was 2.6% for DA, 14.0% for SRT, 3.2% for GABA and 1.8% for ACh. Therefore, intra- and interday variations < 15% were considered both reliable and reproducible due to high precision.

Table 6: Method validation parameters: accuracy for low, middle and high analyte concentrations and intraday and interday precision. How parameters were assessed is listed in section 4.4.5.

	Accuracy [%]			Precision [RSD%]	
	Low	Middle	High	Intraday	Interday
DA	114.8 ± 8.8	111.1 ± 7.9	112.7 ± 4.1	3.1	2.6
SRT	84.9 ± 1.3	85.6 ± 1.5	81.1 ± 1.8	6.1	14.0
GABA	95.3 ± 8.7	108.2 ± 5.2	116.4 ± 5.4	3.4	3.2
ACh	98.5 ± 4.9	96.6 ± 1.0	99.8 ± 0.6	7.6	1.8

3.2.4. Neurotransmitter Levels in Wildtype Worms and cat-2Δ and ace-1Δ::ace-2Δ Deletion Mutants

By using the validated LC-MS/MS method, we investigated the impact of the genetic background of *C. elegans* strains cat-2Δ and ace-1Δ::ace-2Δ on neurotransmitter levels. The deletion mutant cat-2Δ lacks the enzyme tyrosine hydroxylase, which catalyzes the hydroxylation of tyrosine to L-DOPA (L-3,4-dihydroxyphenylalanine), the precursor of DA [271]. Consequently, DA synthesis in cat-2Δ worms is restricted. *C. elegans* strain ace-1Δ::ace-2Δ displays a loss of acetylcholinesterase (AChE), which is the major enzyme to hydrolyze ACh into acetic acid and choline [272]. As a result, this deletion mutant should not be capable of degrading ACh.

The analysis of dopamine levels (Figure 16A) revealed 2.18 ± 0.19 ng DA per mg protein in wildtype worms and 2.26 ± 0.15 ng DA per mg protein in ace-1Δ::ace-2Δ deletion mutants. cat-2Δ worms displayed 0.11 ± 0.04 ng DA per mg protein or 0.54 nM DA in sample extracts; thus, DA levels were significantly lower compared to wildtype worms. This demonstrates that cat-2Δ worms do not suffer a total loss of DA, but nevertheless present a very low level of DA, which is higher than the LOD, but lower than the LOQ. As a result, cat-2Δ worms exhibited 95% less DA compared to wildtype worms. The quantification of SRT revealed no differences in the deletion mutants used compared to wildtype worms. SRT levels (Figure 16B) amounted to 0.067 ± 0.012 ng SRT per mg protein in wildtype worms, 0.063 ± 0.006 ng SRT per mg protein in cat-2Δ worms and 0.067 ± 0.009 ng SRT per mg protein in ace-1Δ::ace-2Δ worms. Wildtype worms contained 196 ± 30 ng GABA per mg protein (Figure 16C). Interestingly, cat-2Δ worms displayed a significantly lower amount of 121 ± 9 ng GABA per mg protein, whereas the deletion mutant ace-1Δ::ace-2Δ had the lowest amount of 104 ± 4 ng GABA per mg protein, which significantly differed compared to wildtype worms. The next neurotransmitter we quantified was ACh (Figure 16D); 6.24 ± 0.64 ng ACh was contained per mg protein in wildtype worms and 4.97

ng ACh per mg protein in cat-2Δ worms, representing a slight decrease, although it was statistically indistinguishable from wildtype worms. In contrast, the deletion mutant ace-1Δ::ace-2Δ contained a significantly higher amount of ACh compared to wildtype worms, with 113 ± 9 ng ACh per mg protein. Thus, ace-1Δ::ace-2Δ worms contained 18-fold greater ACh levels compared to wildtype worms.
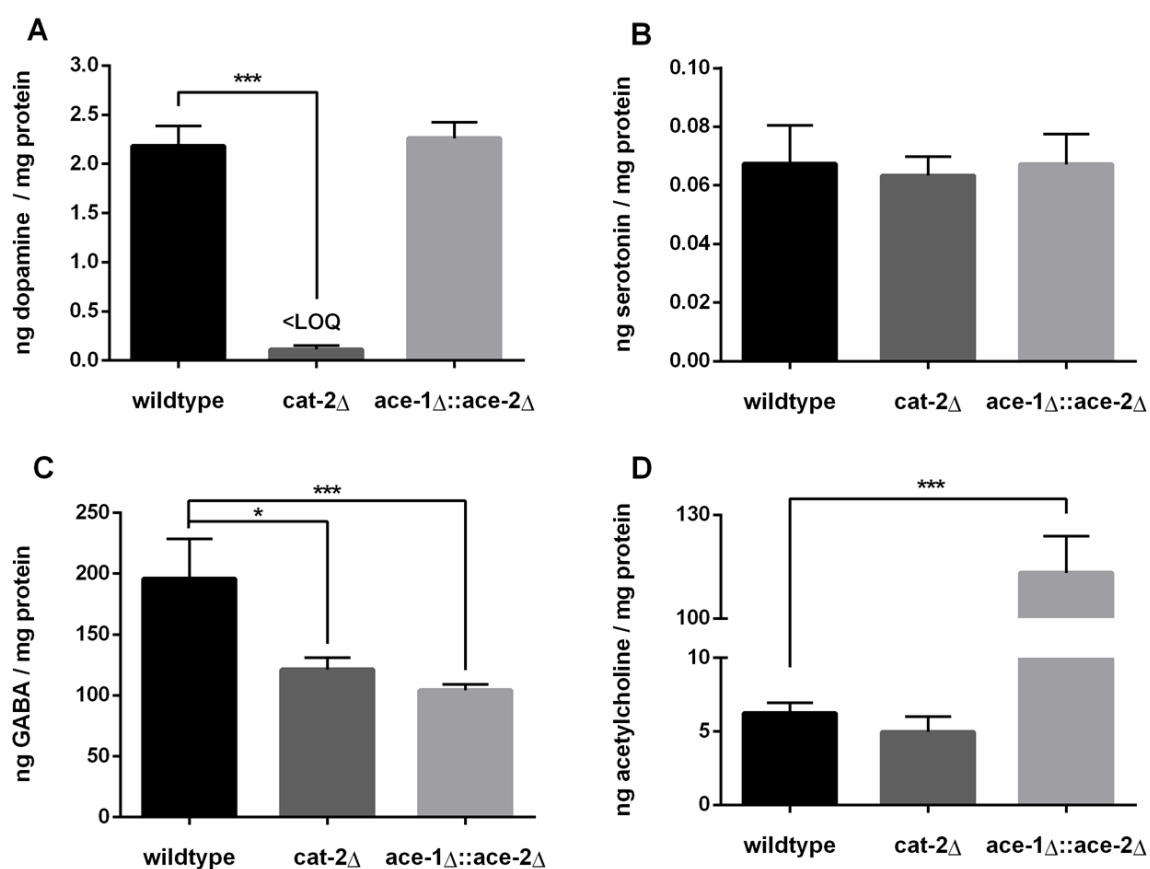
Figure 16: Levels in ng per mg protein of dopamine (**A**), serotonin (**B**), GABA (**C**) and acetylcholine (**D**) in L4 stage worms (wildtype, cat-2Δ and ace-1Δ::ace-2Δ) quantified via LC-MS/MS. Data presented are mean values of $n = 4$ independent experiments + SEM. Statistical analysis using unpaired t-test. Significance levels with $\alpha = 0.05$: *: $p \leq 0.05$ and ***: $p \leq 0.001$ compared to wildtype worms.

3.2.5. Aldicarb-Induced Paralysis Assay

To investigate the consequences of our findings regarding the neurotransmitter quantification of the two deletion mutants, cat-2Δ and ace-1Δ::ace-2Δ, compared to wildtype worms, a classical applied behavioral assay was performed. Aldicarb is an AChE inhibitor, which leads to an accumulation of ACh, and therefore to a persistent activation of muscles followed by paralysis. The aldicarb-induced paralysis assay examines alterations in the synaptic transmission of *C. elegans* [273]. Aldicarb resistance, compared to wildtype worms, results in decreased synaptic transmission. By implication, aldicarb hypersensitivity leads to increased synaptic transmission [274].

Results are presented in Figure 17 and demonstrate the paralysis rate in all three tested worm strains over a time span of 240 min. The cat-2Δ strain showed an earlier onset of paralysis compared to wildtype worms, with only 65% ± 14% of worms moving after 60 min (wildtype: 74% ± 7%) and 15% ± 8% after 120 min (wildtype: 22% ± 7%) when exposed to aldicarb, but the difference did not attain statistical significance. ace-1Δ::ace-2Δ worms, in contrast, showed significant aldicarb resistance compared to wildtype worms, with 94% ± 2% of worms moving after 60 min and 45% ± 10% after 120 min of aldicarb exposure. Taken together, these findings establish that the loss of AChE leads to reduced synaptic transmission in *C. elegans* due to aldicarb resistance.
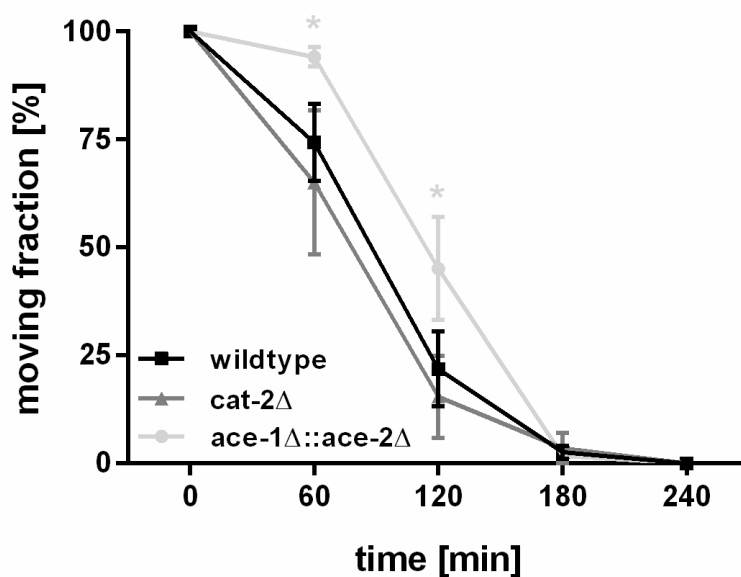
Figure 17: Aldicarb-induced paralysis assay in wildtype worms (black), cat-2Δ (dark grey) and ace-1Δ::ace-2Δ (light grey) deletion mutants. Displayed are fractions of moving worms [%] plotted against assay procedure times [min]. Data presented are mean values of n = 4 independent experiments ± SEM. Statistical analysis using unpaired t-test. Significance levels with α = 0.05: *: $p \le 0.05$ compared to wildtype worms at the same time point.

3.3. Discussion

Tight regulation of the neurotransmitters is required to avoid adverse consequences of deficiency or excess, since various neurological diseases are characterized by a disturbed neurotransmitter homeostasis. Diseases associated with dysregulated neurotransmitters include PD, AD or depression, among others [275]. In this context, it is important to underline that in most clinical disorders, more than a single neurotransmitter is altered in its homeostasis [184,276]. Therefore, we have developed an LC-MS/MS-based method to simultaneously quantify multiple neurotransmitters within a single sample and run, which allows the quantification of DA, SRT, GABA and ACh, as well as the identification of potential changes in neurotransmitter ratios. It is important to note that this, to our knowledge, is the first method proposed to quantify multiple neurotransmitters, especially GABA and ACh, in *C. elegans*. To verify the optimized and validated method, we took advantage of the fact that

57

C. elegans is easily genetically manipulated, and used worms that cannot synthesize DA (cat-2Δ) or degrade ACh (ace-1Δ::ace-2Δ), analyzed their neurotransmitter profiles, and characterized their impacts on synaptic transmission by a further independent assay, which refers to classically performed behavioral assays.

Our method for neurotransmitter quantification distinguishes itself from other published MS-based methods given its advantages. First, only a low quantity of worms is necessary for an analysis. Furthermore, there is only minimal sample preparation required, as the extraction buffer has been optimized regarding pH and organic modifiers for all analytes, so further time-consuming extraction steps are not required. The pH value of the buffer used is particularly important for neurotransmitter extraction, since DA autoxidizes easily at a neutral pH value [277], and extraction must therefore take place in an acidified milieu. GABA, on the other hand, displayed the best extraction in the neutral to slightly acidic pH range, with the result that we found a good compromise of pH = 4 for maximal extraction, which provides a higher overall sensitivity. The limits of detection for all analytes in matrix are in the very low nM range, which is advantageous compared to other LC-MS-based methods for the quantification of neurotransmitters in other matrices, as well as in standard solutions only [267,269,278,279]. Tufi *et al.* present an LOQ for SRT of 1.7 nM in zebrafish *Danio rerio*, which is roughly comparable to our data, whereas for other neurotransmitters like DA and GABA, two-digit nM quantification limits are displayed [269]. Huang *et al.* and Wang *et al.*'s LOQ for GABA in mice brain tissue is lower than that presented by us at 10 nM; however, their LOQs for DA and SRT are above 1 nM, and thus higher than those demonstrated in our study [247,278]. Olesti *et al.* demonstrate LOQs in the two-digit nM range in rat plasma and brain homogenates [279], while in Blanco *et al.*'s study, the average values of DA and ACh in mouse cerebrospinal fluid are below the LOQ [248]. However, the sensitivity is increased enough in the presently evaluated method to quantify

the four neurotransmitters in a few 100 worms, which would allow high-throughput analyses in order to identify, for example, neurotoxic or neuroprotective substances. The method also offers high accuracy, as we use the respective isotope-labeled standards for each analyte throughout the entire sample preparation to compensate for losses in recovery and allow for an unequivocal identification of the neurotransmitters. The use of isotope-labeled standards is also a special feature of this method, which is often unconsidered [247,268,280]. Another advantage that underlines the specificity of our method is the use of a tandem mass spectrometer. The fragment pattern, characterized by the *m/z* ratios of the precursor ion and fragment ions, is as unique as a fingerprint for each molecule [281] and enables us to specifically identify our targeted analytes, rather than using retention times only. Other types of detection, such as quantification by fluorescent dyes [263–265], are less specific than the method described herein. Neurotransmitter quantification by HPLC with fluorescence detection is also both less specific and less sensitive, since it is necessary to derivatize the analytes into a fluorescent product. In addition, external calibration is commonly necessary [261,262]. In addition, other methods, such as that proposed by Zhang *et al.*, combine precolumn derivatization with LC-MS/MS analysis to increase the specificity and sensitivity [282]. This provides LOQs in the single-digit nM range comparable to those produced by our method, but an additional derivatization step must be performed, which bears a further opportunity for error and takes another 30 min.

The roundworm *C. elegans* has become a prominent model organism and multipurpose tool to study neurotoxicity. Since only very few neurodegenerative diseases are linked to genetic factors, growing evidence strongly implicates environmental factors in their respective etiology. Therefore, the worm, with its existing neurodegenerative disease models (mostly transgenic worms), offers the opportunity for testing potential neurodegenerative substances and treatments, which may reflect or even accelerate the progression of

neurodegenerative disorders. The quantification of neurotransmitter levels allows for precise identification of mechanisms that mediate neurotoxicity, and identifies putative targets for efficient therapeutic approaches and neuroprotective strategies. A special feature of *C. elegans* is its short life cycle, which allows a huge sample quantity in a short time period, and in combination with the presented analysis offers an effective high-throughput method. A further advantage of the worm is its completely sequenced genome, allowing its simple genetic manipulation. As a result, especially for neurobehavioral assays, chemicals or toxins are often not used as positive controls; rather, worms with specific mutations are. A commonly used assay is the basal slowing response, which examines dopamine-dependent behavior in the presence of food [175]. cat-2Δ worms are a popular positive control, since they show reduced food sensing due to its deficiency in DA synthesis [283,284]. Mutations of *C. elegans* are also often used to model neurodegenerative diseases like PD [251] and AD [253]. Despite the extensive use of mutants of this worm in neurobehavioral assays, its neurotransmitter profile has not been characterized, to our knowledge. Despite the usage of behavioral assays and the microscopy of fluorescence-tagged neurons, only a few chromatographic approaches have been carried out in *C. elegans* to quantify DA. Only Schumacher et al. displayed a validated LC-MS/MS-based method to analyze DA and SRT in *C. elegans*, but they excluded GABA and ACh [38], which are, however, essential for the investigation of neurotoxicity [242,285]. Using our method, we were able to determine neurotransmitter profiles in wildtype worms, as well as in cat-2Δ and ace-1Δ::ace-2Δ worms. As suggested in the literature, cat-2Δ worms had lesser DA levels compared to wildtype worms, which was corroborated by our LC-MS/MS method. In addition, we could also identify altered GABA levels. The same applied to ace-1Δ::ace-2Δ worms, wherein we could detect increased ACh levels as expected, but also reduced GABA levels, which underlines the interdependence and homeostatic dependence of different neurotransmitters. Muñoz *et al.* demonstrated interactions between the dopaminergic and

serotonergic systems in PD [286]. Qi *et al.* reported how different neurotransmitters modulate neurotransmitter balance, and therefore regulate the function of different brain regions [245]. This emphasizes the importance of simultaneously quantifying multiple neurotransmitters, which has been achieved with this LC-MS/MS-based method. In contrast, behavioral assays do not constitute quantitative methods, but merely provide an insight into the consequences of an eventual neurotransmitter dyshomeostasis. It is noteworthy that the combination of instrumental analytics (especially mass spectrometry) and behavioral assays complement each other remarkably well. Therefore, the worm strains mentioned above were subjected to the aldicarb-induced paralysis assay in addition to neurotransmitter quantification.

Aldicarb, an AChE inhibitor, promotes the accumulation of ACh in locomotor neuromuscular junctions in *C. elegans* [287]. This results in hyperexcitability and excessive muscle contraction, causing paralysis [288]. If a mutant strain displays higher ACh levels, it should undergo paralysis faster. However, it has been shown that not only ACh itself is involved in aldicarb-induced paralysis, but the entire cholinergic system. Upon aldicarb treatment, mutants with impaired cholinergic function accumulate synaptic ACh at a slower rate, resulting in slower paralysis, and therefore aldicarb resistance, compared to wildtype worms [289].

This is consistent with our data, where ace-1Δ::ace-2Δ mutants showed a slower onset of paralysis, which was also demonstrated by Oppermann and Chang [290]. Hypothetically, it is not an increase in total ACh levels that leads to the onset of paralysis, but increased ACh levels in the neuromuscular junction. Giles *et al.* [289]reported that worms with disrupted inhibitory GABA function had a faster paralysis rate due to a loss of relaxation. Thus, given the GABA deficiency, cat-2Δ worms should paralyze faster in the presence of aldicarb compared to wildtype worms, which does not appear to be the case. It appears that behavior is a not fully understood yet complex construct in

C. elegans, and further research is required to understand the underlying mechanisms of behavioral assays like the aldicarb-induced paralysis assay. This underscores that the combination of behavioral assays for *C. elegans* and the quantitative and validated methods such as the LC-MS/MS-based method developed herein provide the means for altered functional characterization along with its underpinning mechanisms. It is also noteworthy that the behavioral assays mentioned are species-specific, in this case *C. elegans*-specific. However, our LC-MS/MS method for the quantification of neurotransmitters is universally applicable and can be applied to other model systems and tissues in the future with the eventual adaption of sample preparation.

3.4. Materials and Method

3.4.1. *C. elegans* Handling and Cultivation

C. elegans strains Bristol N2 (wildtype) and deletion mutants (Δ) CB1112 (cat-2Δ) and GG201 (ace-1Δ::ace-2Δ) were obtained from the Caenorhabditis Genetics Center (CGC, Minneapolis, MN, USA), which is funded by the National Institutes of Health Office of Research Infrastructure Programs. Cultivation of *C. elegans* was maintained on 8P agar plates coated with the *Escherichia coli* (*E. coli*) strain NA22 at 20 °C as previously described [291,292]. To generate age-synchronous worm populations, gravid adults were treated with bleach solution (1% NaOCl and 0.5 M NaOH) to release eggs, which were allowed to hatch overnight in M9 buffer. Synchronous L1-stage larvae were placed on nematode growth (NGM) agar plates coated with *E. coli* strain OP50 for 48 h to reach L4 stage.

3.4.2. Neurotransmitter Standard Solutions

Dopamine hydrochloride (Alfa Aesar, Kandel, Germany) and 2-(3,4-dihydroxy-phenyl)ethyl-1,1,2,2-d4-amine HCl (DA$_{d4}$) (CDN Isotopes, Pointe-Claire, Canada) were dissolved in 200 mM HClO$_4$ (Sigma-Aldrich, Steinheim, Germany), whereas γ-aminobutyric acid (Sigma-Aldrich, Steinheim, Germany)

and 4-aminobutyric-2,2,3,3,4,4-d6 acid (GABA$_{d6}$) (EQ Laboratories GmbH, Augsburg, Germany) stock solutions were prepared in 10% methanol (MeOH) (LC-MS grade, Thermo Fisher Scientific, Waltham, MA, USA). Serotonin hydrochloride (Alfa Aesar), serotonin-α,α,β,β-d4 creatinine sulfate complex (SRT$_{d4}$) (CDN Isotopes, Pointe-Claire, Canada), acetylcholine chloride (Sigma-Aldrich, Steinheim, Germany) and acetylcholine-1,1,2,2-d4 chloride (ACh$_{d4}$) (EQ Laboratories GmbH, Augsburg, Germany) were dissolved in bidistilled water. The deuterated analogue of the respective neurotransmitter was taken as an internal standard.

3.4.3. Sample Preparation and Neurotransmitter Extraction

Synchronous L4 stage wildtype, cat-2Δ and ace-1Δ::ace-2Δ worms were washed off from NGM agar plates using 85 mM NaCl + 0.01% Tween. The washing procedure was repeated three times to ensure samples were free of *E. coli*. Of each respective strain, 3000 worms were pelletized in 50 µL 85 mM NaCl by centrifugation at 380 g, frozen in liquid nitrogen and stored at −80 °C. Extraction buffer (2 mM sodium thiosulfate, 2.5 mM HClO$_4$, 10% MeOH LC-MS grade, 25 mM DA$_{d4}$, 25 mM SRT$_{d4}$, 25 mM ACh$_{d4}$ and 500 mM GABA$_{d6}$) was freshly prepared right before sample preparation. Samples were kept on ice during sample preparation and extracted samples were analyzed immediately by LC-MS/MS. In the first step, worm pellets were defrosted and 100 µL extraction buffer was added, as well as zirconia beads (biolab products, Bebensee, Germany). To homogenize the samples: 4× freeze–thaw cycles (1 min 37 °C, 1 min liquid nitrogen) followed by 4 × 20 sec bead beating by usage of a Bead Ruptor (biolab products, Bebensee, Germany). After centrifugation for 10 min at 16,060 × *g* at 4 °C, 100 µL of the supernatant was transferred to a Spin-X® Centrifuge Tube Filter 0.22 µm (Corning, Amsterdam, The Netherlands) and centrifugation was repeated. An aliquot was transferred to a vial with insert and analyzed via LC-MS/MS, while the rest was used for

protein quantification for normalization measured by bicinchoninic acid assay [293].

3.4.4. LC-MS/MS Parameters

All analyses were conducted using an Agilent 1290 Infinity II liquid chromatography system (Agilent, Waldbronn, Germany) coupled with a Sciex QTRAP 6500+ triple quadrupole mass spectrometer (Sciex, Darmstadt, Germany) interfaced with an electrospray ion source, which operated in positive ion mode. Chromatographic separation was performed using a YMC-Triart PFP (pentafluorophenyl) column (3 µm, 3 × 150 mm) and an additional precolumn (3 µm, 3 × 10 mm) of the same column material. The elution of neurotransmitters was carried out with bidistilled water + 10 mM formic acid (FA) (LC-MS grade, Thermo Fisher Scientific, Waltham, MA, USA) and acetonitrile (ACN) (LC-MS grade, VWR, Darmstadt, Germany) + 10 mM FA. Three µL of the sample was injected. Analytes were eluted with a flow of 0.425 mL min^{-1} from the column, which was pre-heated to 30 °C. Total run time was 12 min, which was divided in a gradient with 0% ACN for 3 min, 0 to 60% ACN for 6 min, 60 to 100% ACN for 0.5 min, 100% ACN for another 0.5 min, 100 to 0% ACN for 0.5 min and 0% ACN for re-equilibration for 1.5 min. Analysis was carried out in scheduled multiple reaction monitoring (sMRM) mode with detection windows of ±40 sec of the respective retention times (Table 4). Ion source parameters optimization was performed with standard solutions of DA, SRT, GABA and ACh using the Compound Optimization software wizard of the Sciex Analyst Software (Version 1.7.2). The following parameters were determined: ion spray voltage = 4000 V, curtain gas (N2) = 40 psi, nebulizer gas = 60 psi, drying gas = 50 psi, collision (CAD) gas = medium, temperature = 600 °C, entrance potential = 10 V. The dwell time for all analytes and deuterated standards was set to 20 ms. Mass transitions for the analytes and internal standards as well as the respective optimized collision energy (CE), declustering potential (DP) and collision cell exit potential (CXP) are listed in Table 4.

3.4.5. Method Validation

Method validation was carried out according the "ICH guideline Q2(R2) on validation of analytical procedures" of the European Medicines Agency. Linear range, limit of detection (LOD), limit of quantification (LOQ), recovery, accuracy and intraday and interday precision were assessed for method validation. To investigate linear ranges, LODs and LOQs, solutions with fixed amounts of matrix (wildtype) and deuterated internal standards were added with neurotransmitter standards in a range of 0–500 nM for DA, SRT and ACh and 0–10 µM for GABA, and analyzed twice. Peak areas of the analytes were normalized to the respective internal standards, plotted against the added concentrations and afterwards examined for linear correlation. Signal-to-noise ratios (S/N) were calculated using Multiquant Software (Sciex, Version 3.0.3) and plotted against the added concentrations; the slopes were determined subsequently. LOD and LOQ were defined as $LOD = 3 \times SD_y/b$ (SD_y = standard deviation of analyte concentration in ≥12 blank measurements, b = slope of calibration curve) and $LOQ = 10 \times SD_y/b$. To assess the recovery of the deuterated internal standards in matrix, eight samples containing extraction buffer only and eight samples with worm matrix in extraction buffer were analyzed. Recovery was defined as the ratio of the area of internal standards with to that without matrix. For accuracy, matrix-free samples with low (25 nM), middle (250 nM) and high (2.5 µM) amounts of all neurotransmitters added along with 250 nM of deuterated standards were analyzed twelve times. Accuracy was calculated in percent by how much of the neurotransmitters was actually detected. To determine precision, intraday variation of eight wildtype worm samples pelletized and analyzed on the same day, and interday variation of six wildtype worm samples, each pelletized and analyzed on six different days, were assessed. Samples were normalized for protein content for examination of intraday as well as interday precision. Precision is stated as relative standard deviation in percent (RSD%) of the above-mentioned samples.

3.4.6. Aldicarb-Induced Paralysis Assay

Synchronous L1 stage worms were placed on NGM plates as mentioned above for 72 h until the young adult stage. The assay was performed based on Mahoney et al. [27]. In brief, a 100 mM aldicarb (Sigma-Aldrich, Steinheim, Germany) stock solution was prepared in 70% ethanol. For plates with 2 mM aldicarb, NGM agar was set up as previously described [270,271] and added with aldicarb for desired concentration. Three mL portions were poured into 3.5 cm petri dishes and stored at 4 °C. The plates were coated at the very beginning of the experiment with 2 μL of *E. coli* strain OP50 to concentrate worms in the middle of the plates. The assay was always performed as a blinded experiment. Of each genotype, 20–25 worms were placed on an aldicarb-containing plate, which were left at room temperature during the assay procedure. Every 60 min, the number of total and paralyzed worms was counted. Worms were defined as paralyzed if they demonstrated no movement after prodding carefully with a platinum wire against head and tail.

3.4.7. Statistics

Statistical analysis was performed using GraphPad Prism 6 (GraphPad Software, La Jolla, CA, USA) via unpaired *t*-test. Significance levels with $\alpha = 0.05$ are depicted as *: $p \leq 0.05$, **: $p \leq 0.01$ and ***: $p \leq 0.001$, compared to wildtype worms.

3.5. Conclusion

In summary, here (1) we developed a novel liquid chromatography–tandem mass spectrometry (LC-MS/MS) method, which enables simultaneous neurotransmitter quantification of dopamine (DA), serotonin (SRT), γ-aminobutyric acid (GABA) and acetylcholine (ACh) in the nematode, *C. elegans*, an assay (2) which can readily be applied to other matrices. (3) Furthermore, the LC-MS/MS method combined with isotope-labeled standards provides exquisite sensitivity and specificity, (4) providing a validated

analytical method for the assessment of altered neurotransmission and neurotoxicity. Our analytical method allows the quantification of neurotransmitters and their ratios as a convenient tool for the identification of mechanisms that mediate neurotoxicity, and it should be helpful in identifying possible putative therapeutic approaches and targets. Neurotoxicity assessment in *C. elegans* is commonly carried out by behavioral assays, which provide a sensitive assay for altered neurological behaviors, but are unable to characterize neurotransmitter levels. Other than *C. elegans* species-specific behavioral assays, our method is equally applicable to other tissues and matrices.

3.6. Author Contributions

Conceptualization, A.-K.W., L.K. and J.B.; methodology, A.-K.W. and L.R.; validation, A.-K.W.; formal analysis, A.-K.W.; investigation, A.-K.W.; data curation, A.-K.W.; writing—original draft preparation, A.-K.W.; writing—review and editing, L.K., T.S., M.A. and J.B.; visualization, A.-K.W.; supervision, J.B.; project administration, J.B.; funding acquisition, J.B. and T.S. All authors have read and agreed to the published version of the manuscript.

3.7. Funding

3.8. Data Availability Statement

The data that support the findings of this study are available from the corresponding author upon reasonable request.

3.9. Key words

Mass spectrometry; liquid chromatography; neurotransmitters; neurodegenerative diseases; *C. elegans*

Abstract

Copper (Cu) is an essential trace element, however an excess is toxic due to its redox properties. Cu homeostasis therefore needs to be tightly regulated via cellular transporters, storage proteins and exporters. An imbalance in Cu homeostasis has been associated with neurodegenerative disorders such as Wilson's disease, but also Alzheimer's or Parkinson's disease. In our current study, we explored the utility of using *Caenorhabditis elegans* (*C. elegans*) as a model of Cu dyshomeostasis. The application of excess Cu dosing and the use of mutants lacking the intracellular Cu chaperone atox-1 and major Cu storage protein ceruloplasmin facilitated the assessment of Cu status, functional markers including total Cu levels, labile Cu levels, Cu distribution and the gene expression of homeostasis-related genes. Our data revealed a decrease in total Cu uptake but an increase in labile Cu levels due to genetic dysfunction, as well as altered gene expression levels of Cu homeostasis-associated genes. In addition, the data uncovered the role ceruloplasmin and atox-1 play in the worm's Cu homeostasis. This study provides insights into suitable functional Cu markers and Cu homeostasis in *C. elegans*, with a focus on labile Cu levels, a promising marker of Cu misregulation during disease progression.

Chapter 4 – Dysfunction in atox-1 and ceruloplasmin alters labile Cu levels and consequently Cu homeostasis in *C. elegans*

Chapter 4 – Dysfunction in atox-1 and ceruloplasmin alters labile Cu levels and consequently Cu homeostasis in *C. elegans*

4.1. Introduction

The essential trace element and micronutrient copper (Cu) functions as a catalytic cofactor for a variety of enzymes in biological processes, including mitochondrial respiration and the synthesis of biocompounds [163]. Cu is widely used in industry and agriculture, both a major contributor of soil and water pollution [294,295]. An excess in Cu (beyond the physiological need) can be harmful to organisms due to its redox properties and the ability to promote the formation of reactive oxygen species (ROS) [296]. In humans, altered Cu levels lead to oxidative stress and in consequence can result in the onset of neurodegenerative disorders [297], as well as cancer [298]. Therefore, the tightly controlled homeostasis of Cu levels is of importance to cellular and organismal well-being [299]. Mammals and other organisms are therefore endowed with a complex network of proteins which are involved in the regulation of Cu homeostasis. These proteins work in concert to coordinate the import, export and intracellular utilization of Cu, thus maintaining cellular levels within a specific range, thereby preventing the consequences of Cu overload [163]. The reduced form of Cu (Cu^+) enters the cell mainly in via a high affinity copper uptake protein (CTR-1) dependent on intracellular Cu levels [300], while oxidized Cu^{2+} is taken up via the divalent metal transporter 1 (DMT-1) [54] (Figure 18). Antioxidant protein 1 (ATOX-1), a Cu metallochaperone protein which obtains Cu from CTR-1, engages in the intracellular transport of Cu to target organelles such as the nucleus or golgi [56]. As Cu serves as cofactor for a variety of mitochondrial enzymes, cytochrome c oxidase copper chaperone (COX-17) regulates mitochondrial Cu import [57]. The major Cu-carrier in the

blood is the multifunctional protein ceruloplasmin, which stores up to 90% of total Cu [58] and displays ferroxidase activity [103]. Furthermore, ceruloplasmin serves as an extracellular scavenger for reactive species and therefore limits oxidative damage [103]. Likewise, metallothioneins bind metal ions like cadmium, zinc and Cu for detoxification and protection against oxidative stress [59]. Cu excretion is mediated by ATP7B, which either delivers Cu to ceruloplasmin [62] for subsequent elimination via the bile [301] or translocates from the golgi to the plasma membrane to efflux Cu via vesicular sequestration [302,303].
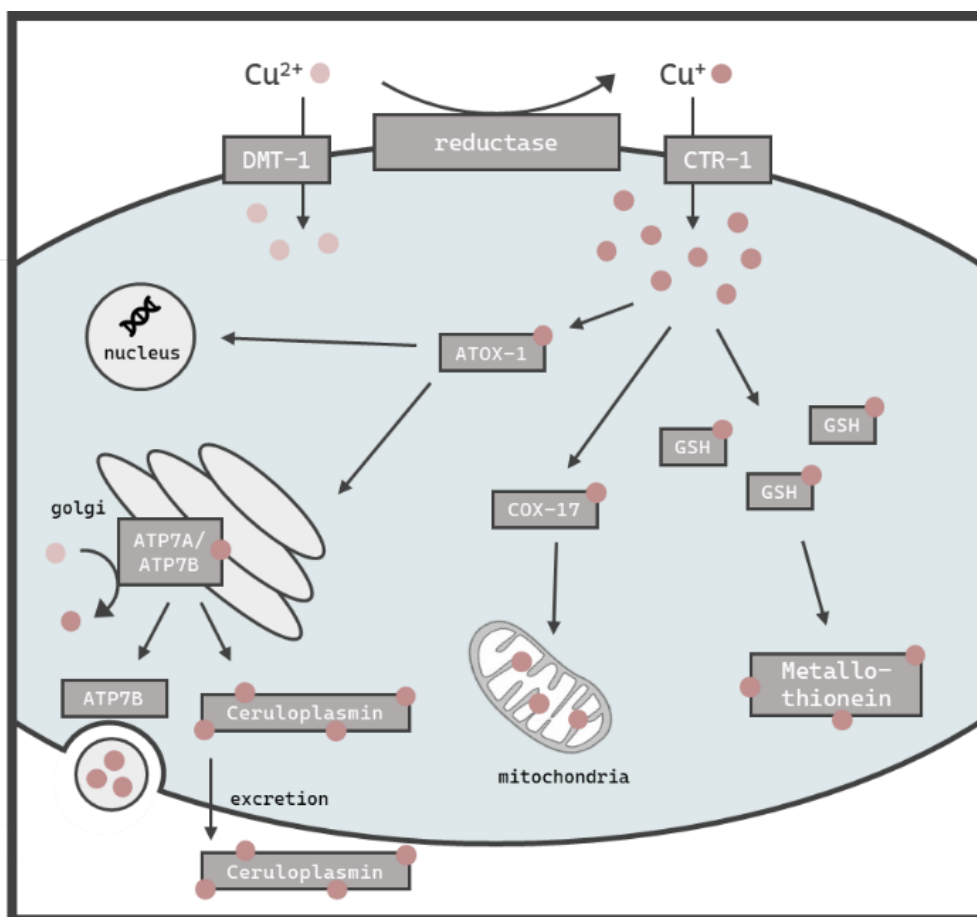
Figure 18: Schematic overview of the assumed intracellular Cu import, distribution, storage and excretion in *C. elegans*. Cu is taken up primarily as Cu^+ via CTR-1 or alternately as Cu^{2+} via DMT-1. ATOX-1 mediates Cu distribution to the golgi, nucleus or mitochondria via COX-17. GSH and metallothionein is thought to be involved in the chelating of excess Cu, while the majority is stored in the ceruloplasmin. The efflux of excess Cu is mediated by ATP7B via vesicular sequestration.

To date, serum or plasma Cu status is derived solely by determining total Cu or ceruloplasmin levels [94,304]. Cellular copper is partitioned between tightly-bound pools in cuproenzymes, which bind copper with K_d values in the 10^{-15} M and tighter, and labile pools, defined as loosely bound to low-molecular weight ligands with K_d values that are orders of magnitude weaker, typically in the 10^{-10} to 10^{-14} range, which can regulate diverse transition metal signaling processes [109,165,305–308]. The labile Cu fraction provides an estimation of Cu activity and may thus serve as a better functional marker than total Cu as Cu participates in transition metal signaling pathways beyond traditional roles in metabolism [309,310]. Indeed, labile Cu was recently identified as a marker for the Cu status in human serum [83,311]. This study aims to further our knowledge base regarding Cu homeostasis and dyshomeostasis, with a particular focus on labile Cu levels. This will shed light on the regulatory mechanisms involved when an organism is challenged with an oversupply of total Cu and/or labile Cu, respectively. For this purpose, we use the model organism *Caenorhabditis elegans* (*C. elegans*), which is an *in vivo* invertebrate model organism suitable to study metal homeostasis and toxicity [312]. An additional advantage of using *C. elegans* is the wide range of available deletion (Δ) mutants. Although the metallomic underpinning of Cu homeostasis in *C. elegans* shares many homologies to mammals, studies using the nematode in research on Cu homeostasis are scarce [64,65,68]. Here, we studied Cu dyshomeostasis by excess Cu feeding as well as by using models displaying genetic Cu disbalance, such as the mutant ceruloplasminΔ, which lacks the major Cu storage protein, as well as an atox-1Δ mutant. Taken together, we define the role of ceruloplasmin and atox-1 in Cu homeostasis and identify suitable functional markers in the model *C. elegans*.

4.2. Materials and Methods

4.2.1. *C. elegans* handling and Cu treatment

C. elegans strain Bristol N2 (wildtype) and deletion mutants *mtl-1*(gk125) obtained from the Caenorhabditis Genetics Center (CGC, Minneapolis, USA), which is funded by the National Institutes of Health Office of Research Infrastructure Programs. Deletion mutants *atox-1* (tm1220), *mtl-1*(tm1770) and the ceruloplasmin mutant (tm14205) were obtained from the Mitani laboratory at Tokyo Women's Medical University. Worm strains *mtl-1;mtl-2*(zs1), and P*mtl-1*::GFP and P*mtl-2*::mcherry (integrated into the genome by Mos1-mediated single-copy insertion (MosSCI)) were generated by the Stephen Stürzenbaum laboratory. Note, the P*mtl-2*::mcherry strain contained an addition nuclear localization signal (NLS). All strains were cultivated on agar plates coated with *Escherichia coli* (*E. coli*) at 20 °C as previously described [292]. Worms were synchronized as described in [313] and placed on NGM plates until L4 larval stage. L4 stage worms were treated with copper-enriched inactivated *E. coli* (OP50) on NGM plates for 24 hours. The bacteria were inactivated for 4 h at 70 °C [314]. Stock solutions of $CuSO_4$ (≥99.99%, Sigma Aldrich) were prepared fresh in bidistilled water.

4.2.2. lethality studies after Cu exposure

For lethality testing, worms were counted manually as alive or dead after 24 h of Cu exposure. Worms were defined as dead if they demonstrated no movement after prodding with a platinum wire.

4.2.3. Total Cu quantification via ICP-OES

Total Cu content in worms was quantified using inductively coupled plasma-optical emission spectrometry (ICP-OES) (Avio 220 Max, Perkin Elmer). Following 24 h Cu exposure, 1000 worms per condition were washed 4x using 85 mM NaCl + 0.01 % Tween 20, pelleted by centrifugation, frozen in liquid nitrogen and stored at -80 °C. Pellets were homogenized using an ultrasonic

probe (UP100H, Hielscher) and subsequently dried at 95 °C. Yttrium (Y) (ROTI®STAR, Carl Roth) was added as internal standard and the samples were digested at 95 °C using 500 µL of a 1:1 mixture (v:v) of HNO_3 (Suprapur®, Merck KGaA) and H_2O_2 (for ultratrace analysis, Sigma Aldrich) and re-dissolved in 2% HNO_3. The following parameters were used for measurements: Plasma power: 1500 W, cooling gas: 8 L/min, auxiliary gas: 0.2 L/min, nebulizer (MicroMist™) gas: 0.7 L/min, wavelengths: Cu – 327.939 and Y – 371.029. The analysis was performed using external calibration (multi element mix (spectec-645) + Y) and verified by measuring certified reference material BCR®-274 (Single cell protein, Institute for Reference Materials and Measurement of the European Commission) and SRM®-1643f (Trace Elements in Natural Water, National Institute of Standards and Technology). The Cu content was normalized to the protein amount determined using a BCA assay [293] using bovine serum albumin (Sigma Aldrich) for external calibration.

4.2.4. Quantification of labile Cu by fluorescent dye CF4

Labile Cu levels were assessed using the fluorescent dye Copper Fluor-4 (CF4), which has an apparent K_d value of 2.9×10^{-13} M for a 1:1 copper:probe stoichiometry that is well-matched to monitor labile Cu pools by reversible Cu binding without depleting the total Cu stores [108]. Stock solutions were prepared in DMSO (5 mM). Following Cu treatment, worms were exposed to 10 µM CF4 for 3 h in the dark in incubation buffer (25 mM HEPES, 120 mM NaCl, 5.4 mM KCl, 5 mM Glucose, 1.3 mM $CaCl_2$, 1 mM $MgCl_2$, 1 mM NaH_2PO_4, pH=7.35, 0.01 % Tween 20). Thereafter, fluorescence intensity was assessed by either fluorescence microscopy or plate reader measurement. Worms were transferred to 4% agarose pads on microscope slides and anesthetized by 5 mM levamisole (Sigma Aldrich). Fluorescence images as well as intensities were obtained with a DM6 B fluorescence microscope and the Leica LAS X software (Leica Microsystems GmbH) using a triple band excitation filter and constant settings as well as light exposure times. 400 worms per well in

triplicates were transferred into a 96 well plate for plate reader measurements, while another aliquot was stored for protein measurement. Bottom reads were performed using a microplate reader Infinite® M Plex (Tecan) with wavelengths of 415 nm for excitation and 660 nm for emission.

4.2.5. Cu imaging by ToF-SIMS

Worms were incubated with 2 mM $CuSO_4$, following 3x washing steps with 85 mM NaCl and 3x washing steps with Rotipuran Ultra (Carl Roth). Subsequently, about 20 worms per strain were transferred to indium tin oxide (ITO) coated glass slides. In order to locate the 3-dimensional Cu distribution in non-fluorescent-labeled worms, ToF-SIMS 3D depth profiling analysis was performed using an IONTOF "ToF.SIMS[5]". Sputtering was performed using a O_2^+, 2 keV ion beam with a maximum current of 650 nA rastered across 700 × 700 μm^2. Analysis was performed using a Bi_1^+, 30 keV, 0.5 pA ion beam in spectrometry mode, rastered across 500 × 500 μm^2 within the center of the sputter crater. Secondary ions of positive polarity were mass analyzed.

4.2.6. Gene expression via quantitative real-time PCR analysis

Total RNA content was isolated using the Trizol method, published by Bornhorst et al [219], of which 1 μg was transcribed using the High Capacity cDNA Reverse Transcription Kit (Applied Biosystems, Thermo Fisher Scientific) following the manufacturer's protocol. Quantitative real-time PCR was carried out on the AriaMx Real-Time PCR System in duplicate wells for each gene using TaqMan Gene Expression Assay probes (Applied Biosystems, Thermo Fisher Scientific) according the manufacturer's instructions. The *AFDN* homolog *afd-1* was used as housekeeping gene for normalization by the comparative $2^{-\Delta\Delta Ct}$ method [315]. The probes used were: *afd-1* (Ce0241573_m1), *ctr-1* (Ce02417730_g1), *mtl-1* (Ce02551471_s1), *mtl-2* (Ce0251627_s1), *cua-1* (Ce02454392_m1), *cuc-1* (Ce02449329_g1), *f21d5.3/ceruloplasmin* (Ce02456979_m1) and *cox-17* (Ce02442285_m1).

4.2.7. Metallothionein expression

To assess metallothionein expression, mtl-1::GFP and mtl-2::mcherry transgenes were used. After Cu treatment and 4x washing steps with 85 mM NaCl + 0.01 % Tween 20, excess liquid was aspirated to yield 1600 worms in 400 μL. 3x 100 μL were transferred as triplicate into a 96 well plate, the remaining 100 μL were used for protein quantification. Bottom read measurements were conducted at 488 nm (excitation) and 509 nm (emission) for GFP-tagged worms and 561 nm (excitation) and 610 nm (emission) for mcherry-tagged worms using a Tecan microplate reader Infinite® M Plex (Tecan, Switzerland). Additionally, worms were transferred to 4% agarose pads on microscope slides, followed by anesthesia using 5 mM levamisole (Sigma Aldrich). Images were taken using a Leica DM6 B fluorescence microscope (Leica Microsystems GmbH) with constant settings and light exposure time.

4.2.8. Statistical analysis

Statistical analyses were carried out with GraphPad Prism 6 (GraphPad Software, La Jolla, CA, USA). Statistical tests and significance levels are listed in figure captions.

4.3. Results

4.3.1. Lethality after Cu exposure

Lethality testing following 24 h Cu exposure revealed no toxic effect up to 2 mM in wildtype worms, while atox-1Δ and ceruloplasminΔ deletion mutants presented a significant reduction of survival of about 10% after 2 mM Cu treatment (Figure 19). During lethality testing we noticed that worms exposed to 2 mM Cu started to display shortened and thinner phenotype, which indicated the onset of a developmental delay. Concentrations above 2 mM were not considered, since worms were previously shown to avoid higher amounts of Cu, as described in Guo et al. [316] and Munro et al. [317].
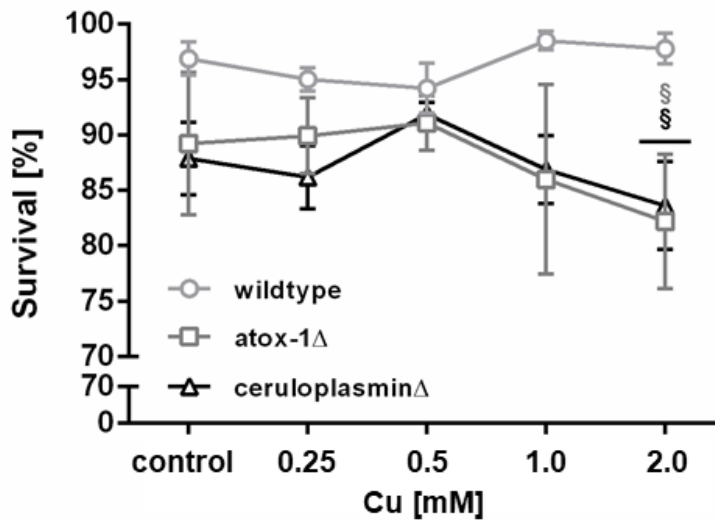
Figure 19: Lethality in wildtype worms, atox-1Δ and ceruloplasminΔ deletion mutants following an exposure to Cu for 24 h at age-synchronized L4 larvae stage. Data presented are mean values of n ≥ 4 experiments ± SEM. Statistical analysis using 2-way ANOVA with Tukey's multiple comparison. Significance level with α = 0.05: §: $p ≤ 0.05$ compared to wildtype in same condition.

4.3.2. Total Cu vs. labile Cu

Following 24 h of treatment with $CuSO_4$-enriched *E. coli* up to 2 mM, total Cu levels of wildtype, atox-1Δ and ceruloplasminΔ deletion mutants were quantified by ICP-OES (Figure 20A). Cu basal levels were indistinguishable in all 3 worm strains with 0.42 ± 0.05 ng Cu per µg protein in wildtype worms respectively. In addition, a concentration-dependent increase in Cu levels was observed for all strains. However, mutants with impaired Cu homeostasis displayed significantly lower total Cu levels than wildtype worms, in particular ceruloplasmin-deficient worms. labile Cu levels were determined by fluorescent dye CF4 (Figure 20B). labile Cu levels tended to be elevated following Cu treatment of wildtype and atox-1Δ worms, furthermore, a higher basal level of labile Cu levels was observed in untreated ceruloplasmin-deficient worms. In general, labile Cu levels appeared to be higher in worms characterized by a disturbed Cu homeostasis (Figure 20C-E).
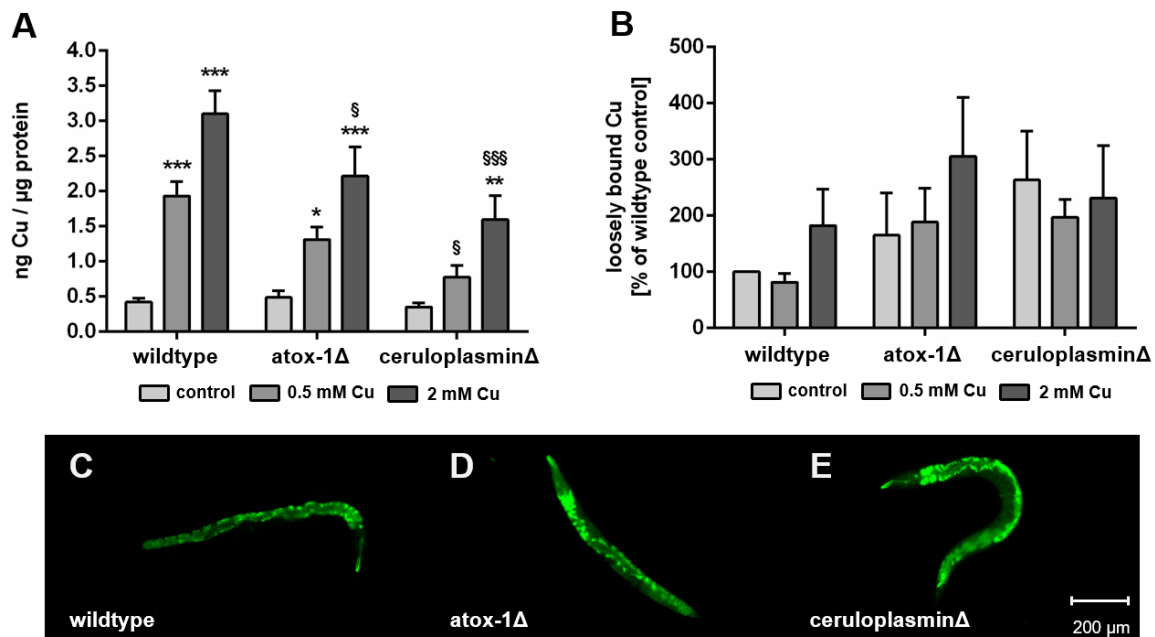
Figure 20: (A) Total Cu levels quantified by ICP-OES and (B) labile Cu levels assessed by using fluorescent dye Copper Fluor-4 (CF4). Displayed are representative images of (C) wildtype worms, (D) atox-1- and (E) ceruloplasmin-deficient worms after CF4 treatment (control, not treated with Cu). Data presented are mean values of $n \geq 4$ independent experiments + SEM. Statistical analysis using 2-way ANOVA with Tukey's multiple comparison. Significance level with $\alpha = 0.05$: *: $p \leq 0.05$; **: $p \leq 0.01$; ***: $p \leq 0.001$ compared to untreated control and §: $p \leq 0.05$ and §§§: $p \leq 0.001$; compared to wildtype in same condition.

4.3.3. Cu imaging and depth profiling by ToF-SIMS

The location of Cu in worms exposed to 2 mM Cu for 24 h was investigated by Time-of-Flight Secondary Ion Mass Spectrometry (ToF-SIMS). 3D depth profiles were created to determine the Cu distribution in relation to the worms' depth. In "dual-beam-mode" of ToF-SIMS depth profiling each sample surface was continuously sputtered by an ion beam (O_2^+), while a second ion beam (Bi^+) was used to image the respective intensity of Cu in the resulting crater surface (Figure 21A). Subsequently, the lateral distribution over the total sputtered depth excluding the first sputter seconds in order to exclude surface contaminants as well as the regional depth profile at the worm positions were calculated from the ToF-SIMS raw data stream. Images of the isotopes $^{63}Cu^+$ and $^{65}Cu^+$ (Figure 21A) were comparable in distribution. Figure 21A shows that the highest Cu intensity

is located in the middle part of the worm corpus for all three strains. The highest Cu intensity was detected in wildtype worms, whereas the ceruloplasmin-deficient worms demonstrated the lowest Cu intensity (Figure 21B).
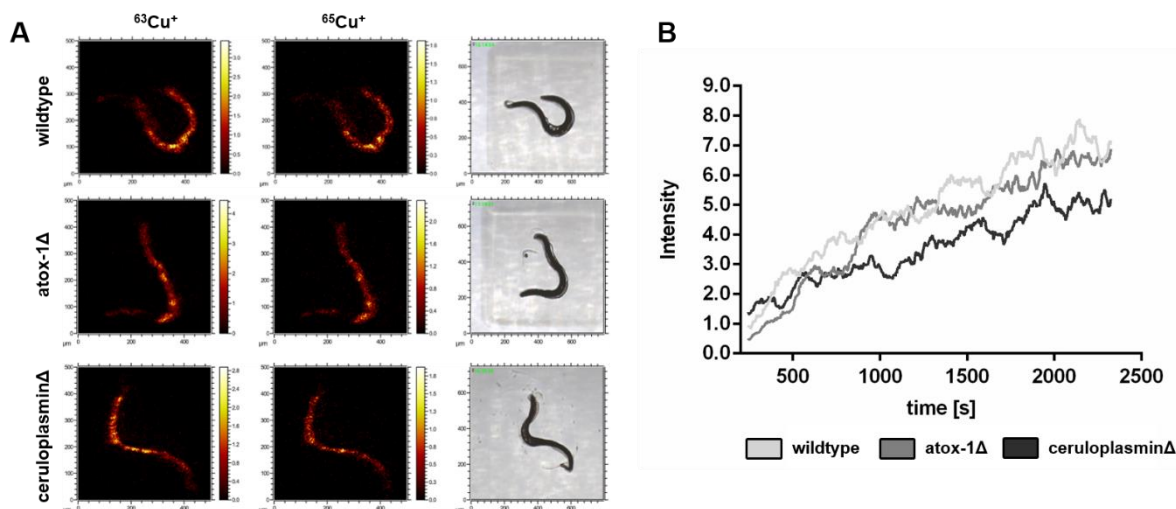
Figure 21: ToF-SIMS analysis of wildtype, atox-1Δ and ceruloplasminΔ worms following 2 mM Cu treatment for 24 h. (A) Distribution of 63Cu+ and 65Cu+ over the total sputtered depth (excluding the first 250 sputter seconds). (B) Depth distribution of 63Cu+ for all 3 worm strains (O2+ sputtering) covering approximately half of the worm's depth.

4.3.4. Gene expression of Cu homeostasis-related genes upon Cu exposure

The relative mRNA levels of Cu transport- and storage-related genes were determined via RT-qPCR in wildtype and mutants treated with Cu for 24 h (Figure 22). Target genes were Cu importer *ctr-1* (ortholog to human high affinity copper uptake protein 1 encoded by *SLC31A1*), cytochrome c oxidase copper chaperone *cox-17*, intracellular transporter *atox-1*, *atp7a/b* (ortholog of human *ATP7A* and *ATP7B*) and storage-related genes *ceruloplasmin*, *mtl-1* and *mtl-2* (orthologs to human metallothionein *MT1A* and *MT2A*). In wildtype worms, Cu treatment resulted in an upregulation of *ctr-1*, while atox-1Δ worms displayed already elevated basal levels. Mitochondrial Cu importer *cox-17* expression was elevated in atox-1Δ deletion mutants at the basal level as also following Cu exposure. *Atox-1* mRNA levels did not increase due to Cu exposure but were

altered in ceruloplasminΔ worms. Mammalian genomes encode for two isoforms per Cu exporter (*ATP7A* and *ATP7B*), whilst *C. elegans* carries only a single gene of *atp7a/b*, albeit with high sequence similarity to human homologs [64]. Cu treatment lead to an increase in *atp7a/b* mRNA levels in wildtype worms, which were already significantly elevated in both untreated deletion mutants. Gene expression of *ceruloplasmin* was amplified due to Cu treatment, in addition, atox-1Δ worms displayed significantly higher levels in untreated controls compared to wildtype worms. mRNA levels of *mtl-1* were significantly reduced by about 90% in wildtype worms upon treatment with 2 mM Cu. The basal level of *mtl-1* was lower in atox-1Δ and ceruloplasminΔ deletion mutants (compared to wildtype) but exposure to 2 mM Cu lowered *mtl-1* gene expression further. The expression of *mtl-2* increased at low level exposures (0.5 mM Cu) but reduced at the higher exposure concentration (2mM), this trend was observed in wildtype and the two deletion mutants, but the expression levels were notably higher in the atox-1Δ mutant.
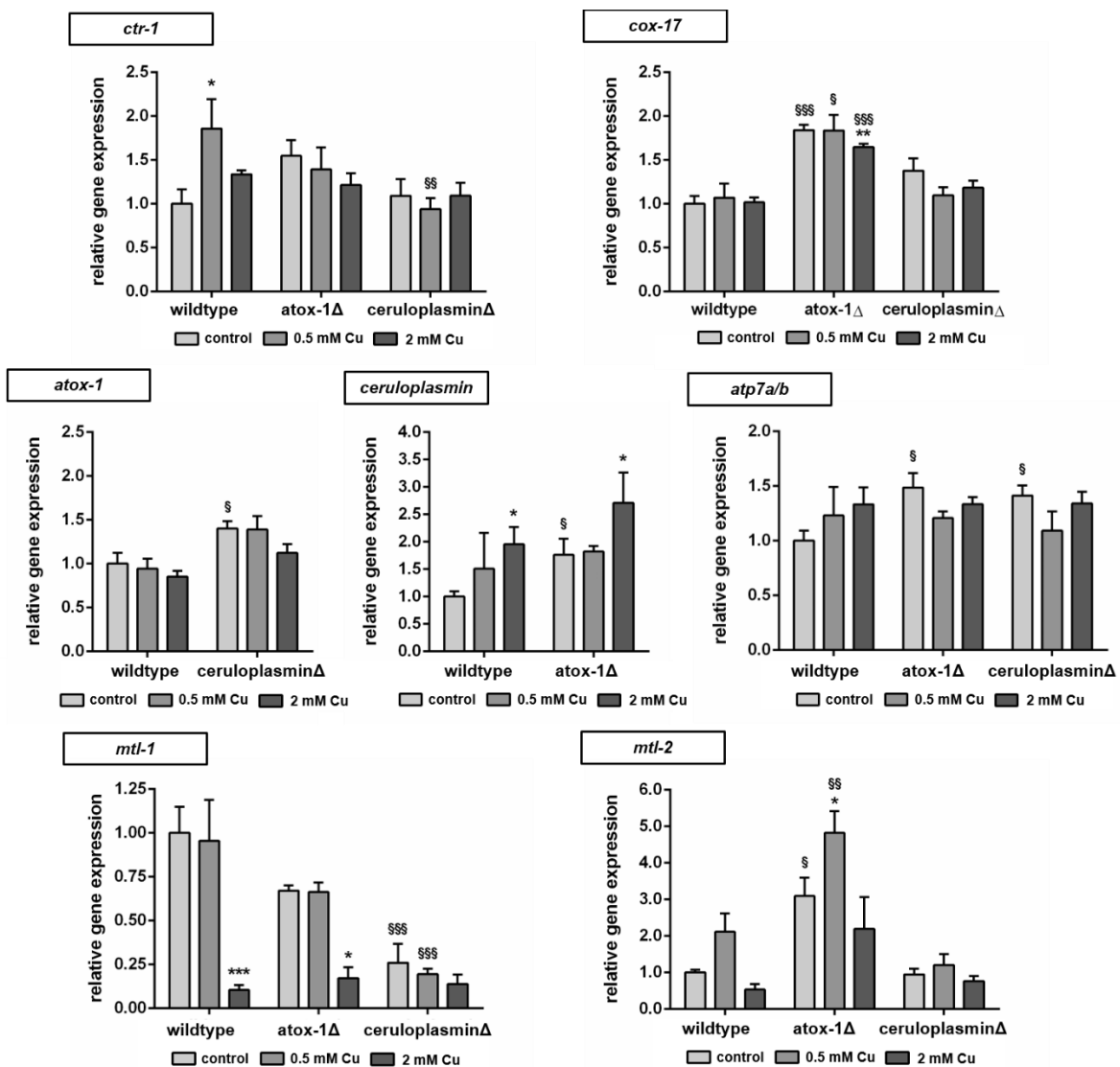
Figure 22: Relative mRNA levels of Cu transport and storage-related genes following 24 h Cu treatment determined by RT-qPCR normalized to *afd-1* (*AFDN* homologue) as housekeeper. Data presented are mean values of n = 4 independent experiments + SEM. Statistical analysis using 2-way ANOVA with Tukey's multiple comparison. Significance level with α = 0.05: *: $p \leq 0.05$; **: $p \leq 0.01$; ***: $p \leq 0.001$ compared to untreated control and §: $p \leq 0.05$; §§: $p \leq 0.01$ and §§§: $p \leq 0.001$ compared to wildtype in same condition.

4.3.5. Metallothionein expression and alterations of Cu uptake in mtl-KO mutants

Since Cu oversupply resulted in decrease of *mtl-1* and *mtl-2* expression, the involvement of metallothionein in Cu homeostasis was further investigated. Therefore, single knockout mutants of mtl-1 (*mtl-1*(tm1770)) and mtl-2

(*mtl-2*(gk125)), as well as the double knockout mutant (*mtl-1*;*mtl-2*(zs1) were incubated with Cu as described and total Cu levels were determined by ICP-OES. Results revealed a concentration-dependent Cu uptake for all tested strains, however, mtl-1KO (*mtl-1*(tm1770)) worms displayed significant less Cu uptake after 2 mM $CuSO_4$ treatment (Figure 23A), but also lower levels in other trace elements (Supplementary Figure 38). Although mRNA is required for protein synthesis, it does not inversely dictate that mRNA levels and mRNA induction levels are universally proportional to each other [318]. Consequently, we investigated the induction of *mtl-1* and *mtl-2* using the fluorescence-tagged transgenes P*mtl-1*::GFP and P*mtl-2*::mcherry, generated by the Mos1-mediated single-copy insertion (MosSCI) techniques, note the latter modified to contain a nuclear localization signal (NLS). Fluorescence plate reader measurements revealed a marginal increase in *mtl-1* expression but *mtl-2* levels remained, at large, unaffected by Cu exposure (Figure 23B), which was also visualized by fluorescence microscopy (Figure 23C).
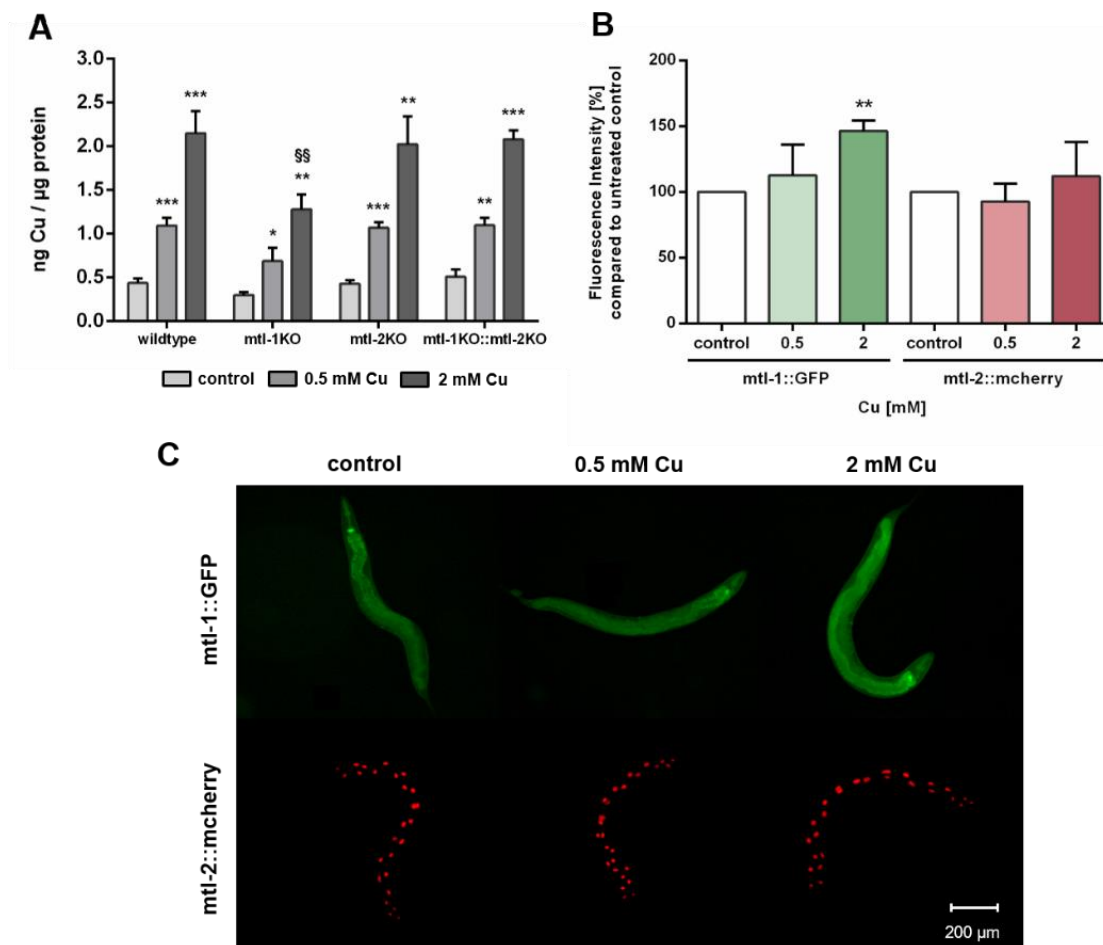
Figure 23: (A) Total Cu levels quantified by ICP-OES in wildtype, and the metallothionein knockout strains (*mtl-1*(tm1770), *mtl-2*(gk125) and the double knockout *mtl-1;mtl-2*(zs1). (B) Fluorescence intensity [%] compared to untreated control in P*mtl-1*::GFP and P*mtl-2*::mcherry worms. (C) representative fluorescence microscopy images. Data presented are mean values of n = 4 independent experiments + SEM. Statistical analysis using 2-way ANOVA with Tukey's multiple comparison. Significance level with α = 0.05: *: $p \leq 0.05$; **: $p \leq 0.01$; ***: $p \leq 0.001$ compared to untreated control and §§: $p \leq 0.01$ compared to wildtype in same condition.

4.4. Discussion

Cu is an essential trace element, serving as an enzyme cofactor due to its redox properties [163]. In excess, however, Cu tends to promote adverse health effects, which are mainly caused by the excessive formation of reactive oxygen species at the cellular level [164]. Excess Cu, beyond the homeostatic range, has been linked to the onset of numerous neurodegenerative diseases, and foremost Wilsons disease (WD) [14,319]. It is therefore of importance to have

mechanisms in place that allow an efficient regulation of Cu homeostasis. It is crucial to gain a better understanding of how Cu homeostasis is balanced and characterize these regulatory mechanisms. Two key players are ceruloplasmin and atox-1 and the consequences of their loss of function should be investigated. In addition, suitable markers and new tools to assess Cu status are needed, and the nematode *C. elegans* is a powerful model to address these shortcomings.

Others have demonstrated that high doses of Cu can result in cellular toxicity in different modes of applications [10,64,65]. Our study focused on metal homeostasis and investigated physiological endpoints rather than toxicology. Accordingly, Cu was applied via *E. coli* on agar plates up to 2 mM for a 24 h duration, which did not impact majorly on lethality rates. Having said that, mutants with disturbed Cu homeostasis presented a reduced survival rate of about 10% and are consequently Cu-hypersensitive. In addition, concentrations above 2 mM were avoided, as worms move away from the exposed *E. coli* and starve [316,317]. Cu^{2+}, as used in our study, is reduced to Cu^+ by a yet unknown reductase in *C. elegans* and subsequently taken up by importer CTR-1. The transcription of *ctr-1* increased in wildtype worms exposed to 0.5 mM Cu, which is in contrast to observations made by Clifford et al. [300], however *ctr-1* expression was not modulated in worms challenged with the higher dosage of Cu (2 mM). Total Cu uptake increased in a concentration-dependent manner [64,65], yet significantly less in the atox-1 and ceruloplasmin deletion mutants, suggesting that these mutants are characterized by an altered storage capacity. Factors that may further contribute to a disturbed homeostasis may include a reduced influx, an increased efflux or a lack of sufficient storage capacity, or a combination thereof. Li et al. display normal Cu levels in ceruloplasmin-KO mice in the cerebral cortex and hippocampus [320]. The brain is, after the liver, the organ with the highest Cu occurrence [296]. Consequently, we investigated whether Cu accumulates in specific areas of the worm. ToF-SIMS analysis

revealed a universal distribution of Cu across the worm body, but it should be noted that neurons are present not only in the head region but over the entire body of the worm [36]. Even if ToF-SIMS analysis goes further than microscopy, as an additional depth profile analysis is included, the resolution is not sufficient to localize Cu within a cell (subcellular). Therefore, future studies should focus on neuronal cells by using techniques such as NanoSIMS (Nano Secondary Ion Mass Spectrometry) [321]. With respect to the total Cu amount, the ToF-SIMS results matched our ICP-OES data, where the highest Cu concentrations were measured in wildtype worms and the lowest in ceruloplasmin-deficient worms, following a 24h treatment with 2 mM Cu (Figure 24).
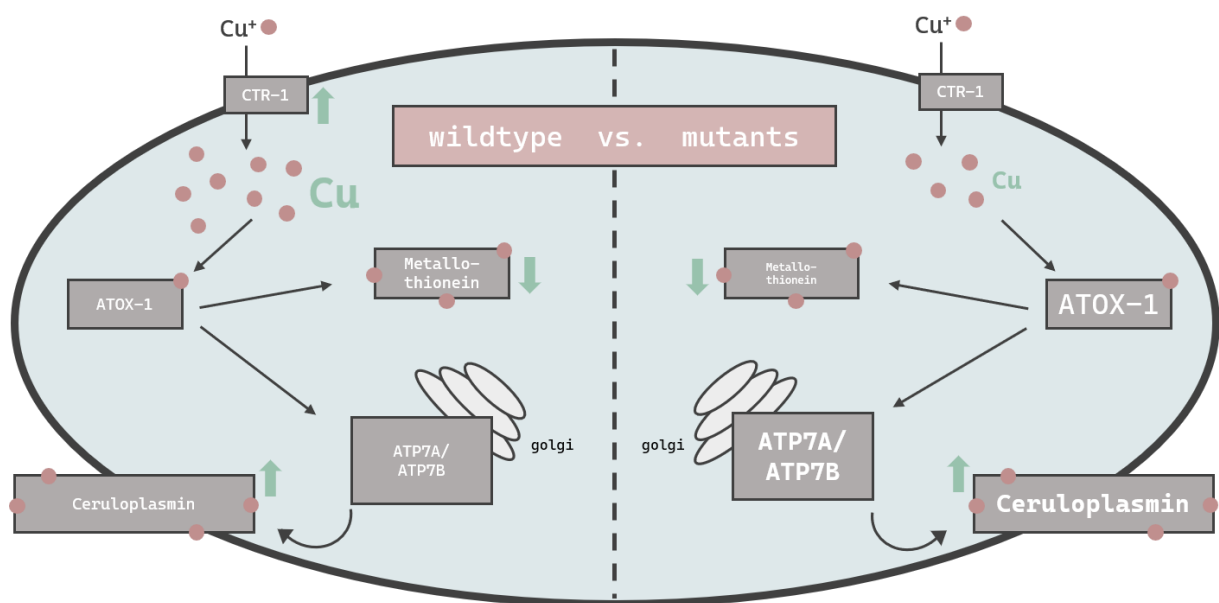
Figure 24: Schematic overview of the changes in the bioavailability and expression of genes responsible for Cu homeostasis in *C. elegans*. Displayed are changes in wildtype worms (left) vs. mutant worms (atox-1Δ or ceruloplasminΔ) (right). Up- and downregulation of mRNA levels by excessive Cu feeding are indicated by green arrows, while differences in basal levels due to genetics compared to wildtype worms is indicated by smaller or larger font size.

Studies in *ATOX-1*KO mice and cell culture revealed a disturbed Cu homeostasis [75,322]. Furthermore, Zhang et al. displayed the phenotype of a *C. elegans atox-1*KO model in form of reduced brood size and distal tip cell

migration defects [69]. However, data on the Cu status were lacking, which are critical for the evaluation of Cu toxicity. In humans, the highest mRNA levels of ATOX-1 in the brain were detected in the cerebral cortex and hippocampus, with elevated ATOX-1 activity due to increased Cu levels [76]. Moreover, ATOX-1 is thought to possess antioxidative properties [76], as increased endogenous ATOX-1 levels protect against oxidative stress and promote neuronal survival [77]. In our study, *cox-17* expression was elevated in the atox-1Δ deletion mutant, which might indicate an increased Cu transport into mitochondria. Whilst atox-1 participates in intracellular Cu distribution, ceruloplasmin is the major Cu storage protein responsible for the binding of 90% of total Cu [58]. Genetic loss of ceruloplasmin can lead to the autosomal recessive disorder "aceruloplasminemia", which is characterized by progressive neurodegeneration [80]. Elevated Cu or labile Cu levels are not the only concern in aceruloplasminemia observed in aging worms [323]. Due to ceruloplasmin's ferroxidase activity, it is essential for iron (Fe) oxidation during cellular export, resulting in cellular Fe accumulation in aceruloplasminemia [324]. Despite its importance in Cu storage protein in mammals, to date no research has focused on the role of ceruloplasmin in Cu homeostasis in *C. elegans*. Our data revealed that Cu levels were altered due to Cu supplementation in ceruloplasmin-deficient worms, but Fe levels seem to be unaffected in this mutant compared to wildtype worms (Supplementary Figure 37). In addition to neurodegeneration, obesity and steatosis have been reported in ceruloplasmin-KO mice [325], highlighting that ceruloplasmin is essential for Cu and Fe homeostasis. Our data revealed that Cu induced *ceruloplasmin* mRNA expression in wildtype and atox-1 deletion mutants (Figure 24), possibly due to the excretion of excess Cu bound to ceruloplasmin. In addition, excess Cu is excreted by atp7b, which in humans, among others, participates in providing Cu to ceruloplasmin [301].

In mammals, the two major functions of ATP7B are the supply of Cu to ceruloplasmin in the golgi and the excretion of excess Cu into the bile [62].

ATP7B translocalizes to the plasma membrane which enables the efflux of excess Cu in the form of vesicular sequestration [302,303]. This aligns with our data where *atp7a/b* mRNA levels were elevated in wildtype worms following Cu treatment. Similar observations were made by Li et al. after Cu treatment [294]. The notion that ATP7B is essential for proper functioning Cu homeostasis is supported by experiments in ATP7B-KO models [323]. Our data reveal an increase of *atp7a/b* mRNA levels due to Cu treatment in wildtype worms, but further display that untreated atox-1 and ceruloplasmin deletion mutants already exhibit elevated *atp7a/b* levels (Figure 24). Interestingly, Cu treatment does not increase *atp7a/b* in those mutants further. The fact that atox-1Δ and ceruloplasminΔ mutants demonstrate greater *atp7b* expression but lower total Cu levels compared to wildtype worms is unexpected. This suggests that one should not focus exclusively on total Cu levels, but also on labile Cu levels, which differ among the worms used in this study and are notably increased in atox-1 and ceruloplasmin deletion mutants.

Traditionally, Cu status is assessed by measuring serum or plasma total Cu and ceruloplasmin levels [94,304], whereas for WD diagnosis a liver biopsy is required [102]. Besides ceruloplasmin protein levels, its enzyme activity and mRNA level also affect the maintenance of Cu homeostasis [326]. Furthermore, labile Cu has recently emerged as a marker of Cu status, as it is assumed to be readily bioavailable and reflects more accurately Cu activity compared to total Cu [327,328]. Our data reveal that atox-1Δ and ceruloplasminΔ mutants displayed reduced total Cu levels compared to wildtype worms following Cu treatment, as well as severe alterations of Cu homeostasis, e.g. increased mRNA levels of *atp7a/b*. This could be linked to elevated levels of labile Cu. Nevertheless, relying on labile Cu levels is currently not considered sufficient due to the complexity of analysis and lack of methodologies available [15,108,165,329]. Having said that, in combination with total Cu and ceruloplasmin measurements, the analysis of labile Cu promises to be a

valuable and powerful tool to assess the Cu status and thus the risk or diagnosis for Cu dyshomeostasis-related diseases [14]. Squitti et al. observed a subpopulation of patients diagnosed with Alzheimer's disease (AD) displaying higher than normal non-ceruloplasmin bound Cu in serum, similar to WD patients, stating that labile Cu identifies a Cu subtype of AD (CuAD) [319,330]. They further hypothesize that Cu dyshomeostasis results in a shift of protein-bound metal pools to labile metal pools, which is associated with the loss of energy production but also altered antioxidant function [330]. Labile Cu pools are increased even by physiological Cu amounts in different brain cells [331], which can exert neurotoxicity [19]. Elevated Cu levels promote the formation of reactive oxygen species, lipid peroxidation, apoptosis and decreased mitochondrial membrane potential, leading to oxidative stress [164,294]. Borchard et al. report that labile Cu is cell toxic with mitochondria as vulnerable target, which in turn can be avoided by Cu chelation [332]. Several studies reveal that Cu chelation reduces or even prevents Cu-mediated toxicity [18,65,166,333], while studies in WD models demonstrate that chelation lowers systemic Cu levels into the homeostatic range as possible therapeutic approach [63,334,335]. Chelator therapy also suggests that Cu toxicity is mainly mediated by labile Cu rather than by pre-protein bound Cu like in ceruloplasmin. Local concentrations of Cu as well as cellular distribution of Cu transporters, storage and excretion proteins are important to maintain a steady state [296] and tight regulation of Cu homeostasis, as dyshomeostasis is associated with the pathogenesis of neurodegenerative diseases such as WD, but also AD [163,163,299,336].

Metallothionein binds excess metal ions to maintain homeostasis, thus the downregulation of *mtl-1* mRNA levels after Cu treatment (Figure 24) seems surprising but supports Zhang et al. who too report a reduction of metallothionein mRNA levels in Cu exposed *C. elegans* [10]. In contrast, Tapia et al. was not able to identify alterations in metallothionein mRNA levels in rat fibroblast cells

[337], which suggests either the presence of tissue- or species- specific differences in metallothionein transcription. *C. elegans* metallothioneins seem to be strongly induced by other trace elements, such as zinc [314,338] as well as cadmium [72,339,340]. Notably, mRNA levels are not necessarily proportional to protein levels [318], this also applies to metallothionein [341]. Our data suggest slight changes in mtl-1, but not mtl-2 expression. Since mtl-2 is present in larger quantities in *C. elegans* [59,340], alterations in mtl-1 are marginal with respect to total metallothionein levels. Nevertheless, mtl-1 still seems to be important for metal uptake, as mtl-1 knockouts take up less Cu and other trace elements in our but also previous studies [314,337]. Additionally, metallothionein preserves Cu-induced neurotoxicity [342].

In summary, we were able to uncover that ceruloplasmin and atox-1 play a key role in Cu homeostasis in *C. elegans*. ICP-OES and ToF-SIMS analysis revealed that total Cu levels were reduced in the ceruloplasmin and atox-1 deletion mutants compared to wildtype worms, in contrast they displayed increased levels of labile Cu. Furthermore, ToF-SIMS analysis is a powerful tool applied in this study enabling firstly a 3D Cu localization in worms. Accordingly, a genetic Cu dyshomeostasis and Cu oversupply can result in a shifted ratio of total Cu vs. labile Cu pools. The dyshomeostasis is further reflected by an altered gene expression of crucial participants in Cu homeostasis like *atp7a/b*, *atox-1*, *ceruloplasmin* and *metallothionein*. As demonstrated here, labile Cu is a potential marker of the Cu status in the organism *C. elegans*. Taken together, the *C. elegans* genome encodes a suite of evolutionary conserved genes involved in Cu homeostasis and thus serves as an exquisite model to study Cu dyshomeostasis linked to neurodegenerative diseases. However, some aspects remain unanswered and require further investigation, such as the mechanistic regulation of atox-1 and ceruloplasmin in *C. elegans*. Our study demonstrates early observations of a defective Cu homeostasis in *C. elegans*, but also reveals a lack of knowledge of underlying mechanisms due to complexity, which should

be addressed in future studies. Altogether, the Cu status should be monitored by multiple functional markers including total Cu, labile Cu as well as gene expression of Cu homeostasis-related genes in order to provide specificity and sensitivity to detect potential alterations in Cu homeostasis.

4.5. Author Contributions

AKW: conceptualization, data curation, formal analysis, investigation, visualization, writing – original draft. KL: resources, investigation, data curation, visualization. ET: resources, investigation, data curation, visualization. ATP: resources, writing – review & edit. CDM: resources. TS: funding acquisition, writing – review & edit. MA: writing – review & edit. CJC: resources, writing – review & edit. SS: supervision, resources, writing – review & edit. JB: conceptualization, funding acquisition, project administration, supervision, writing – review & edit.

4.6. Funding

4.7. Acknowledgements

4.8. Key words

Copper, homeostasis, total vs. labile copper, ToF-SIMS, *C. elegans*

Abstract

While copper (Cu) is an essential trace element for biological systems due to its redox properties, excess levels may lead to adverse effects partly due to overproduction of reactive species. Thus, a tightly regulated Cu homeostasis is crucial for health. Cu dyshomeostasis and elevated labile Cu levels are associated with oxidative stress and neurodegenerative disorders, but the underlying mechanisms have yet to be fully characterized. Here, we used *Caenorhabditis elegans* loss-of-function mutants of the Cu chaperone atox-1 and Cu storage protein ceruloplasmin to model Cu dyshomeostasis, as they display a shifted ratio of total Cu towards labile Cu. We applied highly selective and sensitive techniques to quantify metabolites associated to oxidative stress with focus on mitochondrial integrity, oxidative DNA damage and neurodegeneration all in the context of a disrupted Cu homeostasis. Our novel data reveal elevated oxidative stress, compromised mitochondria displaying reduced ATP levels and cardiolipin content. Cu dyshomeostasis further induced oxidative DNA damage and impaired DNA damage response as well as neurodegeneration characterized by behavior and neurotransmitter analysis. Our study underscores the essentiality of a tightly regulated Cu homeostasis as well as mitochondrial integrity for both genomic and neuronal stability.

Chapter 5 – Dysfunctional Copper Homeostasis in *Caenorhabditis elegans* affects neuronal and genomic stability

Based on:

Ann-Kathrin Weishaupt, Anna Gremme, Torben Meiners, Vera Schwantes, Karsten Sarnow, Alicia Thiel, Tanja Schwerdtle, Michael Aschner, Heiko Hayen and Julia Bornhorst

Chapter 5 – Dysfunctional Copper Homeostasis in *Caenorhabditis elegans* affects neuronal and genomic stability
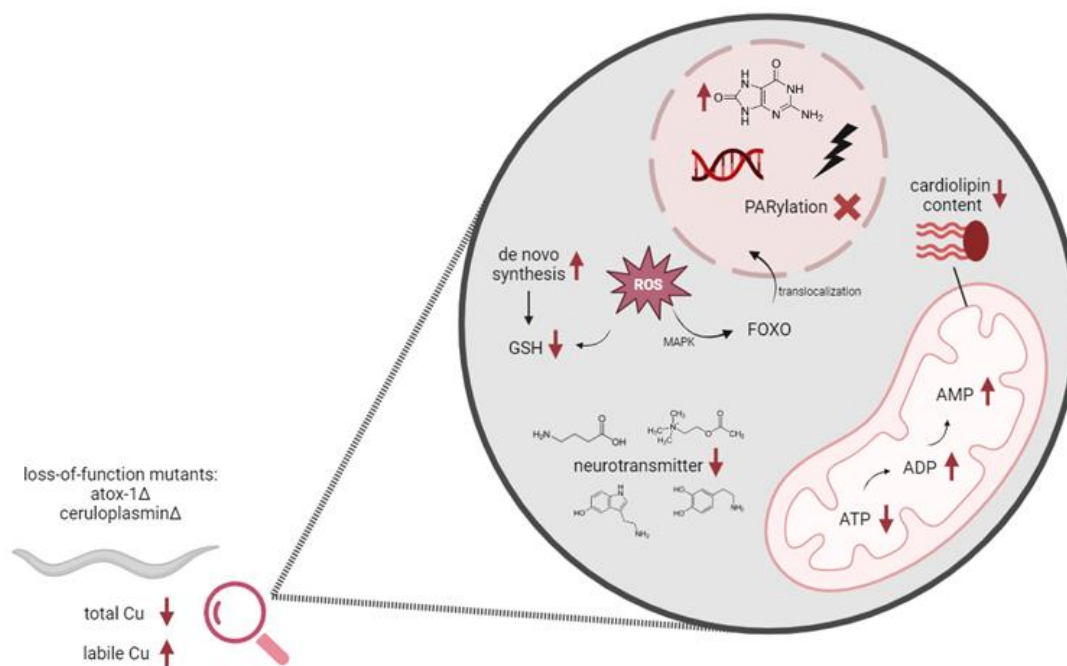
Figure 25: Graphical abstract of: Dysfunctional Copper Homeostasis in *Caenorhabditis elegans* affects neuronal and genomic stability.

5.1. Introduction

Copper (Cu) is an essential trace element and micronutrient, participating in many physiological pathways as an enzyme cofactor [163]. Due to the overuse of Cu-containing chemicals and fungicides in industry and agriculture, Cu is increasingly introduced into the environment, leading to a global concern [144]. When exceeding the physiological range, Cu leads to the formation of reactive oxygen and nitrogen species (RONS) due to its redox activity, which may affect macromolecules such as lipids or the DNA [164]. Therefore, a tightly regulated Cu homeostasis is crucial, since a Cu imbalance has been reported to induce oxidative stress as well as neurodegeneration [18,332]. In a previous study, we demonstrated that a dysregulated Cu homeostasis results in elevated labile Cu levels in *Caenorhabditis elegans* (*C. elegans*) [55]. Besides total Cu levels and

the activity of the Cu storage protein ceruloplasmin, labile Cu is discussed to be an additional marker for Cu status, as it is readily available for cellular uptake [104]. As previously shown, a Cu imbalance leads to a shift from bound Cu towards pools of labile Cu [55], which is associated with the loss of antioxidant defense, impaired energy production and in turn mitochondrial deficits [18]. Indeed, Alzheimer's disease (AD) has been posited to result from Cu imbalance based on a correlation between brain Cu levels and the prevalence of AD [343]. The underlying mechanisms remain unknown, but are often linked to oxidative stress, which is induced by an imbalance of RONS and antioxidants [137]. Cells are equipped with a variety of enzymes and small molecules for antioxidative defenses [138]. Reduced and oxidized glutathione are key markers for oxidative stress [137,138]. As previously stated, RONS can damage macromolecules, such as lipids. Malondialdehyde (MDA), a degradation product of lipid peroxidation of polyunsaturated fatty acids is a common biomarker of oxidative stress [143]. A unique type of phospholipid class, exclusively present in mitochondria, are cardiolipins (CL) [151]. CLs have recently emerged in the focus of neurodegenerative diseases, as a reduction in CL levels has been linked to oxidative stress and mitochondrial dysfunction in AD [344]. Wilson's disease (WD), a Cu metabolism disorder resulting in neurological deficits, is characterized by a mutation in the *Atp7b* gene. This results in non-expression of the Cu exporter protein Atp7b, thereby leading to Cu accumulation, primarily in the liver, but also in the brain [332]. Studies reveal a progressive degradation of CLs in liver mitochondria of a WD mouse model (*Atp7b$^{-/-}$*) [345], which underlines the link between CLs and the pathogenesis of neurodegenerative diseases [151]. Massive RONS formation induced by Cu may further increase DNA lesions. An induction of DNA damage in response to elevated brain Cu levels was observed in AD, Parkinson's disease (PD), as well as in WD [346]. However, the mode of action of Cu-induced toxicity and neurotoxicity is still under debate.

This study aims to investigate the molecular mechanisms of labile Cu redox biology using the model organism *C. elegans*. The nematode is a well-established model to examine metal-induced oxidative stress and neurotoxicity [178]. In addition, *C. elegans* conserved similar proteins related to the mammalian Cu metabolism, making it suitable for its investigation. Furthermore, we recently demonstrated that the nematode can model Cu homeostasis. Our previous study revealed that deletion mutants lacking the intracellular Cu chaperone atox-1 and the Cu storage protein ceruloplasmin take up less total Cu, but display elevated levels of labile Cu compared to wildtype worms [55]. Our aim is to elucidate the toxic mechanisms upon a disrupted Cu homeostasis regarding oxidative stress, with special focus on mitochondrial integrity in terms of energy-related nucleotides such as ATP, as well as total CL levels and the CL profile. Furthermore, the consequences of oxidative stress on genomic and neuronal stability due to Cu dyshomeostasis in *C. elegans* will be investigated.

5.2. Material and Methods

5.2.1. *C. elegans* handling and treatment

C. elegans strain Bristol N2 (wildtype) and TJ356 (daf-16::GFP) were obtained from the Caenorhabditis Genetics Center (CGC, Minneapolis, USA), which is funded by the National Institutes of Health Office of Research Infrastructure Programs. Additionally, deletion mutants (Δ) tm1220 (atox-1Δ) and tm14205 (ceruloplasminΔ) were obtained from the Mitani Lab at Tokyo Women's Medical University. All strains were cultivated on 8P and NGM agar plates, which have been coated with *Escherichia coli* (*E. coli*) and maintained at 20 °C as previously described [292]. All experiments were performed using synchronous worms [313], which were placed on NGM agar plates until L4 larval stage. L4 stage worms were treated with Cu-enriched inactivated *E. coli* (CuSO$_4$ ≥99.99%, Sigma Aldrich) on NGM plates for 24 h up to 2 mM for every experiment as

previously shown [55]. Optionally, 100 mM paraquat (PQ)-enriched *E. coli* for 24 h (Sigma Aldrich) or 6.5 mM *tert*-butyl hydroperoxide (*t*-BOOH) (Sigma Aldrich) for 1 h in 85 mM NaCl solution were used as positive controls, but in wildtype worms only to verify assay procedures.

5.2.2. daf-16 translocalization in daf-16::GFP mutants

Worm strain daf-16::GFP was used to assess daf-16 translocalization by fluorescence microscopy. After Cu treatment, worms were transferred to 4% agarose pads on microscope slides and anesthetized using 5 mM levamisole (Sigma-Aldrich). Analysis was performed using DM6 B fluorescence microscope and the Leica LAS X software (Leica Microsystem GmbH). GFP localization was assessed and categorized as 1) present in cytosol, 2) as intermediate or 3) localized into nucleus. For each experiment, ~ 25 worms were analyzed for each condition.

5.2.3. Gene expression via quantitative real-time PCR analysis

For gene expression assessment, RNA was isolated in pellets containing 500 worms as previously published using the Trizol method [219], which was transcribed using the High Capacity cDNA Reverse Transcription Kit (Applied Biosystems, Thermo Fisher Scientific) as stated in the manufacturer's protocol. Quantitative real-time PCR was carried out using TaqMan Gene Expression Assay probes (Applied Biosystems, Thermo Fisher Scientific) on an AriaMx Real-Time PCR System (Agilent). For normalization by the comparative $2^{-\Delta\Delta Ct}$ method, we used *AFDN* homolog *afd-1* as housekeeping gene [315]. The following probes were used: *afd-1* (Ce0241573_m1), *sod-1* (Ce02434432_g1), *sod-4* (Ce02451138_g1), *skn-1* (Ce02434432_g1), *bli-3* (Ce02413442_m1), *mpk-1* (Ce02445290_m1), *pmk-1* (Ce02456381_g1), *nsy-1* (Ce02432208_g1), *daf-16* (Ce02422838_m1), *gcs-1* (Ce02436726_g1), *pme-1* (Ce02415136_m1) and *pme-2* (Ce02437339_g1).

5.2.4. Glutathione (GSH and GSSG) levels quantification by HPLC-MS/MS

Reduced (GSH) and oxidized (GSSG) glutathione levels were assessed by liquid-chromatography tandem-mass spectrometry (HPLC-MS/MS). Following Cu treatment, pellets were prepared by centrifugation of 1000 worms in 100 µL 85 mM NaCl. Sample preparation and GSH/GSSG analysis was performed as previously published [140].

5.2.5. HPLC-DAD analysis of energy-related adenine and pyridine nucleotides

Sample preparation as well as analysis by ion-pair reversed phase HPLC were performed according Bornhorst et al. [347]. 2000 worms were pelletized per condition in 100 µL 85 mM NaCl and immediately prepared as stated. The analysis was performed on an Agilent 1260 Infinity II liquid chromatography system with a photodiode array detector (DAD). Nucleotide contents were evaluated by external calibration of standard solutions of adenosine triphosphate (ATP), adenosine diphosphate (ADP), adenosine monophosphate (AMP), nicotinamide adenine dinucleotide phosphate (NADPH) and nicotinamide adenine dinucleotide (NADH and NAD^+). Detection by DAD was performed at 259 nm and data analysis was carried out using the OpenLab (version 3.6) software (Agilent).

5.2.6. Quantification of malondialdehyde

Unbound and bound MDA were determined by high performance liquid chromatography with fluorescence detection (HPLC-FLD). The sample preparation was based on Grintzalis et al. [348] and optimized for *C. elegans* matrix. Phosphate buffer (3.54 g/L KH_2PO_4, 7.24 g/L Na_2HPO_4, pH 7.0) was stored at 4 °C. Following pelletizing of 2000 worms in 100 µL 85 mM NaCl, 200 µL phosphate buffer and 1.5 µL 0.1 M 2-and-3-*tert*-butyl-4-hydroxyanisol (BHA) (Sigma Aldrich) were added and the pellet was stored at -80 °C up to one week. Samples were homogenized by 3 × freeze-thaw cycles (1 min liquid nitrogen,

1 min 37 °C), 3 × sonication with an ultrasonic probe (20 sec, cycle 1, amplitude 100%; UP100H, Hielscher) and in an ultrasonic bath (5 min). After centrifugation (5 min, 18620 rcf, 4 °C), 30 µL were transferred for protein measurement. 63 µL of 100 % trichloroacetic acid (TCA) (Carl Roth) were added, following 5 min incubation on ice. Samples were centrifuged (15 min, 20000 rcf, 4 °C) and the entire supernatant (unbound MDA fraction) was transferred to a new tube and stored on ice until further use. For alkaline hydrolysis, 250 µL 1 M NaOH were added to the remaining pellet and incubated for 30 min at 60 °C. The hydrolyzed samples (bound MDA fraction) were cooled on ice and 25 µL conc. HCl was added. 1,1,3,3-Tetramethoxypropane (TMP) (Sigma Aldrich) was used for external calibration (20 – 500 nM), which forms an MDA-TBA product by derivatization with 2-Thiobarbituric acid (TBA) (Sigma Aldrich). For derivatization, 12.5 g/L TBA solution was prepared just before use by mixing solution A (100 % TCA, conc. HCl, ratio 5:1) and solution B (25 g/L TBA in 0.2 M NaOH) in a ratio of 1:1. 50 µL 12.5 g/L TBA and 3 µL 0.1 M BHA were added to 200 µL of each a) unbound, b) bound MDA sample and c) TMP calibration solution. All solutions were heated at 100 °C for 20 min and 300 µL butanol was added after cooling. Following centrifugation (5 min, 20 000 rcf, 4 °C), MDA levels were analyzed in an aliquot of the 1-butanol phase. Settings for the HPLC-FLD analysis as well as method validation parameters are listed in the Supplementary.

5.2.7. Cardiolipin levels and distribution by 2D-LC-HRMS

Cardiolipins were analyzed by 2D-HPLC-HRMS analysis. A detailed overview of the sample preparation and instrument parameters is listed in the Supplementary.

5.2.8. 8oxodG measurement via ELISA

8-oxoguanine (8oxodG) has been quantified by the OxiSelect™ Oxidative DNA Damage ELISA kit (Cell Biolabs). 2000 worms were treated with Cu and pelletized as stated above. In the first step, DNA was isolated of each sample

using the Qiagen Tissue and Blood DNA extraction kit, following the manufacturer's instruction. The amount of DNA was quantified by NanoDrop measurements and portioned in 40 µg aliquots, which were dried. In the second step, DNA was hydrolyzed by enzymes to obtain mononucleotides as described by Nicolai et al. [349]. As third step, 8-oxodG measurement was performed according the above-mentioned manufacturer's kit instructions.

5.2.9. HPLC-MS/MS analysis of PARylation levels

Sample preparation for poly-(ADP-ribose) (PAR) extraction was done in pellets of 1000 worms and according [349]. Analysis was performed by HPLC-MS/MS using an Agilent 1290 Infinity II liquid chromatography system (Agilent, Waldbronn, Germany), which is coupled to a Sciex QTRAP 6500+ triple quadrupole mass spectrometer (Sciex, Darmstadt, Germany). PAR quantification was assessed as described in [349], with minor changes in chromatography: Chromatographic separation was performed using a Hypersil Gold aQ 150 x 2.1 mm and corresponding 10 x 2.1 mm pre-column. Elution was carried out with bidistilled water + 0.1% formic acid (FA) and acetonitrile + 0.1% FA and a flow of 0.3 mL/min. Total run time was 5 min, starting with 0 – 25% of ACN in 2.5 min, to 100% ACN in 0.5 min, 100% ACN for 1 min, following re-equilibration to 0% ACN. Results were normalized to DNA content determined by Hoechst method [158].

5.2.10. Neurotransmitter quantification via HPLC-MS/MS

Dopamine, serotonin, γ-amino butyric acid and acetylcholine levels were determined by HPLC-MS/MS. Pellets of 1000 worms per 50 µL 85 mM NaCl were prepared after Cu incubation. Samples were added with 100 µL extraction buffer, processed and analyzed according to [178]. Results were normalized to protein content analyzed by BCA assay (Sigma-Aldrich).

5.2.11. Aldicarb-induced paralysis assay

The assay is based on Mahoney et al. [256] and was performed as previously published [178]. Plates with 2 mM aldicarb (stock solution in 70% EtOH) were always prepared fresh and the assay was performed as a blinded experiment at all times.

5.2.12. Statistical analysis

Statistical analysis was carried out using GraphPad Prism 6 (GraphPad Software, La Jolla, USA) using 2-way ANOVA with Tukey's multiple comparison or impaired t-test for one-to-one comparison. Significance level with $\alpha = 0.05$: *: $p \leq 0.05$; **: $p \leq 0.01$ ***: $p \leq 0.001$ compared to untreated control and §: $p \leq 0.05$ §§: $p \leq 0.01$ and §§§: $p \leq 0.001$ compared to wildtype in same condition.

5.3. Results

5.3.1. daf-16 translocation visualized by daf-16::GFP fluorescence microscopy and mRNA levels of mitogen-activated protein kinases

Protein kinases activated by stress, such as c-Jun N-terminal kinases (JNK) and p38 mitogen-activated kinases (MAPK), can stimulate Forkhead box O-class proteins (FoxO) expression and translocation from cytosol to nucleus, where it acts as transcription factor participating in DNA repair, RONS detoxification and apoptosis (Figure 26A) [350]. The homolog of human FOXO4 is daf-16 in *C. elegans*, which can be visualized in the transgenic strain daf-16::GFP by fluorescence microscopy (Figure 26B). 24 h treatment with $CuSO_4$ or PQ used as positive control leads to a significant translocation of daf-16 from cytosol into the nucleus (Figure 26C). Furthermore, we examined mRNA levels of *daf-16/FOXO4* itself, but also representatives of MAPK's subgroups p38, JNK and ERK1/2 (extracellular signal-regulated kinases): *pmk-1/MAPK11*, *nsy-1/MAP3K5* and *mpk-1/MAPK1*. Gene expression of *daf-16/FOXO4* as well

103

as of the p38 and JNK kinases *pmk-1/MAPK11* and *nsy-1/MAP3K5* are not altered due to Cu treatment (Supplementary Figure 40), while ERK1/2 MAP kinase *mpk1/MAPK1* is upregulated in wildtype worms in a dose-dependent manner (Figure 26D). Cu does not elevate mRNA levels of *mpk-1/MAPK1* in atox-1 and ceruloplasmin-deficient worms, but basal levels are already increased to the level of Cu-treated wildtype worms.
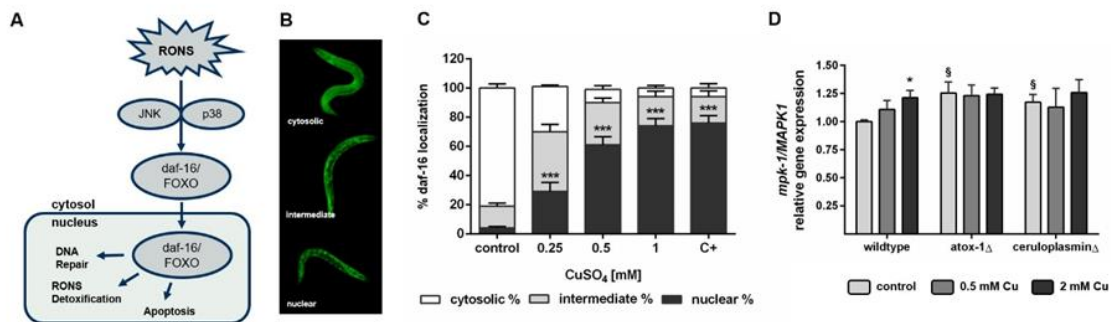
Figure 26: (A) Schematic daf-16 translocation from cytosol into the nucleus under oxidative stress conditions. (B) Exemplary fluorescence images of worms displaying cytosolic, intermediate or nuclear localized daf-16 in mutant worm daf-16::GFP. (C) daf-16 localization [%] of worms treated 24 h with CuSO4 or PQ as positive control (C+). Presented are mean values of n = 3 (N = 25) independent experiments + SEM. (D) Relative mRNA levels of mpk-1/MAPK1 following 24 h Cu incubation. Data presented are mean values of n = 4 independent experiments + SEM.

5.3.2. Reduced and oxidized glutathione, *gcs-1/GCLC* mRNA levels and energy-related nucleotides

As a marker for the antioxidative capacity, reduced (GSH) and oxidized (GSSG) glutathione were quantified by HPLC-MS/MS. Cu exposure (2 mM) significantly reduced GSH levels by 23% in wildtype worms, 34% in atox-1 and 38% in ceruloplasmin deletion mutants (Figure 27A). Inversely, Cu elevates oxidized GSSG levels in all strains (Figure 27B), however, ceruloplasmin-deficient worms display significantly lower GSSG levels after 2 mM Cu treatment compared to wildtype worms. *Gcs-1/GCLC*, which is involved in GSH synthesis, is not altered upon Cu incubation in *C. elegans,* but mutants with impaired Cu homeostasis display elevated mRNA levels (Figure 27C). Energy-related nucleotides of

interest, namely ATP, ADP, AMP, NADPH, NADH and NAD^+ were assessed by HPLC-DAD analysis (Figure 27D-I). For all analytes tested, no alterations were detected by Cu treatment in wildtype worms. On the other hand, altered nucleotide levels were observed for the mutants displaying Cu dyshomeostasis, with ceruloplasmin-deficient worms seem to be specifically affected. Ceruloplasmin deletion mutants displayed reduced ATP levels compared to wildtype worms, which are further reduced following Cu incubation. Furthermore, ADP and AMP levels were increased by Cu in atox-1 as well as ceruloplasmin mutants. While NADPH levels were elevated in atox-1-deficient worms, they were significantly reduced in ceruloplasmin-deficient worms. Moreover, both mutants contained lesser NADH levels compared to wildtype worms, and this effect was more pronounced in ceruloplasmin-deficient worms and was further exacerbated by Cu treatment. In addition, ceruloplasmin-deficient worms showed increased NAD^+ levels following Cu treatment.
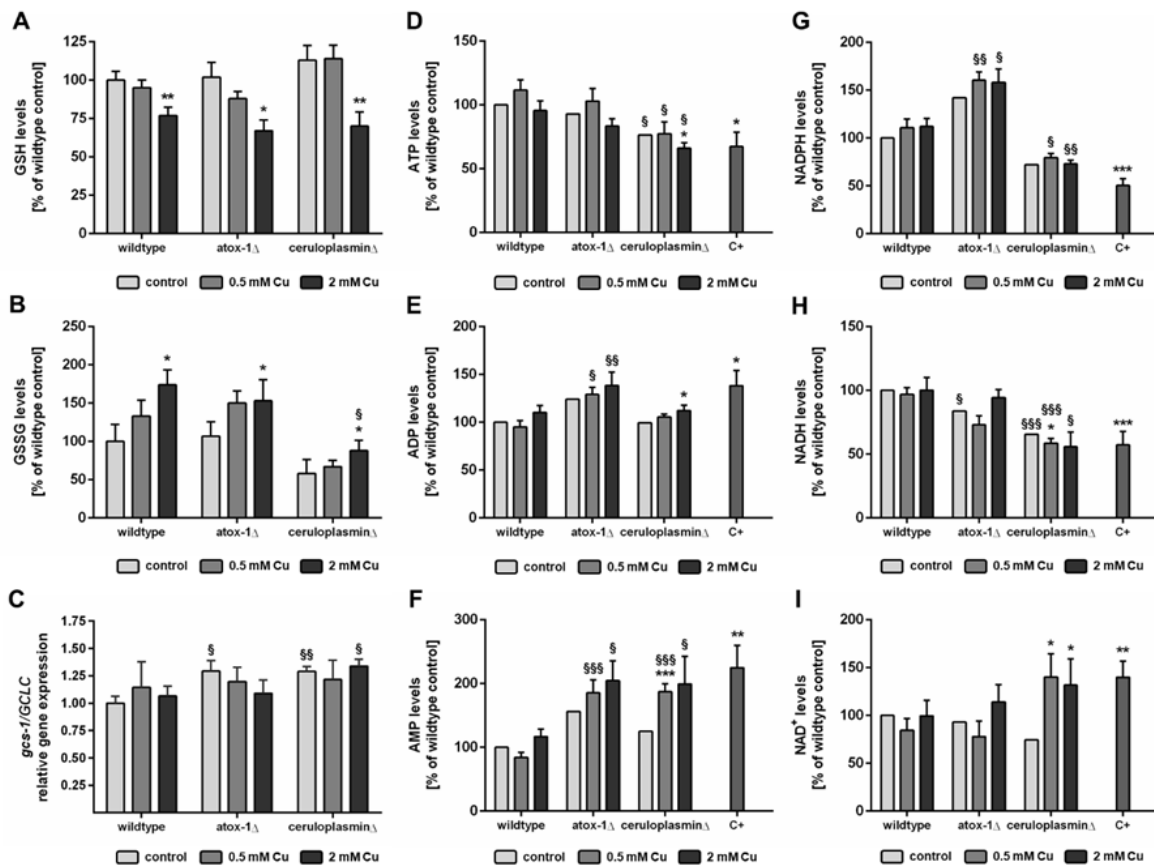
Figure 27: (A) GSH and (B) GSSG levels normalized to wildtype control [%]. (C) Relative mRNA levels of gcs-1/GCLC. Levels of (D) ATP, (E) ADP, (F) AMP, (G) NADPH, (H) NADH and (I) NAD+ compared to wildtype control [%]. PQ was used as positive control (C+) in wildtype worms. Data presented are mean values of n ≥ 4 independent experiments + SEM.

5.3.3. Malondialdehyde quantification and total cardiolipin levels and distribution

Using alkaline hydrolysis, unbound MDA as well as bound MDA, for example bound to proteins or DNA, were assessed. Our data reveal no alterations induced by Cu or t-BOOH on the amount of bound MDA (Supplementary Figure 42). However, unbound MDA levels increased significantly by t-BOOH in wildtype worms as well as by Cu treatment in the deletion mutants atox-1 and ceruloplasmin (Figure 28A). CLs are exclusively found in mitochondria and are fundamental for the mitochondrial membrane [344]. Our data showed no significant alterations in the CL profile induced by Cu supplementation in the

tested worm strains but of the total CL content in the deletion mutant ceruloplasmin was reduced compared to wildtype worms (Figure 28B). Furthermore, our data revealed no alterations induced either by Cu supplementation or genetic Cu dyshomeostasis on the relative distribution of CL species with respect to chain length and the degree of saturation (Figure 28C and Supplementary Figure 43).
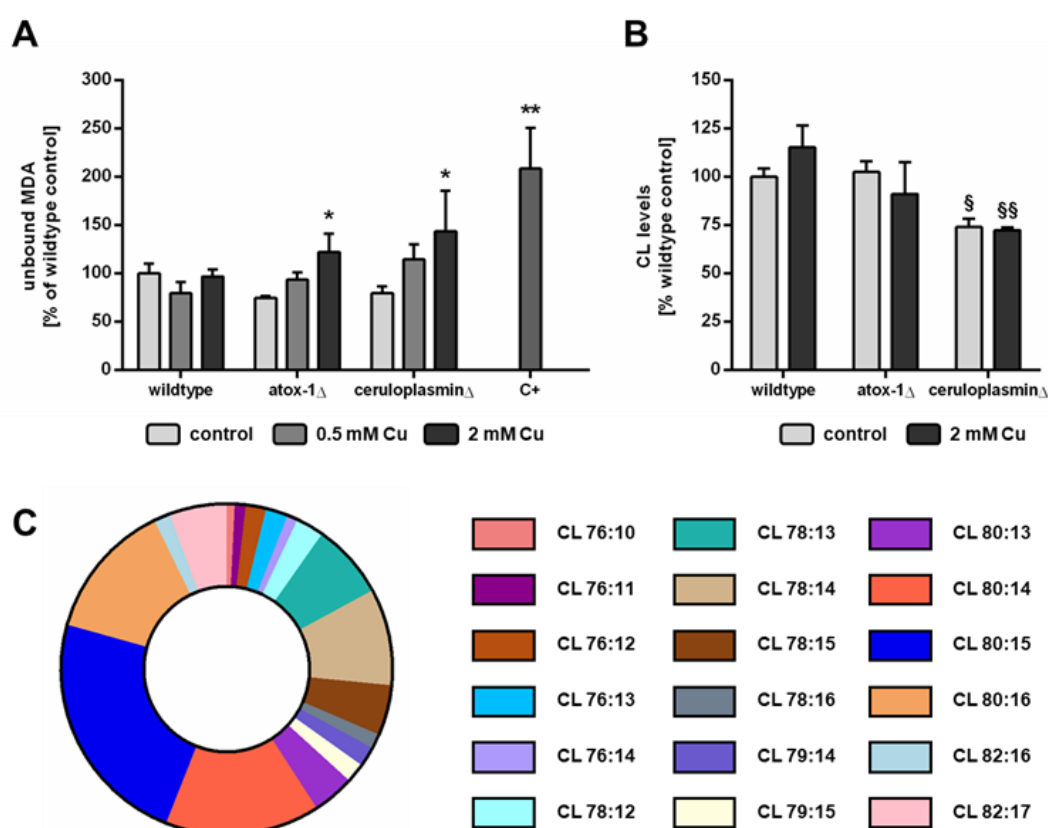
Figure 28: (A) MDA levels (unbound) normalized to wildtype control [%].(B) Total CL levels normalized to protein content and to wildtype control [%]. Data presented are mean values of n ≥ 3 independent experiments + SEM. (C) Representative distribution of CL species in terms of chain length and degree of saturation for untreated wildtype worms. *t*-BOOH was used as positive control (C+) in wildtype worms.

5.3.4. Oxidative DNA damage (8oxodG), DNA damage response (PARylation) and *pme/PARP* mRNA levels

We assessed levels of 8-oxoguanine (8oxodG), which is the most common DNA lesion initialized by RONS [351], as well as poly-(ADP-ribosylation) (PARylation)

as a marker for DNA damage response. Data reveal increased 8oxodG levels for ceruloplasmin-deficient worms up to 350% following 2 mM Cu treatment, while wildtype and atox-1-deficient worms remained unaffected (Figure 29A). PAR levels showed no alterations in wildtype and ceruloplasmin mutants due to Cu supplementation. In contrast, untreated atox-1 mutants displayed reduced PAR levels compared to wildtype worms, but increased PARylation following Cu treatment (Figure 29B). Furthermore, mRNA levels of NAD^+-dependent poly (ADP-ribose) polymerases (PARP), were examined (Figure 29C+D). While *pme-1/PARP1* remained unchanged, *pme-2/PARP2* was downregulated to about 50% in untreated atox-1-deficient mutants compared to wildtype worms, yet it was upregulated in response to Cu treatment.
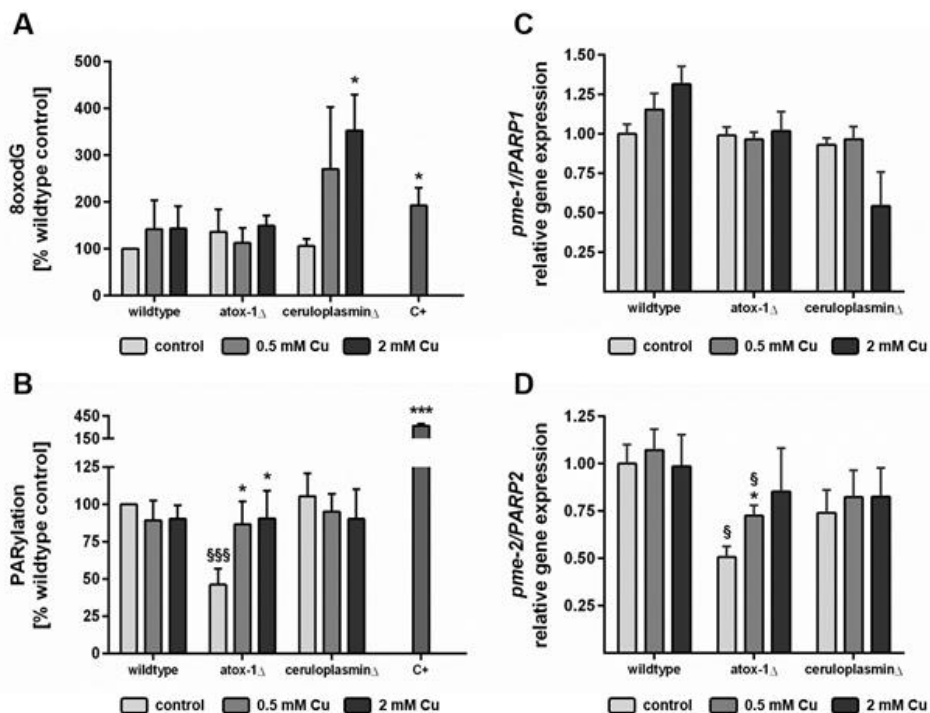
Figure 29: Relative (A) 8oxodG and (B) PARylation levels normalized to wildtype control Relative mRNA levels of (C) pme-1/PARP1 and (D) pme-2/PARP2 following 24 h Cu incubation. Data presented are mean values of n = 4 independent experiments + SEM. [%]. As positive control (C+) *t*-BOOH was used in wildtype worms.

5.3.5. Quantification of neurotransmitters DA, SRT, GABA and ACh levels and aldicarb-induced paralysis assay

HPLC-MS/MS-based quantification of the four neurotransmitters DA, SRT, GABA and ACh revealed different quantities of all analytes in *C. elegans* (Figure 30A-D). Untreated wildtype worms in young adult stage displayed 2.89 ng DA, 0.78 ng SRT, 529 ng GABA and 11.21 ng ACh each per mg of protein. Cu treatment failed to alter levels of all tested neurotransmitters compared to untreated controls in wildtype worms. In addition, in ceruloplasmin-deficient worms, Cu failed to induce any alterations in neurotransmitter levels, however, mutant strain ceruloplasmin displayed significantly reduced GABA levels compared to the wildtype. In contrast, atox-1-deficient worms had the similar basal levels of neurotransmitters in comparison to wildtype worms, but levels of DA, SRT, GABA and ACh were reduced upon treatment with 2 mM Cu for 24 h. The aldicarb-induced paralysis assay was used to examine alterations in the synaptic transmission rate at the neuromuscular junction in *C. elegans* [256,352]. Results revealed significant differences between wildtype and ceruloplasmin-deficient worms, as they displayed aldicarb resistance starting at 240 min aldicarb treatment compared to wildtype worms (Figure 30E). Cu failed to alter the aldicarb-induced paralysis (Supplementary Figure 44) and thus did not lead to changes in the synaptic transmission rate at the neuromuscular junction.
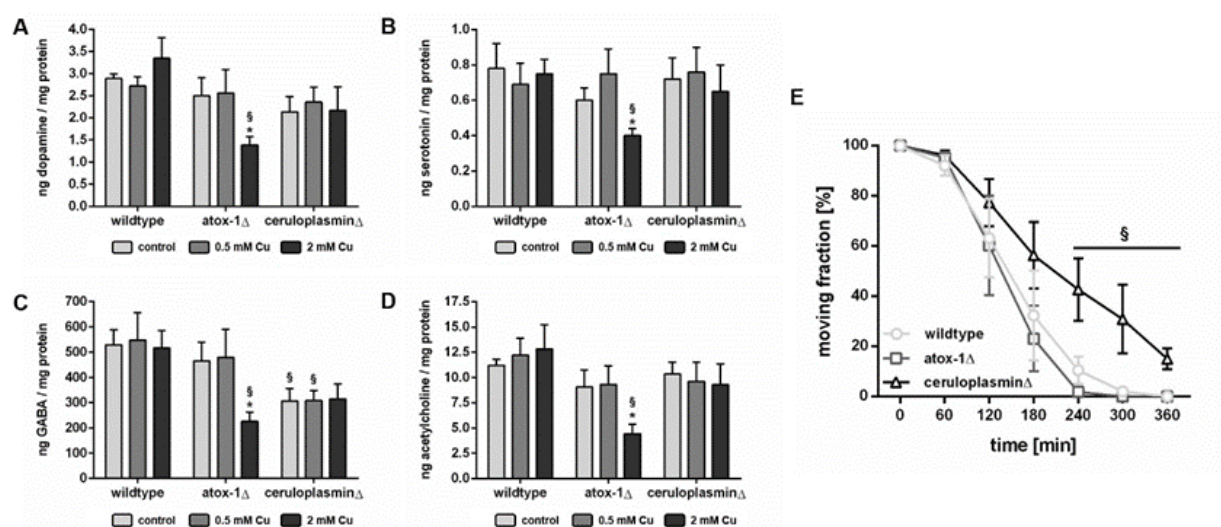
Figure 30: Neurotransmitter levels in ng per mg protein in *C. elegans* quantified via HPLC-MS/MS. Assessed were levels of (A) DA, (B) SRT, (C) acid GABA and (D) ACh. Aldicarb-induced paralysis assay in (E) untreated wildtype (light grey), atox-1Δ (dark grey) and ceruloplasminΔ (black) worms. Plotted are the fraction of moving worms [%] against the assay procedure time [min]. Data presented are mean values of n ≥ 4 independent experiments ± SEM.

5.4. Discussion

Cu is an essential trace element, but is toxic when exceeding the homeostatic range, leading to oxidative stress [298]. Especially labile Cu, namely readily available Cu, is redox active and associated with neurodegenerative diseases, such as Wilson's disease (WD), Alzheimer's disease (AD) and Parkinson's disease (PD) [18,332]. However, the exact underlying mechanisms of Cu toxicity and neurotoxicity are poorly understood. It is therefore of paramount importance to shed light on molecular mechanisms of (labile) Cu-induced oxidative stress and neurotoxicity, which was addressed herein. We used *C. elegans* mutants with a disrupted Cu homeostasis and quantified, by a variety of highly specific and sensitive techniques, oxidative stress-related metabolites. Worm mutants lacking Cu chaperone atox-1 or Cu storage protein ceruloplasmin display elevated labile Cu levels, which was characterized in detail in our previous work [55].

MAP kinases induced by, among others, oxidative stress activate transcription factors like skn-1/NRF2 or daf-16/FOXO4, which then translocate into the

nucleus to induce apoptosis, antioxidative defense or DNA repair [353]. Cu treatment led to a significant activation and translocalization of daf-16/FOXO4 in a concentration-dependent manner, corroborating earlier studies [354] and similar effects by other divalent metals like manganese (Mn) [355]. mRNA levels of *daf-16/FOXO4* remained unaffected after 24 h. However, as this is one of the first pathways affected by RONS, mRNA levels may have returned to normal. Urban et al. investigated gene expression levels of the antioxidant defense system over a time period of 10 days and display different time frames of up- and downregulation of genes related to oxidative stress [356]. Other studies reported Mn- and zinc-induced oxidative stress and neurotoxicity, but in that scenario *daf-16/FOXO4* mRNA levels were unaffected as well [314]. Gene expression studies of representatives of the MAPK family revealed Cu-induced increase in *mpk-1/MAPK1* levels in wildtype worms, as well as altered basal levels in both deletion mutants of atox-1 and ceruloplasmin. He et al. corroborate these findings by displaying Cu-mediated cell death via p38 MAPK activation in vascular endothelial cells [9], while Wang et al. report the absence of Cu-induced apoptosis in *C. elegans* loss-of-function mutants of JNK and p38 MAP kinases [357], indicating the participation of MAPKs in the regulation of Cu-induced oxidative stress.

Cu overload increases the formation of RONS and leads to oxidative stress, which alters, among others, SOD or GPX activity, which then leads to oxidative stress [144,164]. It was shown that the GSH/GSSG ratio is reduced by Cu nanoparticles [9], supporting our data of reduced GSH and increased GSSG levels following Cu treatment. Notably, GSH levels were reduced by 23% in wildtype worms, whereas by 38% in ceruloplasmin-deficient worms, indicating a higher demand or consumption. A higher demand results in an increased synthesis [358], mediated by increased mRNA levels of *gcs-1/GCLC* in ceruloplasmin- and atox-1-deficient mutants. As stated above, Cu mediates p38 downstream activation of transcription factors like daf-16/FOXO4 or

skn-1/NRF2, which activates gcs-1/GCLC expression [138]. GSH synthesis is ATP-dependent [359], potentially reducing ATP levels in ceruloplasmin-deficient worms, which are even further lowered by Cu treatment. Baldissera et al. also showed reduced hepatic ATP levels by Cu in *Cichlasoma amazonarum* [8]. In turn, levels of ADP and AMP, which are formed during ATP consumption [148], are increased by Cu supplementation in atox-1- and ceruloplasmin-deficient worms. In addition to GSH, Cu also alters GSSG levels in wildtype and atox-1 mutants, but significantly less in ceruloplasmin-deficient worms. This may indicate a higher rate of recycling or reducing GSSG back to GSH. This process is, among several others, NADPH-dependent, and is decreased in ceruloplasmin-deficient worms. Although this could be a possible explanation, it is noteworthy that energy-related nucleotides take part in other metabolic pathways as well. Thus, NAD^+ is formed in the GSH/GSSG cycling, which gets elevated by Cu treatment in ceruloplasmin-deficient worms. The Cu-sensing transcription factor Mac1 activates BNA expression and in turn quinolinic acid synthesis which results in *de novo* NAD^+ synthesis, which has been demonstrated in yeast [360,361]. Furthermore, Li et al. described a Cu-dependent S-Adenosylhomocysteine hydrolase inhibition, which results in a shift towards NAD^+ in the $NADH/NAD^+$ pool [362].

Recent studies have uncovered a rise in MDA levels subsequent to Cu treatment across various organisms [9,363,364], including *C. elegans* [144]. Our findings in wildtype worms demonstrated no alterations in either bound or unbound MDA levels, potentially attributed to our administration of (in wildtype worms) non-lethal Cu concentrations. Surprisingly, mutants deficient in atox-1 and ceruloplasmin exhibited comparable baseline levels of unbound MDA, yet notably heightened levels post-Cu treatment compared to wildtype worms. This suggests an increased hypersensitivity to Cu-induced oxidative stress or impaired antioxidative response under conditions of disrupted Cu homeostasis. CLs are vulnerable to oxidative damage due to their exclusive location within

the inner mitochondrial membrane, where RONS are generated as byproduct of cellular respiration [147]. Oxidative stress can result in lipid oxidation and therefore in the formation of oxidized CL species [365]. Our findings indicate no observable formation of oxidized cardiolipins following Cu incubation (data not shown). Blume et al. demonstrated a slight reduction in the total CL content following iron or manganese treatment, but no formation of oxidation products in *C. elegans* [366]. Furthermore, the distribution of individual CL species, known as the CL profile, remains unaffected by Cu exposure or the genetic makeup of the worms. It is noteworthy, however, that our analysis may not quantify all existing CL species, thus limiting our analysis to those above the detection threshold. Moreover, the data presented herein were solely in reference to untreated wildtype worms, as the establishment of improved standards and normalization procedures was essential for facilitating quantitative assessments. Nevertheless, the total sum of analyzed CL reveals a notable reduction in ceruloplasmin-deficient worms compared to the wildtype. Monteiro-Cardoso et al. stated that the total CL content drops significantly in the brain of an AD mouse model [344]. Several studies have also indicated that the dysregulation of CL content, as well as alterations of its structure and distribution, mediated neuronal dysfunction. These abnormalities are associated with the aging process and play a pivotal role in the pathogenesis of various neurodegenerative disorders, including AD and PD [151]. Aberrant levels of CLs have been linked to mitochondrial dysfunction, oxidative stress and impaired synaptic transmission, which are all hallmarks of AD and PD pathology. Understanding the mechanisms underlying cardiolipin-mediated neurodegeneration may offer novel therapeutic strategies aimed at preserving mitochondrial function and mitigating oxidative stress-related neuronal damage [151,344,367].

Cu and Cu nanoparticles have been shown to disrupt genomic integrity by causing oxidative DNA damage and DNA strand breaks [11,12]. Thus, it is

surprising that Cu failed to induce PARylation. This leads to a first assumption that possible DNA damages may already be repaired and that PAR was already degraded in our chronic exposure scenario of 24 h. However, 8oxodG, which is the most common DNA lesion [351], was significantly increased in ceruloplasmin-deficient worms following 24 h Cu incubation, refuting our first assumption. Like wildtype worms, ceruloplasmin mutants exhibited no alterations of PARylation levels, also this strain revealed Cu-induced DNA damage observed characterized by increased 8oxodG levels. PARylation is one of the largest consumers of NAD^+ [159]. Our data reveal normal levels of NAD^+ in wildtype worms and even further increased levels in ceruloplasmin mutants. At first glance, this indicates that NAD^+ deficiency can be ruled out as cause for normal PARylation levels. But it must be noted, that our data only reflect the total NAD^+ content instead of organell-specific selective NAD^+ levels. mRNA levels of *pme-1/PARP1* and *pme-2/PARP2* also remained unchanged in wildtype and ceruloplasmin-deficient worms. Taken together, these findings suggest that Cu inhibited PARylation, as previously hypothesized by Schwerdtle et al. [368]. Basal levels of PARylation were reduced in atox-1 mutants, possibly due to reduced Cu transport into the nucleus by the lack atox-1, but partially compensated by P-type ATPase ATP7B [369]. In addition, atox-1 interacts with PARPs in a detoured manner. Atox-1 induced the expression of MDC1, a crucial protein for double strand repair [370]. MDC1 interacts with aprataxin [371], which in turn works in concert with PARP's [372], which could explain lowered PARylation and *pme-2/PARP2* mRNA levels in atox-1-deficient mutants compared to wildtype worms. This needs to be further elucidated in *C. elegans*. Although 8oxodG levels were not altered in atox-1-deficient worms, Cu appeared to adversely affect the genomic stability of this mutants, as Cu treatment increased both PARylation and *pme-2/PARP2* mRNA levels. The low basal PARylation raise further concerns, since inhibited PAR has been linked to cellular toxicity as well as neurological dysfunction [162]. Although herein

excess Cu failed to cause genotoxicity in wildtype worms, our data underline the importance of a properly functioning Cu homeostasis for genomic integrity.

The loss of proper antioxidant capacity and energy production as well as impaired genomic integrity may cause neuronal death [18,373]. Cu is known to cause neurotoxicity and is associated with neurodegenerative diseases, such as WD [374,375]. Labile bound Cu is commonly mentioned in the context of Cu-induced neurotoxicity [319,332], but knowledge on underlying mechanisms is scarce. Ceruloplasmin-deficient worms revealed aldicarb-resistance, reflecting decreased synaptic transmission rate at the neuromuscular junction [352]. Dabbish et al. demonstrated a correlation between aldicarb-sensitivity and reduced GABA levels [376]. This is contrary to our findings, as ceruloplasmin mutants displayed, next to aldicarb-resistance, reduced GABA levels compared to wildtype worms, indicating that further unknown factors may be involved. One likely mechanism of reduced GABA levels in ceruloplasmin-deficient worms might be that excess Cu, as described by D'Ambrosi et al. [377], reduces GABA receptor activity, resulting in altered GABA levels. Atox-1 deletion mutant's basal levels of neurotransmitters remained unchanged compared to wildtype worms but were reduced due to 2 mM Cu treatment. Kelner et al. noted that atox-1 suppressed oxidative damage and promoted neuronal survival [77]. Furthermore, atox-1 is known to interact with α-synuclein and inhibit amyloid formation [378]. This is in agreement with our findings on Cu-mediated reduction in neurotransmitter levels due to the lack of atox-1, reflecting Cu-induced neurodegeneration upon loss of atox-1. Our data support that the dysregulation of Cu homeostasis leads to oxidative stress and subsequent detrimental effects on neurocellular pathways, underlining the importance of a properly working Cu homeostasis.

5.5. Conclusion

A comprehensive approach was adopted, employing specific and sensitive techniques to quantify metabolites related to oxidative stress with special focus on mitochondria, oxidative DNA damage, DNA damage response as well as neurodegeneration in the context of disrupted Cu homeostasis. Loss-of-function mutants of Cu chaperone atox-1 and Cu storage protein ceruloplasmin displayed increased labile Cu levels despite lowered total Cu uptake [55] concomitant with increased oxidative stress, reduced mitochondrial ATP levels and CL content, as well as oxidative DNA damage and impaired neuronal health. Our data underline the essentiality of a proper Cu homeostasis and the importance of valuable markers, such as labile Cu, to diagnose Cu dyshomeostasis. Furthermore, our study highlights the importance of mitochondrial integrity for genomic and neuronal health. As a future perspective, understanding the intricate interplay of CL dysregulation and neurodegenerative processes holds significant promise for the development of therapeutic interventions preserving genomic and neuronal stability.

5.6. Funding information

5.7. Author's contributions

Conceptualization: A.W., J.B.; Investigation/Experiments: A.W., A.G., T.M., V.S., K.S.; Methodology: A.W., A.G., V.S., A.T.; Supervision: J.B.; H.H.; Funding acquisition: J.B.; Visualization: A.W.; Writing-original draft and revision: A.W.; Writing-review and editing: A.G., T.M., V.S., K.S., A.T., T.S., M.A., H.H., J.B.; All authors have read and agreed this version of the manuscript.

5.8. Acknowledgement

5.9. Keywords

Copper dyshomeostasis, oxidative stress, mitochondrial impairment, cardiolipins, genomic and neuronal instability

Abstract

The mechanisms associated with neurodegenerative diseases, such as Alzheimer's disease (AD) and Parkinson's disease (PD) have yet to be fully characterized, and genetic as well as environmental factors in their disease etiology are under appreciated. While mutations in genes such as PARKIN and LRRK2 have been linked to PD, the idiopathic component of the disease suggests a contribution of environmental risk factors, including metals such as copper (Cu). Cu overexposure has been reported to cause oxidative stress and neurotoxicity, but its role in neurodegenerative diseases is rarely studied. Using *Caenorhabditis elegans* (C. elegans) as a model organism for neurotoxicity, we assessed the effects of Cu oversupply in AD and PD models. Our findings reveal that while copper treatment did not induce neurodegeneration in wildtype worms or the AD model, it significantly exacerbated neurodegeneration in the PD-associated mutants PARKIN and LRRK2. These results suggest that genetic predisposition for PD enhances the sensitivity to copper toxicity, highlighting the multifactorial nature of neurodegenerative diseases. Furthermore, our study provides insights into the mechanisms underlying Cu-induced neurotoxicity in PD models, including disruptions in dopamine levels, altered dopamine-dependent behavior and degraded dopaminergic neurons. Overall, our novel findings contribute to a better understanding of the complex interactions between genetic susceptibility, environmental factors, and neurodegenerative disease pathogenesis, emphasizing the importance of a tightly regulated Cu homeostasis in the etiology of PD.

Chapter 6 – Copper-mediated neurotoxicity and genetic vulnerability in the background of neurodegenerative diseases in *C. elegans*

Based on:

Ann-Kathrin Weishaupt, Lysann Ruecker, Torben Meiners, Tanja Schwerdtle, Daiana Avila, Michael Aschner and Julia Bornhorst

Chapter 6 – Copper-mediated neurotoxicity and genetic vulnerability in the background of neurodegenerative diseases in *C. elegans*

6.1. Introduction

Neurodegenerative diseases like Alzheimer's disease (AD) and Parkinson's disease (PD) are neurodegenerative disorders exhibiting a diverse range of pathological patterns, making their onset mechanisms complex and often elusive [319]. Symptoms of PD are multifaceted, including among others, bradykinesia, tremor, rigidity as well as numerous non-motor symptoms [216]. Although the majority of PD cases are idiopathic, mutations in several genes have been connected to the disease including *PARK2/parkin* and *LRRK2* [219]. Parkin serves as a ubiquitin E3 protein ligase and acts as a versatile protective agent, especially for mitochondria [379]. Disturbance in the ligase activity of parkin is reported to contribute to the pathogenesis of both sporadic and familial forms of PD [380]. Loss-of-function mutations in Parkin can disrupt cellular processes, contributing to disturbances in cell function and ultimately leading to broader pathological changes [381]. LRRK2 (leucine-rich repeat kinase 2) plays an important role in various pathways and cellular signaling processes, including the regulation of protein translation, vesicle trafficking, and neurite outgrowth [217]. The most prevalent *LRRK2* mutation is the G2019S variation [382]. The *LRRK2* G2019S mutation is associated with a gain-of-function effect, which may lead to alterations in autophagy-lysosomal pathways and dysregulation of protein synthesis mechanisms, as well as oxidative stress [383]. Variations in the *PARKIN* and *LRRK2* genes may result in typical clinical symptoms and age-dependent characteristics of PD [382] by affecting dopamine metabolism and causing selective dopaminergic neurodegeneration [379,384]. The progressive loss of dopaminergic neurons and lowered dopamine (DA) levels are the

hallmark of PD [191,380]. AD is also characterized by neurotransmitter disruptions. In addition to reduced DA levels, reduction in choline acetyl transferase and acetylcholine (ACh) synthesis, as well as altered choline uptake and release are inherent to brain tissue of AD patients [215]. One key player to alter central cholinergic functions are plaques of aggregated β-amyloid protein (Aβ) [385]. Aβ formation and neurofibrillary tangles binding tau protein are in the center of attention in the pathology of AD [386]. The toxic range of Aβ extends from mitochondrial alterations, over synaptic dysfunction to oxidative stress [387]. Elevated concentrations of metals like copper (Cu), zinc or iron are bound to Aβ peptides in plaques of AD patients [212]. Some studies have therefore stated, that AD can be considered as a type of metal dyshomeostasis [212]. In AD and PD, overabundance of Cu has been implied as an environmental factor in disease etiology [123,388]. Due to excessive industrial and agricultural use, Cu is increasingly introduced into the environment [144]. Cu overexposure has been reported to cause neurotoxicity with oxidative stress as potential underlying mechanism [164]. In general, neuronal damage due to oxidative stress is an often-discussed mechanism in the onset of neurodegenerative diseases [123]. However, other studies report Cu-induced neurotoxicity, but less is known about its role in AD and PD [296].

In this work, the invertebrate *Caenorhabditis elegans* (*C. elegans*) with a well-elucidated nervous system was applied [178]. Neurotoxicity in *C. elegans* can be examined on different levels. This includes molecular trafficking of, for example, neurotransmitters, but also behavioral assessment. In addition, the transparency of the worm offers an opportunity to probe mutants with fluorescent tags to study neuronal morphology. Another advantage is the large variety of mutants, which, among others, simulate genetic AD and PD [178]. Within this study, we use a deletion mutant (Δ) of pdr-1 (mammalian Parkin), as well as a mutant harboring the g2019s variant of LRRK2 as models of PD. Additionally, an Aβ-expressing mutant was used as AD model. The etiology of

most neurodegenerative diseases has yet to be fully understood, but it has been hypothesized that it represents a multisystemic pathology due to the interaction of a challenging environment and susceptible genetic factors [221,389]. Therefore, the aim of this study was to investigate how an oversupply of the essential trace element Cu affects an individual with a genetic predisposition to AD and PD using the *in vivo* model organism *C. elegans*.

6.2. Material and methods

6.2.1. *C. elegans* handling and treatment

The following strains were obtained from the Caenorhabditis Genetics Center (CGC, Minneapolis, USA), which is funded by the National Institute of Health Office of Research Infrastructure Program: Bristol N2 (wildtype), the deletion mutants VC1024 *pdr-1* (*gk448*) and CB1112 *cat-2* (*e1112*) as well as the transgenic strains CL2006 which expresses $A\beta_{1-42}$ in the cytoplasm of body wall muscle cells and WLZ3 which presents the g2019s mutation in LRRK2. The BY200 strain [vtls1(*dat-1*p::GFP; *rol-6*)] was kindly gifted by the laboratory of Michael Aschner. All strains were cultivated on *Escherichia coli* (*E. coli*) coated NGM agar plates as previously described [292] and maintained at 20 °C, with the exception of CL2006 which was maintained at 16 °C. All experiments were conducted in age-synchronous worms [313], which were placed on NGM plates until L4 larval stage. For Cu treatment, L4 stage worms were fed with Cu-supplemented ($CuSO_4$ ≥ 99.99%, Sigma Aldrich) and heat-inactivated *E. coli* suspension on NGM plates for 24 h with up to 2 mM [390].

6.2.2. Total Cu levels via ICP-OES

Total Cu content was determined by inductively coupled plasma-optical emission spectrometry (ICP-OES) (Avio 220 Max, Perkin Elmer). The analysis was conducted as previously published [390].

6.2.3. Cu lethality assessment

To determine Cu-induced hypersensitivity and lethality of the used mutant strains, a survival assay was performed. Worms were counted as dead or alive after 24 h Cu exposure and survival rate in % was calculated. Worms were defined as dead if they demonstrated no further movement when being prodded with a platinum wire.

6.2.4. GSH and GSSG quantification by LC-MS/MS

Levels of reduced GSH and oxidized GSSG were determined by an LC-MS/MS method previously published by Thiel et al. [140]. Therefore, 1000 Cu-treated worms were pelletized by centrifugation in 100 µL 85 mM NaCl following LC-MS/MS analysis and protein normalization [293].

6.2.5. Aldicarb-induced paralysis assay

The aldicarb-induced paralysis assay was performed as previously described [178] to assess the worm's synaptic transmission rate. Aldicarb-hypersensitivity indicates a reduced synaptic transmission rate, while aldicarb-resistance indicates an increased synaptic transmission rate. For this purpose, NGM plates added with 2 mM aldicarb were always prepared fresh and coated with 2 µL *E. coli* (OP50) right before the experiment. All experiments were performed blinded to avoid a bias in counting worms as paralyzed.

6.2.6. Neurotransmitter quantification via LC-MS/MS

Neurotransmitter (DA, SRT, GABA and ACh) levels of dopamine (DA), serotonin (SRT), γ-amino butyric acid (GABA) and acetylcholine (ACh) were assessed by a previously published method [178]. Pellets were prepared by centrifugation of 1000 worms treated for 24 h with Cu in 50 µL 85 mM NaCl. Samples were prepared and analyzed as previously described [178] and normalized to protein content [293].

6.2.7. Basal slowing response (BSR) assay

After 24 h Cu incubation, worms were washed off plates using S-basal buffer, following 3 additional washing steps to get rid of excess *E. coli*. Five to ten worms were then transferred to uncoated and *E. coli*-coated (circle-shaped) plates each. After 5 min, the number of body bends per 20 sec were counted on both plates [175]. Data was calculated as body bends per 20 sec on uncoated plates minus body bends per 20 sec on coated plates (Δ body bends / 20 sec). Worm strain cat-2, which is restricted in DA synthesis [178] was used as positive control.

6.2.8. Fluorescence microscopy of dopaminergic neurons

In order to examine the integrity of dopaminergic neurons in the PD models using fluorescence microscopy, they were crossed with the BY200 strain. Successful crossing was verified by single worm PCR using the following primers: pdr-1 forward: CATGACTGCGAGGACTAGTGTGC, reverse: CACC-ACACGTAGAAGCTTCCGAG. g2019s forward: AGCTTCCTCACGAGTT-CACTTT, reverse: TCACTTAACTGCAGTGTGGGTCT. Following Cu incubation, worms were washed 3 times with 85 mM NaCl and transferred to 4% agarose pads and got anesthetized using 5 mM levamisole. Fluorescence images were obtained with a DM6 B fluorescence microscope and the Leica LAS X software (Leica Microsystems GmbH) equipped with a x63 magnification objective, excitation at 460 – 500 nm, emission range of 512 – 542 nm, constant settings and light exposure times. A series of z-stacks was carried out by optical sectioning (25 steps of about 0.5 µm) and were superimposed by the Leica LAS X software (Leica Microsystems GmbH). For evaluation, 5 – 10 worms per condition were analyzed and scored as: no alterations, irregularities (kinks and bends of dendrites, shrunken soma) and severe amendments (loss of dendrites or soma). As positive control, 6-hydroxydopamine (6-OHDA) was used. Adult worms (24 h after L4 stage) of strain BY200 were treated with 25 mM 6-OHDA for 1 h in 85 mM NaCl, following fluorescence microscopy analysis.

6.2.9. Statistical analysis

Statistical analysis was carried out using GraphPad Prism 6 (GraphPad Software, La Jolla, USA). Which statistical test has been applied as well as significance levels are stated in all figure legends.

6.3. Results

6.3.1. Total Cu levels analyzed with ICP-OES and worm lethality assessment

Cu treatment via *E. coli* for 24 h led to a dose-dependent Cu uptake, which was observed in all tested worm strains (Figure 31A). This observation ruled out that different effects of Cu in the mutant strains were Cu uptake dependent. Survival testing after 24 h Cu incubation revealed no lethal effects for all tested worm strains (Figure 31B), indicating that the applied Cu doses were in the sub-toxic range. Higher doses than 2 mM Cu were not considered, as previous studies have shown that worms avoid higher Cu doses [390].
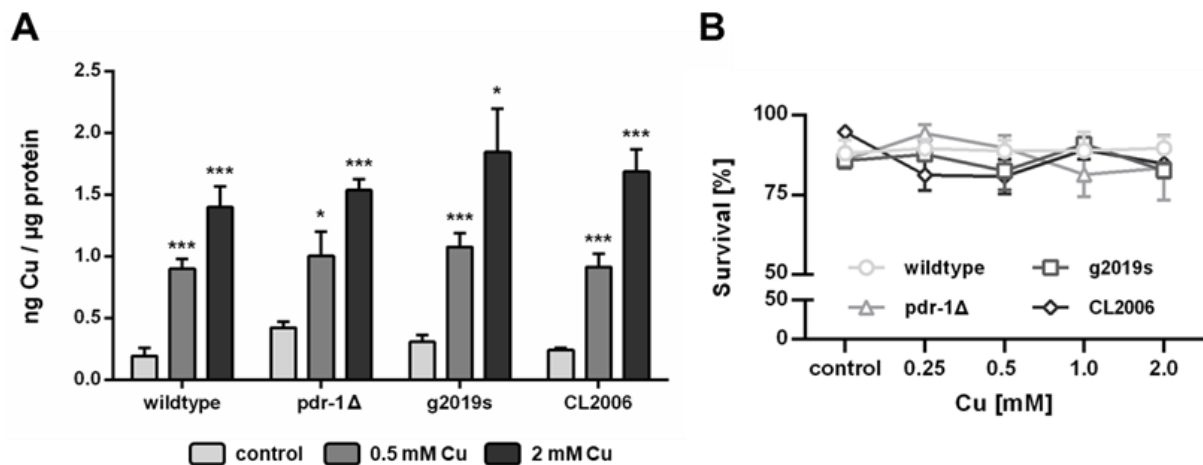
Figure 31: (A) Total Cu levels [ng/µg protein] and (B) survival [%] following 24 h of Cu incubation in wildtype worms, pdr-1, g2019s and CL2006 mutants. Data presented are mean values of n = 4 experiments ± SEM. Statistical analysis using 2-way ANOVA test with Tukey's multiple comparison. Significance level with α = 0.05: *: p ≤ 0.05; ***: p ≤ 0.001 compared to untreated control.

6.3.2. GSH and GSSG quantification by LC-MS/MS

As a marker for oxidative stress we quantified reduced GSH (Figure 32A) and oxidized GSSG (Figure 32B). Cu treatment significantly reduced GSH levels in wildtype and mutant worms. In addition, basal levels of GSH were reduced in mutant worms to 56% (pdr-1), 30% (g2019s) and 22% (CL2006) compared to wildtype worms. Moreover, Cu increased GSSG levels in all worm strains, except for CL2006.
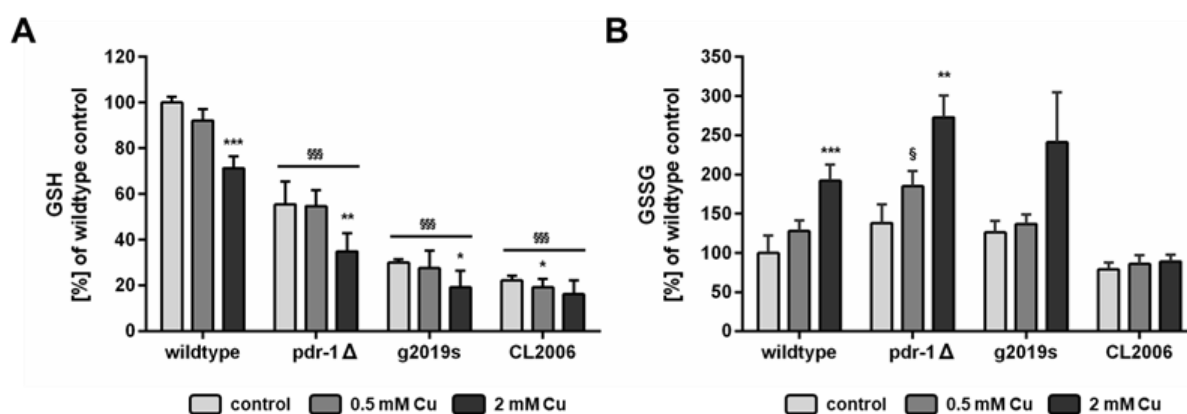
Figure 32: Relative levels of (A) reduced GSH and (B) oxidized GSSG normalized to untreated wildtype control [%] following 24 h Cu treatment quantified by LC-MS/MS. Data presented are mean values of n ≥ 4 independent experiments + SEM. Statistical analysis using 2-way ANOVA test with Tukey's multiple comparison. Significance level with α = 0.05: *: $p ≤ 0.05$; **: $p ≤ 0.01$ and ***: $p ≤ 0.001$ compared to untreated control and §: $p ≤ 0.05$ and §§§: $p ≤ 0.001$ compared to wildtype in same condition.

6.3.3. Aldicarb-induced paralysis assay

The synaptic transmission rate at the neuromuscular junction can be monitored using the aldicarb-induced paralysis assay [256]. Figure 33 reveals a significant hypersensitivity to aldicarb of the PD models pdr-1Δ and g2019s compared to wildtype worms, indicating increased synaptic transmission. On the other hand, strain CL2006 displayed a resistance to aldicarb compared to wildtype worms, indicating a lowered synaptic transmission rate. Cu does not alter the synaptic transmission rate in any of the tested worm strains (Supplementary Figure 45).
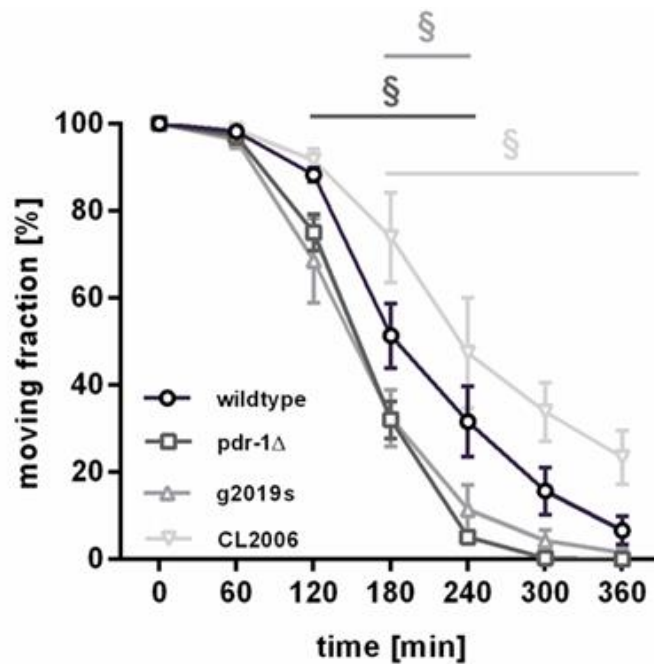
Figure 33: Aldicarb-induced paralysis assay in untreated worms. Plotted is the fraction of moving worms [%] against the assay procedure time [min]. Data presented are mean values of n = 4 independent and blinded experiments ± SEM. Statistical analysis using 2-way ANOVA test with Tukey's multiple comparison. Significance level with α = §: p ≤ 0.05 compared to wildtype in same condition.

6.3.4. Neurotransmitter quantification via LC-MS/MS

The four neurotransmitters DA, SRT, GABA and ACh were quantified by LC-MS/MS (Figure 34A – D). The analysis revealed that Cu treatment in wildtype worms does not result in altered neurotransmitter levels. Compared to wildtype worms, the AD model CL2006 had reduced DA levels and concomitantly increased GABA and ACh levels. The PD models pdr-1Δ and g2019s had reduced basal levels of DA (Figure 34A). In contrast to wildtype worms, the DA levels were significantly reduced by Cu in the PD strains, pdr-1Δ and g2019s.
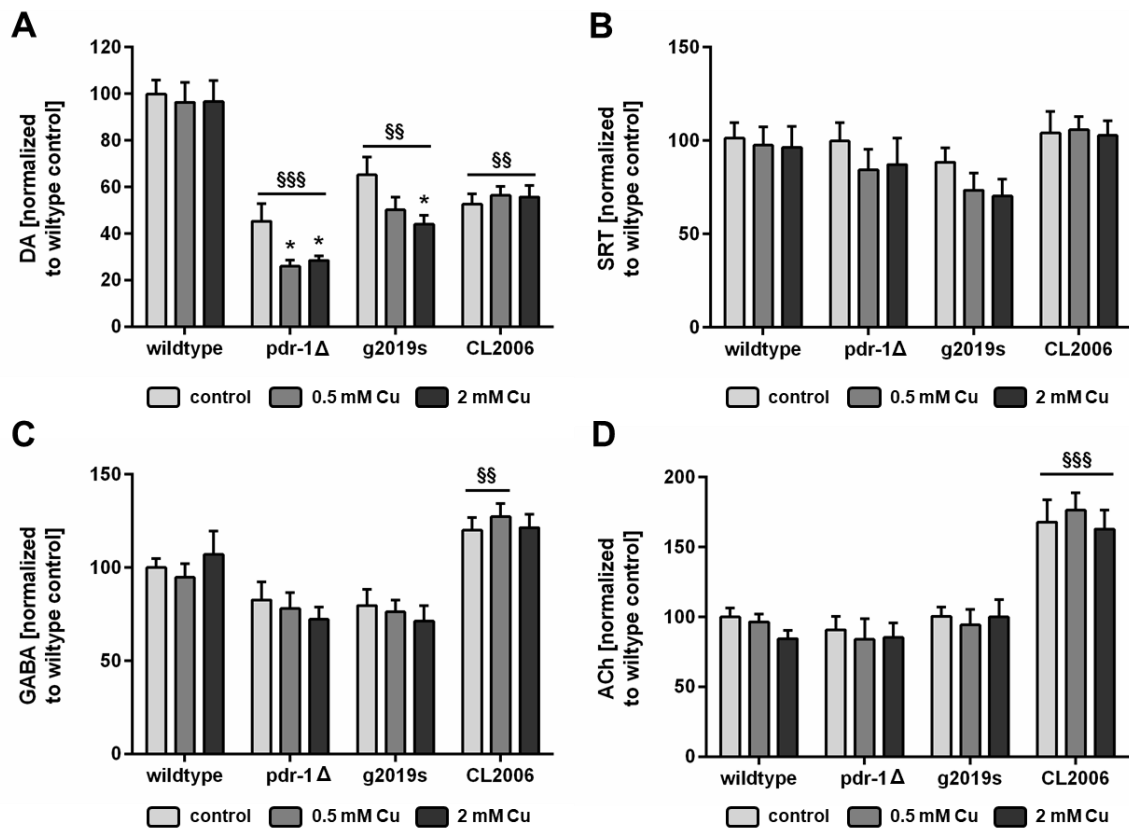
Figure 34: Neurotransmitter levels of (A) DA, (B) SRT, (C) GABA) and (D) ACh in ng per mg protein following Cu treatment. Data presented are mean values of n ≥ 4 independent experiments + SEM. Statistical analysis using 2-way ANOVA test with Tukey's multiple comparison. Significance level with α = 0.05: *: $p \leq 0.05$ compared to untreated control and §§: $p \leq 0.01$ and §§§: $p \leq 0.001$ compared to wildtype in same condition.

6.3.5. Basal slowing response (BSR) assay

Due to reduced DA levels and the Cu sensitivity of the PD models, we investigated DA-dependent the behavior using the BSR assay in pdr-1Δ and g2019s worms. BSR was evaluated as the difference (Δ) of body bends per 20 sec off-food and on-food (Figure 35). The worm strain cat-2Δ serves as positive control due to its restriction in DA synthesis. Cu exposure failed to induce alterations in the BSR in wildtype worms. Of note was the reduced BSR in the untreated PD model pdr-1 compared to untreated wildtype worms. Interestingly, Cu treatment reduced BSR in g2019s mutants.
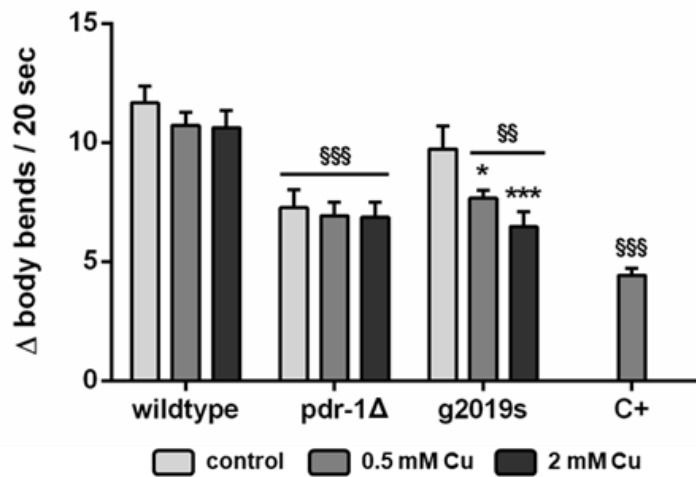
Figure 35: Basal slowing response following Cu treatment. The difference of body bends per 20 sec on uncoated plates and body bends per 20 sec on coated plates (Δ body bends / 20 sec) was assessed. cat-2Δ worms, which are restricted in DA synthesis, are used as positive control (C+). Data presented are mean values of n = 3 independent experiments + SEM. Statistical analysis using 2-way ANOVA test with Tukey's multiple comparison. Significance level with α = 0.05: *: $p ≤ 0.05$ and ***: $p ≤ 0.001$ compared to untreated control and §§: $p ≤ 0.01$ and §§§: $p ≤ 0.001$ compared to wildtype in same condition.

6.3.6. Fluorescence microscopy of dopaminergic neurons

In addition to Cu-reduced DA levels and impaired DA-dependent behavior in the PD models pdr-1 and g2019s, we investigated the morphology of dopaminergic neurons. For this purpose, we used the worm strain BY200, which expresses a green fluorescent protein (GFP) under the control of a promoter for the dopamine re-uptake transporter 1 [117]. For evaluation, an objective scoring system of 3 different events was used (Figure 36B): no alterations, irregularities (kinks and bends of dendrites, shrunken soma) and severe amendments (loss of dendrites or soma). 6OHDA was used as positive control in wildtype worms and results in severe amendments like the loss of dendrites (Figure 36C). Cu led to increased irregularities such as kinks and bends in dendrites in wildtype worms (Figure 36D – E). Both PD models pdr-1 and g2019s displayed alterations in the dopaminergic neuron morphology under untreated conditions, which worsened in response to Cu treatment.
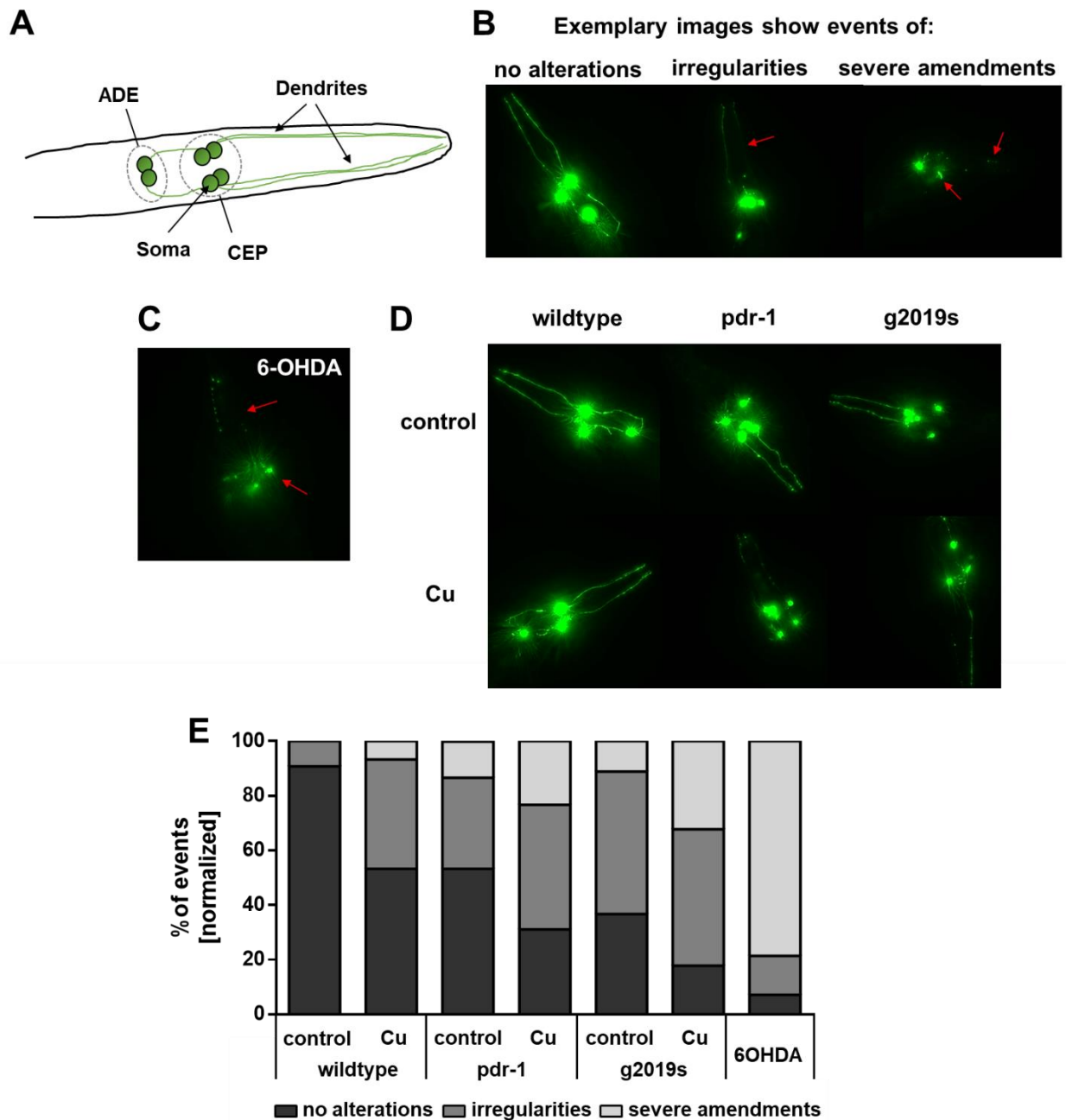
Figure 36: (A) Schematic overview of the dopaminergic neurons (ADE and CEP) in *C. elegans'* head region which can be visualized by fluorescence microscopy in the BY200 strain. (B) Exemplary images show different events of the neurons morphology marked by red arrows: no alterations, irregularities (kinks and bends of dendrites, shrunken soma) and severe amendments (loss of dendrites or soma). (C) 6-OHDA (25 mM) was used as positive control in wildtype worms. (D) Exemplary fluorescence images of wildtype worms (BY200), pdr-1 and g2019s (which were each crossed with strain BY200). Images display either untreated worms or supplemented with 2 mM Cu for 24h. (E) Overview of the number of events [%] counted in N = 5 – 10 worms per group. Data presented are mean values of n = 3 independent experiments.

6.4. Discussion

In addition to genetics, environmental factors also play a critical role in the etiology of neurodegenerative diseases. (Heavy) metals, such as Cu, are often discussed in the context of neurotoxicity [123]. The excessive use of Cu-containing chemicals and pesticides in both industry and agriculture has led to increased introduction of Cu into the environment [144]. Although redox-active Cu is associated with oxidative stress and consequently PD [123], studies on underlying mechanisms, especially in *C. elegans*, are rare. Here, we aimed to assess the interplay between environmental factors, such as Cu, and a genetic predisposition for AD and PD, as both are multifactorial diseases [389]. To this end, we used various *C. elegans* mutants that experimentally model AD or PD. In addition, we have previously shown that the nematode conserves orthologs of a mammalian-like Cu homeostasis and is a suitable model to study dyshomeostasis by excess Cu feeding [390]. Therefore, we investigated the neurotoxic consequences of Cu oversupply in *C. elegans* models of AD and PD to gain a better understanding on the interplay between genetic and environmental factors in the etiology of neurodegenerative diseases.

Toxicity testing up to 2 mM Cu treatment revealed no lethality in wildtype or mutant worms. Higher doses were not considered, as worms move away from their Cu-enriched food source and starve [390]. Although the applied doses were non-lethal, their administration led to a dose-dependent increase in total Cu levels in all tested worm strains. As wildtype and mutant worms did not significantly differ in total Cu levels, toxic effects in subsequent experiments due to differences in Cu uptake was ruled out. A limitation of the *C. elegans* model is that we can only assess Cu levels in the total worm body due to the lack of organs. Several studies reported reduced levels of Cu in the brain of AD [16] and PD [17] patients. Ejaz et al. also showed lower total Cu levels but elevated labile Cu levels in different brain areas in AD, indicating abnormal Cu homeostasis probably due to an increment in labile Cu ions and a reduced

attachment to cuproproteins [391]. Some studies point out that AD patients should be supplemented with Cu due to significantly reduced brain concentrations, while others stated that (labile) Cu levels should be further reduced [212]. Singh et al. propose that metal imbalances contribute to neurodegenerative diseases like AD and PD. They furthermore state that, in particular Cu chelation therapy is promising for AD treatment [392]. Labile Cu can bind cysteine residues in proteins, which is a proposed mechanism for the participation of Cu in the pathogenesis of PD [46]. Furthermore, Genoud et al. hypothesized that Cu homeostasis was disturbed in the brain of patients of PD and that redox-active labile Cu increased the oxidative load due to dysfunctional Cu proteins [388].

The Aβ pathway is prominently involved in AD pathophysiology, as Aβ aggregation leads to neuronal loss [212]. AD is therefore often characterized by amyloid plaques in the brain, which are formed by peptides and trace elements including iron and zinc, and especially Cu. Bagheri et al. posited that AD should be considered a disease of metal dyshomeostasis due to the integration of redox-active metals in Aβ plaques [212]. Indeed, redox-active metals like Cu can induce oxidative stress, which plays a critical role in AD pathophysiology [18]. Our data revealed a reduction of GSH in the AD model CL2006 down to 22 % compared to wildtype worms, which gets further reduced by Cu treatment. Moreover, we demonstrate increased CL2006 worms' synaptic transmission rate due to aldicarb resistance compared to wildtype worms. Meftah et al. suggested that Aβ may play a role in disease progression due to synaptic dysfunction [393]. Analysis of brain tissue of AD patients revealed altered choline acetyltransferase activity, ACh synthesis, as well as choline uptake and release, resulting in cholinergic neurodegeneration. Furthermore, some AD patients' brain regions display loss of dopaminergic neurons [215]. This finding was corroborated by neurotransmitter analysis in the CL2006 mutant worms, herein. CL2006 worms had significantly elevated levels of ACh and reduced DA

levels. Additionally, GABA levels were increased in CL2006 mutants compared to wildtype worms. Our study also corroborated neurodegeneration in the CL2006 AD model compared to wildtype worms, likely due to disturbed neurotransmitter levels and altered behavior. As already stated, AD patients often have altered brain Cu homeostasis, which results in an increased labile Cu pool, but not total Cu levels [231]. Other studies also showed neuronal instability due to a catecholamine misbalance induced by the loss of Cu homeostasis [394]. However, we failed to note further alterations due to excess Cu feeding in the AD model CL2006 compared to wildtype worms.

Parkin, a ubiquitin E3 protein ligase, acts as multipurpose protective agent, for instance in manganese-induced cell death or against dopaminergic toxicity [379]. Impairment of Parkin's ligase activity is considered to play a pathogenic role in the onset of both sporadic or familiar PD [380]. Therefore, we used a *C. elegans* deletion mutant of pdr-1 (mammalian Parkin), since a mutation in the mitophagy gene causes familial PD in worms [395]. PARKIN-KO mice are characterized by neuronal loss and fragmented mitochondria in dopaminergic neurons [396]. The loss of pdr-1 in *C. elegans* results in lowered ATP production and a reduced mitochondrial membrane potential [397], indicative of elevated oxidative stress compared to wildtype worms. This is supported by our data of reduced GSH basal levels compared to wildtype. Furthermore, Cu treatment led to decreased GSH levels and elevated GSSG formation. Other trace elements like manganese comparably enhance oxidative stress and dopaminergic neurodegeneration upon *pdr-1* deletion compared to wildtype worms [219]. Moreover, our data showed lowered basal levels of DA, altered DA-dependent behavior and disturbed dopaminergic neurons in *pdr-1* mutants compared to wildtype worms. Therefore, *pdr-1* mutants seem to display heightened sensitivity even in under normal exposure conditions, and upon over exposure to Cu, these effects are significantly magnified. Cu treatment in *pdr-1* mutants led to significantly reduced DA levels and damaged dopaminergic neurons.

Thus, excess Cu exacerbates preexisting neurodegeneration in *pdr-1* mutants and underlines the neurotoxic potential of Cu in a genetic predisposed PD-like worm strain.

The most common variation in Lrrk2 is g2019s, with patients displaying typical clinical symptoms and age-dependent characteristics of PD [382]. The pathogenic mutation g2019s enhances Lrrk2 kinase activity, which induces neurodegeneration [398] due to impaired synaptic vesicle endocytosis, which leads to alterations in the DA metabolism [384]. Moreover, it results in increased DA oxidation and aggravation of DA-specific stress in dopaminergic neurons [399]. Our data established Cu-induced reduced GSH levels (down to 30%) in g2019s-positive mutants compared to wildtype worms. G2019s-positive mutants displayed, similar to pdr-1 deletion mutants, reduced DA basal levels and destructed dopaminergic neurons. Similar findings of reduced DA levels were seen in the striatum of a g2019s-positive mouse model [400]. Other studies have shown the progressive dysfunction of DA transporters [401] and higher caspase activity [402] in DA neurons due to the g2019s mutation. The effects of Cu in g2019s-positive worms were significantly greater than in wildtype worms, characterized by reduced DA levels and demolished DAergic neurons. Furthermore, Cu treatment impaired the basal slowing response, and in turn, DA-dependent behavior. hence, the effects of Cu on DA metabolism were exacerbated in worms with genetic predisposition for PD, namely G2019s-positive mutants.

In conclusion, our study corroborated DA-dependent alterations in PD models of *C. elegans* [191,192]. Additionally, we identified alterations in DA levels, dopaminergic neuron morphology, and DA-dependent behavior, which were worsened by excess Cu feeding in genetic PD models. The deletion mutant of pdr-1/Parkin and the mutant with g2019s variation in Lrrk2 were hypersensitive to Cu exposure compared to wildtype worms. This raises the question as to whether individuals genetically predisposed to PD might have different

requirements for Cu and other trace elements, and the need for special nutritional recommendations. Furthermore, it suggests that certain mutations (but not all, see below) sensitize these genetically predisposed individuals to develop neurodegenerative diseases, such as PD and AD. Consistent with this suggestion, Cu supplementation failed to induce neurodegeneration in wildtype worms. In addition, the AD model CL2006 failed to display elevated neurodegeneration due to Cu treatment. Taken together, our novel study on excess Cu feeding in *C. elegans* models of neurodegenerative diseases demonstrates that PD is a multifactorial disorder, probably due to a combination of genetics and environmental factors [221,389].

6.5. Funding

6.6. Acknowledgements

6.7. Impact statement

Copper oversupply exacerbated neurodegeneration in *Caenorhabditis elegans* models of Parkinson's disease, highlighting the genetic susceptibility and emphasizing the crucial role of a tightly regulated copper homeostasis in Parkinson's disease pathogenesis.

6.8. Key words

Neurodegenerative diseases, Genetic Predisposition, Copper toxicity, *C. elegans*

Chapter 7 – Final Discussion and Future Perspectives

Chapter 7 – Final Discussion and Future Perspectives

Cu is an essential trace element, mainly taken up via drinking water and foods like fish, nuts and legumes. Daily requirements of 1.3 to 1.6 mg for adults per day are usually met, therefore Cu deficiency is rare [3]. Excess Cu enters the environment from various human activities like industrial operations, agriculture, urban runoff and improper waste disposal. This poses risks to ecosystems and human health if not managed properly [49,50]. On the one hand, Cu plays a crucial role within redox biology of living organisms. Thus, Cu serves as electron donor essential for the proper function of diverse enzymes and biological processes [6]. On the other hand, Cu in excess is able to lead to the formation of RONS, which are capable of attacking biological macromolecules like lipids or DNA [164]. Due to its ability to catalyze Fenton-like reactions, Cu is discussed in terms of oxidative stress, mitochondrial impairment and neurodegeneration [343]. Therefore, it is of paramount importance to be able to assess reliable markers with selective and sensitive techniques, which provide significant insights into the Cu status of an individual, especially for Cu-related diseases like WD [104]. Moreover, little is known on how Cu toxicity is mediated. In particular, molecular mechanisms of labile Cu toxicity with focus on oxidative stress and neurodegeneration remain unknown [137].

Within this work, the molecular mechanism of Cu toxicity should be investigated. Suitable models displaying Cu dyshomeostasis were analyzed for their total and labile Cu levels along with the consequences on the Cu homeostasis. Furthermore, markers for oxidative stress and genotoxicity as well as neurotoxicity were assessed in terms of a disrupted Cu homeostasis. Subsequently, the consequences of excess Cu on an individuum genetically predisposed to neurodegenerative diseases like AD and PD were investigated. To examine neurodegenerative processes, the development of a highly sensitive and specific technique to quantify neurotransmitters was the first step.

Method development for neurotransmitter quantification as highly sensitive marker for neurotoxicity in *C. elegans*

C. elegans has increasingly been used as alternative to animal experiments in the field of neurotoxicity, offering a wide variety of endpoints to analyze [403]. Features of the nematode have been described in section 2.1., allowing to assess neuronal development, connectivity, physiology and behavior impacted by both environmental and genetic factors in a simplified *in vivo* setting [39,404]. Behavioral assays are the primary method for evaluating neurotoxicity in *C. elegans* [405]. These typically involve, among others, to gauge the basal slowing response, which analyzes DA-dependent behavior on and off food [175], determining serotonin-dependent pharyngeal pumping [255], evaluating synaptic transmission at neuromuscular junctions with the aldicarb-induced paralysis assay [256] and analyzing functional alterations in locomotion [175]. Another important tool to elucidate neurotoxicity in *C. elegans* is to study the morphology of neurons. The morphological evaluation of neurons relies on the activation of a fluorescent protein like GFP regulated by specific promoters for each neuron type's genes [284,405]. The following mutant strains can be used to study different categories of neurons: BY200 for dopaminergic neurons [117,283,406], LX929 for cholinergic neurons [407] or EG1285 for GABAergic neurons [408]. In addition, all neurons can be observed simultaneously using strain OH441 with pan-neuronal GFP expression [409]. While this approach can provide valuable initial insights, it also presents challenges in distinguishing between individual neuron types. Behavioral assays as well as microscopy of neuron morphology lack the opportunity to make quantitative statements regarding neurotransmitter levels. Assays like locomotion are dependent on several neurotransmitters like DA and ACh, which can be difficult to interpret. Hence, the concurrent measurement of multiple neurotransmitters proves to be a valuable and potent technique. Unlike behavioral assays and neuronal microscopy, which merely provide insights into outcomes of a neurotransmitter dyshomeostasis, quantifying neurotransmitters allows for the evaluation of

underlying causes. Our findings indicate that the cat-2Δ strain, deficient in tyrosyl hydroxylase and thus limited in DA synthesis, also exhibits decreased GABA levels. This highlights the interconnectedness and homeostatic interdependence of various neurotransmitters, underscoring once more the significance of simultaneously quantifying multiple neurotransmitters.

To simultaneously quantify neurotransmitters, we developed an LC-MS/MS-based method. Meeting the requirements of such a technique presents challenges. On one hand, the analysis must be tailored to each individual neurotransmitter for specificity, while on the other hand, it necessitates high sensitivity due to the low basal levels of neurotransmitters in *C. elegans*. Furthermore, neurotransmitters exhibit poor stability, adding another layer of complexity to the process. Mass spectrometry in MRM mode was the chosen technique due to its unmatched specificity. Distinctive mass transitions of precursor as well as fragment ions were analyzed for each analyte, which allows for unequivocal identification, since the fragment pattern of a molecule is as unique as a fingerprint [281]. Moreover, mass spectrometry permits the utilization of isotope-labeled standards. These standards correspond analogously to their respective analyte throughout the entire analytical procedure, from sample preparation to detection. This makes our method a top-notch tool for the analysis of biological samples [266]. In this work, this technique was established for measurements in *C. elegans*. Subsequently, this method was also optimized for mouse brain tissue. The method was extended to incorporate the neurotransmitter glutamate and adjustments were made to the sample preparation to accommodate the matrix. Optimization of the preparation was carried out for five distinct brain regions: cortex, hippocampus, striatum, cerebellum and brain stem. Subsequently, the analysis was employed in a collaborative study to investigate neurotransmitter levels in mice fed both a standard diet and a western diet. The findings unveiled region-specific dysregulation of neurotransmitters within the brain of the western diet-fed mice, with strongest differences observed in the cortex [410]. In addition,

neurotransmitter levels in *C. elegans* were analyzed for further projects within the Bornhorst working group as part of this dissertation project by using the presented LC-MS/MS method [117,411]. In the future, this method could be further expanded to encompass other neurotransmitters, such as tyramine and octopamine [412]. Furthermore, the quantification of neurotransmitter metabolites, such as DOPAC or homovanillic acid could be integrated as well to detect neurotransmitter changes in disease state or following toxin treatment [413]. Furthermore, future investigations could elucidate neurotransmitter alterations post-treatment with established neurotoxins in *C. elegans*. While dopamine-selective toxins like 1-methyl-4-phenylpyridinium (MPP$^+$) [414,415] and 6-OHDA [40] have demonstrated damage to dopaminergic neurons, the nematode's neurotransmitter levels post-treatment remain unexplored.

In the nervous system, neurotransmitters are pivotal in transmitting information at chemical synapses. Even minor changes within the neurotransmitter homeostasis can result in neurotoxicity and consequently neurodegenerative diseases [416,417]. This underscores the essentiality of quantifying neurotransmitters in exploring mechanisms of neurotoxicity and, moreover, in identifying potential therapeutic interventions. While neurotransmitter analysis is pivotal, it is insufficient as a standalone endpoint for evaluating neurodegeneration. To estimate neurotoxic effects and neurodegenerative processes, a combination of different approaches and techniques should be applied [418]. *C. elegans* presents the opportunity to quantify molecular-level alterations in neurotransmitter content, manifested through various behavioral changes and morphological alterations in different types of neurons. Taken together, these attributes make *C. elegans*, combined with highly sensitive and specific analytical approaches, a reliable and powerful tool for investigations in the field of neurotoxicity.

Cu homeostasis and labile Cu levels are disturbed due to the loss of crucial Cu chaperone atox-1 and Cu storage protein ceruloplasmin in *C. elegans*

Exceeding the physiological range, Cu has been associated with the emergence of neurodegenerative diseases like WD, AD and PD [14,319]. Hence, it is vital to have mechanisms in place which regulate the Cu homeostasis in an efficient way. Therefore it is crucial to gain a better insight into the interplay of Cu-related proteins and their regulatory mechanisms. Ongoing research focuses particularly on labile Cu, as it is readily accessible for cellular absorption and has been suggested to potentially breach the blood-brain barrier in the form of a low molecular weight Cu complex [104]. Given Cu's redox properties, a stringent regulation is essential to protect cells from increasing labile Cu levels, which can trigger the formation of RONS [15,419]. In this study, we investigated Cu dyshomeostasis through excessive Cu feeding and utilized models which exhibit genetic imbalances in Cu homeostasis. The deletion mutant of ceruloplasmin lacks the primary Cu storage protein, while the main Cu chaperone is absent in mutant strain atox-1. Collectively, our findings delineate the roles of ceruloplasmin and atox-1 in Cu homeostasis and identify functional markers in the model organism *C. elegans*.

Our study revealed that the applied doses up to 2 mM for 24 h did not induce lethality in wildtype worms, but ceruloplasmin and atox-1 deletion mutants displayed reduced survival rates down to about 90%, indicating Cu hypersensitivity. Total Cu levels saw a concentration-dependent increase in all three tested worm strains, but notably less in ceruloplasmin and atox-1 deletion mutants. This implies that mutants with disrupted Cu homeostasis possess an altered storage capacity for Cu, which can be caused by a diminished influx, enhanced efflux, inadequate storage capacity or a combination thereof. ToF-SIMS analysis unveiled a uniform distribution of Cu throughout the worm's body. Additionally, depth profiling analysis corroborated the total Cu data

quantified by ICP-OES, demonstrating that wildtype worms exhibited the highest total Cu content, while ceruloplasmin-deficient worms displayed the lowest levels after 24 hours of treatment with 2 mM Cu. Moreover, our findings suggested that disturbances in Cu levels and Cu dysregulation accompany alterations in the gene expression of key players in the Cu homeostasis, such as *atp7a/b*, *atox-1*, *ceruloplasmin*, *mtl-1* and *mtl-2*. The fact that atox-1 and ceruloplasmin deletion mutants display lowered total Cu levels but elevated mRNA levels of Cu exporter *atp7a/b* is unexpected. This could indicate that, instead of total Cu content, labile Cu is causing the alterations in gene expression levels. Despite lower total Cu levels, labile Cu levels of the tested mutant strains assessed by fluorescent dye CF4 were higher than in wildtype worms. These findings underline that labile Cu could be a valuable marker that should be included in the methodology for determining the Cu status, thereby aiding in the risk assessment or diagnosis of Cu dysregulation-related disorders. Taken together, this study underlines the importance of a proper functioning Cu homeostasis and that the Cu status of an individual should be monitored by multiple functional markers, including labile Cu, in order to provide selectivity and sensitivity to detect alterations in Cu homeostasis.

Nevertheless, this study also presents several limitations. Mammals encode two separate genes for both P-type ATPases, one each for *ATP7A* and *ATP7B*. *C. elegans*, on the other hand, carries only one single gene of *atp7a/b*, albeit with high sequence similarity to human homologs [64]. Therefore, neurodegenerative diseases like WD and MD cannot be imitated in *C. elegans*. Chun et al. displayed, that a deletion mutant of *atp7a/b* (strain cua-1Δ) fails to lay eggs, indicating that atp7a and atp7b are required for normal growth and health in *C. elegans* [64]. Studies using analytical imaging techniques like ToF-SIMS in *C. elegans* are rare. Next to our work, only a handful of studies exist using such techniques in the nematode [420–422]. Within this study, the distribution of Cu could be observed over the entire worm body by ToF-SIMS. However, the resolution of this technique is not sufficient enough to investigate

the localization of Cu on a subcellular level. This would require the use of techniques with higher resolution, such as NanoSIMS [321]. Sample preparation for NanoSIMS is complex as fixation of cells and tissue is needed due to the high vacuum requirements of the analysis [423]. Future studies should therefore focus on the establishment of a sample preparation protocol for *C. elegans* samples for NanoSIMS analysis, to apply this unparalleled technique for the first time in worms to visualize subcellular metal localization. Another limitation of *C. elegans* is its lack of organs or specific tissue that can be isolated and analyzed individually. However, examining neuronal cells or isolated brain tissue is advantageous in the evaluation of neurotoxicity. For instance, research across various *in vitro* and *in vivo* models has demonstrated the presence of labile Cu pools within neurons and the brain [108,308,331,424]. In our study, the fluorescent probe CF4 was used to determine labile Cu (I) levels. In future studies, probes specifically designed for the detection of labile Cu (II) could also be utilized in *C. elegans* [15,104]. Since oxidative stress and neurodegeneration are often associated with mitochondrial dysfunction, future studies should focus on the isolation of mitochondria in the here used worm strains to determine mitochondrial Cu content [425,426]. As evidenced by our data and other studies, mRNA expression of metallothioneins *mtl-1* and *mtl-2* did not align with their respective protein expression levels [341]. Therefore, genes of which mRNA levels were assessed, the encoded protein content should be investigated as well, which is usually determined by western blot analysis. This underlines an additional limitation of *C. elegans*, as there is a lack of suitable antibodies available for the nematode [427,428]. A transcriptome analysis should also be carried out in future studies. Although this does not provide quantitative results like qPCR assessments, it does give a broad overview of differentially expressed genes within the complete set of RNA transcripts. In particular, transcription profiling of atox-1 and ceruloplasmin deletion mutants can be used to pinpoint alterations linked to the mutant's phenotype [429]. The transcriptome analysis could therefore provide information on which metabolic pathways are

affected by excess Cu feeding or genetic Cu dyshomeostasis in *C. elegans*. This would provide a useful basis for the conduction of targeted mechanistic studies in the future [430].

Cu-mediated oxidative stress results in genomic and neuronal instability in *C. elegans*

Although Cu is vital as a trace element for biological individuals, excessive Cu can result in an overproduction of RONS due to its redox properties [163]. Therefore, maintaining a tightly regulated Cu homeostasis is crucial for overall health [330,332]. Dysregulation of Cu levels and increased (labile) Cu levels are linked to oxidative stress and neurodegenerative disorders, yet the underlying mechanisms are still poorly understood. Therefore, this study aimed to investigate the molecular mechanisms of Cu redox biology using the model organism *C. elegans*. Chapter 4 revealed that transgenic loss-of-function strains of atox-1 and ceruloplasmin took up less total Cu compared to wildtype worms following 24 h Cu treatment. Simultaneously, the data demonstrated that the mutants with genetic-based Cu dyshomeostasis revealed elevated labile Cu levels compared to wildtype worms. Consequently, Chapter 5 elucidated the toxic mechanisms upon a disrupted Cu homeostasis and excess Cu regarding oxidative stress and the resulting consequences for genomic and neuronal stability.

Our data revealed only few adverse effects induced by Cu in wildtype worms. However, it must be considered, that the applied doses in this study were non-lethal. Cu treatment led to a significant translocation of daf-16/FOXO4 in a concentration-dependent manner, while mRNA levels of daf-16/FOXO4 remained unchanged. Furthermore, Cu supplementation resulted in reduced GSH and elevated GSSG levels in wildtype worms. Mutants with Cu dyshomeostasis, namely deletion mutants of atox-1 and ceruloplasmin, exhibited altered conditions regarding oxidative stress markers. Particularly noteworthy is the loss-of-function mutant ceruloplasmin, which demonstrated

reduced ATP levels and increased mRNA levels of *gcs-1/GCLC*, suggesting enhanced GSH synthesis. A significant finding of our study was the decreased CL content in ceruloplasmin-deficient worms, indicating impaired mitochondrial function and well-being. Additionally, ceruloplasmin-deficient mutants displayed lower GABA levels compared to wildtype worms, indicating neuronal instability in this transgenic worm model. Cu treatment resulted in decreased GSH and increased GSSG levels in both deletion mutants. Additionally, the cleavage products of ATP, ADP and AMP, were elevated, indicating a higher energy demand. Moreover, both mutant strains exhibited an increase in unbound MDA levels, demonstrating that Cu supplementation in the context of Cu dyshomeostasis induces lipid peroxidation in *C. elegans*. Cu induced DNA damage in terms of 8oxodG formation in ceruloplasmin-deficient worms. Surprisingly, PARylation levels remained unchanged following Cu treatment, contradicting expectations. Also, the mRNA levels of *pme-1/PARP1* and *pme-2/PARP2* remained unaffected, suggesting that Cu inhibits PARylation. These findings underscore the importance of ceruloplasmin for genomic stability in Cu toxicity in *C. elegans*. In atox-1 deletion mutants, basal levels of neurotransmitters remained unaltered compared to wildtype worms, but decreased upon 2 mM Cu treatment. This confirms the necessity of the Cu chaperone atox-1 and once again highlights the importance of a balanced Cu homeostasis for neuronal well-being in *C. elegans*. One notable highlight of this study was the analysis of CLs. Given the limited knowledge and possibilities for quantification, being able to detect this variety of species in the nematode is promising. Although no alterations in the pattern of CLs or the formation of oxidized CLs were detected, our study unveiled a decrease in the total CL content in ceruloplasmin-deficient worms.

Studies suggest that disrupted CL levels and structure contribute to neuronal dysfunction and neurodegenerative diseases [151]. Abnormal levels of CLs are linked to mitochondrial dysfunction and are common features of AD and PD. Therefore, future studies should focus on understanding the role of CL in the

onset of neurodegeneration [344]. The brain lipidome is vast and complex and a variety of further lipid species take part in neurogenesis and the modulation of synaptic transmission. Studies indicate that in particular phosphatidylcholine (PC) and phosphatidylethanolamine (PE) are altered in serum and the brain in neurodegenerative diseases like AD and PD [431–433]. PEs and PCs should therefore be analyzed in addition to CLs in the future as well. Our study revealed neuronal instability in ceruloplasmin-deficient worms and Cu-mediated neurotoxicity in atox-1-deficient worms. To confirm these findings, the loss-of-function mutant of ceruloplasmin should be crossed with strain EG1285, to visualize GABAergic neurons by fluorescence microscopy [408]. Furthermore, atox-1-deficient worms should be crossed with the pan-neuronal GFP-tagged strain OH441 [409]. This would allow a comprehensive overview about the neuron's morphology following Cu treatment. Our findings revealed an increase in 8oxodG levels but a lack of PARylation in ceruloplasmin-deficient worms following Cu incubation. In future investigations, it would be valuable to assess additional markers of DNA damage, such as the alkaline unwinding assay, to identify single-strand breaks [434]. Confirming Cu's genotoxicity in ceruloplasmin loss-of-function mutants would underscore its ability to inhibit PARylation. To address the possibility of a fully recovered PARylation after 24 hours, Cu could be applied to ceruloplasmin mutants for a shorter duration, for example only one hour, followed by PARylation measurement. Moreover, treating the ceruloplasmin mutant with PAR inhibitors, such as Olaparib [349], and assessing 8oxodG levels post-Cu incubation could further elucidate Cu's impact on PARylation in *C. elegans* strains deficient in ceruloplasmin. If the same results regarding 8oxodG as in this study are obtained, it would indicate that Cu inhibits PARylation in *C. elegans* transgenic strain of ceruloplasmin. Additionally, deletion mutants of atox-1 exhibited diminished levels of both total PAR and mRNA of *pme-1/PARP1*. The correlation between atox-1 and its involvement in genotoxicity and DNA damage response, particularly PARylation, remains poorly understood and warrants further investigation in

future studies. As oxidative stress is believed to be the key player in the onset of genotoxicity as well as neurotoxicity, underlying mechanisms should be further investigated. Primarily the focus should be on mitochondria, as mitochondrial stress is assumed to cause the onset of genomic and neuronal instability [435]. The mitochondrial morphology in *C. elegans* can be observed using mitochondria-specific fluorescent dyes. Following dye incubation, mitochondrial structures can be visualized by confocal microscopy [395]. Using a Seahorse Xf^{e}24 Extracellular Flux Analyzer delivers data on fundamental parameters like, among others, the basal oxygen consumption rate, ATP-linked respiration or proton leak within the mitochondrial respiratory chain. This analysis would allow a comprehensive understanding of mitochondrial metabolism and provides fast and reliable data on mitochondrial health in *C. elegans* [436]. A further meaningful marker is the total number of mitochondria, which can be analyzed via the mitochondrial DNA (mtDNA) copy number by RT-PCR, which allows to evaluate mitochondrial health [425,437]. Elevated levels of RONS are able to damage cellular components, such as DNA, proteins and lipids. This cellular damage can trigger signaling pathways, which can lead to cell death. Identifying and quantifying cell death mechanisms provides valuable insights into the impact of oxidative stress on cellular damage [438,439]. Future experiments should continue the here presented study by investigating the interplay between Cu dyshomeostasis and mitochondrial integrity as well as cell death mechanisms in the *in vivo* model organism *C. elegans*.

Genetic predisposition to Parkinson's disease leads to hypersensitivity towards Cu-induced neurotoxicity in *C. elegans*

The characterization of the mechanisms behind neurodegenerative diseases like AD and PD remains incomplete, with both genetic and environmental factors playing pivotal roles. While the majority of patients diagnosed with PD are idiopathic, mutations in several genes have been linked to the disease, for

example *PARK2/parkin* and *LRRK2*. Additionally, metal dyshomeostasis, among others disturbed Cu levels, has been implicated as an environmental risk factor in disease development [123,388]. Cu overexposure as well as dysbalanced Cu homeostasis have been linked to neurotoxicity, potentially mediated by oxidative stress [164]. While Cu as well as oxidative stress are frequently discussed in the onset of neurodegenerative diseases, its role in AD and PD remains unknown [296]. In this study, we utilized the nematode *C. elegans*, known for its well-characterized nervous system. We employed models of PD using a loss-of-function mutant of pdr-1/PARKIN and a mutant carrying the g2019s variant of LRRK2. An Aβ-expressing mutant (CL2006) was utilized as model for AD. By excess Cu feeding we investigated the interplay of Cu and neurotoxicity on individuals with a genetic predisposition to AD and PD.

Exposure up to 2 mM Cu revealed no lethal effects among wildtype or mutant worms. Despite that, all strains revealed a dose-dependent increase in total Cu levels. Notably, no significant differences in total Cu were observed between wildtype and mutants worms, ruling out variations in Cu uptake as a cause for toxic effects in subsequent experiments. Our data revealed a reduction of total GSH and an increase in total GSSG in all tested strains following Cu treatment. Furthermore, GSH was significantly less present in PD models, which was even worsened in the AD model CL2006. This finding is in line with literature, revealing that neurodegenerative diseases are associated with oxidative stress and cell death [219]. GSH depletion exacerbates oxidative stress, potentially leading to protein aggregation and neuronal cell death, which is prominent in AD and PD [440,441]. Moreover, this study demonstrated changes in synaptic transmission rates in all mutant strains, with AD and PD models revealing opposite alterations. These findings are supported by literature, since alterations in synaptic transmission contribute to cognitive and neurodevelopmental deficits [442,443]. Neurotransmitter analysis revealed no alterations in wildtype worms induced by Cu treatment. In contrast to wildtype worms, mutant strain CL2006 displayed reduced DA and increased ACh levels, common for AD [215], but no

further impairments by Cu incubation. We revealed significantly lowered total DA levels in both tested PD models. Interestingly, DA levels got further reduced in pdr-1Δ and g2019s mutants following Cu treatment. We verified Cu-induced alterations of the dopaminergic apparatus in PD models, as we assessed Cu-induced alterations of the basal slowing rate as well as impaired morphology of dopaminergic neurons by fluorescence microscopy. Our data underline that the tested PD models pdr-1Δ and g2019s are hypersensitive to Cu overexposure compared to wildtype worms. It further indicates that PD is a multifactorial disorder, due to a combination of genetics and environmental factors. This raises the question whether individuals that are genetically predisposed to PD might have different requirements for Cu and other trace elements, as well as the need for special nutritional recommendations.

In this work, reduced GSH levels were demonstrated in PD and AD models following Cu treatment. Since oxidative stress is considered as a trigger for neurotoxicity [444], future studies should further investigate the underlying mechanisms of Cu-mediated oxidative stress in individuals predisposed to neurodegenerative diseases such as AD and PD. Additionally, Chapter 5 revealed that a Cu imbalance leads to genomic instability, which should also be investigated in PD and AD models following Cu treatment.

Furthermore, the interplay between neurodegenerative diseases and Cu dyshomeostasis should be investigated. For instance, deletion mutants of atox-1 and ceruloplasmin could be crossed with the PD model g2019s. Neurotoxic endpoints regarding behavioral changes, alterations of neuronal morphology as well as neurotransmitter levels should be examined. Additionally, markers for the Cu status should be investigated, with a special focus on labile Cu levels. It would also be interesting to see whether the localization of Cu changes across the worm body and accumulates in the head area as a result of the genetic predisposition to PD and the loss of either atox-1 or ceruloplasmin. The Cu localization in these transgenic worms could be determined using ToF-SIMS.

AD can only be modeled to a limited extent in *C. elegans*. To study Aβ toxicity in the nematode is impossible per se, as *C. elegans* is unable to generate Aβ peptides due to the absence of the enzyme β-secretase [445]. To circumvent this, a transgenic line was obtained (CL2006), which expresses human Aβ in body wall muscle cells. This strain demonstrated an AD-like phenotype and its extensive Aβ deposits reacted with typical anti-Aβ antibodies [446]. However, a limitation of CL2006 is that Aβ is expressed in body wall muscle cells instead of neurons. Subsequently, a pan-neuronal Aβ-expression transgenic line (*snb-1*) has been developed. Although this strain presents intraneuronal Aβ deposits, they do not express an obvious phenotype [447]. The available Aβ-carrying transgenic strains all offer only an approximation to AD, but all have their limitations [445]. Even if experiments in Aβ models cannot be fully transferred to mammals, they offer the great opportunity to gain initial impressions of neurotoxic mechanisms. Although Cu did not alter neurotransmitter levels in strain CL2006, the effect of Cu on Aβ should be further investigated. Total Aβ content can be quantified using Western blot analysis, as described by Tangrodchanapong et al. [448]. Additionally, Aβ-specific dyes, such as Thioflavin S, can be employed for visualizing Aβ by fluorescence microscopy and for counting Aβ deposits [449]. Metal ions have been identified as a critical factor in modulating the aggregation of Aβ in AD [450]. To elevate our understanding, the quantity of Cu within Aβ fibrils could be observed and analyzed using imaging techniques such as NanoSIMS [321,451]. As ACh levels are elevated in the transgenic strain CL2006, acetylcholinesterase activity should be monitored as described by Stefanello et al. [452]. Additionally, GABA levels were significantly elevated compared to wildtype worms. In future studies, CL2006 should be crossed with strain LX929 and EG1285. This would allow to examine the morphology of cholinergic and GABAergic neurons, affected by Aβ deposits. Furthermore, strain CL2006 could be supplemented with substances like diethyl maleate to further deplete its already reduced GSH levels [356]. Subsequently, the effect of GSH depletion on Cu hypersensitivity in the context

of AD could be compared to wildtype worms. Additionally, supplementing CL2006 worms with N-acetyl cysteine (NAC), a GSH precursor [453], could reveal if NAC has a protective effect. If proven effective, NAC could be explored as a potential treatment for AD.

In summary, this thesis highlights the multifaceted role of the essential trace element Cu, addressing the risks associated with excess Cu and a disturbed Cu homeostasis. Next to Cu's pivotal role in biological processes as enzyme cofactor, elevated as well as disturbed Cu levels can lead to the formation of RONS, contributing to oxidative stress and, as shown in this thesis, leading to genomic and neuronal instabilities. Therefore, a variety of reliable and highly specific and sensitive techniques were established and applied in *C. elegans* to quantify metabolites related to oxidative stress, with special focus on mitochondria, oxidative DNA damage, DNA damage response as well as neurodegeneration in the context of a disrupted Cu homeostasis. These findings emphasize the critical need for well-regulated (labile) Cu levels and a tightly controlled Cu homeostasis and underscore the significance of reliable markers for the Cu status. Moreover, it underlines the vital role of RONS balance and mitochondrial health in maintaining both genomic and neuronal integrity. Not only does Cu dyshomeostasis pose a risk for Cu toxicity, but also genetic predisposition for PD. Data revealed Cu-mediated neurotoxicity on dopaminergic neurons in individuals with PD assessed by a comprehensive approach consisting of the analysis of DA levels, DA-dependent behavior as well as the morphology of dopaminergic neurons. This emphasizes a hypersensitivity to Cu due to a genetic predisposition to PD in *C. elegans*.

Appendix – Supplementary Material

Appendix – Supplementary Material

Supplementary for Chapter 4: Dysfunction in atox-1 and ceruloplasmin alters labile Cu levels and consequently Cu homeostasis in *C. elegans*
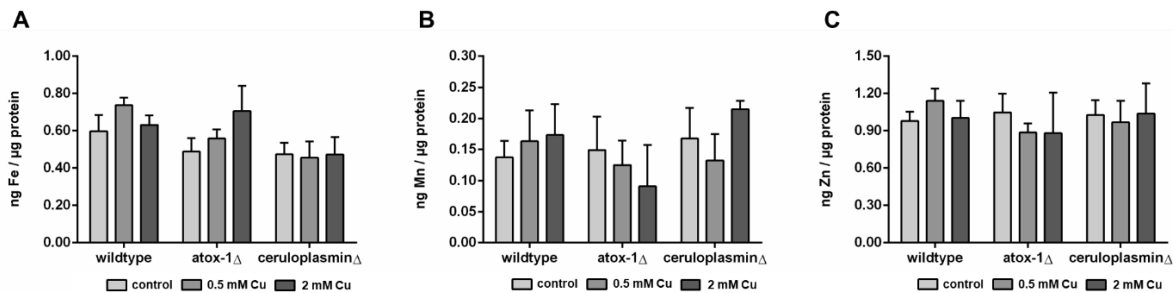
Figure 37: Total (A) Fe, (B) Mn and (C) Zn levels quantified by ICP-OES in wildtype, atox-1Δ and ceruloplasminΔ mutants following 24 h Cu treatment. Data presented are mean values of n ≥ 4 independent experiments + SEM.
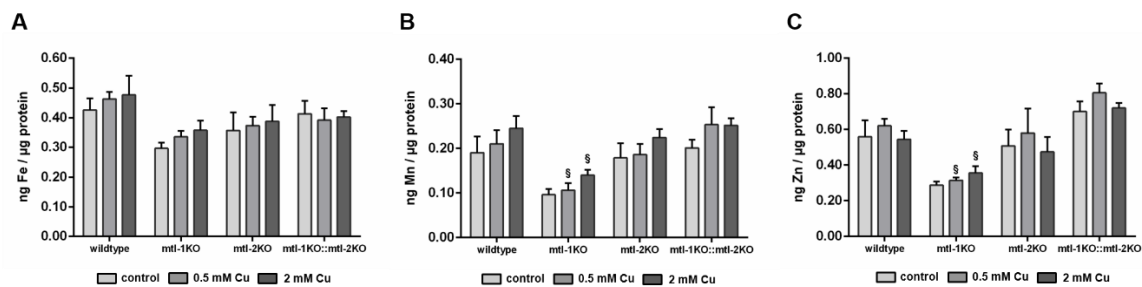
Figure 38: Total (A) Fe, (B) Mn and (C) Zn levels quantified by ICP-OES in wildtype, mtl-1KO, mtl-2KO and mtl-1KO::mtl-2KO mutants following 24 h Cu treatment. Data presented are mean values of n = 4 independent experiments + SEM. Statistical analysis using 2-way ANOVA with Tukey's multiple comparison. Significance level with α = 0.05: *: $p \leq 0.05$; compared to untreated control and §: $p \leq 0.05$; §§: $p \leq 0.01$; §§§: $p \leq 0.001$ compared to wildtype in same condition.

Supplementary for Chapter 5: Dysfunctional Copper Homeostasis in *Caenorhabditis elegans* affects genomic and neuronal stability

MDA: Settings for LC-FLD analysis and method validation parameters

LC-FLD parameters for MDA quantification

Analysis was performed by LC-FLD using an Agilent 1260 Infinity II liquid chromatography system. The chromatographic separation was performed using a Chromolith Performance RP-18 100 x 4.6 mm column at 40 °C. 5 mM KH_2PO_4 (pH 7) and MeOH were used as eluents. At a flow rate of 0.7 mL/min, the total run time was 9 min. The measurement started with 0 – 100% of MeOH in 1 min, 100% MeOH for 5 min, 100 – 0% in 2 min and 1 min equilibration at 0% MeOH. Detection was performed by a FLD at extinction of 515 nm and emission of 553 nm.

Method validation parameters

The method for determination of MDA using LC-FLD was validated according to the "ICH guideline Q2(R2) on a validation of analytical procedures" of the European Medicines Agency. All samples and standards were derivatized with 2-Thiobarbituric acid (TBA) before the measurements. The linearity, limit of detection (LOD) and limit of quantification (LOQ) were determined by adding a defined amount of homogenized worm (wild type) matrix to TMP standards before derivatization with TBA. The concentration range of the standards was between 0 – 500 nM TMP. The LOD and LOQ were determined using following formulas: LOD = 3 x SD_y/b and LOQ = 10 x SD_y/b (SD_y = standard deviation of analyte concentration in 4 blank measurements, b = slope of calibration curve). To determine the accuracy, 20 nM, 200 nM and 500 nM TMP were analyzed five times each. The ratio of the measured concentration to the expected concentration was calculated to determine the accuracy. The recovery was determined by analyzing four samples with a defined amount of worm matrix, four samples with a defined TMP concentration and four samples containing

both. To calculate the recovery, the ratio of the measured standard with matrix and the quantity of the standard without matrix was determined. To determine the intraday precision, five samples were pelletized on one day and for interday determination, five samples were pelletized on five different days. The unbound and bound MDA concentrations of these samples were normalized to protein content and the precision is stated as the relative standard deviation of the samples in percent (RSD%).

Table 7: Overview of linearity, LOD, LOQ, accuracy and recovery of the MDA method validation.

Correlation coefficient [R^2]	0.9995		
LOD [nM]	9		
LOQ [nM]	30		
Accuracy [%]	20 nM TMP	200 nM TMP	500 nM TMP
	134 ± 13	98 ± 10	100 ± 6
Recovery [%]	98 ± 8		

Table 8: Overview of intraday and interday of unbound and bound MDA.

	unbound MDA	bound MDA
intraday	16 %	10 %
interday	19 %	29 %

Experimental procedure for cardiolipin analysis

Chemicals and materials

Methanol (MeOH), acetonitrile (ACN), 2-propanol (LC/MS grade), formic acid (99-100% p.a.) and acetic acid (≥99.99%) were obtained from VWR International GmbH (Darmstadt, Germany). Methyl-*tert*-butylether (MtBE) (LC grade) was purchased from Merck KGaA (Darmstadt, Germany). Ammonium formate (≥99.995%) was purchased from Sigma Aldrich (Steinheim,

Germany). Ammonium acetate (≥99.99%) was delivered by Honeywell (Seelze, Germany). 18:2 Cardiolipin-d5 (> 99%) (d5-CL 72:8) was obtained from Avanti Polar Lipids (Birmingham, AL, USA). Water was purified by a Milli-Q EQ 7000-System (18.2 MΩcm; 0.2 µm filter; Millipore, Molsheim, France). All chemicals were used as received.

Lipid extraction

Lipid extraction of *C. elegans* samples was carried out according to a modified protocol of Matyash et al. [454] including an additional extraction cycle previously described by Helmer et al [365]. *C. elegans* nematodes in the fourth larvae stadium (L4) were extracted in pellets of 4500 worms. For resuspension of the pellet, 100 µL of water was added. Additionally, 20 µL of 65 mM BHT as an antioxidant was added before three freeze-thaw cycles in liquid nitrogen were performed. This step was followed by sonication (UP200St, Hielscher Ultrasonics GmbH, Germany) of the sample after adding 1.5 mL MeOH and 20 µL 5 µM d5-CL 72:8 as internal standard (IS). Lipid extraction was induced by adding 5 mL MtBE to the sample in 12 mL glass vials with Teflon caps. The sample was shaken for 1 h at 600 rpm at room temperature. For phase separation, 1.25 mL water was added to the extraction mixture followed by an additional 10 min incubation at room temperature. After centrifugation of the sample for 10 min at 2500 rpm (Centrifuge 5804, Eppendorf SE, Germany), the upper organic phase was collected. A second extraction cycle was then applied to the aqueous phase by adding 2 mL MtBE/MeOH/water (10:3:2.5; v/v/v). Pooled organic supernatants were dried utilizing a gentle nitrogen flow. The residue was resuspended in 200 µL of 2-propanol, resulting in a concentration of 0.5 µM IS and 6.5 mM BHT. Lipid extracts were then directly used for analysis.

Cardiolipin analysis via 2D-LC-HRMS

2D-LC-HRMS analysis was carried out utilizing a Thermo Scientific Vanquish Flex Duo UHPLC-system (Thermo Fisher Scientific, Dreieich, Germany) hyphenated to a Q Exactive Plus mass spectrometer (Thermo Fisher Scientific,

Bremen, Germany). The instrument setup was controlled via the XCalibur 4.1 software using the SII plug-in. The instrument and heart-cut setup was applied as previously described by Blume et al. [366] and Helmer et al. [365,455]. In first dimension (^{1}D) HILIC separation of phospholipid classes was performed utilizing an iHILIC Fusion(+) column (20 x 2.1 mm, 5 μm, 100 Å) (HILICON AB, Umeå, Sweden). Gradient elution was performed using an aqueous ammonium formate buffer (35 mM, pH 3.5, 5% ACN) (A) and ACN (B) as organic solvent [455]. Equilibration of the stationary phase at 60% B for 20 min took place beforehand to ensure reproducible retention times. In second dimension (^{2}D) RP separation was optimized for efficient separation of CL species on an Xselect Premier CSH C18 column (100 x 2.1 mm, 2,5 μm) (Waters Corporation, France). For gradient elution, aqueous ammonium acetate buffer (10 mM, 0.01% acetic acid, 5% MeOH) (A) and MeOH/2-isopropanol (60:40 (*v/v*), 10 mM ammonium acetate, 0.01% acetic acid). The gradient started at 80% B with an equilibration step during the HILIC separation in first dimension [365]. Table 9 gives a detailed gradient overview of ^{1}D HILIC and ^{2}D RP separation. For the heart-cut approach, a transfer window from 5.8 min to 6.4 min was applied. A six-port valve integrated into the column compartment was equipped with a 400 μL stainless-steel sample loop for the heart-cut setup as described earlier [365,366]. Analyte transfer onto the RP column in ^{2}D was carried out by back-flushing the sample loop. Gradient elution as described in Table 9 started simultaneously. The total run time including both separation dimensions was 28 min with a sample injection volume set to 5 μL.

Table 9: Gradient overview containing both gradients for the HILIC separation in the first and the RP separation in the second dimension and the switching positions of the six-port-valve for the heart-cut setup.

^{1}D HILIC gradient			^{2}D RP gradient			Valve set-up	
time /min	flow /mLmin^{-1}	%B	time /min	flow /mLmin^{-1}	%B	time /min	position
0.00	0.3	97	0.00	0.3	80	0.00	2_1
0.2	0.3	97	7.70	0.3	80	5.80	1_6
0.5	0.3	93	8.70	0.3	92	6.40	2_1
2.75	0.3	93	22.70	0.3	98	7.70	1_6
7.50	0.3	60	23.10	0.3	100	25.00	2_1
11.00	0.3	60	26.90	0.3	100		
11.50	0.3	97	27.40	0.3	80		
14.00	0.3	97	28.00	0.3	80		
14.10	0.05	97					
24.50	0.05	97					
28.00	0.3	97					
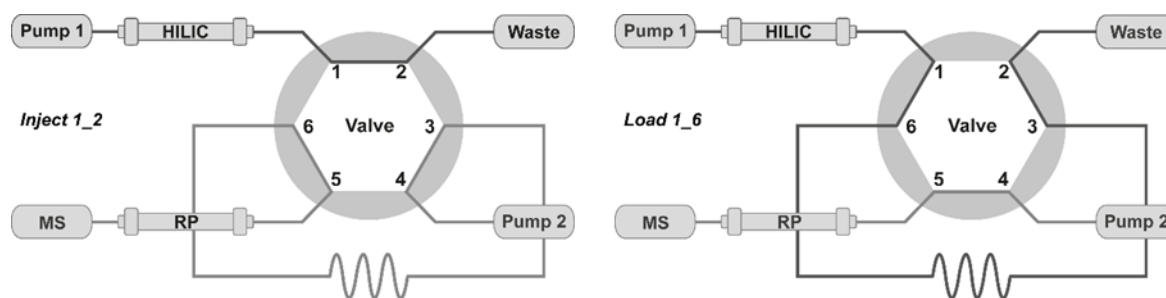
Figure 39: Six-port-valve positions for the heart-cut setup.

Negative electrospray ionization (ESI) was performed by a HESI-II probe (Thermo Fisher Scientific, Bremen, Germany) prior mass spectrometric detection. Probe parameters were set to the following values: source voltage -3.5 kV, probe heater 300 °C, sheath gas flow rate 45 arbitrary units, auxiliary

gas flow rate 10 arbitrary units, spare gas flow rate 1 arbitrary unit, capillary temperature 325 °C. The s-lens rf level was set to 85. Data-dependent MS/MS experiments for structural elucidation were performed at a normalized collision energy of 24 eV (based on a m/z of 500) by HCD with a resolution of 17,500 (at m/z 200). Full scan resolution was set to 140,000. An isolation window of 1.5 Da for precursors was set to avoid isotopic interferences. The maximum C-trap injection time was set to 100 ms in full scan mode and 50 ms for MS/MS experiments.

Data processing

For data processing of the HRMS data, the open source software MZmine 3 [456] (version 3.4.21) was utilized. CL annotation was performed by the lipid search module based on accurate mass and matching MS^2 spectra. A batch processing method was created using the processing wizard. The UHPLC-Orbitrap-DDA setup was chosen. Polarity was set to negative with a noise level of 5000 for MS^1 and 1000 for MS^2 level. A mass tolerance of 10 ppm was set for the ADAP chromatogram builder [457]. Subsequently, the created feature lists were aligned and gap filled.

For the analysis of the CL distribution, all peak areas of identified CL species were normalized to the peak area of the IS (0.5 µM d5-CL 72:8) in addition to the protein content. Subsequently, all normalized peak areas of identified CL species were summed up and the relative abundance of all CL species in comparison to the overall CL amount was calculated. An absolute quantification was not carried out. Due to the normalization of the data set, comparable results in wild-type and mutant samples could be observed.

Lipid nomenclature

Lipids were named according to the shorthand notation proposed by Liebisch et al. [458] The total number of carbon atoms in the fatty acyl residues is given together with the number of double bonds i.e. CL 72:8.

Supplementary Figures
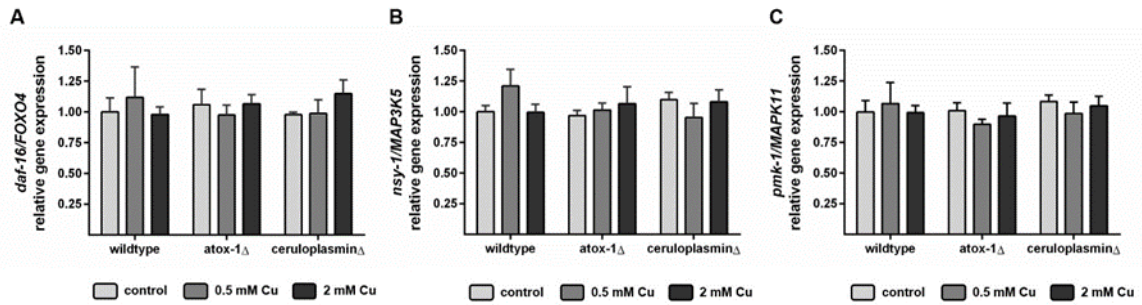
Figure 40: Relative mRNA levels of (A) daf-16/FOXO4, (B) nsy-1/MAP3K5 and (C) pmk-1/MAPK11 following 24 h Cu incubation. Data presented are mean values of n = 4 independent experiments + SEM.
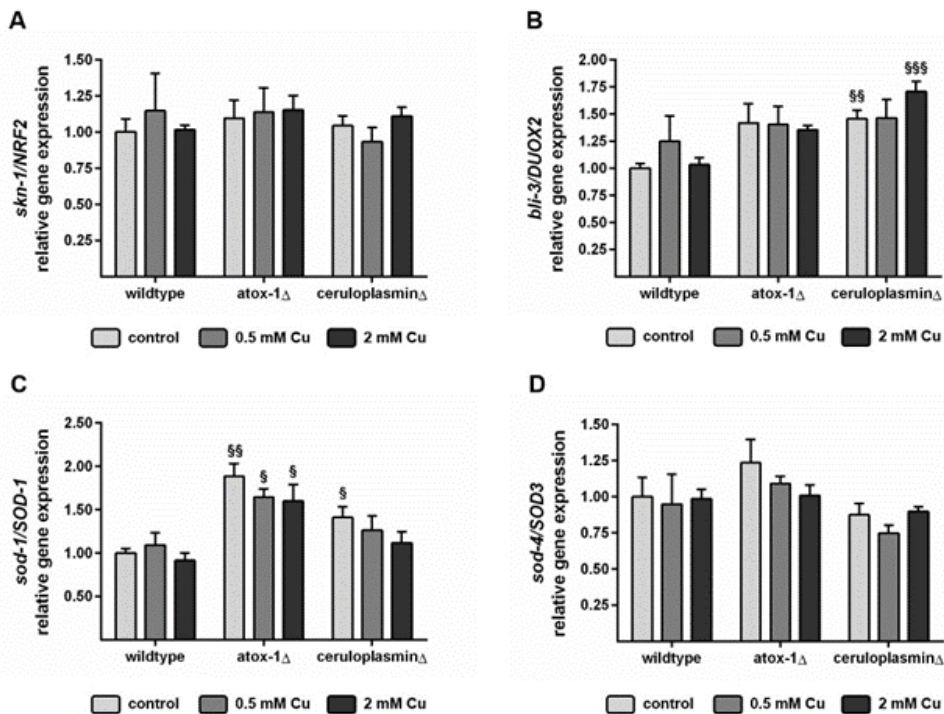
Figure 41: Relative mRNA levels of (A) skn-1/NRF2, (B) bli-3/DUOX2, (C) sod-1/SOD-1 and (D) sod-4/SOD-3 following 24 h Cu incubation. Data presented are mean values of n = 4 independent experiments + SEM.
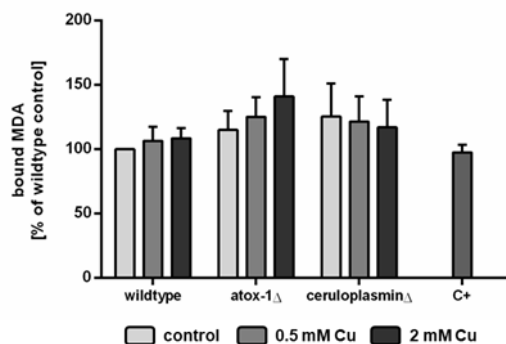
Figure 42: MDA levels (bound) normalized to wildtype control [%]. PQ was used as positive control (C+) in wildtype worms. Data presented are mean values of n = 4 independent experiments + SEM.
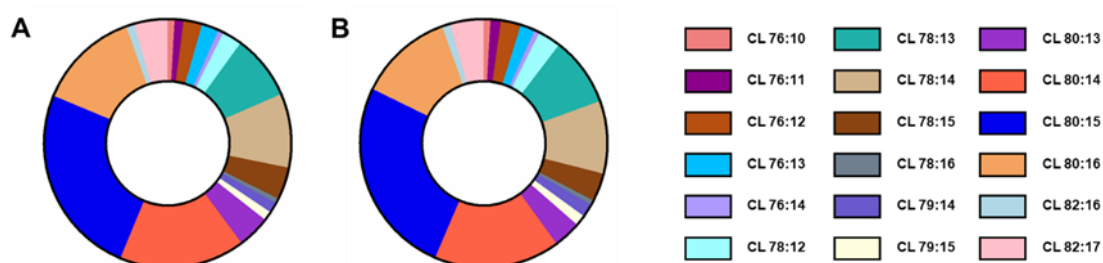
Figure 43: Representative distribution of CL species in terms of chain length and degree of saturation for untreated (A) atox-1 and (B) ceruloplasmin deletion mutants.
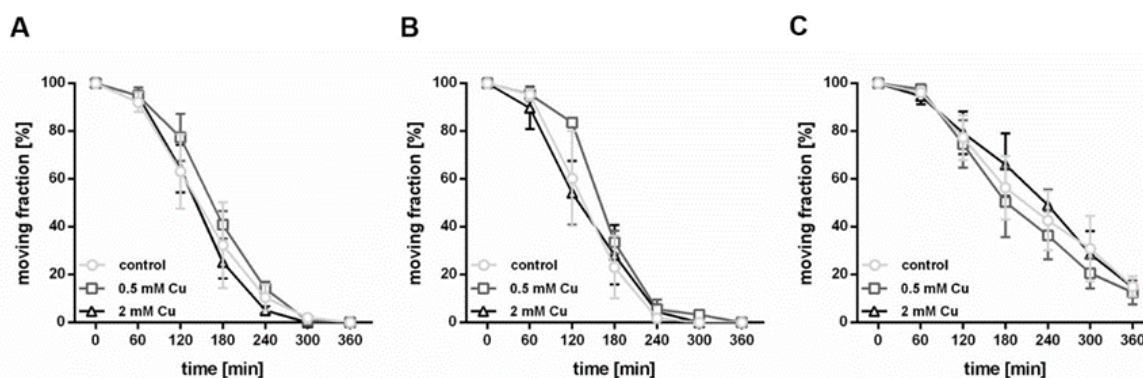
Figure 44: Aldicarb-induced paralysis assay in (A) wildtype, (B) atox-1Δ and (C) ceruloplasminΔ worms treated with 0 mM (light grey), 0.5 mM (dark grey) or 2 mM (black) CuSO₄ for 24 h. Plotted are the fraction of moving worms [%] against the assay procedure time [min]. Data presented are mean values of n = 3 independent and blinded experiments ± SEM.

Supplementary for Chapter 6: Copper-mediated neurotoxicity and genetic vulnerability in the background of neurodegenerative diseases in *C. elegans*
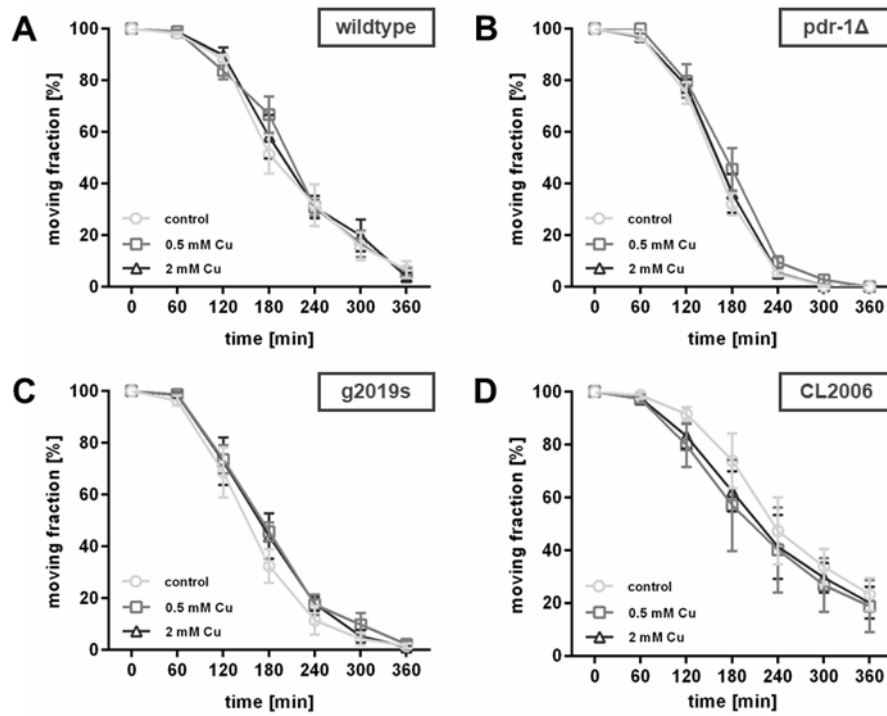
Figure 45: Aldicarb-induced paralysis assay in (A) wildtype worms and (B) pdr-1Δ, (C) g2019s and (D) CL2006 mutants. Worms were treated with either 0 mM (light grey), 0.5 mM (dark grey) or 2 mM (black) $CuSO_4$ for 24 h. Plotted are the fraction of moving worms [%] against the assay procedure time [min]. Data presented are mean values of n = 3 independent and blinded experiments ± SEM.

References

[1] H.-W. Hsu, S.C. Bondy, M. Kitazawa, Environmental and Dietary Exposure to Copper and Its Cellular Mechanisms Linking to Alzheimer's Disease, Toxicol. Sci. 163 (2018) 338–345. https://doi.org/10.1093/toxsci/kfy025.

[2] G.J. Brewer, Copper-2 Ingestion, Plus Increased Meat Eating Leading to Increased Copper Absorption, Are Major Factors Behind the Current Epidemic of Alzheimer's Disease, Nutrients 7 (2015) 10053–10064. https://doi.org/10.3390/nu7125513.

[3] Scientific Opinion on Dietary Reference Values for copper, EFSA Journal 13 (2015) 4253. https://doi.org/10.2903/j.efsa.2015.4253.

[4] G.-C. Fang, Y.-S. Wu, Y.-L. Huang, Measurement and modeling of concentrations of ambient air particles, chromium, copper and lead pollutants concentrations, as well as dry deposition in central Taiwan, J. Environ. Sci. Health A Tox. Hazard. Subst. Environ. Eng. 46 (2011) 394–407. https://doi.org/10.1080/02773813.2010.542396.

[5] K.J. Rader, R.F. Carbonaro, E.D. van Hullebusch, S. Baken, K. Delbeke, The Fate of Copper Added to Surface Water: Field, Laboratory, and Modeling Studies, Environ. Toxicol. Chem. 38 (2019) 1386–1399. https://doi.org/10.1002/etc.4440.

[6] T.C.B. Pereira, M.M. Campos, M.R. Bogo, Copper toxicology, oxidative stress and inflammation using zebrafish as experimental model, J. Appl. Toxicol. 36 (2016) 876–885. https://doi.org/10.1002/jat.3303.

[7] A.B. Swaminathan, V.M. Gohil, The Role of COA6 in the Mitochondrial Copper Delivery Pathway to Cytochrome c Oxidase, Biomolecules 12 (2022). https://doi.org/10.3390/biom12010125.

[8] M.D. Baldissera, C.F. Souza, D.C. Barroso, R.S. Pereira, K.O. Alessio, C. Bizzi, B. Baldisserotto, A.L. Val, Acute exposure to environmentally relevant concentrations of copper affects branchial and hepatic phosphoryl transfer network of Cichlasoma amazonarum: Impacts on bioenergetics homeostasis, Comparative Biochemistry and Physiology Part C: Toxicology & Pharmacology 238 (2020) 108846. https://doi.org/10.1016/j.cbpc.2020.108846.

[9] H. He, Z. Zou, B. Wang, G. Xu, C. Chen, X. Qin, C. Yu, J. Zhang, Copper Oxide Nanoparticles Induce Oxidative DNA Damage and Cell Death via Copper Ion-Mediated P38 MAPK Activation in Vascular Endothelial Cells, Int. J. Nanomedicine 15 (2020) 3291–3302. https://doi.org/10.2147/IJN.S241157.

[10] Y. Zhang, C. Zhao, H. Zhang, Q. Lu, J. Zhou, R. Liu, S. Wang, Y. Pu, L. Yin, Trans-generational effects of copper on nerve damage in Caenorhabditis elegans, Chemosphere 284 (2021) 131324. https://doi.org/10.1016/j.chemosphere.2021.131324.

[11] R. Sadiq, Q.M. Khan, A. Mobeen, A.J. Hashmat, In vitro toxicological assessment of iron oxide, aluminium oxide and copper nanoparticles in prokaryotic and eukaryotic cell types, Drug Chem. Toxicol. 38 (2015) 152–161. https://doi.org/10.3109/01480545.2014.919584.

[12] N. Husain, R. Mahmood, Copper(II) generates ROS and RNS, impairs antioxidant system and damages membrane and DNA in human blood cells, Environ. Sci. Pollut. Res. Int. 26 (2019) 20654–20668. https://doi.org/10.1007/s11356-019-05345-1.

[13] M.-C. Boll, M. Alcaraz-Zubeldia, S. Montes, C. Rios, Free copper, ferroxidase and SOD1 activities, lipid peroxidation and NO(x) content in the CSF. A different marker profile in four neurodegenerative diseases, Neurochem. Res. 33 (2008) 1717–1723. https://doi.org/10.1007/s11064-008-9610-3.

[14] S. Shribman, A. Poujois, O. Bandmann, A. Czlonkowska, T.T. Warner, Wilson's disease: update on pathogenesis, biomarkers and treatments, J. Neurol. Neurosurg. Psychiatry 92 (2021) 1053–1061. https://doi.org/10.1136/jnnp-2021-326123.

[15] A.T. Pezacki, C.D. Matier, X. Gu, E. Kummelstedt, S.E. Bond, L. Torrente, K.L. Jordan-Sciutto, G.M. DeNicola, T.A. Su, D.C. Brady, C.J. Chang, Oxidation state-specific fluorescent copper sensors reveal oncogene-driven redox changes that regulate labile copper(II) pools, Proc. Natl. Acad. Sci. U. S. A. 119 (2022) e2202736119. https://doi.org/10.1073/pnas.2202736119.

[16] J. Xu, S.J. Church, S. Patassini, P. Begley, H.J. Waldvogel, M.A. Curtis, R.L.M. Faull, R.D. Unwin, G.J.S. Cooper, Evidence for widespread, severe brain copper deficiency in Alzheimer's dementia, Metallomics 9 (2017) 1106–1119. https://doi.org/10.1039/c7mt00074j.

[17] M. Scholefield, S.J. Church, J. Xu, S. Patassini, F. Roncaroli, N.M. Hooper, R.D. Unwin, G.J.S. Cooper, Widespread Decreases in Cerebral Copper Are Common to Parkinson's Disease Dementia and Alzheimer's Disease Dementia, Front. Aging Neurosci. 13 (2021) 641222. https://doi.org/10.3389/fnagi.2021.641222.

[18] R. Squitti, P. Faller, C. Hureau, A. Granzotto, A.R. White, K.P. Kepp, Copper Imbalance in Alzheimer's Disease and Its Link with the Amyloid Hypothesis: Towards a Combined Clinical, Chemical, and Genetic Etiology, J. Alzheimers. Dis. 83 (2021) 23–41. https://doi.org/10.3233/JAD-201556.

[19] M. Ugarte, N.N. Osborne, L.A. Brown, P.N. Bishop, Iron, zinc, and copper in retinal physiology and disease, Surv. Ophthalmol. 58 (2013) 585–609. https://doi.org/10.1016/j.survophthal.2012.12.002.

[20] M.E. Hahn, K.C. Sadler, Casting a wide net: use of diverse model organisms to advance toxicology, Dis. Model. Mech. 13 (2020). https://doi.org/10.1242/dmm.043844.

[21] S.B. Hedges, The origin and evolution of model organisms, Nat. Rev. Genet. 3 (2002) 838–849. https://doi.org/10.1038/nrg929.

[22] C. Rodriguez Perez, K. Persson, R.M. Cajiga Morales, B.S. Elger, D.M. Shaw, Russell and Burch's 3Rs then and now: The case of Switzerland, ALTEX 40 (2023) 635–648. https://doi.org/10.14573/altex.2303061.

[23] P.R. Hunt, The C. elegans model in toxicity testing, J. Appl. Toxicol. 37 (2017) 50–59. https://doi.org/10.1002/jat.3357.

[24] A.K. Corsi, B. Wightman, M. Chalfie, A Transparent Window into Biology: A Primer on Caenorhabditis elegans, Genetics 200 (2015) 387–407. https://doi.org/10.1534/genetics.115.176099.

[25] Y. Yue, S. Li, P. Shen, Y. Park, Caenorhabditis elegans as a model for obesity research, Curr. Res. Food Sci. 4 (2021) 692–697. https://doi.org/10.1016/j.crfs.2021.09.008.

[26] J.G. White, E. Southgate, J.N. Thomson, S. Brenner, The structure of the nervous system of the nematode Caenorhabditis elegans, Philos. Trans. R. Soc. Lond. B Biol. Sci. 314 (1986) 1–340. https://doi.org/10.1098/rstb.1986.0056.

[27] P.M. Meneely, C.L. Dahlberg, J.K. Rose, 2019. Working with Worms: Caenorhabditis elegans as a Model Organism. CP Essential Lab Tech 19, e35. https://doi.org/10.1002/cpet.35.

[28] R. Dhakal, M. Yosofvand, M. Yavari, R. Abdulrahman, R. Schurr, N. Moustaid-Moussa, H. Moussa, Review of Biological Effects of Acute and Chronic Radiation Exposure on Caenorhabditis elegans, Cells 10 (2021). https://doi.org/10.3390/cells10081966.

[29] P.J. Hu, Dauer, WormBook (2007) 1–19. https://doi.org/10.1895/wormbook.1.144.1.

[30] J. Kimble, C. Nüsslein-Volhard, The great small organisms of developmental genetics: Caenorhabditis elegans and Drosophila melanogaster, Dev. Biol. 485 (2022) 93–122. https://doi.org/10.1016/j.ydbio.2022.02.013.

[31] E.A. Cox-Paulson, T.M. Grana, M.A. Harris, J.M. Batzli, Studying human disease genes in Caenorhabditis elegans: a molecular genetics laboratory project, CBE Life Sci. Educ. 11 (2012) 165–179. https://doi.org/10.1187/cbe-11-06-0045.

[32] T. Ohkumo, C. Masutani, T. Eki, F. Hanaoka, Use of RNAi in C. elegans, Methods Mol. Biol. 442 (2008) 129–137. https://doi.org/10.1007/978-1-59745-191-8_10.

[33] J.K. Heppert, D.J. Dickinson, A.M. Pani, C.D. Higgins, A. Steward, J. Ahringer, J.R. Kuhn, B. Goldstein, Comparative assessment of fluorescent proteins for in vivo imaging in an animal model system, Mol. Biol. Cell 27 (2016) 3385–3394. https://doi.org/10.1091/mbc.E16-01-0063.

[34] T. Kaletta, M.O. Hengartner, Finding function in novel targets: C. elegans as a model organism, Nat. Rev. Drug Discov. 5 (2006) 387–398. https://doi.org/10.1038/nrd2031.

[35] E. Culetto, D.B. Sattelle, A role for Caenorhabditis elegans in understanding the function and interactions of human disease genes, Hum. Mol. Genet. 9 (2000) 869–877. https://doi.org/10.1093/hmg/9.6.869.

[36] M. Gendrel, E.G. Atlas, O. Hobert, A cellular and regulatory map of the GABAergic nervous system of C. elegans, Elife 5 (2016). https://doi.org/10.7554/eLife.17686.

[37] M.W. Moyle, K.M. Barnes, M. Kuchroo, A. Gonopolskiy, L.H. Duncan, T. Sengupta, L. Shao, M. Guo, A. Santella, R. Christensen, A. Kumar, Y. Wu, K.R. Moon, G. Wolf, S. Krishnaswamy, Z. Bao, H. Shroff, W.A. Mohler, D.A. Colón-Ramos, Structural and developmental principles of neuropil assembly in C. elegans, Nature 591 (2021) 99–104. https://doi.org/10.1038/s41586-020-03169-5.

[38] F. Schumacher, S. Chakraborty, B. Kleuser, E. Gulbins, T. Schwerdtle, M. Aschner, J. Bornhorst, Highly sensitive isotope-dilution liquid-chromatography-electrospray ionization-tandem-mass spectrometry approach to study the drug-mediated modulation of dopamine and serotonin levels in Caenorhabditis elegans, Talanta 144 (2015) 71–79. https://doi.org/10.1016/j.talanta.2015.05.057.

[39] J.A. Ruszkiewicz, A. Pinkas, M.R. Miah, R.L. Weitz, M.J.A. Lawes, A.J. Akinyemi, O.M. Ijomone, M. Aschner, C. elegans as a model in developmental neurotoxicology, Toxicol. Appl. Pharmacol. 354 (2018) 126–135. https://doi.org/10.1016/j.taap.2018.03.016.

[40] R. Nass, D.H. Hall, D.M. Miller, R.D. Blakely, Neurotoxin-induced degeneration of dopamine neurons in Caenorhabditis elegans, Proc. Natl. Acad. Sci. U. S. A. 99 (2002) 3264–3269. https://doi.org/10.1073/pnas.042497999.

[41] N.D. Peterson, R. Pukkila-Worley, Caenorhabditis elegans in high-throughput screens for anti-infective compounds, Curr. Opin. Immunol. 54 (2018) 59–65. https://doi.org/10.1016/j.coi.2018.06.003.

[42] D. Gems, D.L. Riddle, Defining wild-type life span in Caenorhabditis elegans, J. Gerontol. A Biol. Sci. Med. Sci. 55 (2000) B215-9. https://doi.org/10.1093/gerona/55.5.b215.

[43] T.E. Johnson, Advantages and disadvantages of Caenorhabditis elegans for aging research, Exp. Gerontol. 38 (2003) 1329–1332. https://doi.org/10.1016/j.exger.2003.10.020.

[44] D.L. de Romaña, M. Olivares, R. Uauy, M. Araya, Risks and benefits of copper in light of new insights of copper homeostasis, J. Trace Elem. Med. Biol. 25 (2011) 3–13. https://doi.org/10.1016/j.jtemb.2010.11.004.

[45] R.B. Rucker, T. Kosonen, M.S. Clegg, A.E. Mitchell, B.R. Rucker, J.Y. Uriu-Hare, C.L. Keen, Copper, lysyl oxidase, and extracellular matrix protein cross-linking, Am. J. Clin. Nutr. 67 (1998) 996S-1002S. https://doi.org/10.1093/ajcn/67.5.996S.

[46] G. Gromadzka, B. Tarnacka, A. Flaga, A. Adamczyk, Copper Dyshomeostasis in Neurodegenerative Diseases-Therapeutic Implications, Int. J. Mol. Sci. 21 (2020). https://doi.org/10.3390/ijms21239259.

[47] Grundlagen der Toxikologie, WILEY-VCH, Weinheim, 2010.

[48] D.G. Barceloux, Copper, J. Toxicol. Clin. Toxicol. 37 (1999) 217–230. https://doi.org/10.1081/clt-100102421.

[49] T. Ameh, C.M. Sayes, The potential exposure and hazards of copper nanoparticles: A review, Environ. Toxicol. Pharmacol. 71 (2019) 103220. https://doi.org/10.1016/j.etap.2019.103220.

[50] Z. Shabbir, A. Sardar, A. Shabbir, G. Abbas, S. Shamshad, S. Khalid, Natasha, G. Murtaza, C. Dumat, M. Shahid, Copper uptake, essentiality, toxicity, detoxification and risk assessment in soil-plant environment, Chemosphere 259 (2020) 127436. https://doi.org/10.1016/j.chemosphere.2020.127436.

[51] L.M. Gaetke, C.K. Chow, Copper toxicity, oxidative stress, and antioxidant nutrients, Toxicology 189 (2003) 147–163. https://doi.org/10.1016/s0300-483x(03)00159-8.

[52] T. Tsang, C.I. Davis, D.C. Brady, Copper biology, Curr. Biol. 31 (2021) R421-R427. https://doi.org/10.1016/j.cub.2021.03.054.

[53] X. Wang, S.R. Flores, J.-H. Ha, C. Doguer, R.R. Woloshun, P. Xiang, A. Grosche, S. Vidyasagar, J.F. Collins, Intestinal DMT1 Is Essential for Optimal Assimilation of Dietary Copper in Male and Female Mice with Iron-Deficiency Anemia, J. Nutr. 148 (2018) 1244–1252. https://doi.org/10.1093/jn/nxy111.

[54] A. Shawki, S.R. Anthony, Y. Nose, M.A. Engevik, E.J. Niespodzany, T. Barrientos, H. Öhrvik, R.T. Worrell, D.J. Thiele, B. Mackenzie, Intestinal DMT1 is critical for iron absorption in the mouse but is not required for the absorption of copper or manganese, Am. J. Physiol. Gastrointest. Liver Physiol. 309 (2015) G635-47. https://doi.org/10.1152/ajpgi.00160.2015.

[55] A.-K. Weishaupt, K. Lamann, E. Tallarek, A.T. Pezacki, C.D. Matier, T. Schwerdtle, M. Aschner, C.J. Chang, S.R. Stürzenbaum, J. Bornhorst, 2024. Dysfunction in atox-1 and ceruloplasmin alters labile Cu levels and consequently Cu homeostasis in C. elegans. Front. Mol. Biosci. 11, 1354627. https://doi.org/10.3389/fmolb.2024.1354627.

[56] T. Kamiya, K. Takeuchi, S. Fukudome, H. Hara, T. Adachi, Copper chaperone antioxidant-1, Atox-1, is involved in the induction of SOD3 in THP-1 cells, Biometals 31 (2018) 61–68. https://doi.org/10.1007/s10534-017-0067-1.

[57] F.A. Punter, D.L. Adams, D.M. Glerum, Characterization and localization of human COX17, a gene involved in mitochondrial copper transport, Hum. Genet. 107 (2000) 69–74. https://doi.org/10.1007/s004390000339.

[58] N.E. Hellman, J.D. Gitlin, Ceruloplasmin metabolism and function, Annu. Rev. Nutr. 22 (2002) 439–458. https://doi.org/10.1146/annurev.nutr.22.012502.114457.

[59] M. Höckner, R. Dallinger, S.R. Stürzenbaum, Nematode and snail metallothioneins, J. Biol. Inorg. Chem. 16 (2011) 1057–1065. https://doi.org/10.1007/s00775-011-0826-3.

[60] Z. Tümer, L.B. Møller, N. Horn, Mutation spectrum of ATP7A, the gene defective in Menkes disease, Adv. Exp. Med. Biol. 448 (1999) 83–95. https://doi.org/10.1007/978-1-4615-4859-1_7.

[61] S.G. Kaler, ATP7A-related copper transport diseases-emerging concepts and future trends, Nat. Rev. Neurol. 7 (2011) 15–29. https://doi.org/10.1038/nrneurol.2010.180.

[62] K.H. Weiss, J.C. Lozoya, S. Tuma, D. Gotthardt, J. Reichert, R. Ehehalt, W. Stremmel, J. Füllekrug, Copper-induced translocation of the Wilson disease protein ATP7B independent of Murr1/COMMD1 and Rab7, Am. J. Pathol. 173 (2008) 1783–1794. https://doi.org/10.2353/ajpath.2008.071134.

[63] C. Einer, D.E. Munk, E. Park, B. Akdogan, J. Nagel, J. Lichtmannegger, C. Eberhagen, T. Rieder, M.H. Vendelbo, B. Michalke, R. Wimmer, A. Blutke, A. Feuchtinger, P. Dershwitz, A.M. DiSpirito, T. Islam, R.E. Castro, B.-K. Min, T. Kim, S. Choi, D. Kim, C. Jung, H. Lee, D. Park, W. Im, S.-Y. Eun, Y.-H. Cho, J.D. Semrau, C.M.P. Rodrigues, S. Hohenester, T. Damgaard Sandahl, A.A. DiSpirito, H. Zischka, ARBM101 (Methanobactin SB2) Drains Excess Liver Copper via Biliary Excretion in Wilson's Disease Rats, Gastroenterology 165 (2023) 187-200.e7. https://doi.org/10.1053/j.gastro.2023.03.216.

[64] H. Chun, A.K. Sharma, J. Lee, J. Chan, S. Jia, B.-E. Kim, The Intestinal Copper Exporter CUA-1 Is Required for Systemic Copper Homeostasis in Caenorhabditis elegans, J. Biol. Chem. 292 (2017) 1–14. https://doi.org/10.1074/jbc.M116.760876.

[65] S. Yuan, A.K. Sharma, A. Richart, J. Lee, B.-E. Kim, CHCA-1 is a copper-regulated CTR1 homolog required for normal development, copper accumulation, and copper-sensing behavior in Caenorhabditis elegans, J. Biol. Chem. 293 (2018) 10911–10925. https://doi.org/10.1074/jbc.RA118.003503.

[66] V.A. Ohse, L.-O. Klotz, J. Priebs, Copper Homeostasis in the Model Organism C. elegans, Cells 13 (2024) 727. https://doi.org/10.3390/cells13090727.

[67] C. Au, A. Benedetto, J. Anderson, A. Labrousse, K. Erikson, J.J. Ewbank, M. Aschner, SMF-1, SMF-2 and SMF-3 DMT1 orthologues regulate and are regulated differentially by manganese levels in C. elegans, PLoS One 4 (2009) e7792. https://doi.org/10.1371/journal.pone.0007792.

[68] T. Wakabayashi, N. Nakamura, Y. Sambongi, Y. Wada, T. Oka, M. Futai, Identification of the copper chaperone, CUC-1, in Caenorhabditis elegans: tissue specific co-expression with the copper transporting ATPase, CUA-1, FEBS Lett. 440 (1998) 141–146. https://doi.org/10.1016/S0014-5793(98)01431-8.

[69] X. Zhang, S. Blockhuys, R. Devkota, M. Pilon, P. Wittung-Stafshede, The Caenorhabditis elegans homolog of human copper chaperone Atox1, CUC-1, aids in distal tip cell migration, Biometals 33 (2020) 147–157. https://doi.org/10.1007/s10534-020-00239-z.

[70] T. Nevitt, H. Ohrvik, D.J. Thiele, Charting the travels of copper in eukaryotes from yeast to mammals, Biochim. Biophys. Acta 1823 (2012) 1580–1593. https://doi.org/10.1016/j.bbamcr.2012.02.011.

[71] L.T. Jensen, V.C. Culotta, Activation of CuZn superoxide dismutases from Caenorhabditis elegans does not require the copper chaperone CCS, J. Biol. Chem. 280 (2005) 41373–41379. https://doi.org/10.1074/jbc.M509142200.

[72] Y.J. Essig, O.I. Leszczyszyn, N. Almutairi, A. Harrison-Smith, A. Blease, S. Zeitoun-Ghandour, S.M. Webb, C.A. Blindauer, S.R. Stürzenbaum, Juggling cadmium detoxification and zinc homeostasis: A division of labour between the two C. elegans metallothioneins, Chemosphere 350 (2023) 141021. https://doi.org/10.1016/j.chemosphere.2023.141021.

[73] W. Kim, R.S. Underwood, I. Greenwald, D.D. Shaye, OrthoList 2: A New Comparative Genomic Analysis of Human and Caenorhabditis elegans Genes, Genetics 210 (2018) 445–461. https://doi.org/10.1534/genetics.118.301307.

[74] Y. Hatori, S. Lutsenko, The Role of Copper Chaperone Atox1 in Coupling Redox Homeostasis to Intracellular Copper Distribution, Antioxidants (Basel) 5 (2016). https://doi.org/10.3390/antiox5030025.

[75] I. Hamza, A. Faisst, J. Prohaska, J. Chen, P. Gruss, J.D. Gitlin, The metallochaperone Atox1 plays a critical role in perinatal copper homeostasis, Proc. Natl. Acad. Sci. U. S. A. 98 (2001) 6848–6852. https://doi.org/10.1073/pnas.111058498.

[76] S. Lutsenko, A. Bhattacharjee, A.L. Hubbard, Copper handling machinery of the brain, Metallomics 2 (2010) 596–608. https://doi.org/10.1039/c0mt00006j.

[77] G.S. Kelner, M. Lee, M.E. Clark, D. Maciejewski, D. McGrath, S. Rabizadeh, T. Lyons, D. Bredesen, P. Jenner, R.A. Maki, The copper transport protein Atox1 promotes neuronal survival, J. Biol. Chem. 275 (2000) 580–584. https://doi.org/10.1074/jbc.275.1.580.

[78] B. Wang, X.-P. Wang, Does Ceruloplasmin Defend Against Neurodegenerative Diseases?, Curr. Neuropharmacol. 17 (2019) 539–549. https://doi.org/10.2174/1570159X16666180508113025.

[79] G. Vashchenko, R.T.A. MacGillivray, Multi-copper oxidases and human iron metabolism, Nutrients 5 (2013) 2289–2313. https://doi.org/10.3390/nu5072289.

[80] S. Kono, Aceruloplasminemia, Curr. Drug Targets 13 (2012) 1190–1199. https://doi.org/10.2174/138945012802002320.

[81] I. Scheiber, R. Dringen, J.F.B. Mercer, Copper: effects of deficiency and overload, Met. Ions Life Sci. 13 (2013) 359–387. https://doi.org/10.1007/978-94-007-7500-8_11.

[82] Bundesinstitut für Risikobewertung, Aktualisierte Höchstmengenvorschläge für Vitamine und Mineralstoffe in Nahrungsergänzungsmitteln und angereicherten Lebensmitteln: Stellungnahme Nr. 009/2021 des BfR vom 15. März 2021, Bundesbehörden und Einrichtungen im Geschäftsbereich des Bundesministeriums für Ernährung und Landwirtschaft (BMEL), 2021.

[83] M. Tuchtenhagen, M. Stiboller, B. Witt, T. Schwerdtle, A novel approach for the determination of exchangeable copper in serum using protein precipitation, J. Anal. At. Spectrom. 38 (2023) 587–594. https://doi.org/10.1039/D2JA00355D.

[84] J. Bornhorst, A.P. Kipp, H. Haase, S. Meyer, T. Schwerdtle, The crux of inept biomarkers for risks and benefits of trace elements, TrAC Trends in Analytical Chemistry 104 (2018) 183–190. https://doi.org/10.1016/j.trac.2017.11.007.

[85] S.M. Müller, C. Dawczynski, J. Wiest, S. Lorkowski, A.P. Kipp, T. Schwerdtle, Functional Biomarkers for the Selenium Status in a Human Nutritional Intervention Study, Nutrients 12 (2020). https://doi.org/10.3390/nu12030676.

[86] C.M. Pfeiffer, A.C. Looker, Laboratory methodologies for indicators of iron status: strengths, limitations, and analytical challenges, Am. J. Clin. Nutr. 106 (2017) 1606S-1614S. https://doi.org/10.3945/ajcn.117.155887.

[87] M. Maares, J. Hackler, A. Haupt, R.A. Heller, M. Bachmann, J. Diegmann, A. Moghaddam, L. Schomburg, H. Haase, Free Zinc as a Predictive Marker for COVID-19 Mortality Risk, Nutrients 14 (2022). https://doi.org/10.3390/nu14071407.

[88] M. Siotto, S. Bucossi, R. Squitti, Copper status abnormalities and how to measure them in neurodegenerative disorders, Recent Pat. CNS Drug Discov. 5 (2010) 182–194. https://doi.org/10.2174/157488910793362395.

[89] M. Bost, S. Houdart, M. Oberli, E. Kalonji, J.-F. Huneau, I. Margaritis, Dietary copper and human health: Current evidence and unresolved issues, J. Trace Elem. Med. Biol. 35 (2016) 107–115. https://doi.org/10.1016/j.jtemb.2016.02.006.

[90] J. Bertinato, A. Zouzoulas, Considerations in the development of biomarkers of copper status, J. AOAC Int. 92 (2009) 1541–1550.

[91] L.J. Harvey, K. Ashton, L. Hooper, A. Casgrain, S.J. Fairweather-Tait, Methods of assessment of copper status in humans: a systematic review, Am. J. Clin. Nutr. 89 (2009) 2009S-2024S. https://doi.org/10.3945/ajcn.2009.27230E.

[92] R.F. Pfeiffer, Wilson's disease, Handb. Clin. Neurol. 100 (2011) 681–709. https://doi.org/10.1016/B978-0-444-52014-2.00049-5.

[93] X. Lu, S. Li, W. Zhang, Y. Lin, Z. Lu, Y. Cai, X. Su, Y. Shao, Z. Liu, H. Sheng, Y. Huang, L. Liu, C. Zeng, Assessment of the diagnostic value of serum ceruloplasmin for Wilson's disease in children, BMC Gastroenterol 22 (2022). https://doi.org/10.1186/s12876-022-02186-0.

[94] M. Olivares, M.A. Méndez, P.A. Astudillo, F. Pizarro, Present situation of biomarkers for copper status, Am. J. Clin. Nutr. 88 (2008) 859S-62S. https://doi.org/10.1093/ajcn/88.3.859S.

[95] G. Gromadzka, M. Grycan, A.M. Przybyłkowski, Monitoring of Copper in Wilson Disease, Diagnostics (Basel) 13 (2023). https://doi.org/10.3390/diagnostics13111830.

[96] E. González-Jiménez, J. Schmidt-Riovalle, L. Sinausía, M. Carmen Valenza, J.S. Perona, Predictive value of ceruloplasmin for metabolic syndrome in adolescents, Biofactors 42 (2016) 163–170. https://doi.org/10.1002/biof.1258.

[97] J.A. Kim, H.J. Kim, J.M. Cho, S.H. Oh, B.H. Lee, G.-H. Kim, J.-H. Choi, K.M. Kim, H.-W. Yoo, Diagnostic Value of Ceruloplasmin in the Diagnosis of Pediatric Wilson's Disease, Pediatr. Gastroenterol. Hepatol. Nutr. 18 (2015) 187–192. https://doi.org/10.5223/pghn.2015.18.3.187.

[98] H.M. Salman, M. Amin, J. Syed, Z. Sarfraz, A. Sarfraz, M. Sarfraz, M.J. Farfán Bajaña, M. Felix, I. Cherrez-Ojeda, Biochemical testing for the diagnosis of Wilson's disease: A systematic review, J. Clin. Lab. Anal. 36 (2022) e24191. https://doi.org/10.1002/jcla.24191.

[99] U. Merle, M. Schaefer, P. Ferenci, W. Stremmel, Clinical presentation, diagnosis and long-term outcome of Wilson's disease: a cohort study, Gut 56 (2007) 115–120. https://doi.org/10.1136/gut.2005.087262.

[100] D.B. Milne, Copper intake and assessment of copper status, Am. J. Clin. Nutr. 67 (1998) 1041S-1045S. https://doi.org/10.1093/ajcn/67.5.1041S.

[101] R. Danzeisen, M. Araya, B. Harrison, C. Keen, M. Solioz, D. Thiele, H.J. McArdle, How reliable and robust are current biomarkers for copper status?, Br. J. Nutr. 98 (2007) 676–683. https://doi.org/10.1017/S0007114507798951.

[102] I. Mohr, K.H. Weiss, Biochemical Markers for the Diagnosis and Monitoring of Wilson Disease, Clin. Biochem. Rev. 40 (2019) 59–77. https://doi.org/10.33176/AACB-18-00014.

[103] M.C. Linder, Ceruloplasmin and other copper binding components of blood plasma and their functions: an update, Metallomics 8 (2016) 887–905. https://doi.org/10.1039/c6mt00103c.

[104] M. Maares, A. Haupt, C. Schüßler, M. Kulike-Koczula, J. Hackler, C. Keil, I. Mohr, L. Schomburg, R.D. Süssmuth, H. Zischka, U. Merle, H. Haase, A fluorometric assay to determine labile copper(II) ions in serum, Sci. Rep. 13 (2023) 12807. https://doi.org/10.1038/s41598-023-39841-9.

[105] T. Kirsipuu, A. Zadorožnaja, J. Smirnova, M. Friedemann, T. Plitz, V. Tõugu, P. Palumaa, Copper(II)-binding equilibria in human blood, Sci. Rep. 10 (2020) 5686. https://doi.org/10.1038/s41598-020-62560-4.

[106] T.D. Rae, P.J. Schmidt, R.A. Pufahl, V.C. Culotta, T.V. O'Halloran, Undetectable intracellular free copper: the requirement of a copper chaperone for superoxide dismutase, Science 284 (1999) 805–808. https://doi.org/10.1126/science.284.5415.805.

[107] M. Arredondo, M. González, M. Olivares, F. Pizarro, M. Araya, Ceruloplasmin, an indicator of copper status, Biol. Trace Elem. Res. 123 (2008) 261–269. https://doi.org/10.1007/s12011-008-8110-2.

[108] T. Xiao, C.M. Ackerman, E.C. Carroll, S. Jia, A. Hoagland, J. Chan, B. Thai, C.S. Liu, E.Y. Isacoff, C.J. Chang, Copper regulates rest-activity cycles through the locus coeruleus-norepinephrine system, Nat. Chem. Biol. 14 (2018) 655–663. https://doi.org/10.1038/s41589-018-0062-z.

[109] K.P. Carter, A.M. Young, A.E. Palmer, Fluorescent sensors for measuring metal ions in living systems, Chem. Rev. 114 (2014) 4564–4601. https://doi.org/10.1021/cr400546e.

[110] P. Rajendran, N. Nandakumar, T. Rengarajan, R. Palaniswami, E.N. Gnanadhas, U. Lakshminarasaiah, J. Gopas, I. Nishigaki, Antioxidants and human diseases, Clin. Chim. Acta 436 (2014) 332–347. https://doi.org/10.1016/j.cca.2014.06.004.

[111] G. Pizzino, N. Irrera, M. Cucinotta, G. Pallio, F. Mannino, V. Arcoraci, F. Squadrito, D. Altavilla, A. Bitto, Oxidative Stress: Harms and Benefits for Human Health, Oxid. Med. Cell. Longev. 2017 (2017) 8416763. https://doi.org/10.1155/2017/8416763.

[112] J.Q. Wu, T.R. Kosten, X.Y. Zhang, Free radicals, antioxidant defense systems, and schizophrenia, Prog. Neuropsychopharmacol. Biol. Psychiatry 46 (2013) 200–206. https://doi.org/10.1016/j.pnpbp.2013.02.015.

[113] T. Takeshima, K. Usui, K. Mori, T. Asai, K. Yasuda, S. Kuroda, Y. Yumura, Oxidative stress and male infertility, Reprod. Med. Biol. 20 (2021) 41–52. https://doi.org/10.1002/rmb2.12353.

[114] D.A. Averill-Bates, The antioxidant glutathione, Vitam. Horm. 121 (2023) 109–141. https://doi.org/10.1016/bs.vh.2022.09.002.

[115] Y. Wang, R. Branicky, A. Noë, S. Hekimi, Superoxide dismutases: Dual roles in controlling ROS damage and regulating ROS signaling, J. Cell Biol. 217 (2018) 1915–1928. https://doi.org/10.1083/jcb.201708007.

[116] H. Sies, C. Berndt, D.P. Jones, Oxidative Stress, Annu. Rev. Biochem. 86 (2017) 715–748. https://doi.org/10.1146/annurev-biochem-061516-045037.

[117] L. Kubens, A.-K. Weishaupt, V. Michaelis, I. Rohn, F. Mohr, J. Bornhorst, Exposure to the environmentally relevant fungicide Maneb: Studying toxicity in the soil nematode Caenorhabditis elegans, Environ. Int. 183 (2024) 108372. https://doi.org/10.1016/j.envint.2023.108372.

[118] M. Khalid, S. Hassani, M. Abdollahi, Metal-induced oxidative stress: an evidence-based update of advantages and disadvantages, Current Opinion in Toxicology 20-21 (2020) 55–68. https://doi.org/10.1016/j.cotox.2020.05.006.

[119] M. Valko, H. Morris, M.T.D. Cronin, Metals, toxicity and oxidative stress, Curr. Med. Chem. 12 (2005) 1161–1208. https://doi.org/10.2174/0929867053764635.

[120] H. Rumgay, N. Murphy, P. Ferrari, I. Soerjomataram, Alcohol and Cancer: Epidemiology and Biological Mechanisms, Nutrients 13 (2021). https://doi.org/10.3390/nu13093173.

[121] F. Ozguner, A. Koyu, G. Cesur, Active smoking causes oxidative stress and decreases blood melatonin levels, Toxicol. Ind. Health 21 (2005) 21–26. https://doi.org/10.1191/0748233705th211oa.

[122] E. Birben, U.M. Sahiner, C. Sackesen, S. Erzurum, O. Kalayci, Oxidative stress and antioxidant defense, World Allergy Organ. J. 5 (2012) 9–19. https://doi.org/10.1097/WOX.0b013e3182439613.

[123] S. Pyatha, H. Kim, D. Lee, K. Kim, Association between Heavy Metal Exposure and Parkinson's Disease: A Review of the Mechanisms Related to Oxidative Stress, Antioxidants (Basel) 11 (2022). https://doi.org/10.3390/antiox11122467.

[124] S.I. Dikalov, D.G. Harrison, Methods for detection of mitochondrial and cellular reactive oxygen species, Antioxid. Redox Signal. 20 (2014) 372–382. https://doi.org/10.1089/ars.2012.4886.

[125] S.-Y. Hong, L.V. Roze, J.E. Linz, Oxidative stress-related transcription factors in the regulation of secondary metabolism, Toxins (Basel) 5 (2013) 683–702. https://doi.org/10.3390/toxins5040683.

[126] Y. Son, S. Kim, H.-T. Chung, H.-O. Pae, Reactive oxygen species in the activation of MAP kinases, Methods Enzymol. 528 (2013) 27–48. https://doi.org/10.1016/B978-0-12-405881-1.00002-1.

[127] J.M. Shin, K.-M. Lee, H.J. Lee, J.H. Yun, C.W. Nho, Physalin A regulates the Nrf2 pathway through ERK and p38 for induction of detoxifying enzymes, BMC Complement. Altern. Med. 19 (2019) 101. https://doi.org/10.1186/s12906-019-2511-y.

[128] M. Farhan, H. Wang, U. Gaur, P.J. Little, J. Xu, W. Zheng, FOXO Signaling Pathways as Therapeutic Targets in Cancer, Int. J. Biol. Sci. 13 (2017) 815–827. https://doi.org/10.7150/ijbs.20052.

[129] S. Du, H. Zheng, Role of FoxO transcription factors in aging and age-related metabolic and neurodegenerative diseases, Cell Biosci. 11 (2021) 188. https://doi.org/10.1186/s13578-021-00700-7.

[130] L. Jiang, Z. Tang, Expression and regulation of the ERK1/2 and p38 MAPK signaling pathways in periodontal tissue remodeling of orthodontic tooth movement, Mol. Med. Rep. 17 (2018) 1499–1506. https://doi.org/10.3892/mmr.2017.8021.

[131] I. Karwaciak, M. Gorzkiewicz, G. Bartosz, L. Pulaski, TLR2 activation induces antioxidant defence in human monocyte-macrophage cell line models, Oncotarget 8 (2017) 54243–54264. https://doi.org/10.18632/oncotarget.17342.

[132] S. Machado, A. Silva, A.L. de Sousa-Coelho, I. Duarte, I. Grenho, B. Santos, V. Mayoral-Varo, D. Megias, F. Sánchez-Cabo, A. Dopazo, B.I. Ferreira, W. Link, Harmine and Piperlongumine Revert TRIB2-Mediated Drug Resistance, Cancers (Basel) 12 (2020). https://doi.org/10.3390/cancers12123689.

[133] P. Sanadhya, P. Bucki, O. Liarzi, D. Ezra, A. Gamliel, S. Braun Miyara, Caenorhabditis elegans susceptibility to Daldinia cf. concentrica bioactive volatiles is coupled with expression activation of the stress-response transcription factor daf-16, a part of distinct nematicidal action, PLoS One 13 (2018) e0196870. https://doi.org/10.1371/journal.pone.0196870.

[134] M. Hammad, M. Raftari, R. Cesário, R. Salma, P. Godoy, S.N. Emami, S. Haghdoost, Roles of Oxidative Stress and Nrf2 Signaling in Pathogenic and Non-Pathogenic Cells: A Possible General Mechanism of Resistance to Therapy, Antioxidants (Basel) 12 (2023). https://doi.org/10.3390/antiox12071371.

[135] T. Nguyen, P. Nioi, C.B. Pickett, The Nrf2-antioxidant response element signaling pathway and its activation by oxidative stress, J. Biol. Chem. 284 (2009) 13291–13295. https://doi.org/10.1074/jbc.R900010200.

[136] M. Jozefczak, T. Remans, J. Vangronsveld, A. Cuypers, Glutathione is a key player in metal-induced oxidative stress defenses, Int. J. Mol. Sci. 13 (2012) 3145–3175. https://doi.org/10.3390/ijms13033145.

[137] G.H. Kim, J.E. Kim, S.J. Rhie, S. Yoon, The Role of Oxidative Stress in Neurodegenerative Diseases, Exp. Neurobiol. 24 (2015) 325–340. https://doi.org/10.5607/en.2015.24.4.325.

[138] G.D. Ferguson, W.J. Bridge, The glutathione system and the related thiol network in Caenorhabditis elegans, Redox Biol. 24 (2019) 101171. https://doi.org/10.1016/j.redox.2019.101171.

[139] I. Rahman, A. Kode, S.K. Biswas, Assay for quantitative determination of glutathione and glutathione disulfide levels using enzymatic recycling method, Nat. Protoc. 1 (2006) 3159–3165. https://doi.org/10.1038/nprot.2006.378.

[140] A. Thiel, A.-K. Weishaupt, M.M. Nicolai, K. Lossow, A.P. Kipp, T. Schwerdtle, J. Bornhorst, Simultaneous quantitation of oxidized and reduced glutathione via LC-MS/MS to study the redox state and drug-mediated modulation in cells, worms and animal tissue, J. Chromatogr. B Analyt. Technol. Biomed. Life Sci. 1225 (2023) 123742. https://doi.org/10.1016/j.jchromb.2023.123742.

[141] C.J. Weydert, J.J. Cullen, Measurement of superoxide dismutase, catalase and glutathione peroxidase in cultured cells and tissue, Nat. Protoc. 5 (2010) 51–66. https://doi.org/10.1038/nprot.2009.197.

[142] I. Rohn, S. Raschke, M. Aschner, S. Tuck, D. Kuehnelt, A. Kipp, T. Schwerdtle, J. Bornhorst, Treatment of Caenorhabditis elegans with Small Selenium Species Enhances Antioxidant Defense Systems, Mol. Nutr. Food Res. 63 (2019) e1801304. https://doi.org/10.1002/mnfr.201801304.

[143] D. Grotto, L.D. Santa Maria, S. Boeira, J. Valentini, M.F. Charão, A.M. Moro, P.C. Nascimento, V.J. Pomblum, S.C. Garcia, Rapid quantification of malondialdehyde in plasma by high performance liquid chromatography-visible detection, J. Pharm. Biomed. Anal. 43 (2007) 619–624. https://doi.org/10.1016/j.jpba.2006.07.030.

[144] Y. Zhang, C. Zhao, H. Zhang, R. Liu, S. Wang, Y. Pu, L. Yin, Integrating transcriptomics and behavior tests reveals how the C. elegans responds to copper induced aging, Ecotoxicol. Environ. Saf. 222 (2021) 112494. https://doi.org/10.1016/j.ecoenv.2021.112494.

[145] J.B. Spinelli, M.C. Haigis, The multifaceted contributions of mitochondria to cellular metabolism, Nat. Cell Biol. 20 (2018) 745–754. https://doi.org/10.1038/s41556-018-0124-1.

[146] G.S. Shadel, T.L. Horvath, Mitochondrial ROS signaling in organismal homeostasis, Cell 163 (2015) 560–569. https://doi.org/10.1016/j.cell.2015.10.001.

[147] P. Kowalczyk, D. Sulejczak, P. Kleczkowska, I. Bukowska-Ośko, M. Kucia, M. Popiel, E. Wietrak, K. Kramkowski, K. Wrzosek, K. Kaczyńska, Mitochondrial Oxidative Stress-A Causative Factor and Therapeutic Target in Many Diseases, Int. J. Mol. Sci. 22 (2021). https://doi.org/10.3390/ijms222413384.

[148] M. Bonora, S. Patergnani, A. Rimessi, E. de Marchi, J.M. Suski, A. Bononi, C. Giorgi, S. Marchi, S. Missiroli, F. Poletti, M.R. Wieckowski, P. Pinton, ATP synthesis and storage, Purinergic Signal. 8 (2012) 343–357. https://doi.org/10.1007/s11302-012-9305-8.

[149] L. Gómez-Virgilio, A. Luarte, D.P. Ponce, B.A. Bruna, M.I. Behrens, Analyzing Olfactory Neuron Precursors Non-Invasively Isolated through NADH FLIM as a Potential Tool to Study Oxidative Stress in Alzheimer's Disease, Int. J. Mol. Sci. 22 (2021). https://doi.org/10.3390/ijms22126311.

[150] J.S. Bhatti, G.K. Bhatti, P.H. Reddy, Mitochondrial dysfunction and oxidative stress in metabolic disorders — A step towards mitochondria based therapeutic strategies, Biochimica et Biophysica Acta (BBA) - Molecular Basis of Disease 1863 (2017) 1066–1077. https://doi.org/10.1016/j.bbadis.2016.11.010.

[151] M. Falabella, H.J. Vernon, M.G. Hanna, S.M. Claypool, R.D.S. Pitceathly, Cardiolipin, Mitochondria, and Neurological Disease, Trends Endocrinol. Metab. 32 (2021) 224–237. https://doi.org/10.1016/j.tem.2021.01.006.

[152] C.T. Chu, J. Ji, R.K. Dagda, J.F. Jiang, Y.Y. Tyurina, A.A. Kapralov, V.A. Tyurin, N. Yanamala, I.H. Shrivastava, D. Mohammadyani, K.Z.Q. Wang, J. Zhu, J. Klein-Seetharaman, K. Balasubramanian, A.A. Amoscato, G. Borisenko, Z. Huang, A.M. Gusdon, A. Cheikhi, E.K. Steer, R. Wang, C. Baty, S. Watkins, I. Bahar, H. Bayir, V.E. Kagan, Cardiolipin externalization to the outer mitochondrial membrane acts as an elimination signal for mitophagy in neuronal cells, Nat. Cell Biol. 15 (2013) 1197–1205. https://doi.org/10.1038/ncb2837.

[153] H. Chao, T.S. Anthonymuthu, E.M. Kenny, A.A. Amoscato, L.K. Cole, G.M. Hatch, J. Ji, V.E. Kagan, H. Bayır, Disentangling oxidation/hydrolysis reactions of brain mitochondrial cardiolipins in pathogenesis of traumatic injury, JCI Insight 3 (2018). https://doi.org/10.1172/jci.insight.97677.

[154] K. Phan, Y. He, R. Pickford, S. Bhatia, J.S. Katzeff, J.R. Hodges, O. Piguet, G.M. Halliday, W.S. Kim, Uncovering pathophysiological changes in frontotemporal dementia using serum lipids, Sci. Rep. 10 (2020) 3640. https://doi.org/10.1038/s41598-020-60457-w.

[155] M. Schlame, J.A. Towbin, P.M. Heerdt, R. Jehle, S. DiMauro, T.J.J. Blanck, Deficiency of tetralinoleoyl-cardiolipin in Barth syndrome, Ann. Neurol. 51 (2002) 634–637. https://doi.org/10.1002/ana.10176.

[156] M.S. Cooke, M.D. Evans, M. Dizdaroglu, J. Lunec, Oxidative DNA damage: mechanisms, mutation, and disease, FASEB J. 17 (2003) 1195–1214. https://doi.org/10.1096/fj.02-0752rev.

[157] A. Valavanidis, T. Vlachogianni, C. Fiotakis, 8-hydroxy-2' -deoxyguanosine (8-OHdG): A critical biomarker of oxidative stress and carcinogenesis, J. Environ. Sci. Health C Environ. Carcinog. Ecotoxicol. Rev. 27 (2009) 120–139. https://doi.org/10.1080/10590500902885684.

[158] C. Neumann, J. Baesler, G. Steffen, M.M. Nicolai, T. Zubel, M. Aschner, A. Bürkle, A. Mangerich, T. Schwerdtle, J. Bornhorst, The role of poly(ADP-ribose) polymerases in manganese exposed Caenorhabditis elegans, J. Trace Elem. Med. Biol. 57 (2020) 21–27. https://doi.org/10.1016/j.jtemb.2019.09.001.

[159] A. Bürkle, Poly(ADP-ribose). The most elaborate metabolite of NAD+, FEBS J. 272 (2005) 4576–4589. https://doi.org/10.1111/j.1742-4658.2005.04864.x.

[160] N. Chatterjee, G.C. Walker, Mechanisms of DNA damage, repair, and mutagenesis, Environ. Mol. Mutagen. 58 (2017) 235–263. https://doi.org/10.1002/em.22087.

[161] Y. Wang, V.L. Dawson, T.M. Dawson, Poly(ADP-ribose) signals to mitochondrial AIF: a key event in parthanatos, Exp. Neurol. 218 (2009) 193–202. https://doi.org/10.1016/j.expneurol.2009.03.020.

[162] J. Bornhorst, S. Meyer, T. Weber, C. Böker, T. Marschall, A. Mangerich, S. Beneke, A. Bürkle, T. Schwerdtle, Molecular mechanisms of Mn induced neurotoxicity: RONS generation, genotoxicity, and DNA-damage response, Mol. Nutr. Food Res. 57 (2013) 1255–1269. https://doi.org/10.1002/mnfr.201200758.

[163] L. Chen, J. Min, F. Wang, Copper homeostasis and cuproptosis in health and disease, Signal Transduct. Target. Ther. 7 (2022) 378. https://doi.org/10.1038/s41392-022-01229-y.

[164] S. Song, X. Zhang, H. Wu, Y. Han, J. Zhang, E. Ma, Y. Guo, Molecular basis for antioxidant enzymes in mediating copper detoxification in the nematode Caenorhabditis elegans, PLoS One 9 (2014) e107685. https://doi.org/10.1371/journal.pone.0107685.

[165] J.A. Cotruvo, A.T. Aron, K.M. Ramos-Torres, C.J. Chang, Synthetic fluorescent probes for studying copper in biological systems, Chem. Soc. Rev. 44 (2015) 4400–4414. https://doi.org/10.1039/c4cs00346b.

[166] J. Lichtmannegger, C. Leitzinger, R. Wimmer, S. Schmitt, S. Schulz, Y. Kabiri, C. Eberhagen, T. Rieder, D. Janik, F. Neff, B.K. Straub, P. Schirmacher, A.A. DiSpirito, N. Bandow, B.S. Baral, A. Flatley, E. Kremmer, G. Denk, F.P. Reiter, S. Hohenester, F. Eckardt-Schupp, N.A. Dencher, J. Adamski, V. Sauer, C. Niemietz, H.H.J. Schmidt, U. Merle, D.N. Gotthardt, G. Kroemer, K.H. Weiss, H. Zischka, Methanobactin reverses acute liver failure in a rat model of Wilson disease, J. Clin. Invest. 126 (2016) 2721–2735. https://doi.org/10.1172/JCI85226.

[167] A. Rakshit, K. Khatua, V. Shanbhag, P. Comba, A. Datta, Cu2+ selective chelators relieve copper-induced oxidative stress in vivo, Chem. Sci. 9 (2018) 7916–7930. https://doi.org/10.1039/C8SC04041A.

[168] S. Mohammad Ahmadi Soleimani, H. Ekhtiari, J.L. Cadet, Drug-induced neurotoxicity in addiction medicine: From prevention to harm reduction, Prog. Brain Res. 223 (2016) 19–41. https://doi.org/10.1016/bs.pbr.2015.07.004.

[169] Y. Cao, B. Li, N. Ismail, K. Smith, T. Li, R. Dai, Y. Deng, Neurotoxicity and Underlying Mechanisms of Endogenous Neurotoxins, Int. J. Mol. Sci. 22 (2021). https://doi.org/10.3390/ijms222312805.

[170] P.S. Spencer, P.J. Lein, Neurotoxicity, in: Encyclopedia of Toxicology, Elsevier, 2014, pp. 489–500.

[171] K. Zhou, W. Luo, T. Liu, Y. Ni, Z. Qin, Neurotoxins Acting at Synaptic Sites: A Brief Review on Mechanisms and Clinical Applications, Toxins (Basel) 15 (2022). https://doi.org/10.3390/toxins15010018.

[172] P. Sweeney, H. Park, M. Baumann, J. Dunlop, J. Frydman, R. Kopito, A. McCampbell, G. Leblanc, A. Venkateswaran, A. Nurmi, R. Hodgson, Protein misfolding in neurodegenerative diseases: implications and strategies, Transl. Neurodegener. 6 (2017) 6. https://doi.org/10.1186/s40035-017-0077-5.

[173] O. Hobert, Specification of the nervous system, WormBook (2005) 1–19. https://doi.org/10.1895/wormbook.1.12.1.

[174] O. Hobert, Neurogenesis in the nematode Caenorhabditis elegans, WormBook (2010) 1–24. https://doi.org/10.1895/wormbook.1.12.2.

[175] E.R. Sawin, R. Ranganathan, H.R. Horvitz, C. elegans locomotory rate is modulated by the environment through a dopaminergic pathway and by experience through a serotonergic pathway, Neuron 26 (2000) 619–631. https://doi.org/10.1016/s0896-6273(00)81199-x.

[176] J.F. Etchberger, E.B. Flowers, R.J. Poole, E. Bashllari, O. Hobert, Cis-regulatory mechanisms of left/right asymmetric neuron-subtype specification in C. elegans, Development 136 (2009) 147–160. https://doi.org/10.1242/dev.030064.

[177] J. Rizo, Molecular Mechanisms Underlying Neurotransmitter Release, Annu. Rev. Biophys. 51 (2022) 377–408. https://doi.org/10.1146/annurev-biophys-111821-104732.

[178] A.-K. Weishaupt, L. Kubens, L. Ruecker, T. Schwerdtle, M. Aschner, J. Bornhorst, A Reliable Method Based on Liquid Chromatography-Tandem Mass Spectrometry for the Simultaneous Quantification of Neurotransmitters in Caenorhabditis elegans, Molecules 28 (2023). https://doi.org/10.3390/molecules28145373.

[179] M. Nimgampalle, H. Chakravarthy, S. Sharma, S. Shree, A.R. Bhat, J.A. Pradeepkiran, V. Devanathan, Neurotransmitter systems in the etiology of major neurological disorders: Emerging insights and therapeutic implications, Ageing Res. Rev. 89 (2023) 101994. https://doi.org/10.1016/j.arr.2023.101994.

[180] D.L. Chase, M.R. Koelle, Biogenic amine neurotransmitters in C. elegans, WormBook (2007) 1–15. https://doi.org/10.1895/wormbook.1.132.1.

[181] L. Pereira, P. Kratsios, E. Serrano-Saiz, H. Sheftel, A.E. Mayo, D.H. Hall, J.G. White, B. LeBoeuf, L.R. Garcia, U. Alon, O. Hobert, A cellular and regulatory map of the cholinergic nervous system of C. elegans, Elife 4 (2015). https://doi.org/10.7554/eLife.12432.

[182] L.G. Costa, Interactions of neurotoxicants with neurotransmitter systems, Toxicology 49 (1988) 359–366. https://doi.org/10.1016/0300-483X(88)90019-4.

[183] K. Heine, A. Taghavi, F. Kalberlah, Project summary: a critical synopsis of mechanisms of action of low-dose xenobiotics in mammalian organisms as a basis for assessing aggregated effects of chemical mixtures and identifying "new" toxicological end points, Environ Sci Eur 23 (2011). https://doi.org/10.1186/2190-4715-23-27.

[184] C.A. Sanchez-Catasus, N.I. Bohnen, N. D'Cruz, M.L.T.M. Müller, Striatal Acetylcholine-Dopamine Imbalance in Parkinson Disease: In Vivo Neuroimaging Study with Dual-Tracer PET and Dopaminergic PET-Informed Correlational Tractography, J. Nucl. Med. 63 (2022) 438–445. https://doi.org/10.2967/jnumed.121.261939.

[185] J.W. McKinley, Z. Shi, I. Kawikova, M. Hur, I.J. Bamford, S.P. Sudarsana Devi, A. Vahedipour, M. Darvas, N.S. Bamford, Dopamine Deficiency Reduces Striatal Cholinergic Interneuron Function in Models of Parkinson's Disease, Neuron 103 (2019) 1056-1072.e6. https://doi.org/10.1016/j.neuron.2019.06.013.

[186] J. Sonne, V. Reddy, M.R. Beato, StatPearls: Neuroanatomy, Substantia Nigra, Treasure Island (FL), 2024.

[187] W. Schultz, Multiple dopamine functions at different time courses, Annu. Rev. Neurosci. 30 (2007) 259–288. https://doi.org/10.1146/annurev.neuro.28.061604.135722.

[188] J. Meiser, D. Weindl, K. Hiller, Complexity of dopamine metabolism, Cell Commun. Signal. 11 (2013) 34. https://doi.org/10.1186/1478-811X-11-34.

[189] D.S. Goldstein, P. Sullivan, C. Holmes, G.W. Miller, S. Alter, R. Strong, D.C. Mash, I.J. Kopin, Y. Sharabi, Determinants of buildup of the toxic dopamine metabolite DOPAL in Parkinson's disease, J. Neurochem. 126 (2013) 591–603. https://doi.org/10.1111/jnc.12345.

[190] J.N. Cobley, M.L. Fiorello, D.M. Bailey, 13 reasons why the brain is susceptible to oxidative stress, Redox Biol. 15 (2018) 490–503. https://doi.org/10.1016/j.redox.2018.01.008.

[191] K.M.L. Cramb, D. Beccano-Kelly, S.J. Cragg, R. Wade-Martins, Impaired dopamine release in Parkinson's disease, Brain 146 (2023) 3117–3132. https://doi.org/10.1093/brain/awad064.

[192] D.B. Miller, J.P. O'Callaghan, Biomarkers of Parkinson's disease: present and future, Metabolism 64 (2015) S40-6. https://doi.org/10.1016/j.metabol.2014.10.030.

[193] H. Xu, F. Yang, The interplay of dopamine metabolism abnormalities and mitochondrial defects in the pathogenesis of schizophrenia, Transl. Psychiatry 12 (2022) 464. https://doi.org/10.1038/s41398-022-02233-0.

[194] P.W. Andrews, C. Bosyj, L. Brenton, L. Green, P.J. Gasser, C.A. Lowry, V.M. Pickel, All the brain's a stage for serotonin: the forgotten story of serotonin diffusion across cell membranes, Proc. Biol. Sci. 289 (2022) 20221565. https://doi.org/10.1098/rspb.2022.1565.

[195] L.F. Mohammad-Zadeh, L. Moses, S.M. Gwaltney-Brant, Serotonin: a review, J. Vet. Pharmacol. Ther. 31 (2008) 187–199. https://doi.org/10.1111/j.1365-2885.2008.00944.x.

[196] S. Jauhar, P.J. Cowen, M. Browning, Fifty years on: Serotonin and depression, J. Psychopharmacol. 37 (2023) 237–241. https://doi.org/10.1177/02698811231161813.

[197] O.A.C. Petroff, GABA and glutamate in the human brain, Neuroscientist 8 (2002) 562–573. https://doi.org/10.1177/1073858402238515.

[198] J. Samardzic, D. Jadzic, B. Hencic, J. Jancic, D.S. Strac, Introductory Chapter: GABA/Glutamate Balance: A Key for Normal Brain Functioning, in: J. Samardzic (Ed.), GABA And Glutamate - New Developments In Neurotransmission Research, InTech, 2018.

[199] C.K. Jones, N. Byun, M. Bubser, Muscarinic and nicotinic acetylcholine receptor agonists and allosteric modulators for the treatment of schizophrenia, Neuropsychopharmacology 37 (2012) 16–42. https://doi.org/10.1038/npp.2011.199.

[200] G.D. Stanciu, A. Luca, R.N. Rusu, V. Bild, S.I. Beschea Chiriac, C. Solcan, W. Bild, D.C. Ababei, Alzheimer's Disease Pharmacotherapy in Relation to Cholinergic System Involvement, Biomolecules 10 (2019). https://doi.org/10.3390/biom10010040.

[201] K. Sharma, Cholinesterase inhibitors as Alzheimer's therapeutics (Review), Mol. Med. Rep. 20 (2019) 1479–1487. https://doi.org/10.3892/mmr.2019.10374.

[202] C.N. Pope, S. Brimijoin, Cholinesterases and the fine line between poison and remedy, Biochemical Pharmacology 153 (2018) 205–216. https://doi.org/10.1016/j.bcp.2018.01.044.

[203] M.B. Colović, D.Z. Krstić, T.D. Lazarević-Pašti, A.M. Bondžić, V.M. Vasić, Acetylcholinesterase inhibitors: pharmacology and toxicology, Curr. Neuropharmacol. 11 (2013) 315–335. https://doi.org/10.2174/1570159X11311030006.

[204] V. Aroniadou-Anderjaska, J.P. Apland, T.H. Figueiredo, M. de Araujo Furtado, M.F. Braga, Acetylcholinesterase inhibitors (nerve agents) as weapons of mass destruction: History, mechanisms of action, and medical countermeasures, Neuropharmacology 181 (2020) 108298. https://doi.org/10.1016/j.neuropharm.2020.108298.

[205] G.M. Mawe, K.N. Browning, F.P. Manfredsson, M. Camilleri, F.A. Hamilton, J.A. Hollander, B.-A. Sieber, P. Greenwel, T. Shea-Donohue, J.W. Wiley, 2021 Workshop: Neurodegenerative Diseases in the Gut-Brain Axis-Parkinson's Disease, Gastroenterology 162 (2022) 1574–1582. https://doi.org/10.1053/j.gastro.2022.02.004.

[206] J. van Schependom, M. D'haeseleer, Advances in Neurodegenerative Diseases, J. Clin. Med. 12 (2023). https://doi.org/10.3390/jcm12051709.

[207] L. Agnello, M. Ciaccio, Neurodegenerative Diseases: From Molecular Basis to Therapy, Int. J. Mol. Sci. 23 (2022). https://doi.org/10.3390/ijms232112854.

[208] X.-X. Zhang, Y. Tian, Z.-T. Wang, Y.-H. Ma, L. Tan, J.-T. Yu, The Epidemiology of Alzheimer's Disease Modifiable Risk Factors and Prevention, J. Prev. Alzheimers. Dis. 8 (2021) 313–321. https://doi.org/10.14283/jpad.2021.15.

[209] C.A. Lane, J. Hardy, J.M. Schott, Alzheimer's disease, Eur. J. Neurol. 25 (2018) 59–70. https://doi.org/10.1111/ene.13439.

[210] S. Musardo, E. Marcello, Synaptic dysfunction in Alzheimer's disease: From the role of amyloid β-peptide to the α-secretase ADAM10, Eur. J. Pharmacol. 817 (2017) 30–37. https://doi.org/10.1016/j.ejphar.2017.06.018.

[211] F. Kametani, M. Hasegawa, Reconsideration of Amyloid Hypothesis and Tau Hypothesis in Alzheimer's Disease, Front. Neurosci. 12 (2018) 25. https://doi.org/10.3389/fnins.2018.00025.

[212] S. Bagheri, R. Squitti, T. Haertlé, M. Siotto, A.A. Saboury, Role of Copper in the Onset of Alzheimer's Disease Compared to Other Metals, Front. Aging Neurosci. 9 (2017) 446. https://doi.org/10.3389/fnagi.2017.00446.

[213] H. Hampel, J. Hardy, K. Blennow, C. Chen, G. Perry, S.H. Kim, V.L. Villemagne, P. Aisen, M. Vendruscolo, T. Iwatsubo, C.L. Masters, M. Cho, L. Lannfelt, J.L. Cummings, A. Vergallo, The Amyloid-β Pathway in Alzheimer's Disease, Mol. Psychiatry 26 (2021) 5481–5503. https://doi.org/10.1038/s41380-021-01249-0.

[214] E.E. Congdon, E.M. Sigurdsson, Tau-targeting therapies for Alzheimer disease, Nat. Rev. Neurol. 14 (2018) 399–415. https://doi.org/10.1038/s41582-018-0013-z.

[215] Z. Yang, Y. Zou, L. Wang, Neurotransmitters in Prevention and Treatment of Alzheimer's Disease, Int. J. Mol. Sci. 24 (2023). https://doi.org/10.3390/ijms24043841.

[216] B.R. Bloem, M.S. Okun, C. Klein, Parkinson's disease, Lancet 397 (2021) 2284–2303. https://doi.org/10.1016/ S0140-6736(21)00218-X.

[217] Y. Xiong, T.M. Dawson, V.L. Dawson, Models of LRRK2-Associated Parkinson's Disease, Adv. Neurobiol. 14 (2017) 163–191. https://doi.org/10.1007/978-3-319-49969-7_9.

[218] J. Tian, J. Guo, L. Wang, Q. Sun, L. Yao, L. Luo, C. Shi, Y. Hu, X. Yan, B. Tang, Mutation analysis of LRRK2, SCNA, UCHL1, HtrA2 and GIGYF2 genes in Chinese patients with autosomal dorminant Parkinson's disease, Neurosci. Lett. 516 (2012) 207–211. https://doi.org/10.1016/j.neulet.2012.03.086.

[219] J. Bornhorst, S. Chakraborty, S. Meyer, H. Lohren, S.G. Brinkhaus, A.L. Knight, K.A. Caldwell, G.A. Caldwell, U. Karst, T. Schwerdtle, A. Bowman, M. Aschner, The effects of pdr1, djr1.1 and pink1 loss in manganese-induced toxicity and the role of α-synuclein in C. elegans, Metallomics 6 (2014) 476–490. https://doi.org/10.1039/c3mt00325f.

[220] S. Martin, S. van Veen, T. Holemans, S. Demirsoy, C. van den Haute, V. Baekelandt, P. Agostinis, J. Eggermont, P. Vangheluwe, Protection against Mitochondrial and Metal Toxicity Depends on Functional Lipid Binding Sites in ATP13A2, Parkinsons. Dis. 2016 (2016) 9531917. https://doi.org/10.1155/2016/9531917.

[221] H.N. Costa, A.R. Esteves, N. Empadinhas, S.M. Cardoso, Parkinson's Disease: A Multisystem Disorder, Neurosci. Bull. 39 (2023) 113–124. https://doi.org/10.1007/s12264-022-00934-6.

[222] K. Jomova, D. Vondrakova, M. Lawson, M. Valko, Metals, oxidative stress and neurodegenerative disorders, Mol. Cell. Biochem. 345 (2010) 91–104. https://doi.org/10.1007/s11010-010-0563-x.

[223] H.C. Çubukçu, M. Yurtdaş, Z.E. Durak, B. Aytaç, H.N. Güneş, B.G. Çokal, T.K. Yoldaş, İ. Durak, Oxidative and nitrosative stress in serum of patients with Parkinson's disease, Neurol. Sci. 37 (2016) 1793–1798. https://doi.org/10.1007/s10072-016-2663-1.

[224] I. Ullah, L. Zhao, Y. Hai, M. Fahim, D. Alwayli, X. Wang, H. Li, "Metal elements and pesticides as risk factors for Parkinson's disease - A review", Toxicol. Rep. 8 (2021) 607–616. https://doi.org/10.1016/j.toxrep.2021.03.009.

[225] L. Cassidy, F. Fernandez, J.B. Johnson, M. Naiker, A.G. Owoola, D.A. Broszczak, Oxidative stress in alzheimer's disease: A review on emergent natural polyphenolic therapeutics, Complement. Ther. Med. 49 (2020) 102294. https://doi.org/10.1016/j.ctim.2019.102294.

[226] G. Eskici, P.H. Axelsen, Copper and oxidative stress in the pathogenesis of Alzheimer's disease, Biochemistry 51 (2012) 6289–6311. https://doi.org/10.1021/bi3006169.

[227] F. Arrigoni, T. Prosdocimi, L. Mollica, L. de Gioia, G. Zampella, L. Bertini, Copper reduction and dioxygen activation in Cu-amyloid beta peptide complexes: insight from molecular modelling, Metallomics 10 (2018) 1618–1630. https://doi.org/10.1039/C8MT00216A.

[228] G.J. Brewer, S.H. Kanzer, E.A. Zimmerman, D.F. Celmins, S.M. Heckman, R. Dick, Copper and ceruloplasmin abnormalities in Alzheimer's disease, Am. J. Alzheimers. Dis. Other Demen. 25 (2010) 490–497. https://doi.org/10.1177/1533317510375083.

[229] R. Squitti, P. Pasqualetti, G. Dal Forno, F. Moffa, E. Cassetta, D. Lupoi, F. Vernieri, L. Rossi, M. Baldassini, P.M. Rossini, Excess of serum copper not related to ceruloplasmin in Alzheimer disease, Neurology 64 (2005) 1040–1046. https://doi.org/10.1212/01.WNL.0000154531.79362.23.

[230] R. Squitti, M. Ventriglia, G. Barbati, E. Cassetta, F. Ferreri, G. Dal Forno, S. Ramires, F. Zappasodi, P.M. Rossini, 'Free' copper in serum of Alzheimer's disease patients correlates with markers of liver function, J. Neural Transm. (Vienna) 114 (2007) 1589–1594. https://doi.org/10.1007/s00702-007-0777-6.

[231] S.A. James, I. Volitakis, P.A. Adlard, J.A. Duce, C.L. Masters, R.A. Cherny, A.I. Bush, Elevated labile Cu is associated with oxidative pathology in Alzheimer disease, Free Radic. Biol. Med. 52 (2012) 298–302. https://doi.org/10.1016/j.freeradbiomed.2011.10.446.

[232] C. Shen, E.J. New, What has fluorescent sensing told us about copper and brain malfunction?, Metallomics 7 (2015) 56–65. https://doi.org/10.1039/c4mt00288a.

[233] D.A. Loeffler, P.A. LeWitt, P.L. Juneau, A.A. Sima, H.U. Nguyen, A.J. DeMaggio, C.M. Brickman, G.J. Brewer, R.D. Dick, M.D. Troyer, L. Kanaley, Increased regional brain concentrations of ceruloplasmin in neurodegenerative disorders, Brain Res. 738 (1996) 265–274. https://doi.org/10.1016/s0006-8993(96)00782-2.

[234] S. Latif, M. Jahangeer, D. Maknoon Razia, M. Ashiq, A. Ghaffar, M. Akram, A. El Allam, A. Bouyahya, L. Garipova, M. Ali Shariati, M. Thiruvengadam, M. Azam Ansari, Dopamine in Parkinson's disease, Clin. Chim. Acta 522 (2021) 114–126. https://doi.org/10.1016/j.cca.2021.08.009.

[235] M.O. Klein, D.S. Battagello, A.R. Cardoso, D.N. Hauser, J.C. Bittencourt, R.G. Correa, Dopamine: Functions, Signaling, and Association with Neurological Diseases, Cell. Mol. Neurobiol. 39 (2019) 31–59. https://doi.org/10.1007/s10571-018-0632-3.

[236] D. Meder, D.M. Herz, J.B. Rowe, S. Lehéricy, H.R. Siebner, The role of dopamine in the brain - lessons learned from Parkinson's disease, Neuroimage 190 (2019) 79–93. https://doi.org/10.1016/j.neuroimage.2018.11.021.

[237] A. Masato, N. Plotegher, D. Boassa, L. Bubacco, Impaired dopamine metabolism in Parkinson's disease pathogenesis, Mol. Neurodegener. 14 (2019) 35. https://doi.org/10.1186/s13024-019-0332-6.

[238] P. de Deurwaerdère, G. Di Giovanni, Serotonin in Health and Disease, Int. J. Mol. Sci. 21 (2020). https://doi.org/10.3390/ijms21103500.

[239] M. Pourhamzeh, F.G. Moravej, M. Arabi, E. Shahriari, S. Mehrabi, R. Ward, R. Ahadi, M.T. Joghataei, The Roles of Serotonin in Neuropsychiatric Disorders, Cell. Mol. Neurobiol. 42 (2022) 1671–1692. https://doi.org/10.1007/s10571-021-01064-9.

[240] S.B. Sarasa, R. Mahendran, G. Muthusamy, B. Thankappan, D.R.F. Selta, J. Angayarkanni, A Brief Review on the Non-protein Amino Acid, Gamma-amino Butyric Acid (GABA): Its Production and Role in Microbes, Curr. Microbiol. 77 (2020) 534–544. https://doi.org/10.1007/s00284-019-01839-w.

[241] A. Sood, K. Preeti, V. Fernandes, D.K. Khatri, S.B. Singh, Glia: A major player in glutamate-GABA dysregulation-mediated neurodegeneration, J. Neurosci. Res. 99 (2021) 3148–3189. https://doi.org/10.1002/jnr.24977.

[242] T.H. Ferreira-Vieira, I.M. Guimaraes, F.R. Silva, F.M. Ribeiro, Alzheimer's disease: Targeting the Cholinergic System, Curr. Neuropharmacol. 14 (2016) 101–115. https://doi.org/10.2174/1570159x13666150716165726.

[243] H. Hampel, M.-M. Mesulam, A.C. Cuello, M.R. Farlow, E. Giacobini, G.T. Grossberg, A.S. Khachaturian, A. Vergallo, E. Cavedo, P.J. Snyder, Z.S. Khachaturian, The cholinergic system in the pathophysiology and treatment of Alzheimer's disease, Brain 141 (2018) 1917–1933. https://doi.org/10.1093/brain/awy132.

[244] S. Habtemariam, Natural Products in Alzheimer's Disease Therapy: Would Old Therapeutic Approaches Fix the Broken Promise of Modern Medicines?, Molecules 24 (2019). https://doi.org/10.3390/molecules24081519.

[245] Z. Qi, F. Tretter, E.O. Voit, A heuristic model of alcohol dependence, PLoS One 9 (2014) e92221. https://doi.org/10.1371/journal.pone.0092221.

[246] N. Huber, S. Korhonen, D. Hoffmann, S. Leskelä, H. Rostalski, A.M. Remes, P. Honkakoski, E. Solje, A. Haapasalo, Deficient neurotransmitter systems and synaptic function in frontotemporal lobar degeneration-Insights into disease mechanisms and current therapeutic approaches, Mol. Psychiatry 27 (2022) 1300–1309. https://doi.org/10.1038/s41380-021-01384-8.

[247] L.-S. Wang, M.-D. Zhang, X. Tao, Y.-F. Zhou, X.-M. Liu, R.-L. Pan, Y.-H. Liao, Q. Chang, LC-MS/MS-based quantification of tryptophan metabolites and neurotransmitters in the serum and brain of mice, J. Chromatogr. B Analyt. Technol. Biomed. Life Sci. 1112 (2019) 24–32. https://doi.org/10.1016/j.jchromb.2019.02.021.

[248] M.E. Blanco, O.B. Mayo, T. Bandiera, D. de Pietri Tonelli, A. Armirotti, LC-MS/MS analysis of twelve neurotransmitters and amino acids in mouse cerebrospinal fluid, J. Neurosci. Methods 341 (2020) 108760. https://doi.org/10.1016/j.jneumeth.2020.108760.

[249] P. Fernandez-Funez, J. Sanchez-Garcia, D.E. Rincon-Limas, Drosophila models of prionopathies: insight into prion protein function, transmission, and neurotoxicity, Curr. Opin. Genet. Dev. 44 (2017) 141–148. https://doi.org/10.1016/j.gde.2017.03.013.

[250] C.A. Taylor, K. Tuschl, M.M. Nicolai, J. Bornhorst, P. Gubert, A.M. Varão, M. Aschner, D.R. Smith, S. Mukhopadhyay, Maintaining Translational Relevance in Animal Models of Manganese Neurotoxicity, J. Nutr. 150 (2020) 1360–1369. https://doi.org/10.1093/jn/nxaa066.

[251] J.F. Cooper, J.M. van Raamsdonk, Modeling Parkinson's Disease in C. elegans, J. Parkinsons. Dis. 8 (2018) 17–32. https://doi.org/10.3233/JPD-171258.

[252] L. Ma, X. Li, C. Liu, W. Yan, J. Ma, R.B. Petersen, A. Peng, K. Huang, Modelling Parkinson's Disease in C. elegans: Strengths and Limitations, Curr. Pharm. Des. 28 (2022) 3033–3048. https://doi.org/10.2174/1381612828666220915103502.

[253] K.A. Caldwell, C.W. Willicott, G.A. Caldwell, Modeling neurodegeneration in Caenorhabditiselegans, Dis. Model. Mech. 13 (2020). https://doi.org/10.1242/dmm.046110.

[254] F.J. Naranjo-Galindo, R. Ai, E.F. Fang, H.L. Nilsen, T. SenGupta, C. elegans as an Animal Model to Study the Intersection of DNA Repair, Aging and Neurodegeneration, Front. Aging 3 (2022) 916118. https://doi.org/10.3389/fragi.2022.916118.

[255] N.F. Trojanowski, D.M. Raizen, C. Fang-Yen, Pharyngeal pumping in Caenorhabditis elegans depends on tonic and phasic signaling from the nervous system, Sci. Rep. 6 (2016) 22940. https://doi.org/10.1038/srep22940.

[256] T.R. Mahoney, Analysis of synaptic transmission in Caenorhabditis elegans using an aldicarb-sensitivity assay, Nat. Protoc. (2006).

[257] T. Ke, A. Tsatsakis, A. Santamaría, F.A. Antunes Soare, A.A. Tinkov, A.O. Docea, A. Skalny, A.B. Bowman, M. Aschner, Chronic exposure to methylmercury induces puncta formation in cephalic dopaminergic neurons in Caenorhabditis elegans, Neurotoxicology 77 (2020) 105–113. https://doi.org/10.1016/j.neuro.2020.01.003.

[258] Z. Yan, X. Cheng, Y. Li, Z. Su, Y. Zhou, J. Liu, Sexually Dimorphic Neurotransmitter Release at the Neuromuscular Junction in Adult Caenorhabditis elegans, Front. Mol. Neurosci. 14 (2021) 780396. https://doi.org/10.3389/fnmol.2021.780396.

[259] B.A. Patel, M. Arundell, K.H. Parker, M.S. Yeoman, D. O'Hare, Simple and rapid determination of serotonin and catecholamines in biological tissue using high-performance liquid chromatography with electrochemical detection, J. Chromatogr. B Analyt. Technol. Biomed. Life Sci. 818 (2005) 269–276. https://doi.org/10.1016/j.jchromb.2005.01.008.

[260] J.Y. Baek, T. an Trinh, W. Huh, J.H. Song, H.Y. Kim, J. Lim, J. Kim, H.J. Choi, T.-H. Kim, K.S. Kang, Electro-Acupuncture Alleviates Cisplatin-Induced Anorexia in Rats by Modulating Ghrelin and Monoamine Neurotransmitters, Biomolecules 9 (2019). https://doi.org/10.3390/biom9100624.

[261] H.-X. Zhao, H. Mu, Y.-H. Bai, H. Yu, Y.-M. Hu, A rapid method for the determination of dopamine in porcine muscle by pre-column derivatization and HPLC with fluorescence detection, J. Pharm. Anal. 1 (2011) 208–212. https://doi.org/10.1016/j.jpha.2011.04.003.

[262] N. Şanlı, S.E. Tague, C. Lunte, Analysis of amino acid neurotransmitters from rat and mouse spinal cords by liquid chromatography with fluorescence detection, J. Pharm. Biomed. Anal. 107 (2015) 217–222. https://doi.org/10.1016/j.jpba.2014.12.024.

[263] J. An, M. Chen, N. Hu, Y. Hu, R. Chen, Y. Lyu, W. Guo, L. Li, Y. Liu, Carbon dots-based dual-emission ratiometric fluorescence sensor for dopamine detection, Spectrochim. Acta A Mol. Biomol. Spectrosc. 243 (2020) 118804. https://doi.org/10.1016/j.saa.2020.118804.

[264] F. Sun, J. Zeng, M. Jing, J. Zhou, J. Feng, S.F. Owen, Y. Luo, F. Li, H. Wang, T. Yamaguchi, Z. Yong, Y. Gao, W. Peng, L. Wang, S. Zhang, J. Du, D. Lin, M. Xu, A.C. Kreitzer, G. Cui, Y. Li, A Genetically Encoded Fluorescent Sensor Enables Rapid and Specific Detection of Dopamine in Flies, Fish, and Mice, Cell 174 (2018) 481-496.e19. https://doi.org/10.1016/j.cell.2018.06.042.

[265] J. Sun, A. Feng, X. Wu, X. Che, W. Zhou, Enhanced Tb(III) fluorescence on gelatin-coated silver nanoparticles in dopamine detection, Talanta 231 (2021) 122334. https://doi.org/10.1016/j.talanta.2021.122334.

[266] J. Wu, R. Wiegand, P. LoRusso, J. Li, A stable isotope-labeled internal standard is essential for correcting for the interindividual variability in the recovery of lapatinib from cancer patient plasma in quantitative LC-MS/MS analysis, J. Chromatogr. B Analyt. Technol. Biomed. Life Sci. 941 (2013) 100–108. https://doi.org/10.1016/j.jchromb.2013.10.011.

[267] F. Carreño, V.E. Helfer, K.J. Staudt, L.B. Olivo, F. Barreto, A.P. Herrmann, S.M.K. Rates, T. Dalla Costa, Quantification of neurotransmitters in microdialysate samples following quetiapine dosing to schizophrenia phenotyped rats using a validated LC-MS/MS method, J. Chromatogr. B Analyt. Technol. Biomed. Life Sci. 1155 (2020) 122282. https://doi.org/10.1016/j.jchromb.2020.122282.

[268] H. Xu, Z. Wang, L. Zhu, Z. Sui, W. Bi, R. Liu, K. Bi, Q. Li, Targeted Neurotransmitters Profiling Identifies Metabolic Signatures in Rat Brain by LC-MS/MS: Application in Insomnia, Depression and Alzheimer's Disease, Molecules 23 (2018). https://doi.org/10.3390/molecules23092375.

[269] S. Tufi, P. Leonards, M. Lamoree, J. de Boer, J. Legler, J. Legradi, Changes in Neurotransmitter Profiles during Early Zebrafish (Danio rerio) Development and after Pesticide Exposure, Environ. Sci. Technol. 50 (2016) 3222–3230. https://doi.org/10.1021/acs.est.5b05665.

[270] I. Fuertes, C. Barata, Characterization of neurotransmitters and related metabolites in Daphnia magna juveniles deficient in serotonin and exposed to neuroactive chemicals that affect its behavior: A targeted LC-MS/MS method, Chemosphere 263 (2021) 127814. https://doi.org/10.1016/j.chemosphere.2020.127814.

[271] S.C. Daubner, T. Le, S. Wang, Tyrosine hydroxylase and regulation of dopamine synthesis, Arch. Biochem. Biophys. 508 (2011) 1–12. https://doi.org/10.1016/j.abb.2010.12.017.

[272] S.F. McHardy, H.-Y.L. Wang, S.V. McCowen, M.C. Valdez, Recent advances in acetylcholinesterase Inhibitors and Reactivators: an update on the patent literature (2012-2015), Expert Opin. Ther. Pat. 27 (2017) 455–476. https://doi.org/10.1080/13543776.2017.1272571.

[273] K.H. Oh, H. Kim, Aldicarb-induced Paralysis Assay to Determine Defects in Synaptic Transmission in Caenorhabditis elegans, Bio Protoc. 7 (2017). https://doi.org/10.21769/BioProtoc.2400.

[274] J.B. Rand, Acetylcholine, WormBook (2007) 1–21. https://doi.org/10.1895/wormbook.1.131.1.

[275] S. Bhat, A. El-Kasaby, M. Freissmuth, S. Sucic, Functional and Biochemical Consequences of Disease Variants in Neurotransmitter Transporters: A Special Emphasis on Folding and Trafficking Deficits, Pharmacol. Ther. 222 (2021) 107785. https://doi.org/10.1016/j.pharmthera.2020.107785.

[276] G. Rizzi, K.R. Tan, Dopamine and Acetylcholine, a Circuit Point of View in Parkinson's Disease, Front. Neural Circuits 11 (2017) 110. https://doi.org/10.3389/fncir.2017.00110.

[277] N. Umek, B. Geršak, N. Vintar, M. Šoštarič, J. Mavri, Dopamine Autoxidation Is Controlled by Acidic pH, Front. Mol. Neurosci. 11 (2018) 467. https://doi.org/10.3389/fnmol.2018.00467.

[278] F. Huang, J. Li, H.-L. Shi, T. Wang, W. Muhtar, M. Du, B. Zhang, H. Wu, L. Yang, Z. Hu, X. Wu, Simultaneous quantification of seven hippocampal neurotransmitters in depression mice by LC-MS/MS, J. Neurosci. Methods 229 (2014) 8–14. https://doi.org/10.1016/j.jneumeth.2014.04.004.

[279] E. Olesti, J. Rodríguez-Morató, A. Gomez-Gomez, J.G. Ramaekers, R. de La Torre, O.J. Pozo, Quantification of endogenous neurotransmitters and related compounds by liquid chromatography coupled to tandem mass spectrometry, Talanta 192 (2019) 93–102. https://doi.org/10.1016/j.talanta.2018.09.034.

[280] X.-M. Han, Y.-J. Qin, Y. Zhu, X.-L. Zhang, N.-X. Wang, Y. Rang, X.-J. Zhai, Y.-N. Lu, Development of an underivatized LC-MS/MS method for quantitation of 14 neurotransmitters in rat hippocampus, plasma and urine: Application to CUMS induced depression rats, J. Pharm. Biomed. Anal. 174 (2019) 683–695. https://doi.org/10.1016/j.jpba.2019.06.043.

[281] F.W. McLafferty, F. Turecek, Interpretation of mass spectra: Zahlr. Tab, fourth. Aufl., University Science Books, Mill Welley, 1993.

[282] M. Zhang, C. Fang, G. Smagin, Derivatization for the simultaneous LC/MS quantification of multiple neurotransmitters in extracellular fluid from rat brain microdialysis, J. Pharm. Biomed. Anal. 100 (2014) 357–364. https://doi.org/10.1016/j.jpba.2014.08.015.

[283] S.W. Caito, M. Aschner, NAD+ Supplementation Attenuates Methylmercury Dopaminergic and Mitochondrial Toxicity in Caenorhabditis Elegans, Toxicol. Sci. 151 (2016) 139–149. https://doi.org/10.1093/toxsci/kfw030.

[284] O.M. Ijomone, M.R. Miah, G.T. Akingbade, H. Bucinca, M. Aschner, Nickel-Induced Developmental Neurotoxicity in C. elegans Includes Cholinergic, Dopaminergic and GABAergic Degeneration, Altered Behaviour, and Increased SKN-1 Activity, Neurotox. Res. 37 (2020) 1018–1028. https://doi.org/10.1007/s12640-020-00175-3.

[285] C. Defaix, A. Solgadi, T.H. Pham, A.M. Gardier, P. Chaminade, L. Tritschler, Rapid analysis of glutamate, glutamine and GABA in mice frontal cortex microdialysis samples using HPLC coupled to electrospray tandem mass spectrometry, J. Pharm. Biomed. Anal. 152 (2018) 31–38. https://doi.org/10.1016/j.jpba.2018.01.039.

[286] A. Muñoz, A. Lopez-Lopez, C.M. Labandeira, J.L. Labandeira-Garcia, Interactions Between the Serotonergic and Other Neurotransmitter Systems in the Basal Ganglia: Role in Parkinson's Disease and Adverse Effects of L-DOPA, Front. Neuroanat. 14 (2020) 26. https://doi.org/10.3389/fnana.2020.00026.

[287] E.G. Govorunova, M. Moussaif, A. Kullyev, K.C.Q. Nguyen, T.V. McDonald, D.H. Hall, J.Y. Sze, A homolog of FHM2 is involved in modulation of excitatory neurotransmission by serotonin in C. elegans, PLoS One 5 (2010) e10368. https://doi.org/10.1371/journal.pone.0010368.

[288] N. Suthakaran, T. Brock, A. Naraine, P. Gonzalez-Lerma, C. Hopkins, K. Dawson-Scully, Atropine reduces aldicarb-induced sensitivity to C. elegans electroshock model, MicroPubl. Biol. 2022 (2022). https://doi.org/10.17912/micropub.biology.000621.

[289] A.C. Giles, M. Desbois, K.J. Opperman, R. Tavora, M.J. Maroni, B. Grill, A complex containing the O-GlcNAc transferase OGT-1 and the ubiquitin ligase EEL-1 regulates GABA neuron function, J. Biol. Chem. 294 (2019) 6843–6856. https://doi.org/10.1074/jbc.RA119.007406.

[290] C.H. Opperman, S. Chang, Effects of Aldicarb and Fenamiphos on Acetycholinesterase and Motility of Caenorhabditis elegans, J. Nematol. 23 (1991) 20–27.

[291] R. Nass, The nematode C. elegans as an animal model to explore toxicology in vivo: solid and axenic growth culture conditions and compound exposure parameters, Curr. Protoc. Toxicol. (2007) Unit1.9.

[292] S. Brenner, The genetics of Caenorhabditis elegans, Genetics (1974).

[293] J.M. Walker, The bicinchoninic acid (BCA) assay for protein quantitation, Methods Mol. Biol. 32 (1994) 5–8. https://doi.org/10.1385/0-89603-268-X:5.

[294] Y. Li, H. Chen, J. Liao, K. Chen, M.T. Javed, N. Qiao, Q. Zeng, B. Liu, J. Yi, Z. Tang, Y. Li, Long-term copper exposure promotes apoptosis and autophagy by inducing oxidative stress in pig testis, Environ. Sci. Pollut. Res. Int. 28 (2021) 55140–55153. https://doi.org/10.1007/s11356-021-14853-y.

[295] R. Vázquez-Blanco, M. Arias-Estévez, E. Bååth, D. Fernández-Calviño, Comparison of Cu salts and commercial Cu based fungicides on toxicity towards microorganisms in soil, Environ. Pollut. 257 (2020) 113585. https://doi.org/10.1016/j.envpol.2019.113585.

[296] Y. An, S. Li, X. Huang, X. Chen, H. Shan, M. Zhang, The Role of Copper Homeostasis in Brain Disease, Int. J. Mol. Sci. 23 (2022). https://doi.org/10.3390/ijms232213850.

[297] E.L. Que, D.W. Domaille, C.J. Chang, Metals in neurobiology: probing their chemistry and biology with molecular imaging, Chem. Rev. 108 (2008) 1517–1549. https://doi.org/10.1021/cr078203u.

[298] E.J. Ge, A.I. Bush, A. Casini, P.A. Cobine, J.R. Cross, G.M. DeNicola, Q.P. Dou, K.J. Franz, V.M. Gohil, S. Gupta, S.G. Kaler, S. Lutsenko, V. Mittal, M.J. Petris, R. Polishchuk, M. Ralle, M.L. Schilsky, N.K. Tonks, L.T. Vahdat, L. van Aelst, D. Xi, P. Yuan, D.C. Brady, C.J. Chang, Connecting copper and cancer: from transition metal signalling to metalloplasia, Nat. Rev. Cancer 22 (2022) 102–113. https://doi.org/10.1038/s41568-021-00417-2.

[299] M. Bisaglia, L. Bubacco, Copper Ions and Parkinson's Disease: Why Is Homeostasis So Relevant?, Biomolecules 10 (2020). https://doi.org/10.3390/biom10020195.

[300] R.J. Clifford, E.B. Maryon, J.H. Kaplan, Dynamic internalization and recycling of a metal ion transporter: Cu homeostasis and CTR1, the human Cu^+ uptake system, J. Cell Sci. 129 (2016) 1711–1721. https://doi.org/10.1242/jcs.173351.

[301] J.R. Prohaska, Role of copper transporters in copper homeostasis, Am. J. Clin. Nutr. 88 (2008) 826S-9S. https://doi.org/10.1093/ajcn/88.3.826S.

[302] J.-F. Monty, R.M. Llanos, J.F.B. Mercer, D.R. Kramer, Copper exposure induces trafficking of the menkes protein in intestinal epithelium of ATP7A transgenic mice, J. Nutr. 135 (2005) 2762–2766. https://doi.org/10.1093/jn/135.12.2762.

[303] M.A. Cater, S. La Fontaine, K. Shield, Y. Deal, J.F.B. Mercer, ATP7B mediates vesicular sequestration of copper: insight into biliary copper excretion, Gastroenterology 130 (2006) 493–506. https://doi.org/10.1053/j.gastro.2005.10.054.

[304] J. Hackler, M. Wisniewska, L. Greifenstein-Wiehe, W.B. Minich, M. Cremer, C. Bührer, L. Schomburg, Copper and selenium status as biomarkers of neonatal infections, J. Trace Elem. Med. Biol. 58 (2020) 126437. https://doi.org/10.1016/j.jtemb.2019.126437.

[305] L. Banci, I. Bertini, S. Ciofi-Baffoni, T. Kozyreva, K. Zovo, P. Palumaa, Affinity gradients drive copper to cellular destinations, Nature 465 (2010) 645–648. https://doi.org/10.1038/nature09018.

[306] D.J. Hare, E.J. New, M.D. de Jonge, G. McColl, Imaging metals in biology: balancing sensitivity, selectivity and spatial resolution, Chem. Soc. Rev. 44 (2015) 5941–5958. https://doi.org/10.1039/c5cs00055f.

[307] C.M. Ackerman, S. Lee, C.J. Chang, Analytical Methods for Imaging Metals in Biology: From Transition Metal Metabolism to Transition Metal Signaling, Anal. Chem. 89 (2017) 22–41. https://doi.org/10.1021/acs.analchem.6b04631.

[308] C.M. Ackerman, C.J. Chang, Copper signaling in the brain and beyond, J. Biol. Chem. 293 (2018) 4628–4635. https://doi.org/10.1074/jbc.R117.000176.

[309] V.N. Pham, C.J. Chang, Metalloallostery and Transition Metal Signaling: Bioinorganic Copper Chemistry Beyond Active Sites, Angew. Chem. Int. Ed Engl. 62 (2023) e202213644. https://doi.org/10.1002/anie.202213644.

[310] C.J. Chang, Searching for harmony in transition-metal signaling, Nat. Chem. Biol. 11 (2015) 744–747. https://doi.org/10.1038/nchembio.1913.

[311] M. Schwarz, C.E. Meyer, A. Löser, K. Lossow, J. Hackler, C. Ott, S. Jäger, I. Mohr, E.A. Eklund, A.A.H. Patel, N. Gul, S. Alvarez, I. Altinonder, C. Wiel, M. Maares, H. Haase, A. Härtlova, T. Grune, M.B. Schulze, T. Schwerdtle, U. Merle, H. Zischka, V.I. Sayin, L. Schomburg, A.P. Kipp, Excessive copper impairs intrahepatocyte trafficking and secretion of selenoprotein P, Nat. Commun. 14 (2023) 3479. https://doi.org/10.1038/s41467-023-39245-3.

[312] M. Aschner, C. Palinski, M. Sperling, U. Karst, T. Schwerdtle, J. Bornhorst, Imaging metals in Caenorhabditis elegans, Metallomics 9 (2017) 357–364. https://doi.org/10.1039/c6mt00265j.

[313] M. Porta-de-la-Riva, L. Fontrodona, A. Villanueva, J. Cerón, Basic Caenorhabditis elegans methods: synchronization and observation, J. Vis. Exp. (2012) e4019. https://doi.org/10.3791/4019.

[314] J. Baesler, V. Michaelis, M. Stiboller, H. Haase, M. Aschner, T. Schwerdtle, S.R. Sturzenbaum, J. Bornhorst, Nutritive Manganese and Zinc Overdosing in Aging C. elegans Result in a Metallothionein-Mediated Alteration in Metal Homeostasis, Mol. Nutr. Food Res. 65 (2021) e2001176. https://doi.org/10.1002/mnfr.202001176.

[315] K.J. Livak, T.D. Schmittgen, Analysis of relative gene expression data using real-time quantitative PCR and the 2(-Delta Delta C(T)) Method, Methods 25 (2001) 402–408. https://doi.org/10.1006/meth.2001.1262.

[316] M. Guo, T.-H. Wu, Y.-X. Song, M.-H. Ge, C.-M. Su, W.-P. Niu, L.-L. Li, Z.-J. Xu, C.-L. Ge, M.T.H. Al-Mhanawi, S.-P. Wu, Z.-X. Wu, Reciprocal inhibition between sensory ASH and ASI neurons modulates nociception and avoidance in Caenorhabditis elegans, Nat. Commun. 6 (2015) 5655. https://doi.org/10.1038/ncomms6655.

[317] C.J. Munro, M.A. Nguyen, C. Falgons, S. Chaudhry, M. Olagunjo, A. Bode, C. Bobé, M.E. Portela, M.R. Knecht, K.M. Collins, Identification of Toxicity Effects of Cu2O Materials on C. elegans as a Function of Environmental Ionic Composition, Environ. Sci. Nano 7 (2020) 645–655.

[318] C. Buccitelli, M. Selbach, mRNAs, proteins and the emerging principles of gene expression control, Nat. Rev. Genet. 21 (2020) 630–644. https://doi.org/10.1038/s41576-020-0258-4.

[319] R. Squitti, C. Catalli, L. Gigante, M. Marianetti, M. Rosari, S. Mariani, S. Bucossi, G. Mastromoro, M. Ventriglia, I. Simonelli, V. Tondolo, P. Singh, A. Kumar, A. Pal, M. Rongioletti, Non-Ceruloplasmin Copper Identifies a Subtype of Alzheimer's Disease (CuAD): Characterization of the Cognitive Profile and Case of a CuAD Patient Carrying an RGS7 Stop-Loss Variant, Int. J. Mol. Sci. 24 (2023). https://doi.org/10.3390/ijms24076377.

[320] Z.-D. Li, H. Li, S. Kang, Y.-G. Cui, H. Zheng, P. Wang, K. Han, P. Yu, Y.-Z. Chang, The divergent effects of astrocyte ceruloplasmin on learning and memory function in young and old mice, Cell Death Dis. 13 (2022) 1006. https://doi.org/10.1038/s41419-022-05459-4.

[321] B. Witt, D. Schaumlöffel, T. Schwerdtle, Subcellular Localization of Copper-Cellular Bioimaging with Focus on Neurological Disorders, Int. J. Mol. Sci. 21 (2020). https://doi.org/10.3390/ijms21072341.

[322] I. Hamza, J. Prohaska, J.D. Gitlin, Essential role for Atox1 in the copper-mediated intracellular trafficking of the Menkes ATPase, Proc. Natl. Acad. Sci. U. S. A. 100 (2003) 1215–1220. https://doi.org/10.1073/pnas.0336230100.

[323] A. Muchenditsi, C.C. Talbot, A. Gottlieb, H. Yang, B. Kang, T. Boronina, R. Cole, L. Wang, S. Dev, J.P. Hamilton, S. Lutsenko, Systemic deletion of Atp7b modifies the hepatocytes' response to copper overload in the mouse models of Wilson disease, Sci. Rep. 11 (2021) 5659. https://doi.org/10.1038/s41598-021-84894-3.

[324] H. Miyajima, Aceruloplasminemia, Neuropathology 35 (2015) 83–90. https://doi.org/10.1111/neup.12149.

[325] S. Raia, A. Conti, A. Zanardi, B. Ferrini, G.M. Scotti, E. Gilberti, G. de Palma, S. David, M. Alessio, Ceruloplasmin-Deficient Mice Show Dysregulation of Lipid Metabolism in Liver and Adipose Tissue Reduced by a Protein Replacement, Int. J. Mol. Sci. 24 (2023). https://doi.org/10.3390/ijms24021150.

[326] P.N. Ranganathan, Y. Lu, L. Jiang, C. Kim, J.F. Collins, Serum ceruloplasmin protein expression and activity increases in iron-deficient rats and is further enhanced by higher dietary copper intake, Blood 118 (2011) 3146–3153. https://doi.org/10.1182/blood-2011-05-352112.

[327] J. Kardos, L. Héja, Á. Simon, I. Jablonkai, R. Kovács, K. Jemnitz, Copper signalling: causes and consequences, Cell Commun. Signal. 16 (2018) 71. https://doi.org/10.1186/s12964-018-0277-3.

[328] S.C. Dodani, A. Firl, J. Chan, C.I. Nam, A.T. Aron, C.S. Onak, K.M. Ramos-Torres, J. Paek, C.M. Webster, M.B. Feller, C.J. Chang, Copper is an endogenous modulator of neural circuit spontaneous activity, Proc. Natl. Acad. Sci. U. S. A. 111 (2014) 16280–16285. https://doi.org/10.1073/pnas.1409796111.

[329] C.D. Quarles, M. Macke, B. Michalke, H. Zischka, U. Karst, P. Sullivan, M.P. Field, LC-ICP-MS method for the determination of "extractable copper" in serum, Metallomics 12 (2020) 1348–1355. https://doi.org/10.1039/d0mt00132e.

[330] R. Squitti, P. Faller, C. Hureau, A. Granzotto, A.R. White, K.P. Kepp, Copper Imbalance in Alzheimer's Disease and Its Link with the Amyloid Hypothesis: Towards a Combined Clinical, Chemical, and Genetic Etiology, J. Alzheimers. Dis. 83 (2021) 23–41. https://doi.org/10.3233/JAD-201556.

[331] S. Lee, C.Y.-S. Chung, P. Liu, L. Craciun, Y. Nishikawa, K.J. Bruemmer, I. Hamachi, K. Saijo, E.W. Miller, C.J. Chang, Activity-Based Sensing with a Metal-Directed Acyl Imidazole Strategy Reveals Cell Type-Dependent Pools of Labile Brain Copper, J. Am. Chem. Soc. 142 (2020) 14993–15003. https://doi.org/10.1021/jacs.0c05727.

[332] S. Borchard, S. Raschke, K.M. Zak, C. Eberhagen, C. Einer, E. Weber, S.M. Müller, B. Michalke, J. Lichtmannegger, A. Wieser, T. Rieder, G.M. Popowicz, J. Adamski, M. Klingenspor, A.H. Coles, R. Viana, M.H. Vendelbo, T.D. Sandahl, T. Schwerdtle, T. Plitz, H. Zischka, Bis-choline tetrathiomolybdate prevents copper-induced blood-brain barrier damage, Life Sci. Alliance 5 (2022). https://doi.org/10.26508/lsa.202101164.

[333] S. Yuan, T. Korolnek, B.-E. Kim, Oral Elesclomol Treatment Alleviates Copper Deficiency in Animal Models, Front. Cell Dev. Biol. 10 (2022) 856300. https://doi.org/10.3389/fcell.2022.856300.

[334] J.-C. Müller, J. Lichtmannegger, H. Zischka, M. Sperling, U. Karst, High spatial resolution LA-ICP-MS demonstrates massive liver copper depletion in Wilson disease rats upon Methanobactin treatment, J. Trace Elem. Med. Biol. 49 (2018) 119–127. https://doi.org/10.1016/j.jtemb.2018.05.009.

[335] D.C. Brady, M.S. Crowe, M.L. Turski, G.A. Hobbs, X. Yao, A. Chaikuad, S. Knapp, K. Xiao, S.L. Campbell, D.J. Thiele, C.M. Counter, Copper is required for oncogenic BRAF signalling and tumorigenesis, Nature 509 (2014) 492–496. https://doi.org/10.1038/nature13180.

[336] L. Mezzaroba, D.F. Alfieri, A.N. Colado Simão, E.M. Vissoci Reiche, The role of zinc, copper, manganese and iron in neurodegenerative diseases, Neurotoxicology 74 (2019) 230–241. https://doi.org/10.1016/j.neuro.2019.07.007.

[337] L. Tapia, M. González-Agüero, M.F. Cisternas, M. Suazo, V. Cambiazo, R. Uauy, M. González, Metallothionein is crucial for safe intracellular copper storage and cell survival at normal and supra-physiological exposure levels, Biochem. J. 378 (2004) 617–624. https://doi.org/10.1042/BJ20031174.

[338] N. Polak, D.S. Read, K. Jurkschat, M. Matzke, F.J. Kelly, D.J. Spurgeon, S.R. Stürzenbaum, Metalloproteins and phytochelatin synthase may confer protection against zinc oxide nanoparticle induced toxicity in Caenorhabditis elegans, Comp. Biochem. Physiol. C. Toxicol. Pharmacol. 160 (2014) 75–85. https://doi.org/10.1016/j.cbpc.2013.12.001.

[339] S.L. Hughes, J.G. Bundy, E.J. Want, P. Kille, S.R. Stürzenbaum, The metabolomic responses of Caenorhabditis elegans to cadmium are largely independent of metallothionein status, but dominated by changes in cystathionine and phytochelatins, J. Proteome Res. 8 (2009) 3512–3519. https://doi.org/10.1021/pr9001806.

[340] S. Zeitoun-Ghandour, J.M. Charnock, M.E. Hodson, O.I. Leszczyszyn, C.A. Blindauer, S.R. Stürzenbaum, The two Caenorhabditis elegans metallothioneins (CeMT-1 and CeMT-2) discriminate between essential zinc and toxic cadmium, FEBS J. 277 (2010) 2531–2542. https://doi.org/10.1111/j.1742-4658.2010.07667.x.

[341] V. Michaelis, L. Aengenheister, M. Tuchtenhagen, J. Rinklebe, F. Ebert, T. Schwerdtle, T. Buerki-Thurnherr, J. Bornhorst, Differences and Interactions in Placental Manganese and Iron Transfer across an In Vitro Model of Human Villous Trophoblasts, Int. J. Mol. Sci. 23 (2022). https://doi.org/10.3390/ijms23063296.

[342] A. Petro, H.G. Sexton, C. Miranda, A. Rastogi, J.H. Freedman, E.D. Levin, Persisting neurobehavioral effects of developmental copper exposure in wildtype and metallothionein 1 and 2 knockout mice, BMC Pharmacol. Toxicol. 17 (2016) 55. https://doi.org/10.1186/s40360-016-0096-3.

[343] G. Tassone, A. Kola, D. Valensin, C. Pozzi, Dynamic Interplay between Copper Toxicity and Mitochondrial Dysfunction in Alzheimer's Disease, Life (Basel) 11 (2021). https://doi.org/10.3390/life11050386.

[344] V.F. Monteiro-Cardoso, M.M. Oliveira, T. Melo, M.R.M. Domingues, P.I. Moreira, E. Ferreiro, F. Peixoto, R.A. Videira, Cardiolipin profile changes are associated to the early synaptic mitochondrial dysfunction in Alzheimer's disease, J. Alzheimers. Dis. 43 (2015) 1375–1392. https://doi.org/10.3233/JAD-141002.

[345] I.L. Yurkova, J. Arnhold, G. Fitzl, D. Huster, Fragmentation of mitochondrial cardiolipin by copper ions in the Atp7b-/- mouse model of Wilson's disease, Chem. Phys. Lipids 164 (2011) 393–400. https://doi.org/10.1016/j.chemphyslip.2011.05.006.

[346] V.K. Wandt, N. Winkelbeiner, J. Bornhorst, B. Witt, S. Raschke, L. Simon, F. Ebert, A.P. Kipp, T. Schwerdtle, A matter of concern - Trace element dyshomeostasis and genomic stability in neurons, Redox Biol. 41 (2021) 101877. https://doi.org/10.1016/j.redox.2021.101877.

[347] J. Bornhorst, F. Ebert, H. Lohren, H.-U. Humpf, U. Karst, T. Schwerdtle, Effects of manganese and arsenic species on the level of energy related nucleotides in human cells, Metallomics 4 (2012) 297–306. https://doi.org/10.1039/c2mt00164k.

[348] K. Grintzalis, D. Zisimopoulos, T. Grune, D. Weber, C.D. Georgiou, Method for the simultaneous determination of free/protein malondialdehyde and lipid/protein hydroperoxides, Free Radic. Biol. Med. 59 (2013) 27–35. https://doi.org/10.1016/j.freeradbiomed.2012.09.038.

[349] M.M. Nicolai, A.-K. Weishaupt, J. Baesler, V. Brinkmann, A. Wellenberg, N. Winkelbeiner, A. Gremme, M. Aschner, G. Fritz, T. Schwerdtle, J. Bornhorst, Effects of Manganese on Genomic Integrity in the Multicellular Model Organism Caenorhabditis elegans, Int. J. Mol. Sci. 22 (2021). https://doi.org/10.3390/ijms222010905.

[350] M.P. Ceballos, J.P. Parody, A.D. Quiroga, M.L. Casella, D.E. Francés, M.C. Larocca, C.E. Carnovale, M.d.L. Alvarez, M.C. Carrillo, FoxO3a nuclear localization and its association with β-catenin and Smads in IFN-α-treated hepatocellular carcinoma cell lines, J. Interferon Cytokine Res. 34 (2014) 858–869. https://doi.org/10.1089/jir.2013.0124.

[351] A.R. Poetsch, The genomics of oxidative DNA damage, repair, and resulting mutagenesis, Comput. Struct. Biotechnol. J. 18 (2020) 207–219. https://doi.org/10.1016/j.csbj.2019.12.013.

[352] A.-K. Weishaupt, L. Kubens, L. Ruecker, T. Schwerdtle, M. Aschner, J. Bornhorst, A Reliable Method Based on Liquid Chromatography–Tandem Mass Spectrometry for the Simultaneous Quantification of Neurotransmitters in Caenorhabditis elegans, Molecules 28 (2023) 5373. https://doi.org/10.3390/molecules28145373.

[353] T.V. Peres, L.P. Arantes, M.R. Miah, J. Bornhorst, T. Schwerdtle, A.B. Bowman, R.B. Leal, M. Aschner, Role of Caenorhabditis elegans AKT-1/2 and SGK-1 in Manganese Toxicity, Neurotox. Res. 34 (2018) 584–596. https://doi.org/10.1007/s12640-018-9915-1.

[354] I. Hamann, K. Petroll, L. Grimm, A. Hartwig, L.-O. Klotz, Insulin-like modulation of Akt/FoxO signaling by copper ions is independent of insulin receptor, Arch. Biochem. Biophys. 558 (2014) 42–50. https://doi.org/10.1016/j.abb.2014.06.004.

[355] P. Gubert, B. Puntel, T. Lehmen, J. Bornhorst, D.S. Avila, M. Aschner, F.A.A. Soares, Reversible reprotoxic effects of manganese through DAF-16 transcription factor activation and vitellogenin downregulation in Caenorhabditis elegans, Life Sci. 151 (2016) 218–223. https://doi.org/10.1016/j.lfs.2016.03.016.

[356] N. Urban, D. Tsitsipatis, F. Hausig, K. Kreuzer, K. Erler, V. Stein, M. Ristow, H. Steinbrenner, L.-O. Klotz, Non-linear impact of glutathione depletion on C. elegans life span and stress resistance, Redox Biol. 11 (2017) 502–515. https://doi.org/10.1016/j.redox.2016.12.003.

[357] S. Wang, L. Wu, Y. Wang, X. Luo, Y. Lu, Copper-induced germline apoptosis in Caenorhabditis elegans: the independent roles of DNA damage response signaling and the dependent roles of MAPK cascades, Chem. Biol. Interact. 180 (2009) 151–157. https://doi.org/10.1016/j.cbi.2009.03.012.

[358] R. Franco, O.J. Schoneveld, A. Pappa, M.I. Panayiotidis, The central role of glutathione in the pathophysiology of human diseases, Arch. Physiol. Biochem. 113 (2007) 234–258. https://doi.org/10.1080/13813450701661198.

[359] C. Cui, M. Kong, Y. Wang, C. Zhou, H. Ming, Characterization of polyphosphate kinases for the synthesis of GSH with ATP regeneration from AMP, Enzyme Microb. Technol. 149 (2021) 109853. https://doi.org/10.1016/j.enzmictec.2021.109853.

[360] T. Croft, P. Venkatakrishnan, S.-J. Lin, NAD+ Metabolism and Regulation: Lessons From Yeast, Biomolecules 10 (2020). https://doi.org/10.3390/biom10020330.

[361] C. James Theoga Raj, T. Croft, P. Venkatakrishnan, B. Groth, G. Dhugga, T. Cater, S.-J. Lin, The copper-sensing transcription factor Mac1, the histone deacetylase Hst1, and nicotinic acid regulate de novo NAD+ biosynthesis in budding yeast, J. Biol. Chem. 294 (2019) 5562–5575. https://doi.org/10.1074/jbc.RA118.006987.

[362] M. Li, Y. Li, J. Chen, W. Wei, X. Pan, J. Liu, Q. Liu, W. Leu, L. Zhang, X. Yang, J. Lu, K. Wang, Copper ions inhibit S-adenosylhomocysteine hydrolase by causing dissociation of NAD+ cofactor, Biochemistry 46 (2007) 11451–11458. https://doi.org/10.1021/bi700395d.

[363] S.O. Anadozie, A.U. Aduma, O.B. Adewale, Alkaloid-rich extract of Buchholzia coriacea seed mitigate the effect of copper-induced toxicity in Drosophila melanogaster, Vegetos (2023). https://doi.org/10.1007/s42535-023-00760-9.

[364] M. Rehman, Z. Maqbool, D. Peng, L. Liu, Morpho-physiological traits, antioxidant capacity and phytoextraction of copper by ramie (Boehmeria nivea L.) grown as fodder in copper-contaminated soil, Environ. Sci. Pollut. Res. Int. 26 (2019) 5851–5861. https://doi.org/10.1007/s11356-018-4015-6.

[365] P.O. Helmer, M.M. Nicolai, V. Schwantes, J. Bornhorst, H. Hayen, Investigation of cardiolipin oxidation products as a new endpoint for oxidative stress in C. elegans by means of online two-dimensional liquid chromatography and high-resolution mass spectrometry, Free Radic. Biol. Med. 162 (2021) 216–224. https://doi.org/10.1016/j.freeradbiomed.2020.10.019.

[366] B. Blume, V. Schwantes, M. Witting, H. Hayen, P. Schmitt-Kopplin, P.O. Helmer, B. Michalke, Lipidomic and Metallomic Alteration of Caenorhabditis elegans after Acute and Chronic Manganese, Iron, and Zinc Exposure with a Link to Neurodegenerative Disorders, J. Proteome Res. 22 (2023) 837–850. https://doi.org/10.1021/acs.jproteome.2c00578.

[367] S. Pope, J.M. Land, S.J.R. Heales, Oxidative stress and mitochondrial dysfunction in neurodegeneration; cardiolipin a critical target?, Biochim. Biophys. Acta 1777 (2008) 794–799. https://doi.org/10.1016/j.bbabio.2008.03.011.

[368] T. Schwerdtle, I. Hamann, G. Jahnke, I. Walter, C. Richter, J.L. Parsons, G.L. Dianov, A. Hartwig, Impact of copper on the induction and repair of oxidative DNA damage, poly(ADP-ribosyl)ation and PARP-1 activity, Mol. Nutr. Food Res. 51 (2007) 201–210. https://doi.org/10.1002/mnfr.200600107.

[369] O. Karginova, C.M. Weekley, A. Raoul, A. Alsayed, T. Wu, S.S.-Y. Lee, C. He, O.I. Olopade, Inhibition of Copper Transport Induces Apoptosis in Triple-Negative Breast Cancer Cells and Suppresses Tumor Angiogenesis, Mol. Cancer Ther. 18 (2019) 873–885. https://doi.org/10.1158/1535-7163.MCT-18-0667.

[370] J. Jin, M. Ma, S. Shi, J. Wang, P. Xiao, H.-F. Yu, C. Zhang, Q. Guo, Z. Yu, Z. Lou, C.-B. Teng, Copper enhances genotoxic drug resistance via ATOX1 activated DNA damage repair, Cancer Lett. 536 (2022) 215651. https://doi.org/10.1016/j.canlet.2022.215651.

[371] O.J. Becherel, B. Jakob, A.L. Cherry, N. Gueven, M. Fusser, A.W. Kijas, C. Peng, S. Katyal, P.J. McKinnon, J. Chen, B. Epe, S.J. Smerdon, G. Taucher-Scholz, M.F. Lavin, CK2 phosphorylation-dependent interaction between aprataxin and MDC1 in the DNA damage response, Nucleic Acids Res. 38 (2010) 1489–1503. https://doi.org/10.1093/nar/gkp1149.

[372] J.L. Harris, B. Jakob, G. Taucher-Scholz, G.L. Dianov, O.J. Becherel, M.F. Lavin, Aprataxin, poly-ADP ribose polymerase 1 (PARP-1) and apurinic endonuclease 1 (APE1) function together to protect the genome against oxidative damage, Hum. Mol. Genet. 18 (2009) 4102–4117. https://doi.org/10.1093/hmg/ddp359.

[373] M.L. Hegde, P.M. Hegde, L.M.F. Holthauzen, T.K. Hazra, K.S.J. Rao, S. Mitra, Specific Inhibition of NEIL-initiated repair of oxidized base damage in human genome by copper and iron: potential etiological linkage to neurodegenerative diseases, J. Biol. Chem. 285 (2010) 28812–28825. https://doi.org/10.1074/jbc.M110.126664.

[374] A.N. Minniti, D.L. Rebolledo, P.M. Grez, R. Fadic, R. Aldunate, I. Volitakis, R.A. Cherny, C. Opazo, C. Masters, A.I. Bush, N.C. Inestrosa, Intracellular amyloid formation in muscle cells of Abeta-transgenic Caenorhabditis elegans: determinants and physiological role in copper detoxification, Mol. Neurodegener. 4 (2009) 2. https://doi.org/10.1186/1750-1326-4-2.

[375] A. Metaxas, Imbalances in Copper or Zinc Concentrations Trigger Further Trace Metal Dyshomeostasis in Amyloid-Beta Producing Caenorhabditis elegans, Front. Neurosci. 15 (2021) 755475. https://doi.org/10.3389/fnins.2021.755475.

[376] N.S. Dabbish, D.M. Raizen, GABAergic synaptic plasticity during a developmentally regulated sleep-like state in C. elegans, J. Neurosci. 31 (2011) 15932–15943. https://doi.org/10.1523/JNEUROSCI.0742-11.2011.

[377] N. D'Ambrosi, L. Rossi, Copper at synapse: Release, binding and modulation of neurotransmission, Neurochem. Int. 90 (2015) 36–45. https://doi.org/10.1016/j.neuint.2015.07.006.

[378] I. Horvath, S. Blockhuys, D. Šulskis, S. Holgersson, R. Kumar, B.M. Burmann, P. Wittung-Stafshede, Interaction between Copper Chaperone Atox1 and Parkinson's Disease Protein α-Synuclein Includes Metal-Binding Sites and Occurs in Living Cells, ACS Chem. Neurosci. 10 (2019) 4659–4668. https://doi.org/10.1021/acschemneuro.9b00476.

[379] T.M. Dawson, V.L. Dawson, The role of parkin in familial and sporadic Parkinson's disease, Mov. Disord. 25 Suppl 1 (2010) S32-9. https://doi.org/10.1002/mds.22798.

[380] Z.D. Zhou, L.X. Yi, D.Q. Wang, T.M. Lim, E.K. Tan, Role of dopamine in the pathophysiology of Parkinson's disease, Transl. Neurodegener. 12 (2023) 44. https://doi.org/10.1186/s40035-023-00378-6.

[381] I. Kamienieva, J. Duszyński, J. Szczepanowska, Multitasking guardian of mitochondrial quality: Parkin function and Parkinson's disease, Transl. Neurodegener. 10 (2021) 5. https://doi.org/10.1186/s40035-020-00229-8.

[382] C. Ren, Y. Ding, S. Wei, L. Guan, C. Zhang, Y. Ji, F. Wang, S. Yin, P. Yin, G2019S Variation in LRRK2: An Ideal Model for the Study of Parkinson's Disease?, Front. Hum. Neurosci. 13 (2019) 306. https://doi.org/10.3389/fnhum.2019.00306.

[383] J.H. Lee, J.-H. Han, H. Kim, S.M. Park, E.-H. Joe, I. Jou, Parkinson's disease-associated LRRK2-G2019S mutant acts through regulation of SERCA activity to control ER stress in astrocytes, Acta Neuropathol. Commun. 7 (2019) 68. https://doi.org/10.1186/s40478-019-0716-4.

[384] M. Nguyen, D. Krainc, LRRK2 phosphorylation of auxilin mediates synaptic defects in dopaminergic neurons from patients with Parkinson's disease, Proc. Natl. Acad. Sci. U. S. A. 115 (2018) 5576–5581. https://doi.org/10.1073/pnas.1717590115.

[385] S. Kar, S.P. Slowikowski, D. Westaway, H.T. Mount, Interactions between β-amyloid and central cholinergic neurons: implications for Alzheimer's disease, J. Psychiatry Neurosci. 29 (2004) 427–441.

[386] M.P. Murphy, H. LeVine, Alzheimer's disease and the amyloid-beta peptide, J. Alzheimers. Dis. 19 (2010) 311–323. https://doi.org/10.3233/JAD-2010-1221.

[387] P. Carrillo-Mora, R. Luna, L. Colín-Barenque, Amyloid beta: multiple mechanisms of toxicity and only some protective effects?, Oxid. Med. Cell. Longev. 2014 (2014) 795375. https://doi.org/10.1155/2014/795375.

[388] S. Genoud, B.R. Roberts, A.P. Gunn, G.M. Halliday, S.J.G. Lewis, H.J. Ball, D.J. Hare, K.L. Double, Subcellular compartmentalisation of copper, iron, manganese, and zinc in the Parkinson's disease brain, Metallomics 9 (2017) 1447–1455. https://doi.org/10.1039/c7mt00244k.

[389] B.A. Veldman, A.M. Wijn, N. Knoers, P. Praamstra, M.W. Horstink, Genetic and environmental risk factors in Parkinson's disease, Clin. Neurol. Neurosurg. 100 (1998) 15–26. https://doi.org/10.1016/s0303-8467(98)00009-2.

[390] A.-K. Weishaupt, K. Lamann, E. Tallarek, A.T. Pezacki, C.D. Matier, T. Schwerdtle, M. Aschner, C.J. Chang, S.R. Stürzenbaum, J. Bornhorst, 2024. Dysfunction in atox-1 and ceruloplasmin alters labile Cu levels and consequently Cu homeostasis in C. elegans. Front. Mol. Biosci. 11, 1354627. https://doi.org/10.3389/fmolb.2024.1354627.

[391] H.W. Ejaz, W. Wang, M. Lang, Copper Toxicity Links to Pathogenesis of Alzheimer's Disease and Therapeutics Approaches, Int. J. Mol. Sci. 21 (2020). https://doi.org/10.3390/ijms21207660.

[392] S.K. Singh, V. Balendra, A.A. Obaid, J. Esposto, M.A. Tikhonova, N.K. Gautam, B. Poeggeler, Copper-mediated β-amyloid toxicity and its chelation therapy in Alzheimer's disease, Metallomics 14 (2022). https://doi.org/10.1093/mtomcs/mfac018.

[393] S. Meftah, J. Gan, Alzheimer's disease as a synaptopathy: Evidence for dysfunction of synapses during disease progression, Front. Synaptic Neurosci. 15 (2023) 1129036. https://doi.org/10.3389/fnsyn.2023.1129036.

[394] S. Lutsenko, C. Washington-Hughes, M. Ralle, K. Schmidt, Copper and the brain noradrenergic system, J. Biol. Inorg. Chem. 24 (2019) 1179–1188. https://doi.org/10.1007/s00775-019-01737-3.

[395] A.L. Luz, J.P. Rooney, L.L. Kubik, C.P. Gonzalez, D.H. Song, J.N. Meyer, Mitochondrial Morphology and Fundamental Parameters of the Mitochondrial Respiratory Chain Are Altered in Caenorhabditis elegans Strains Deficient in Mitochondrial Dynamics and Homeostasis Processes, PLoS One 10 (2015) e0130940. https://doi.org/10.1371/journal.pone.0130940.

[396] S. Noda, S. Sato, T. Fukuda, N. Tada, Y. Uchiyama, K. Tanaka, N. Hattori, Loss of Parkin contributes to mitochondrial turnover and dopaminergic neuronal loss in aged mice, Neurobiol. Dis. 136 (2020) 104717. https://doi.org/10.1016/j.nbd.2019.104717.

[397] K. Palikaras, E. Lionaki, N. Tavernarakis, Coordination of mitophagy and mitochondrial biogenesis during ageing in C. elegans, Nature 521 (2015) 525–528. https://doi.org/10.1038/nature14300.

[398] J. Pallos, S. Jeng, S. McWeeney, I. Martin, Dopamine neuron-specific LRRK2 G2019S effects on gene expression revealed by translatome profiling, Neurobiol. Dis. 155 (2021) 105390. https://doi.org/10.1016/j.nbd.2021.105390.

[399] Z.D. Zhou, W.T. Saw, P.G.H. Ho, Z.W. Zhang, L. Zeng, Y.Y. Chang, A.X.Y. Sun, D.R. Ma, H.Y. Wang, L. Zhou, K.L. Lim, E.-K. Tan, The role of tyrosine hydroxylase-dopamine pathway in Parkinson's disease pathogenesis, Cell. Mol. Life Sci. 79 (2022) 599. https://doi.org/10.1007/s00018-022-04574-x.

[400] A. Tozzi, M. Tantucci, S. Marchi, P. Mazzocchetti, M. Morari, P. Pinton, A. Mancini, P. Calabresi, Dopamine D2 receptor-mediated neuroprotection in a G2019S Lrrk2 genetic model of Parkinson's disease, Cell Death Dis. 9 (2018) 204. https://doi.org/10.1038/s41419-017-0221-2.

[401] F. Longo, D. Mercatelli, S. Novello, L. Arcuri, A. Brugnoli, F. Vincenzi, I. Russo, G. Berti, O.S. Mabrouk, R.T. Kennedy, D.R. Shimshek, K. Varani, L. Bubacco, E. Greggio, M. Morari, Age-dependent dopamine transporter dysfunction and Serine129 phospho-α-synuclein overload in G2019S LRRK2 mice, Acta Neuropathol. Commun. 5 (2017) 22. https://doi.org/10.1186/s40478-017-0426-8.

[402] H. Kim, H.J. Park, H. Choi, Y. Chang, H. Park, J. Shin, J. Kim, C.J. Lengner, Y.K. Lee, J. Kim, Modeling G2019S-LRRK2 Sporadic Parkinson's Disease in 3D Midbrain Organoids, Stem Cell Reports 12 (2019) 518–531. https://doi.org/10.1016/j.stemcr.2019.01.020.

[403] K. Melnikov, S. Kucharíková, Z. Bárdyová, N. Botek, A. Kaiglová, Applications of a powerful model organism Caenorhabditis elegans to study the neurotoxicity induced by heavy metals and pesticides, Physiol. Res. 72 (2023) 149–166. https://doi.org/10.33549/physiolres.934977.

[404] D. Avila, K. Helmcke, M. Aschner, The Caenorhabiditis elegans model as a reliable tool in neurotoxicology, Hum. Exp. Toxicol. 31 (2012) 236–243. https://doi.org/10.1177/0960327110392084.

[405] S.R. Sammi, L.E. Jameson, K.D. Conrow, M.C.K. Leung, J.R. Cannon, Caenorhabditis elegans Neurotoxicity Testing: Novel Applications in the Adverse Outcome Pathway Framework, Front. Toxicol. 4 (2022) 826488. https://doi.org/10.3389/ftox.2022.826488.

[406] O.M. Ijomone, M.R. Miah, T.V. Peres, P.U. Nwoha, M. Aschner, Null allele mutants of trt-1, the catalytic subunit of telomerase in Caenorhabditis elegans, are less sensitive to Mn-induced toxicity and DAergic degeneration, Neurotoxicology 57 (2016) 54–60. https://doi.org/10.1016/j.neuro.2016.08.016.

[407] S.M. Murray, B.M. Waddell, C.-W. Wu, Neuron-specific toxicity of chronic acrylamide exposure in C. elegans, Neurotoxicol. Teratol. 77 (2020) 106848. https://doi.org/10.1016/j.ntt.2019.106848.

[408] M.V. Soares, M.F. Charão, M.T. Jacques, A.L.A. Dos Santos, C. Luchese, S. Pinton, D.S. Ávila, Airborne toluene exposure causes germline apoptosis and neuronal damage that promotes neurobehavioural changes in Caenorhabditis elegans, Environ. Pollut. 256 (2020) 113406. https://doi.org/10.1016/j.envpol.2019.113406.

[409] C. Bessa, P. Maciel, A.J. Rodrigues, Using C. elegans to decipher the cellular and molecular mechanisms underlying neurodevelopmental disorders, Mol. Neurobiol. 48 (2013) 465–489. https://doi.org/10.1007/s12035-013-8434-6.

[410] R.J.P. Custodio, Z. Hobloss, M. Myllys, R. Hassan, D. González, J. Reinders, J. Bornhorst, A.-K. Weishaupt, A.-L. Seddek, T. Abbas, A. Friebel, S. Hoehme, S. Getzmann, J.G. Hengstler, C. van Thriel, A. Ghallab, Cognitive Functions, Neurotransmitter Alterations, and Hippocampal Microstructural Changes in Mice Caused by Feeding on Western Diet, Cells 12 (2023). https://doi.org/10.3390/cells12182331.

[411] O.M. Ijomone, A.-K. Weishaupt, V. Michaelis, O.K. Ijomone, J. Bornhorst, p38- and ERK-MAPK Signalling Modulate Developmental Neurotoxicity of Nickel and Vanadium in the Caenorhabditis elegans Model, Kinases and Phosphatases 2 (2024) 28–42. https://doi.org/10.3390/kinasesphosphatases2010003.

[412] R.T. Wragg, V. Hapiak, S.B. Miller, G.P. Harris, J. Gray, P.R. Komuniecki, R.W. Komuniecki, Tyramine and octopamine independently inhibit serotonin-stimulated aversive behaviors in Caenorhabditis elegans through two novel amine receptors, J. Neurosci. 27 (2007) 13402–13412. https://doi.org/10.1523/JNEUROSCI.3495-07.2007.

[413] E.Z. Poh, D. Hahne, J. Moretti, A.R. Harvey, M.W. Clarke, J. Rodger, Simultaneous quantification of dopamine, serotonin, their metabolites and amino acids by LC-MS/MS in mouse brain following repetitive transcranial magnetic stimulation, Neurochem. Int. 131 (2019) 104546. https://doi.org/10.1016/j.neuint.2019.104546.

[414] P. Pu, W. Le, Dopamine neuron degeneration induced by MPP+ is independent of CED-4 pathway in Caenorhabditis elegans, Cell Res. 18 (2008) 978–981. https://doi.org/10.1038/cr.2008.279.

[415] E. Braungart, M. Gerlach, P. Riederer, R. Baumeister, M.C. Hoener, Caenorhabditis elegans MPP+ model of Parkinson's disease for high-throughput drug screenings, Neurodegener. Dis. 1 (2004) 175–183. https://doi.org/10.1159/000080983.

[416] K.D. Harris, M. Weiss, A. Zahavi, Why are neurotransmitters neurotoxic? An evolutionary perspective, F1000Res. 3 (2014) 179. https://doi.org/10.12688/f1000research.4828.2.

[417] A. Iqubal, M. Ahmed, S. Ahmad, C.R. Sahoo, M.K. Iqubal, S.E. Haque, Environmental neurotoxic pollutants: review, Environ. Sci. Pollut. Res. Int. 27 (2020) 41175–41198. https://doi.org/10.1007/s11356-020-10539-z.

[418] N.R.C. Staff, Environmental Neurotoxicology, National Academies Press, 1992.

[419] C.Y.-S. Chung, J.M. Posimo, S. Lee, T. Tsang, J.M. Davis, D.C. Brady, C.J. Chang, Activity-based ratiometric FRET probe reveals oncogene-driven changes in labile copper pools induced by altered glutathione metabolism, Proc. Natl. Acad. Sci. U. S. A. 116 (2019) 18285–18294. https://doi.org/10.1073/pnas.1904610116.

[420] K. Takahashi, T. Yamagishi, S. Aoyagi, D. Aoki, K. Fukushima, Y. Kimura, 2018. Principal component analysis image fusion of TOF-SIMS and microscopic images and low intensity secondary ion enhancement by pixel reduction. Journal of Vacuum Science & Technology B, Nanotechnology and Microelectronics: Materials, Processing, Measurement, and Phenomena 36, 03F113. https://doi.org/10.1116/1.5013218.

[421] F.M. Geier, S. Fearn, J.G. Bundy, D.S. McPhail, ToF-SIMS analysis of biomolecules in the model organism Caenorhabditis elegans, Surface & Interface Analysis 45 (2013) 234–236. https://doi.org/10.1002/sia.5110.

[422] M.E. Johnson, J. Bennett, A.R. Montoro Bustos, S.K. Hanna, A. Kolmakov, N. Sharp, E.J. Petersen, P.E. Lapasset, C.M. Sims, K.E. Murphy, B.C. Nelson, Combining secondary ion mass spectrometry image depth profiling and single particle inductively coupled plasma mass spectrometry to investigate the uptake and biodistribution of gold nanoparticles in Caenorhabditis elegans, Anal. Chim. Acta 1175 (2021) 338671. https://doi.org/10.1016/j.aca.2021.338671.

[423] C. Grovenor, K.E. Smart, M.R. Kilburn, B. Shore, J.R. Dilworth, B. Martin, C. Hawes, R. Rickaby, Specimen preparation for NanoSIMS analysis of biological materials, Applied Surface Science 252 (2006) 6917–6924. https://doi.org/10.1016/j.apsusc.2006.02.180.

[424] E. Cho, J.-J. Hwang, S.-H. Han, S.J. Chung, J.-Y. Koh, J.-Y. Lee, Endogenous zinc mediates apoptotic programmed cell death in the developing brain, Neurotox. Res. 17 (2010) 156–166. https://doi.org/10.1007/s12640-009-9085-2.

[425] A.L. Luz, T.R. Godebo, L.L. Smith, T.C. Leuthner, L.L. Maurer, J.N. Meyer, Deficiencies in mitochondrial dynamics sensitize Caenorhabditis elegans to arsenite and other mitochondrial toxicants by reducing mitochondrial adaptability, Toxicology 387 (2017) 81–94. https://doi.org/10.1016/j.tox.2017.05.018.

[426] E.-B. Kayser, P.G. Morgan, M.M. Sedensky, Mitochondrial complex I function affects halothane sensitivity in Caenorhabditis elegans, Anesthesiology 101 (2004) 365–372. https://doi.org/10.1097/00000542-200408000-00017.

[427] T.A. Egelhofer, A. Minoda, S. Klugman, K. Lee, P. Kolasinska-Zwierz, A.A. Alekseyenko, M.-S. Cheung, D.S. Day, S. Gadel, A.A. Gorchakov, T. Gu, P.V. Kharchenko, S. Kuan, I. Latorre, D. Linder-Basso, Y. Luu, Q. Ngo, M. Perry, A. Rechtsteiner, N.C. Riddle, Y.B. Schwartz, G.A. Shanower, A. Vielle, J. Ahringer, S.C.R. Elgin, M.I. Kuroda, V. Pirrotta, B. Ren, S. Strome, P.J. Park, G.H. Karpen, R.D. Hawkins, J.D. Lieb, An assessment of histone-modification antibody quality, Nat. Struct. Mol. Biol. 18 (2011) 91–93. https://doi.org/10.1038/nsmb.1972.

[428] J.E. Gilda, R. Ghosh, J.X. Cheah, T.M. West, S.C. Bodine, A.V. Gomes, Western Blotting Inaccuracies with Unverified Antibodies: Need for a Western Blotting Minimal Reporting Standard (WBMRS), PLoS One 10 (2015) e0135392. https://doi.org/10.1371/journal.pone.0135392.

[429] M. Blumenberg, Introductory Chapter: Transcriptome Analysis, in: M. Blumenberg (Ed.), Transcriptome Analysis, IntechOpen, 2019.

[430] M.M. Nicolai, M. Pirritano, G. Gasparoni, M. Aschner, M. Simon, J. Bornhorst, Manganese-Induced Toxicity in C. elegans: What Can We Learn from the Transcriptome?, Int. J. Mol. Sci. 23 (2022). https://doi.org/10.3390/ijms231810748.

[431] D. Patel, S.N. Witt, Ethanolamine and Phosphatidylethanolamine: Partners in Health and Disease, Oxid. Med. Cell. Longev. 2017 (2017) 4829180. https://doi.org/10.1155/2017/4829180.

[432] T. Fraser, H. Tayler, S. Love, Fatty acid composition of frontal, temporal and parietal neocortex in the normal human brain and in Alzheimer's disease, Neurochem. Res. 35 (2010) 503–513. https://doi.org/10.1007/s11064-009-0087-5.

[433] A. Kikuchi, A. Takeda, H. Onodera, T. Kimpara, K. Hisanaga, N. Sato, A. Nunomura, R.J. Castellani, G. Perry, M.A. Smith, Y. Itoyama, Systemic increase of oxidative nucleic acid damage in Parkinson's disease and multiple system atrophy, Neurobiol. Dis. 9 (2002) 244–248. https://doi.org/10.1006/nbdi.2002.0466.

[434] M.M. Nicolai, B. Witt, A. Hartwig, T. Schwerdtle, J. Bornhorst, A fast and reliable method for monitoring genomic instability in the model organism Caenorhabditis elegans, Arch. Toxicol. 95 (2021) 3417–3424. https://doi.org/10.1007/s00204-021-03144-7.

[435] C. Guo, L. Sun, X. Chen, D. Zhang, Oxidative stress, mitochondrial damage and neurodegenerative diseases, Neural Regen. Res. 8 (2013) 2003–2014. https://doi.org/10.3969/j.issn.1673-5374.2013.21.009.

[436] A.L. Luz, L.L. Smith, J.P. Rooney, J.N. Meyer, Seahorse Xfe 24 Extracellular Flux Analyzer-Based Analysis of Cellular Respiration in Caenorhabditis elegans, Curr. Protoc. Toxicol. 66 (2015) 25.7.1-25.7.15. https://doi.org/10.1002/0471140856.tx2507s66.

[437] J.P. Rooney, I.T. Ryde, L.H. Sanders, E.H. Howlett, M.D. Colton, K.E. Germ, G.D. Mayer, J.T. Greenamyre, J.N. Meyer, PCR based determination of mitochondrial DNA copy number in multiple species, Methods Mol. Biol. 1241 (2015) 23–38. https://doi.org/10.1007/978-1-4939-1875-1_3.

[438] Y.-C. Wu, X. Wang, D. Xue, Methods for studying programmed cell death in C. elegans, Methods Cell Biol. 107 (2012) 295–320. https://doi.org/10.1016/B978-0-12-394620-1.00010-2.

[439] Z. Zhou, E. Hartwieg, H.R. Horvitz, CED-1 is a transmembrane receptor that mediates cell corpse engulfment in C. elegans, Cell 104 (2001) 43–56. https://doi.org/10.1016/s0092-8674(01)00190-8.

[440] S. Hashimoto, Y. Matsuba, M. Takahashi, N. Kamano, N. Watamura, H. Sasaguri, Y. Takado, Y. Yoshihara, T. Saito, T.C. Saido, Neuronal glutathione loss leads to neurodegeneration involving gasdermin activation, Sci. Rep. 13 (2023) 1109. https://doi.org/10.1038/s41598-023-27653-w.

[441] I.Y. Iskusnykh, A.A. Zakharova, D. Pathak, Glutathione in Brain Disorders and Aging, Molecules 27 (2022). https://doi.org/10.3390/molecules27010324.

[442] T. Kreko-Pierce, J.R. Pugh, Altered Synaptic Transmission and Excitability of Cerebellar Nuclear Neurons in a Mouse Model of Duchenne Muscular Dystrophy, Front. Cell. Neurosci. 16 (2022) 926518. https://doi.org/10.3389/fncel.2022.926518.

[443] H.-C. Lu, A.A. Mills, Di Tian, Altered synaptic transmission and maturation of hippocampal CA1 neurons in a mouse model of human chr16p11.2 microdeletion, J. Neurophysiol. 119 (2018) 1005–1018. https://doi.org/10.1152/jn.00306.2017.

[444] L.M. Sayre, G. Perry, M.A. Smith, Oxidative stress and neurotoxicity, Chem. Res. Toxicol. 21 (2008) 172–188. https://doi.org/10.1021/tx700210j.

[445] J. Alvarez, P. Alvarez-Illera, J. Santo-Domingo, R.I. Fonteriz, M. Montero, Modeling Alzheimer's Disease in Caenorhabditis elegans, Biomedicines 10 (2022). https://doi.org/10.3390/biomedicines10020288.

[446] C.D. Link, Expression of human beta-amyloid peptide in transgenic Caenorhabditis elegans, Proc. Natl. Acad. Sci. U. S. A. 92 (1995) 9368–9372. https://doi.org/10.1073/pnas.92.20.9368.

[447] C.D. Link, C. elegans models of age-associated neurodegenerative diseases: lessons from transgenic worm models of Alzheimer's disease, Exp. Gerontol. 41 (2006) 1007–1013. https://doi.org/10.1016/j.exger.2006.06.059.

[448] T. Tangrodchanapong, P. Sobhon, K. Meemon, Frondoside A Attenuates Amyloid-β Proteotoxicity in Transgenic Caenorhabditis elegans by Suppressing Its Formation, Front. Pharmacol. 11 (2020) 553579. https://doi.org/10.3389/fphar.2020.553579.

[449] X.-G. Zhang, X. Wang, T.-T. Zhou, X.-F. Wu, Y. Peng, W.-Q. Zhang, S. Li, J. Zhao, Scorpion Venom Heat-Resistant Peptide Protects Transgenic Caenorhabditis elegans from β-Amyloid Toxicity, Front. Pharmacol. 7 (2016) 227. https://doi.org/10.3389/fphar.2016.00227.

[450] A. Abelein, Metal Binding of Alzheimer's Amyloid-β and Its Effect on Peptide Self-Assembly, Acc. Chem. Res. 56 (2023) 2653–2663. https://doi.org/10.1021/acs.accounts.3c00370.

[451] N.C. Wildburger, F. Gyngard, C. Guillermier, B.W. Patterson, D. Elbert, K.G. Mawuenyega, T. Schneider, K. Green, R. Roth, R.E. Schmidt, N.J. Cairns, T.L.S. Benzinger, M.L. Steinhauser, R.J. Bateman, Amyloid-β Plaques in Clinical Alzheimer's Disease Brain Incorporate Stable Isotope Tracer In Vivo and Exhibit Nanoscale Heterogeneity, Front. Neurol. 9 (2018) 169. https://doi.org/10.3389/fneur.2018.00169.

[452] S.T. Stefanello, P. Gubert, B. Puntel, C.R. Mizdal, M.M.A. de Campos, S.M. Salman, L. Dornelles, D.S. Avila, M. Aschner, F.A.A. Soares, Protective effects of novel organic selenium compounds against oxidative stress in the nematode Caenorhabditis elegans, Toxicol. Rep. 2 (2015) 961–967. https://doi.org/10.1016/j.toxrep.2015.06.010.

[453] I. Gusarov, I. Shamovsky, B. Pani, L. Gautier, S. Eremina, O. Katkova-Zhukotskaya, A. Mironov, A.A. Makarov, E. Nudler, Dietary thiols accelerate aging of C. elegans, Nat. Commun. 12 (2021) 4336. https://doi.org/10.1038/s41467-021-24634-3.

[454] V. Matyash, G. Liebisch, T.V. Kurzchalia, A. Shevchenko, D. Schwudke, Lipid extraction by methyl-tert-butyl ether for high-throughput lipidomics, J. Lipid Res. 49 (2008) 1137–1146. https://doi.org/10.1194/jlr.D700041-JLR200.

[455] P.O. Helmer, C.M. Wienken, A. Korf, H. Hayen, Mass spectrometric investigation of cardiolipins and their oxidation products after two-dimensional heart-cut liquid chromatography, J. Chromatogr. A 1619 (2020) 460918. https://doi.org/10.1016/j.chroma.2020.460918.

[456] R. Schmid, S. Heuckeroth, A. Korf, A. Smirnov, O. Myers, T.S. Dyrlund, R. Bushuiev, K.J. Murray, N. Hoffmann, M. Lu, A. Sarvepalli, Z. Zhang, M. Fleischauer, K. Dührkop, M. Wesner, S.J. Hoogstra, E. Rudt, O. Mokshyna, C. Brungs, K. Ponomarov, L. Mutabdžija, T. Damiani, C.J. Pudney, M. Earll, P.O. Helmer, T.R. Fallon, T. Schulze, A. Rivas-Ubach, A. Bilbao, H. Richter, L.-F. Nothias, M. Wang, M. Orešič, J.-K. Weng, S. Böcker, A. Jeibmann, H. Hayen, U. Karst, P.C. Dorrestein, D. Petras, X. Du, T. Pluskal, Integrative analysis of multimodal mass spectrometry data in MZmine 3, Nat. Biotechnol. 41 (2023) 447–449. https://doi.org/10.1038/s41587-023-01690-2.

[457] O.D. Myers, S.J. Sumner, S. Li, S. Barnes, X. Du, One Step Forward for Reducing False Positive and False Negative Compound Identifications from Mass Spectrometry Metabolomics Data: New Algorithms for Constructing Extracted Ion Chromatograms and Detecting Chromatographic Peaks, Anal. Chem. 89 (2017) 8696–8703. https://doi.org/10.1021/acs.analchem.7b00947.

[458] G. Liebisch, J.A. Vizcaíno, H. Köfeler, M. Trötzmüller, W.J. Griffiths, G. Schmitz, F. Spener, M.J.O. Wakelam, Shorthand notation for lipid structures derived from mass spectrometry, J. Lipid Res. 54 (2013) 1523–1530. https://doi.org/10.1194/jlr.M033506.

Acknowledgements

Die Fertigstellung dieser Arbeit wäre ohne die Hilfe vieler Menschen nicht möglich gewesen. Daher möchte ich allen, die mich in den letzten Jahren unterstützt haben, meinen herzlichen Dank aussprechen.

Zuerst möchte ich mich bei meiner Betreuerin Julia Bornhorst bedanken. Danke für die Möglichkeit, dass ich an diesem spannenden Thema arbeiten konnte, für deine fachliche Expertise, konstruktives Feedback und dein Engagement und deine Zeit, welche du in mich und dieses Projekt investiert hast. Ich danke dir für dein Vertrauen, deine Begeisterungsfähigkeit und für deine immer gute Laune. Danke, dass du immer ein offenes Ohr hattest und mich bei allem unterstützt hast.

Ein ganz besonderer Dank geht an Alice, Anna, Vivi und Laura. Danke, dass ihr mich immer bedingungslos unterstützt und mir geholfen habt, ohne euch hätten die ganzen (operator) fails im Labor nicht im Ansatz so viel Spaß gemacht. Danke auch für die schöne Zeit außerhalb der Uni, für all die Ausflüge und Spieleabende.

Bedanken möchte ich mich bei meinen Masterstudenten Torben, Lysann und Karsten, welche dieses Thema tatkräftig unterstützt haben. Danke für all eure Hilfe und den Spaß den wir gemeinsam im Labor hatten.

Ein großer Dank geht an die AG Schebb und AG Simon für das Mitbenutzen der Labore und Geräte. Danke euch für all die Unterstützung über die letzten Jahre! Zudem bedanke ich mich bei Vera Schwantes und Heiko Hayen von der Uni Münster für die Messung der Cardiolipine. Ein großer Dank gilt allen weiteren Kooperationspartnern, insbesondere der Arbeitsgruppe Schwerdtle aus Potsdam und dem Chang Lab aus Berkeley.

Zudem bedanke ich mich bei allen Doktoranden des „Stammtischs" für die schöne und immer lustige Zeit in und außerhalb der Uni. Ein riesiger Dank geht an Timo, der den ganzen „Uni-Kram" seit Tag 1 mit mir durchgestanden hat. Außerdem möchte ich mich bei all meinen Freunden und meiner Familie bedanken, die mir die letzten Jahre bei allem zur Seite gestanden haben. Für all eure Unterstützung, ohne die ich überhaupt nicht studiert hätte, bin ich euch unendlich dankbar.

Declaration

The presented semi-cumulative doctoral thesis is composed of seven independent chapters. Chapter 3 and 4 have been published in peer-reviewed scientific journals, while chapter 5 and 6 have been submitted and are currently undergoing the peer-review process. All published and submitted articles include suggestions made by co-authors, editors and reviewers during the peer-review process.

As the leading author of chapter 3 – 6, the studies were conceptualized together with my supervisor Prof. Dr. Julia Bornhorst. I carried out the majority of experiments, conducted the data analysis and interpretation and wrote the main manuscripts. All work done by co-authors has been described at the end of each publication.

Citations for published data, methods, statements and data interpretation of other researchers are properly cited in the relevant articles and across every chapter of this thesis.

_____

Ann-Kathrin Weishaupt